



PHD

**Isolation, characterization, and SAR of norditerpenoid alkaloids from Delphinium and Aconitum  
(Alternative Format Thesis)**

Qasem, Ashraf M. A.

*Award date:*  
2022

*Awarding institution:*  
University of Bath

[Link to publication](#)

**Alternative formats**

If you require this document in an alternative format, please contact:  
[openaccess@bath.ac.uk](mailto:openaccess@bath.ac.uk)

Copyright of this thesis rests with the author. Access is subject to the above licence, if given. If no licence is specified above, original content in this thesis is licensed under the terms of the Creative Commons Attribution-NonCommercial 4.0 International (CC BY-NC-ND 4.0) Licence (<https://creativecommons.org/licenses/by-nc-nd/4.0/>). Any third-party copyright material present remains the property of its respective owner(s) and is licensed under its existing terms.

**Take down policy**

If you consider content within Bath's Research Portal to be in breach of UK law, please contact: [openaccess@bath.ac.uk](mailto:openaccess@bath.ac.uk) with the details. Your claim will be investigated and, where appropriate, the item will be removed from public view as soon as possible.

**Isolation, characterization, and SAR of norditerpenoid alkaloids  
from *Delphinium* and *Aconitum***

Ashraf Mahmoud Abdelghani Qasem

A thesis submitted for the degree of Doctor of Philosophy

University of Bath

Department of Pharmacy and Pharmacology

September 2022

**COPYRIGHT**

Attention is drawn to the fact that copyright of this thesis rests with the author and copyright of any previously published materials included may rest with third parties. A copy of this thesis has been supplied on condition that anyone who consults it understands that they must not copy it or use material from it except as licenced, permitted by law or with the consent of the author or other copyright owners, as applicable.

Signed .....

Date 22<sup>nd</sup> September 2022

*This thesis is dedicated to my parents who sacrificed everything for me to be what I am now. and to the memory of my late brother who always believed in my ability to be successful*

## **Acknowledgements**

Above all, I am grateful to Almighty Allah, who is my refuge and guiding light throughout my ups and downs, without whose help I would not have completed the research in this thesis.

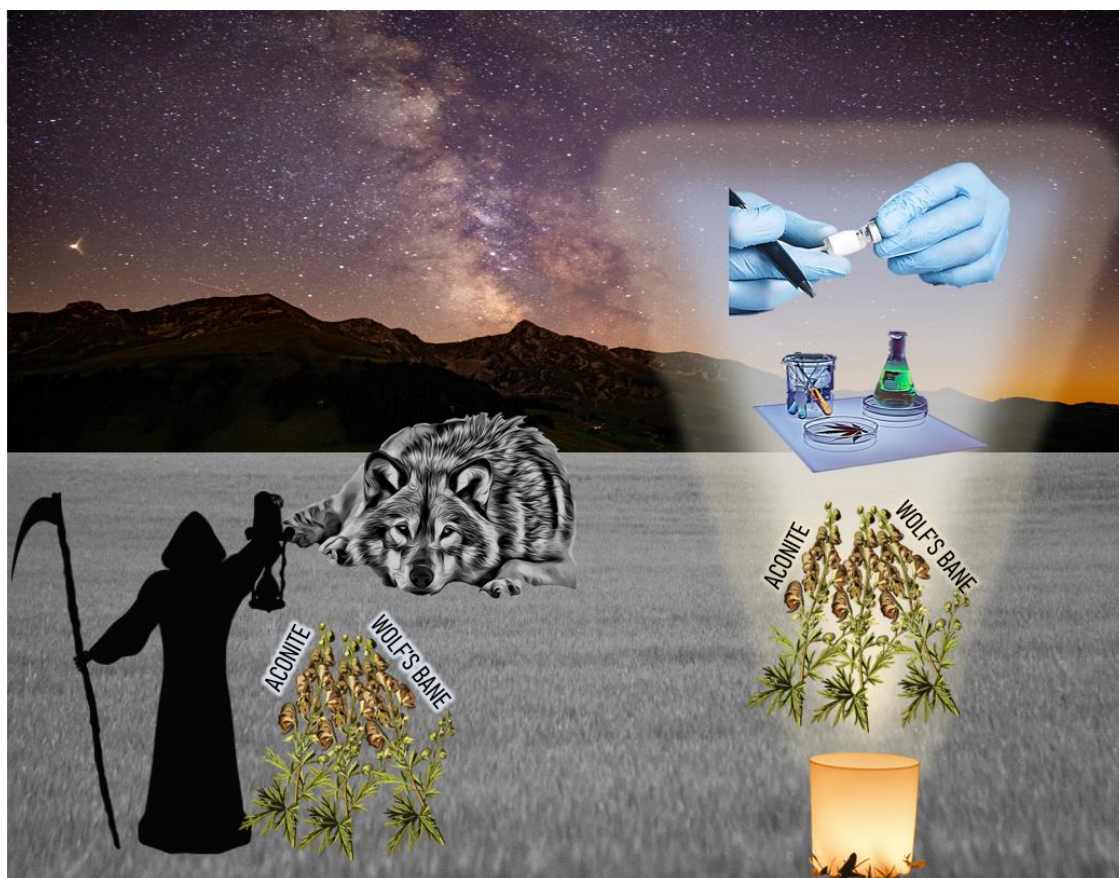
I am eternally grateful to my dear parents who sacrificed their lives for me to be what I am now. I express my sincere thanks to my siblings who supported and encouraged me in the hard times of my PhD journey. I would like to offer special thanks to my late brother, you are gone but your belief in me will last forever. I am also grateful to my friends for being there for me when I really needed you.

My greatest appreciation goes to my supervisors, Dr Ian S. Blagbrough and Dr Michael G. Rowan for their supervision, encouragement, and continuous support throughout my PhD. They have always provided excellent guidance and wise advice, and this PhD thesis would be impossible to have been achieved without their great inputs. I am extremely grateful to them, and it has been my great pleasure to work with such experienced researchers.

I thank Dr Timothy J. Woodman for his assistance with NMR spectroscopy and a lot of good advice. I thank Dr Shaun Reeksting for his Mass Spectrometry assistance. I thank Dr Gabriele Kociok-Kohn for the single-crystal X-ray crystallography data. I also thank all the research and technical staff in the Department of Pharmacy and Pharmacology. I am grateful to Prof Neil S. Millar and Victoria R. Sanders, University College London, for their collaboration in evaluating my compounds biologically.

I acknowledge my colleagues in 5W3.20 and Laboratory 5W3.14 for their help, support, and friendship, especially Dr Abdulaziz Al Khzem, Dr Ziyu Zeng, Dr Rami Alnajadat, Dr Husain A. Naqi, Dr Alexander Disney, and Dr Gerta Cami-Kobeci who helped me in science and in life.

Lastly, but not least, I am grateful to Zarqa University, Jordan, for fully funding this studentship. I also thank the Faculty of Pharmacy at Zarqa University, especially Dr Ahalm Alkilani and Dr Mahmoud Al-sha'er, for their support throughout my PhD.



## **Wolf's Bane Journey into Clinics**

*Aconitum* plants (Aconite) have a famous history due to their toxicity. In the television series “Midsomer Murders”, "Garden of Death" episode, aconite is used as a murder weapon. Aconite also plays a role in Agatha Christie’s “They Do It with Mirrors” and “4.50 From Paddington” novels. *Aconitum* species were used as arrows’ poison for hunting wolves. These plants are called monkshood or wolf’s bane. The name “wolf’s bane” has been used in many poems, movies, and TV shows like Game of Thrones. The clinical studies showed that by controlling the dose, we can avoid their toxicity and make clinically useful drugs. My work focuses on making simplified analogues of the natural products. The biological results show promising activity.

**Winner of “Snap! Your Doctorate” Competition 2022**

## Abstract

Norditerpenoid alkaloids (NDA) are the main bioactive components of the medicinal plants of *Delphinium* and *Aconitum*. This research project is focussed on the characterization of NDA in their natural sources by isolation, some aspects of quantification, and detailed analytical chemistry which leads to a better understanding of their possible 3D-conformations in biological fluids. The synthesis of small molecule AE-bicyclic NDA analogues gave a better understanding of their structure-activity relationships (SAR).

The phytochemical investigation of *D. elatum* seeds results in the isolation of four NDA: methyllycaconitine (MLA), shawurensine A, shawurensine B, which is reported for the first time, and delpheline where the crystal structure is reported for the first time. The safety and effectiveness have been assessed for five *Aconitum* TCM preparations (Zhi'cao'wu, Zhi'chuan'wu, Yan'fu'zi, Bai'fu'pian, and Hei'shun'pian) through the quantification of six norditerpenoid markers. It was found that the total diester diterpenoid alkaloids (DDA) amount is within the Chinese Pharmacopeia limit and therefore they can be safely used. On the other hand, only Zhi'cao'wu met the Chinese Pharmacopeia limit for the total monoester diterpenoid alkaloids (MDA) amount which ensures the preparation efficacy.

The in-solution characterization of NDA using NMR spectroscopy and mass spectrometry (MS) was accomplished where it was observed using NMR spectroscopy that the A-ring in 1-OH NDA adopts a boat conformation compared to a chair conformer in 1-OMe NDA due to the intramolecular H-bonding between that 1-OH group and the piperidine nitrogen. The stability of the NDA skeleton was studied using atmospheric pressure chemical ionization mass spectrometry (APCI-MS) where it was shown that 1-OH NDA are more stable compared to 1-OMe NDA. In addition, the effect of carbon 1 substituent configuration was studied by the synthesis of 1-*epi*-condelphine where it was found that it is less stable in the MS compared to condelphine as the nitrogen is no longer hydrogen bonded to the  $\beta$ -OH at position 1.

The synthesis of AE-bicyclic analogues of methyllycaconitine (MLA) was accomplished with different nitrogen and ester side-chains to get a better SAR understanding of their activity at human  $\alpha 7$  nAChR.

## Abbreviations

∠ angle

Å Ångström

Ac acetyl

aq. aqueous solution

Bz benzoyl

CNS central nervous system

conc. concentrated

COSY correlation spectroscopy

Da Dalton

DEPT Distortionless Enhancement by Polarization Transfer

eq. equivalent

Et ethyl

g gram

h hour

H2BC heteronuclear two bond correlation

HMBC heteronuclear multiple bond correlation

HSQC heteronuclear single quantum coherence

Hz Hertz

IC50 half maximal inhibitory concentration

*J* coupling constant

K degree Kelvin

kg kilogram

LD<sub>50</sub> median lethal dose

M molar

*m/z* mass-to-charge ratio

Me methyl

mg milligram

MHz Mega Hertz  
mL millilitre  
mM millimolar  
mmol millimole  
nM nanomolar  
NMR nuclear magnetic resonance  
NOESY nuclear Overhauser spectroscopy  
°C degree Celsius  
OH hydroxyl  
OMe methoxyl  
pKa acid dissociation constant  
ppm parts per million  
R<sub>f</sub> retention value  
sat. saturated  
TCM Traditional Chinese Medicine  
TLC thin layer chromatography  
w/w weight by weight  
XRD X-ray diffraction  
 $\delta$  chemical shift  
 $\Delta\delta$  difference of chemical shifts  
 $\lambda$  wavelength  
 $\mu\text{L}$  microlitre



<b>Contents</b>	<b>Page</b>
<b>Abstract</b>	<b>5</b>
<b>Abbreviations</b>	<b>6</b>
<b>Chapter 1. General introduction and literature review</b>	<b>9</b>
<b>Chapter 2. Isolation of norditerpenoid alkaloids from <i>Delphinium elatum</i></b>	<b>79</b>
<b>Chapter 3. Quantification and chemical profiling of TCM <i>Aconitum</i> preparations using LC-ESI-MS/MS</b>	<b>100</b>
<b>Chapter 4. The 1<math>\alpha</math>-hydroxy-A-rings of norditerpenoid alkaloids are twisted-boat conformers</b>	<b>125</b>
<b>Chapter 5. Impacts of steric compression, protonation, and intramolecular hydrogen bonding on the <sup>15</sup>N NMR spectroscopy of norditerpenoid alkaloids and their piperidine-ring analogues</b>	<b>141</b>
<b>Chapter 6. Conformational analysis of 1<math>\alpha</math>-methoxy and 1<math>\alpha</math>-hydroxy norditerpenoid alkaloids</b>	<b>153</b>
<b>Chapter 7. Effect of position 1 substituent and configuration on APCI-MS fragmentation of norditerpenoid alkaloids including 1-<i>epi</i>-condelphine</b>	<b>171</b>
<b>Chapter 8. Synthesis and antagonist activity of methyllycaconitine analogues on human <math>\alpha 7</math> nicotinic acetylcholine receptors</b>	<b>190</b>
<b>Chapter 9. Conclusions</b>	<b>221</b>
<b>Appendix 1. Abstracts presented at conferences</b>	<b>227</b>
<b>Appendix 2. Data of single-crystal X-ray determinations of delpheline</b>	<b>235</b>

## Chapter 1

### General introduction and literature review

#### Introduction

Nature is rich with many examples of plants that can be described as medicinal or poisonous plants. The controversy in the description spotlights the fact, well known in pharmacy and the pharmaceutical sciences, that dose and mode of action are very important. Plants from *Aconitum* and *Delphinium* are well-known as herbal medicines, but it is dose dependent as they also contain highly toxic norditerpenoid alkaloids (NDA). NDA have complex highly oxygenated hexacyclic skeletons and are of pharmacological importance where few of them have been clinically approved. For the physical and chemical properties of NDA and their binding modes at their targets, it is important to pay attention to structural details as conformation is an important factor of the pharmacological action. The synthesis and analysis of small molecule analogues will provide a better understanding of their structure activity relationship (SAR).

#### Aims

To characterize NDA in their natural sources by isolation, some aspects of quantification, and detailed analytical chemistry, and to synthesize small molecule AE-bicyclic NDA analogues to get a better understanding of their SAR.

#### Objectives

*Delphinium elatum* seeds will be phytochemically investigated to isolate NDA.

*Aconitum* preparations, used in traditional Chinese medicine (TCM), will be extracted, and chemically profiled where NDA will be quantified to assess the TCM preparations safety and efficacy compared to the Chinese Pharmacopeia limits.

In-solution characterization of NDA using NMR to understand their conformation as free bases and salts.

Atmospheric pressure chemical ionization mass spectrometry (APCI-MS) will be used to assess NDA skeleton stability and correlate it with their 3D configuration.

Simple AE-bicyclic analogues of methyllycaconitine (MLA) will be synthesized with different nitrogen and ester side-chains and their antagonistic activity at human  $\alpha 7$  nAChR will be examined (in collaboration) to get a better understanding of their SAR.

## **Poisonous Piperidine Plants and the Biodiversity of Norditerpenoid Alkaloids for Leads in Drug Discovery: Experimental Aspects**

**Aims:** There are famous examples of simple (e.g., hemlock, *Conium maculatum* L.) and complex (e.g., opium poppy, *Papaver somniferum* L., Papaveraceae) piperidine-alkaloid-containing plants. Many of these are highly poisonous, whilst pepper is well-known gastronomically, and several substituted piperidine alkaloids are therapeutically beneficial as a function of dose and mode of action. This review covers the taxonomy of the genera *Aconitum*, *Delphinium*, and the controversial *Consolida*. As part of studying the biodiversity of norditerpenoid alkaloids (NDAs), the majority of which possess an N-ethyl group, we also quantified the fragment occurrence count in the SciFinder database for NDA skeletons. The wide range of NDA biodiversity is also captured in a review of over 100 recently reported isolated alkaloids. Ring A substitution at position 1 is important to determine the NDA skeleton conformation. In this overview of naturally occurring highly oxygenated NDAs from traditional *Aconitum* and *Delphinium* plants, consideration is given to functional effect and to real functional evidence. Their high potential biological activity makes them useful candidate molecules for further investigation as lead compounds in the development of selective drugs.

<b>This declaration concerns the article entitled:</b>			
Poisonous Piperidine Plants and the Biodiversity of Norditerpenoid Alkaloids for Leads in Drug Discovery: Experimental Aspects			
<b>Publication status (tick one)</b>			
<b>Draft manuscript</b>	<input type="checkbox"/>	<b>Submitted</b>	<input type="checkbox"/>
		<b>In review</b>	<input type="checkbox"/>
		<b>Accepted</b>	<input type="checkbox"/>
		<b>Published</b>	<input checked="" type="checkbox"/>
<b>Publication details (reference)</b>	Qasem, A.M.A.; Rowan, M.G.; Blagbrough, I.S. Poisonous Piperidine Plants and the Biodiversity of Norditerpenoid Alkaloids for Leads in Drug Discovery: Experimental Aspects. <i>Int. J. Mol. Sci.</i> 2022, 23, 12128.		
<b>Copyright status (tick the appropriate statement)</b>			
The material has been published with a CC-BY license		<input checked="" type="checkbox"/>	The publisher has granted permission to replicate the material included here
		<input type="checkbox"/>	
<b>Candidate's contribution to the paper (provide details, and also indicate as a percentage)</b>	<p><b>Formulation of ideas:</b> The candidate considerably contributed to the formulation of the article ideas to cover piperidine containing plants, biodiversity of norditerpenoid alkaloids and the taxonomy of their natural sources. (60%)</p> <p><b>Design of methodology:</b> Critical review of the recent literature. (70%)</p> <p><b>Experimental work:</b> The candidate considerably contributed to the experimental work using Web of science and SciFinder databases (70%).</p> <p><b>Presentation of data in journal format:</b> The candidate considerably contributed to the data presentation through writing, referencing, and preparing the article figures (80%).</p>		
<b>Statement from Candidate</b>	This paper reports on original research I conducted during the period of my Higher Degree by Research candidature.		
<b>Signed (typed signature)</b>	Ashraf Qasem	<b>Date</b>	21/09/2022

## 1. Piperidines: Poisonous, Tasty, and Beneficial

Nature is rich with examples of plants that can be described as medicinal or poisonous. The controversy in the description spotlights the fact, well known in pharmacy and the pharmaceutical sciences, that dose and mode of action are critical. Out of thousands of plants with various types of active principles, many examples can be found of natural sources of alkaloids containing a substituted piperidine nucleus.

There are well-known examples of simple piperidine-alkaloid-containing plants, such as the famous poison hemlock (*Conium maculatum* L.), in the family Apiaceae (formerly Umbelliferae). It is a lethal poison that was given to criminals in ancient Greece and that the Greek philosopher, Socrates, was forced to drink (399 B.C.) [1]. The principal component of poison hemlock is the piperidine alkaloid coniine **1** (Figure 1), which is a nicotinic acetylcholine receptor (nAChR) agonist [1] where the importance of the positive centre was highlighted in the Beers–Reich model [2]. Consumption of *C. maculatum* leads to various degrees of toxicity in animals, where it has been found that it is more poisonous to cattle than to other animals.

Human toxicity signs were described by Socrates' pupil as trembling, staggering, and rapid muscular weakness. Death resulting from hemlock poisoning is mainly due to respiratory failure [1,3]. Another nAChR agonist is anabasine **2**, a natural nicotine **3** like isomer compound from *Nicotiana* spp. (tobacco) of the family Solanaceae. Two important species are *N. glauca* (wild tree tobacco) and *N. tabacum* L. Anabasine **2** is the major component in *N. glauca*, while nicotine **3** is the main constituent in *N. tabacum* L. [3–5]. Another source of piperidine alkaloids is *Lobelia* spp. (Campanulaceae). An important example is the Indian tobacco, *L. inflata* L., which is used traditionally in smoking cessation and in the treatment of respiratory conditions [6]. Lobeline **4** is the major and the most biologically active component of *L. inflata* L. It was found that lobeline **4** can be described as agonist, antagonist, or mixed agonist/antagonist at nAChR [7].

*Lupinus* spp. (Fabaceae) consumption leads to teratogenic crooked calf disease. The teratogenicity was initially suggested to be due to the quinolizidine alkaloid, anagryne **5** [5,8].

As similar teratogenicity happens in livestock due to the consumption of *C. maculatum* and *N. glauca*, which contain mainly piperidine alkaloids [4,9,10], it is now suggested that the main piperidine alkaloid, ammodendrine **6**, which is found in many *Lupinus* spp. such as *L. formosus*, is responsible for such deformations. Keeler and Panter [8] showed that anagyrene **5** exists as a minor component in *L. formosus*, while ammodendrine **6** is the major one, supporting that the piperidine alkaloid **6** is responsible for the teratogenicity.

Black pepper, *Piper nigrum* L. (Piperaceae), is known as the king of spices, and it is the natural source of piperine **7** which shows anti-inflammatory, antioxidant, anticancer, and antimicrobial activities [11–13]. 1-Deoxynojirimycin **8** is another example of a piperidine alkaloid which acts as one of the most potent  $\alpha$ -glycosidase inhibitors and has relevant biological activity in the treatment of hyperglycaemia and obesity. It is naturally occurring in the leaves of white mulberry, *Morus alba* L. (Moraceae) [14,15].

In addition to simple piperidines, there are many famous examples of piperidine-containing plants where the piperidine ring is part of a complex skeleton. *Papaver somniferum* L. (Papaveraceae), also known as opium poppy, is a natural source of the opioids morphine **9** and codeine **10**. These piperidine-containing alkaloids are used as strong analgesics, but are also abused in addiction [16,17]. The potency of morphine **9** is much higher than codeine **10**, and the fact that codeine **10** exerts its analgesic effect after being metabolized into morphine **9** highlights the importance of the phenolic alcohol in the activity at  $\mu$  opioid receptors [18].

Another example is cytisine **11**, which is derived from *Laburnum anagyroides* Medik. (Fabaceae), and it acts as an nAChR agonist. The skeleton of cytisine **11** shows that the piperidine coexists with a quinolizidine ring [3,19] and fits the Beers–Reich model, as cytisine **11** contains a cationic centre and heteroatoms, where the model showed that the distance between them in nAChR ligands is 5.9 Å [2].

There are piperidine-containing alkaloids, which are C-18 and C-19 norditerpenoid alkaloids (NDAs) from *Aconitum* and *Delphinium* (Ranunculaceae), and especially aconitine **12**, lappaconitine **13**, lycoctonine **14**, lycaconitine **15**, and methyllycaconitine (MLA) **16**. The C-19 NDA aconitine **12** was first discovered in 1833 by P. L. Geiger from *A. napellus* [20,21]. It is considered a potent lethal cardiotoxin that acts on voltage-gated sodium channels (VGSC) and

keeps them in an open conformation. In contrast, lappaconitine **13**, which was the first C-18 NDA to be discovered, is a VGSC blocker [22]. The hydrogen bromide (HBr) salt of lappaconitine **13** (allapinine) is used clinically in Russia as an anti-arrhythmic drug. Lappaconitine **13** was first discovered from *A. septentrionale* Koelle by H. V. Rosendahl in 1895 [23,24]. Lycoctonine **14** was first reported in 1865 from *A. lycoctonum* L. [25]. Lycaconitine **15** was first reported in 1884 from *A. lycoctonum* L. [26]. MLA **16**, a C-19 NDA, was first discovered by Manske in 1938 in *D. brownii* Rydb [27]. Goodson (1943) later determined its exact formula [28]. MLA **16** acts as a potent competitive antagonist on  $\alpha 7$ -nAChR [29]. The importance of the piperidine nitrogen of NDAs in the interaction with nAChR was proven, as semi-synthetic analogues with quaternary nitrogen showed higher activity, and that suggests that the nitrogen is a main site of receptor interaction [30]. All the previous examples show alkaloids which contain piperidine alone or they coexist with other heterocycles. Scopolamine (hyoscine) **17**, L-hyoscyamine **18**, and atropine (dl-hyoscyamine) **19** (Figure 1) are examples of alkaloids that contain a piperidine ring fused with pyrrolidine (tropane alkaloids). These alkaloids are antagonists at the muscarinic acetylcholine receptors (mAChR) and are derived from many plants of the nightshades (Solanaceae). These compounds meet the Beers–Reich pharmacophore criteria, as they contain a cationic centre and a Van der Waals surface (heteroatoms). A member of the nightshades is *Datura stramonium* L., which is also known as thornapple and jimsonweed [31,32].





## 2. Taxonomy of *Aconitum*, *Delphinium*, and *Consolida*

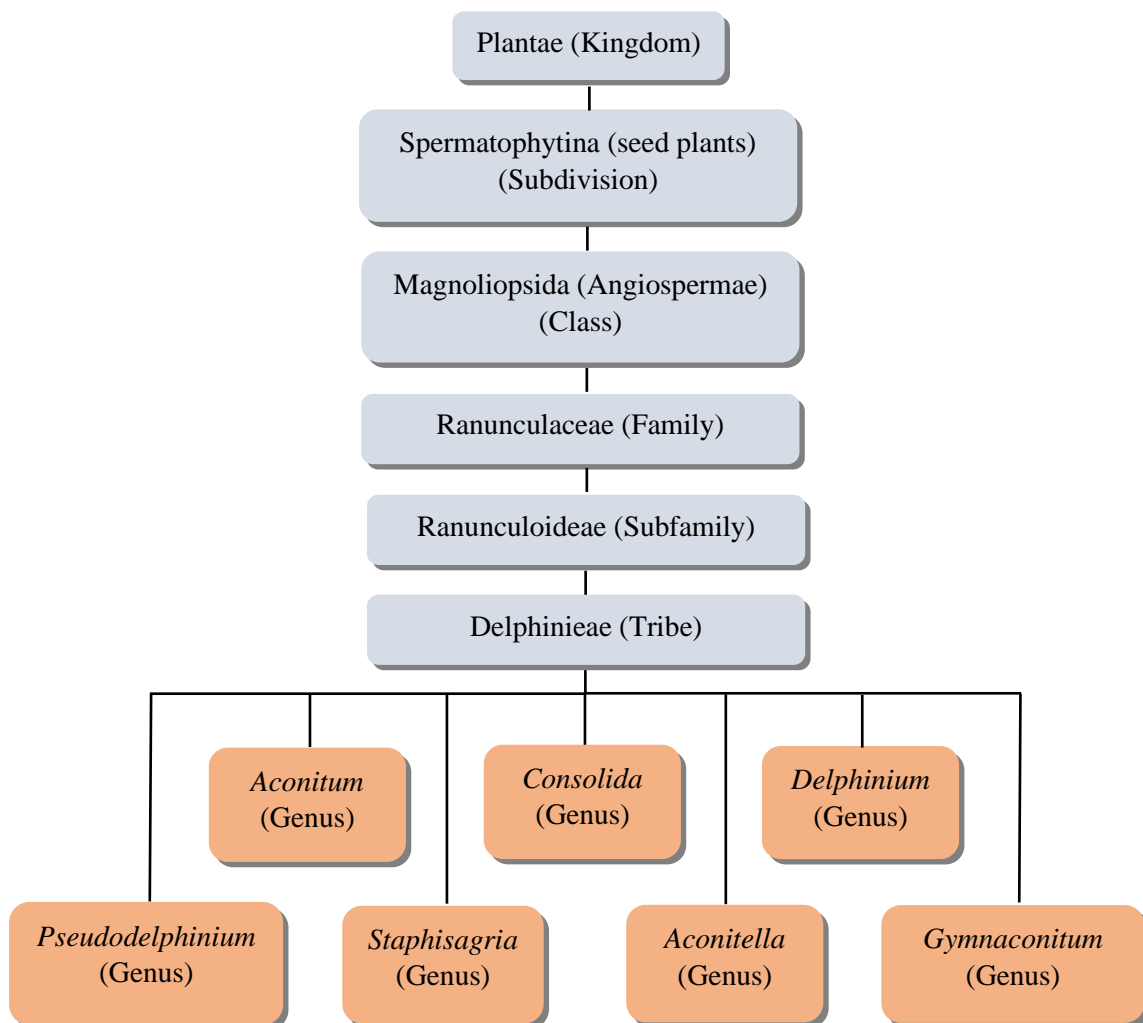
Diterpenoid alkaloids are found mainly in *Aconitum*, *Delphinium*, and *Consolida* within the family Ranunculaceae, and Garrya (silk tassel) from the family Garryaceae. Apart from these genera, three diterpenoid alkaloids, lycoctonine **14**, MLA **16**, and inuline (which is the 2-aminobenzoate ester of lycoctonine **14**) have been reported from *Inula royleana* (Asteraceae) [33]. The three families (Ranunculaceae, Garryaceae, and Asteraceae) are classified under the Angiospermae class (flowering plants) [34–36]. C-18 and C-19 NDAs are derived from only three genera within Ranunculaceae: *Aconitum*, *Delphinium*, and *Consolida*. The Ranunculaceae family contains around 43 genera and more than 2000 species [37]. *Aconitum* L. with around 330 species and *Delphinium* L. with around 450 species are considered the major genera in this family [38,39].

All three of these genera are classified within the tribe Delphinieae of the subfamily Ranunculoideae. [40]. A scientific classification of *Aconitum*, *Delphinium*, and *Consolida* is shown in Scheme 1 [36,40–42].

*Aconitum* L. has been divided into three subgenera (*Aconitum*, *Lycoctonum* (DC.) Peterm., and *Gymnaconitum* (Stapf) Rapes). The *Aconitum* subgenus *Aconitum* produces biennial tuberous roots, while subgenus *Lycoctonum* (DC.) Peterm. species have perennial rhizomes. The only annual species of the *Aconitum* genus can be found in subgenus *Gymnaconitum* (Stapf) Rapes. [43]. The *Delphinium* L. genus is also divided into two subgenera (*Delphinastnim* (DC.) Wang and *Delphinium*) [44], and the species within this genus are usually perennial (occasionally annual) [45]. Due to the shape of flowers of the *Delphinium* species which resemble dolphins, the *Delphinium* genus takes its name from the Greek word delphis [45].

The genus *Consolida* has proved to be more controversial. A. P. De Candolle separated a group of annual species from the genus *Delphinium* L. to form an independent section (*Consolida* DC.). S.F. Gray changed the section *Consolida* to the rank of a genus in 1821 (*Consolida* (DC.) S.F. Gray). Boissier gave the rank of genus to the *Consolida* section of *Delphinium* L. in 1867 and Huth gave it the rank subgenus in 1895 [46]. Huth was the last

worker to include *Consolida* within *Delphinium*. Much more recently, Jabbour and Renner (2011) suggested using a DNA phylogenetic study that *Consolida* should be embedded in *Delphinium* [47]. Commonly, *Delphinium* and *Consolida* species are called larkspur, which is also a name derived from the shape of the flowers [45]. The colourful flowers of the *Delphinium* species gave rise to many cultivated species (cultivars) that are used as ornamental plants in the garden. These hybrid species come from crossing different parent plants and mainly from the tetraploid *D. elatum* L. [48,49]. Examples of the hybrid *Delphinium* varieties are the giant pacific court hybrids which originate from *D. elatum* and other species such as *D. exaltatum* and *D. formosum* [50].



**Scheme 1.** Scientific classification of *Aconitum*, *Delphinium*, and *Consolida* from the Plantae kingdom.

### 3. NDA chemical toxicity

North Americans have divided the *Delphinium* (larkspur) plants into three categories depending on habit of growth and environment. First are the tall larkspurs (such as *D. barbeyi*, *D. occidentale*), which are 1–2 m tall and generally exist at altitudes above 2400 m in moist habitats. Second are the intermediate larkspurs (such as *D. geyeri*, plains larkspur), which are 0.6–1 m tall and grow on the short grass prairies of Nebraska, Wyoming, and Colorado. The third category is low larkspurs (such as *D. andersonii*), which are less than 0.6 m tall and generally grow in the desert/semidesert, foothills, or low mountain ranges [51,52]. *Delphinium* (larkspur) alkaloids cause economically important livestock toxicity across North American ranges [51,53]. Tall larkspurs contain higher amounts of toxic NDAs and are therefore considered a greater threat [54]. Intoxication happens due to the action of NDAs at the  $\alpha$ 1-nAChR expressed at neuromuscular junctions (NMJ) [55].

It was found that the livestock intoxication by larkspurs is controlled by different factors, for example, cattle breed and genetics affect the susceptibility to the intoxication. Age is another factor, where young heifers are more susceptible than mature cows. The cattle sex was reported to be an effective factor, where heifers are more prone to the toxicity than steers and bulls. Lastly, the plant factor plays an important role, where the alkaloid concentration and composition of methylsuccinimidoanthranoyl-lycoctonine (MSAL) and non-MSAL (Figure 2), which depend on the population, species, climate, and the year, affect the toxicity in cattle and the amount needed to develop clinical signs [56,57].

The toxicity of NDAs found in three tall larkspur species (*D. barbeyi*, *D. occidentale*, *D. glaucescens*) was tested in mice. The assay revealed that the 7,8-methylenedioxy-lycoctonine (MDL) alkaloids are the least toxic NDAs. The lycoctonine-type is twice as toxic as MDL, but it is considered to be a low toxic group, where the least toxic alkaloid of this category, brownine **20**, has a toxicity which is comparable to the MDL NDA. The MSAL alkaloids MLA **16** and 14-deacetylindicauline **21** were 10-times more toxic than any other tested NDAs (Figure 2) [54].

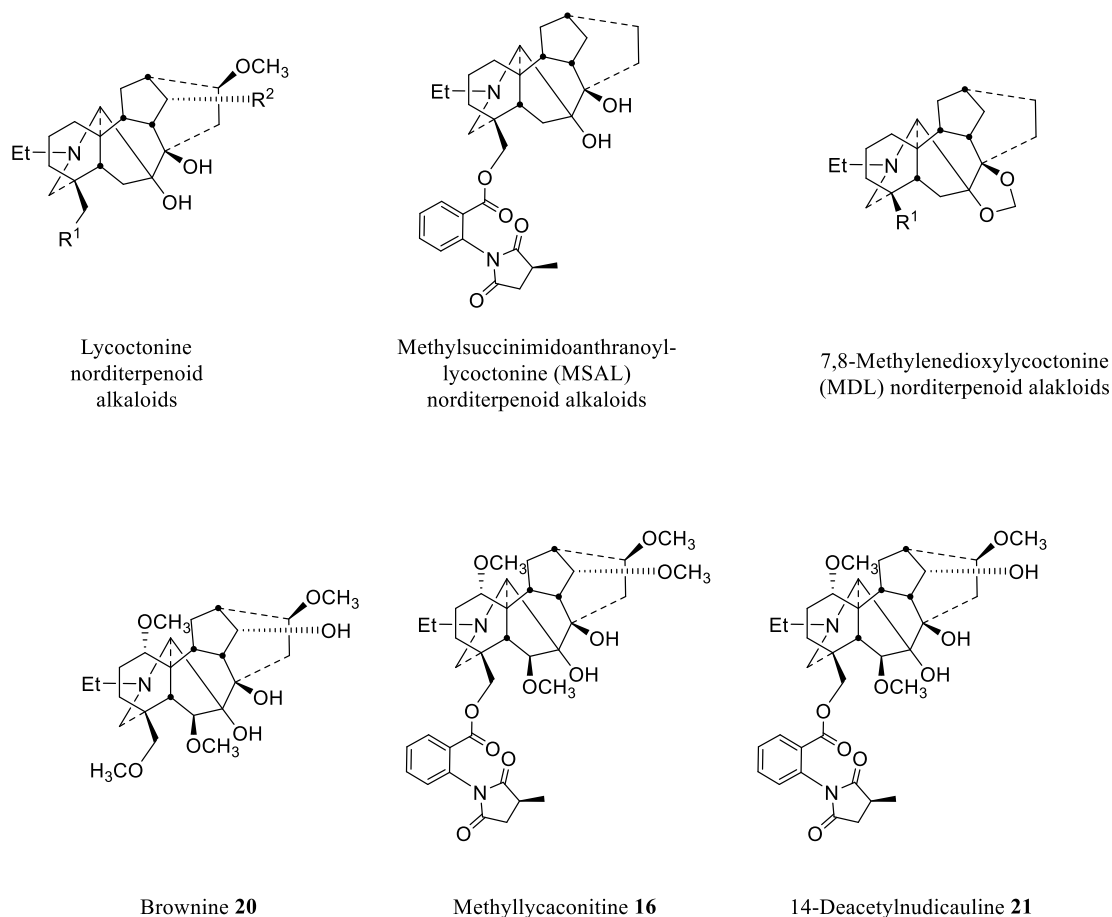


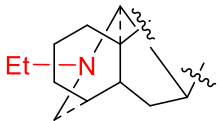
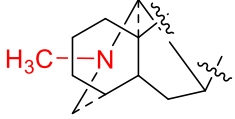
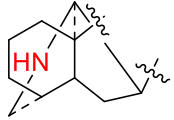
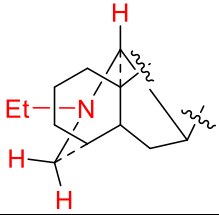
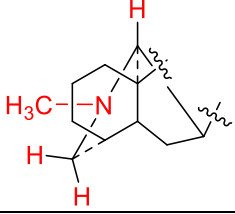
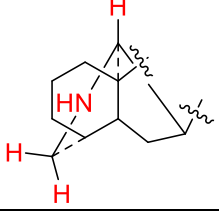
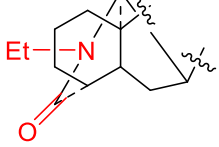
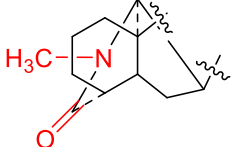
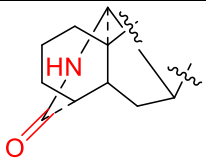
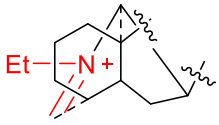
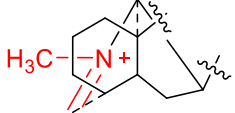
**Figure 2.** NDAs of lycoctonine (**20**), MSAL (**16**), and MDL types.

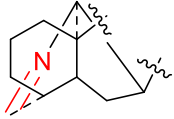
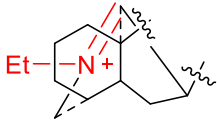
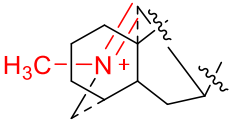
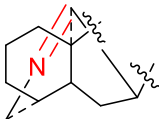
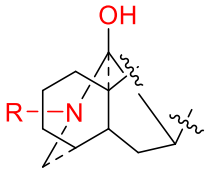
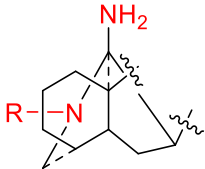
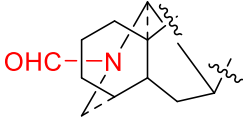
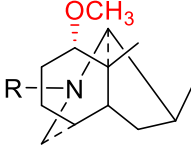
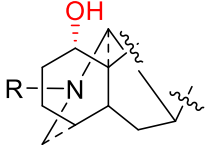
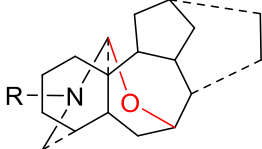
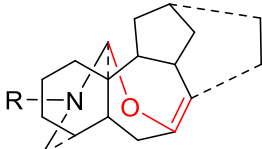
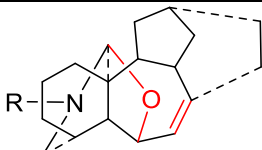
MSAL is much more toxic than MDL, and the MSAL level in the tall larkspurs mainly contributes to livestock poisoning. A report investigated the importance of the MDL alkaloids and found that MDL alkaloids exacerbate the toxicity of the MSAL alkaloids; as the ratio of MDL to MSAL increases, the amount of MSAL that is needed to develop clinical signs decreases. The exact mechanism of this MDL action is not known, but it was suggested that MDL may act as a co-agonist in an allosteric manner or at the orthosteric ligand binding site of the receptor to exacerbate the toxicity of MSAL-type alkaloids on nAChR and therefore increase their toxicity [58]. The observed action could also be due to an effect of MDL alkaloids on metabolic enzymes which results in prolonged exposure to the MSAL alkaloids, but further investigation is needed.

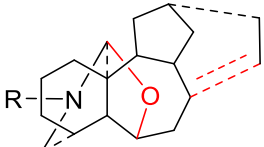
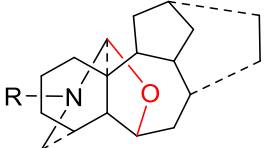
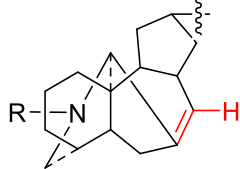
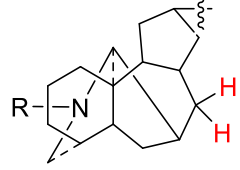
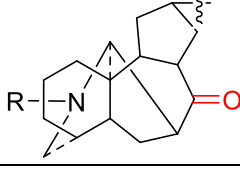
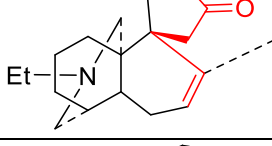
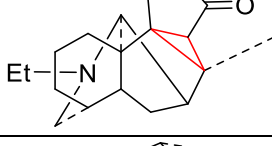
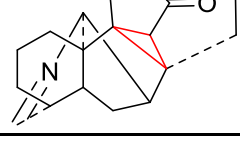
#### 4. Norditerpenoid alkaloid (NDA) biodiversity

NDA's have complex highly oxygenated hexacyclic systems, and as many of them are of pharmacological importance, their structures and 3D configuration are significant factors in their actions at various biological targets [59]. The majority of NDAs possess an *N*-Et group, as shown in Table 1, which shows various NDA skeletons and their abundance in the SciFinder database. Substitution at position 1 is important to determine the NDA skeleton conformation, as ring A in 1-OMe NDA free bases exists in a twisted-chair conformation, and in 1-OH NDA ring A adopts a twisted-boat conformation [60,61]. Table 1 shows that 1-OMe NDA abundance is 10-times higher than 1-OH NDA. The biological activity of NDAs attracts natural product chemists to investigate their sources, and that has resulted in the discovery of interesting NDA skeletons, some of them with pharmacological importance.

**Table 1.** NDA skeletons occurrence count on SciFinder database.

Skeleton <sup>+</sup>	Number of Compounds <sup>++</sup>
	2728
	436
	160
	2598
	427
	128
	78
	5
	13
	13
	4

	67
	0
	0
	0
	0
	0
	36
	3002
	392
	10 (all are <i>N</i> -Et)
	0
	24 (3 <i>N</i> -Pr, 1 <i>N</i> -Me, and 20 <i>N</i> -Et)

	1 ( <i>N</i> -Et)
	5 ( <i>N</i> -Et)
	0
	0
	2
	3
	2
	2

+ R = methyl (Me), ethyl (Et), propyl (Pr); ++ number of compounds includes the free base form and the salt form.



Recent phytochemical investigations reported on *Aconitum* and *Delphinium* species show the wide variety of structural motifs in such NDAs. Chen et al. reported the extraction of a new aconitine-type NDA with a 1-OH substitution, pubescensine **22** from *A. soongaricum* var. pubescens, and this showed a potent insect antifeedant activity ( $EC_{50} < 1 \text{ mg/cm}^2$ ) [62]. Ding and co-workers discovered four new NDAs, vilmorines A–D **23–26** from *A. vilmorinianum* (Figure 3) [63]. Vilmorine D **26** exhibited moderate to weak antioxidant activity ( $Fe^{2+}$  chelation activity) with  $IC_{50} = 33.6 \pm 0.2 \text{ }\mu\text{g/mL}$ , and it showed antibacterial activity against *Staphylococcus aureus* and *Bacillus subtilis* with MICs of 64 and 32  $\mu\text{g/mL}$ , respectively. Vilmorine A **23** has an unusual spiro junction. Only three such compounds were isolated with that characteristic skeleton (Table 1). Vilmorine A **23** also has the really unusual 1- $\beta$ -OMe group, whereas the vast majority of the position 1 substituents have an  $\alpha$ -configuration. Vilmorines B–C **24–25** have an unusual cyclopropyl moiety, and they are rare examples containing an imine (piperidine) (Table 1).

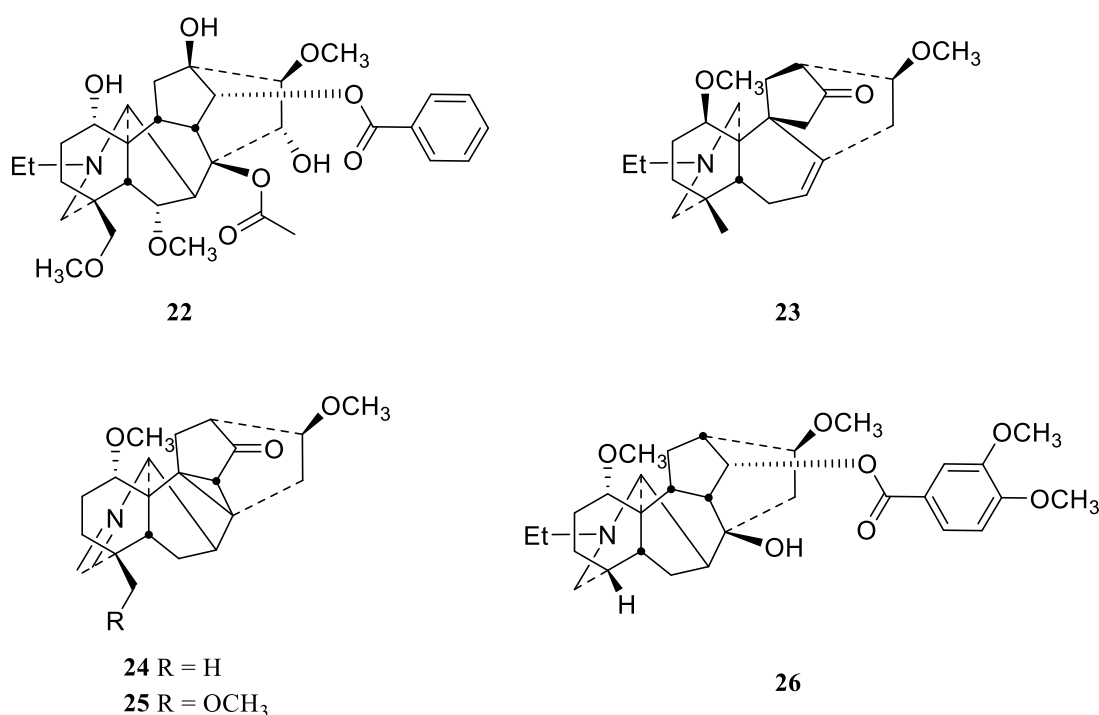
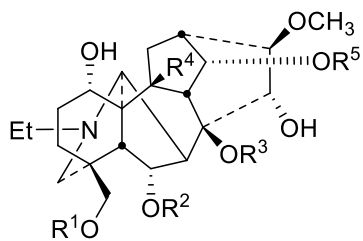
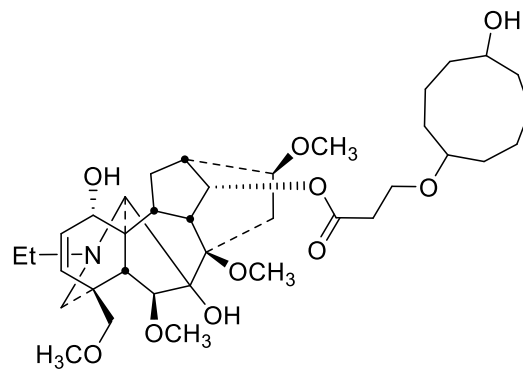


**Figure 3.** NDAs **22–26**.

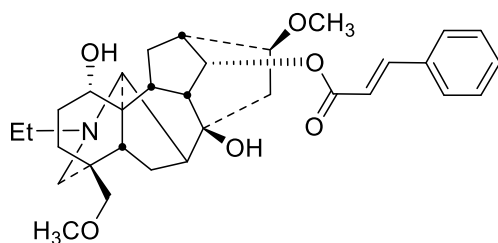
Qin et al. (2015) isolated five new NDA from *A. carmichaelii*, carmichaenine A–E **27-31** [64] with a characteristic 1-OH substitution. Majusine D **32** from *D. majus* W. T. Wang and stapfianine A **33** from *A. stapfianu* were discovered as new C-19 NDA [65,66] with 1-OH substitution. Sharwuphinine B **34** was discovered from *D. shawurensense* as one of the few quaternary C-19 NDA (Figure 4) [67].



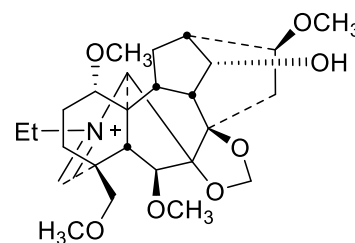
- 27** R<sup>1</sup> = R<sup>2</sup> = CH<sub>3</sub>, R<sup>3</sup> = Bz, R<sup>4</sup> = R<sup>5</sup> = H  
**28** R<sup>1</sup> = R<sup>3</sup> = R<sup>5</sup> = H, R<sup>2</sup> = CH<sub>3</sub>, R<sup>4</sup> = OH  
**29** R<sup>1</sup> = CH<sub>3</sub>, R<sup>2</sup> = R<sup>3</sup> = R<sup>4</sup> = H, R<sup>5</sup> = Bz  
**30** R<sup>1</sup> = R<sup>2</sup> = R<sup>3</sup> = R<sup>4</sup> = H, R<sup>5</sup> = Bz  
**31** R<sup>1</sup> = R<sup>2</sup> = CH<sub>3</sub>, R<sup>3</sup> = Bz, R<sup>4</sup> = OH, R<sup>5</sup> = H



**32**



**33**



**34**

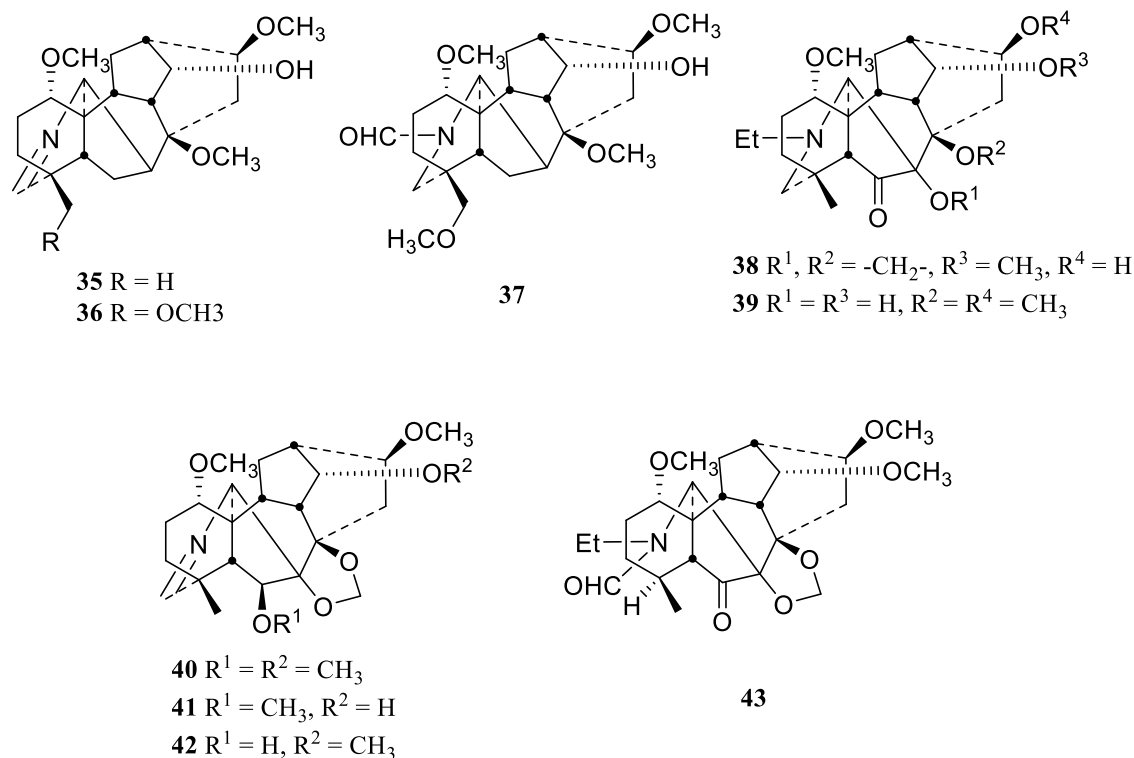


**Figure 4.** NDAs 27-43.

Chen et al. isolated two imine (piperidine)-type NDAs, vilmorrianines F–G **35–36**, in addition to new *N*-desethyl-*N*-formyl-8-*O*-methyltaltisamine **37** from *A. vilmorinianum* Komarov [68]. Six new NDAs, 6-dehydroeladine **38**, elapacidine **39**, iminopaciline **40**, iminoisodelpheline **41**, iminodelpheline **42** (piperidine), and *N*-formyl-4,19-secopacinine **43**, were extracted from *D. elatum* seeds (Figure 4) [69]. Shan et al. reported two new C-18 NDAs, anthriscifoltine A–B **44–45** from *D. anthriscifolium* var. majus [70]. Ding and co-workers also isolated three new NDAs, vilmotenitines A–C **46–48** from *A. vilmorinianum* var. *patentipilum*, (Figure 5) where vilmotenitines A and B **46–47** had an unusual (spiro) rearranged six-membered B ring [71], as they had found in vilmorine A **23** with the inverted substituent stereochemistry at position 1 [63].

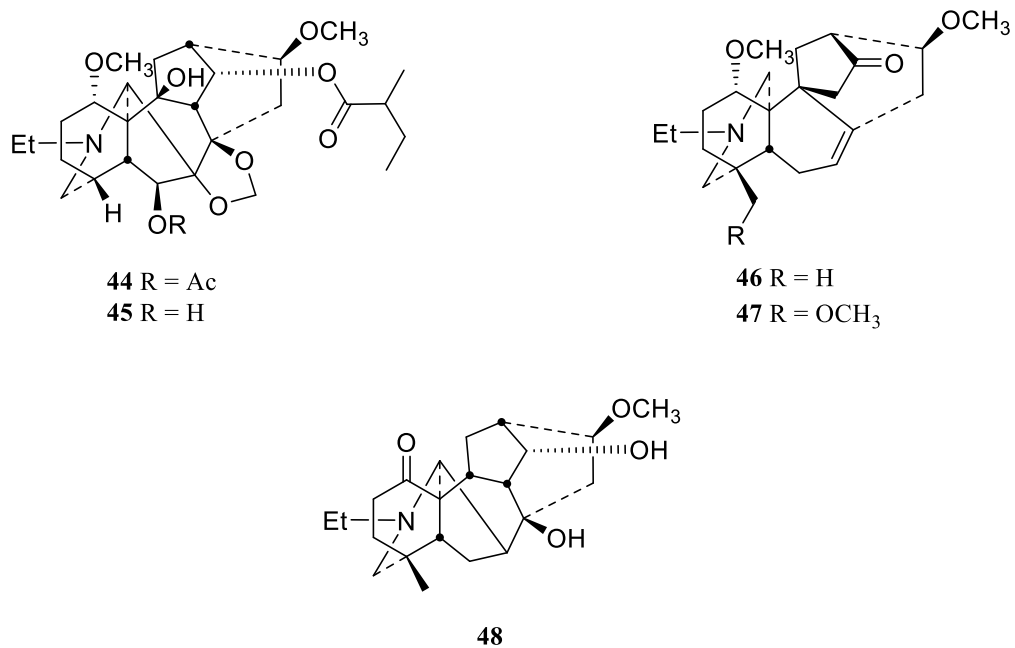


**Figure 5.** NDAs **44-48**.

Two new C19 NDAs, iliensine A and B **49-50**, were isolated from *D. iliense*, where iliensine A **49** had a characteristic glycosidic linkage [72]. Wada et al. isolated four new C19 NDAs with a 7,8-methylenedioxy moiety from *D. elatum* [73], 19-oxoisodelpheline **51**, *N*-deethyl-19-oxoisodelpheline **52**, *N*-deethyl-19-oxodelpheline **53**, and melpheline **54** (Figure 6).

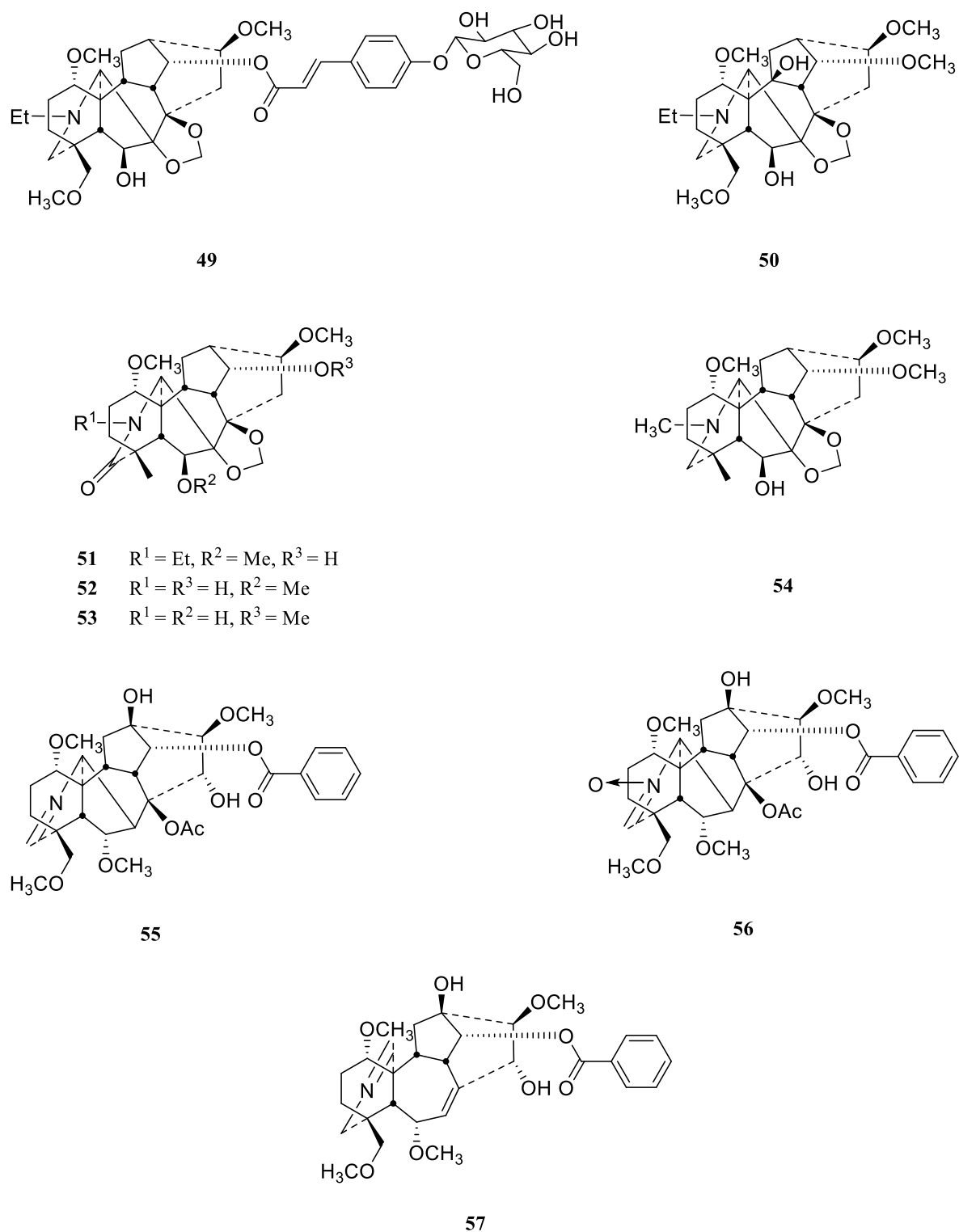


**Figure 6.** NDAs 49-57.

Wang and co-workers discovered three new C19 NDAs, szechenyianine A, B, and C **55–57**, from *A. szechenyianum* [74]. All three compounds were tested against nitric oxide (NO) release inhibition, as they were considered potential anti-inflammatory agents. Szechenyianine A **55**

showed activity with  $IC_{50}$   $36.6 \pm 7 \mu\text{M}$ , while szechenyianine B **56** had  $IC_{50}$   $3.3 \pm 0.1 \mu\text{M}$ , and that highlights the importance of the N-O moiety. Szechenyianine C **57** (Figure 6) which is a 7,17-secoaconitine-type NDA, also showed potent activity, with  $IC_{50}$   $7.5 \pm 0.9 \mu\text{M}$ .

Chao Zhan et al. reported caerulephinine A **58**, a new 1-OH C-19 lycoctonine-type NDA from *D. caeruleum* Jacq. ex Camp [75]. Grandiflorine B **59** was also reported as a new C-19 lycoctonine-type NDA from *D. grandiflorum* [76]. The unusual skeleton of grandiflorine B **59** shows cleavage of the 7–17 bond and N-C19 bond and the formation of an unusual N-C7 bond. Zhao et al. reported three new NDAs, nagaconitine A–C **60–62** from *A. nagarum* var. heterotrichum [77]. Nagaconitine A **60** has a unique acyl group which was reported in only three NDAs. 8,14-Diacetate diester **62** showed antitumor activity against cancer cell line SK-OV-3. Two more new C-19 NDAs, 14-benzoylliljestrandsine **63** and 14-anisoylliljestrandsine **64**, were isolated from *A. tsaii* (Figure 7) [78].

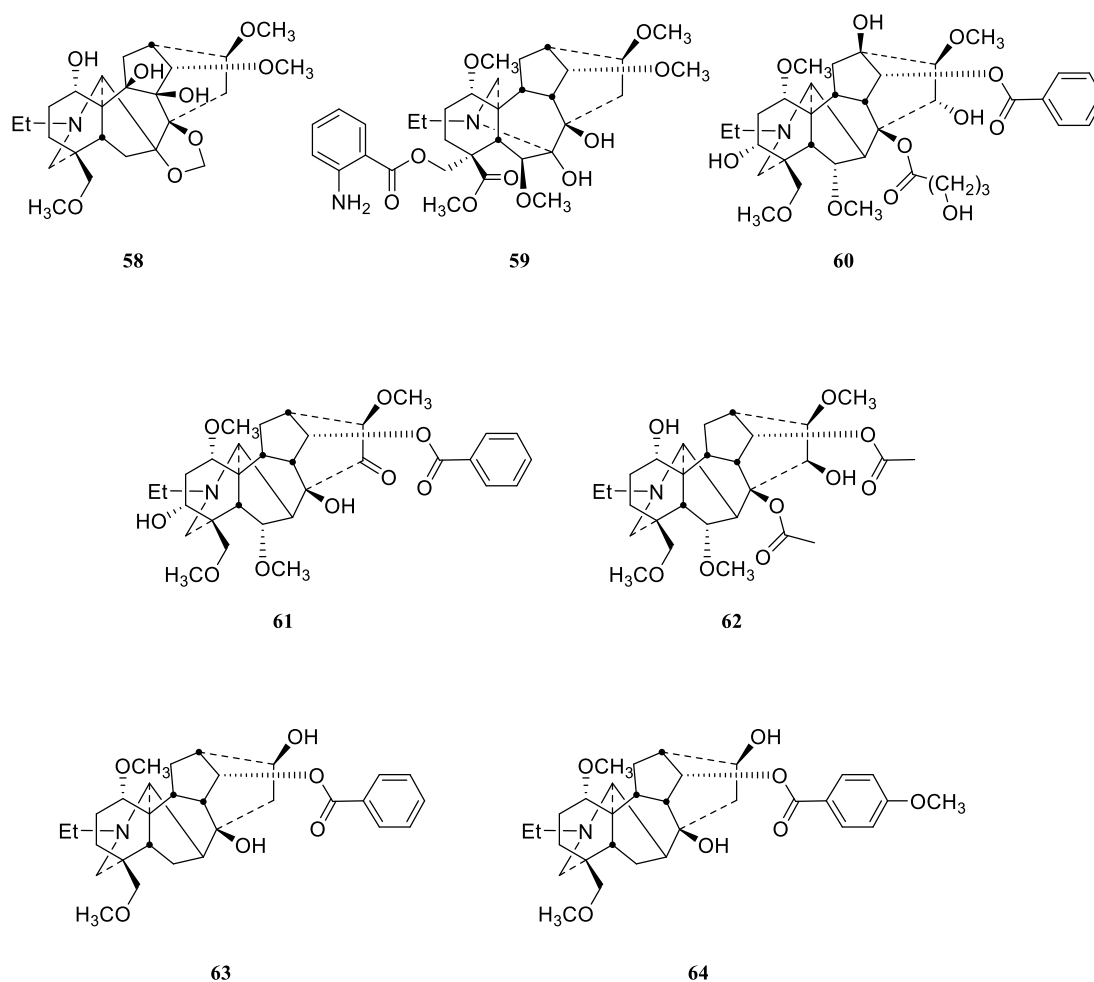


**Figure 7.** NDAs **58-64**.

Extensive phytochemical studies on *D. anthriscifolium* var. majus led to the isolation of six new C-19 NDA with 7,8-methylenedioxy moiety which were named anthrisciflorine A-F **65-70** (Figure 8) [79].

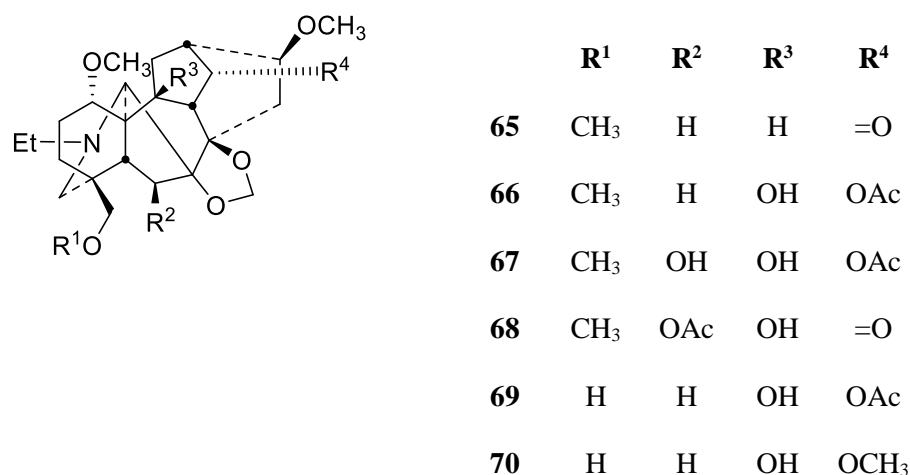


**Figure 8.** NDAs **65-70**.

Guo et al. isolated two new NDAs, 7,8-epoxy-franchetine **71** and *N*-(19)-en-austroconitine A **72**, from *A. iochanicum* [80]. Tested against NO production in macrophages (mouse cell line), they showed weak anti-inflammatory effect. Liang et al. (2017) isolated sinchiangensine A **73** as a new NDA from *A. sinchiangense* W.T. Wang (Figure 9) and it showed significant anti-tumour activity against cancer cell lines A-549, SMCC-7721, MCF-7 and SW-480 [81]. The IC<sub>50</sub> (μM) values of **73** against these cell lines were 12.8, 9.6, 11.8 and 18.8 respectively, and these values were comparable the cisplatin, the positive control, IC<sub>50</sub> (μM) values which were 22.3, 18.6, 28.8 and 18.2. Sinchiangensine A **73** showed also potent anti-bacterial activity against the Gram-positive *S. aureus* ATCC-25923 with MIC value (μmol/mL) 0.15 which is comparable to 0.67, the MIC of the positive control berberine.HCl.

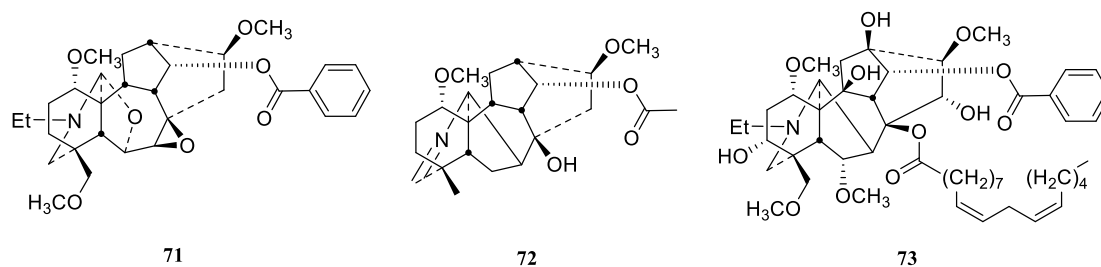


**Figure 9.** NDAs **71-73**.

Ajacisines A-E **74-78** (Figure 10) were isolated as new NDA from *D. ajacis* [82]. They tested the *in vitro* antiviral activity against respiratory syncytial virus (RSV) and the compounds **76-78** showed moderate to weak effect. The IC<sub>50</sub> (μM) of **76-78** against RSV were 75.2 ± 1.1, 35.1 ± 0.6 and 10.1 ± 0.3 while the IC<sub>50</sub> (μM) of ribavirin (the positive control) was 3.1 ± 0.8.

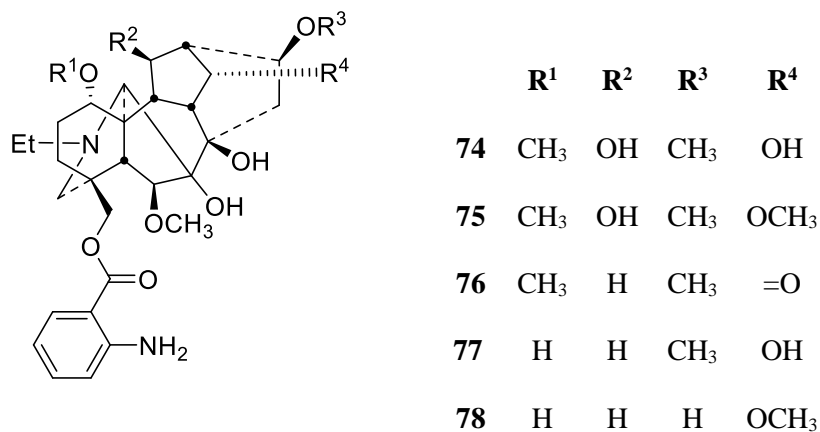


**Figure 10.** NDAs **74-78**.

Meng et al. reported the isolation of four new C-19 NDA, aconicarmichoside A-D **79-82** (Figure 11), from the aqueous extract of fuzi, the lateral roots of *A. carmichaeli* [83]. These four alkaloids are the first examples of glycosidic NDAs where the glycosides are directly attached to the alkaloid skeleton.

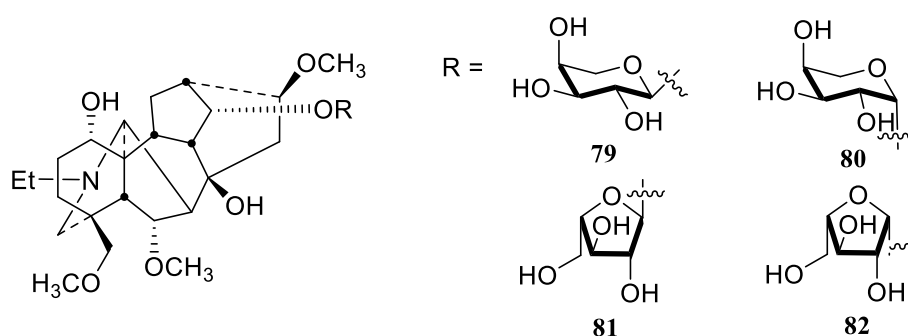


**Figure 11.** Glycosidic NDAs **74-78**.

Fukuyama and co-workers [84] achieved the synthesis of cardiopetaline **83** through Wagner-Meerwein rearrangement of denudatine skeleton into aconitine skeleton without the need of pre-activation of the hydroxy group. This means that there is no need to differentiate the hydroxy groups in the poly-oxygenated system as was needed before. Sarpong and co-workers



[85] developed a unifying strategy to synthesize C-18 NDA (weisaconitine D **84**) and C-19 NDA (liljestrandinine **85**) from a common intermediate. Liu and Qin (2017) [86] highlighted the importance of dearomatization of aromatic compounds that yield *o*-benzoquinones coupled with Diels-Alder cycloaddition in the synthesis of complex structures like **83**, **84**, **85**, and many others. Yang et al. (2017) constructed a unique tricyclo [6.2.1.0] BCD system **86** of the NDA skeleton (Figure 12) [87].

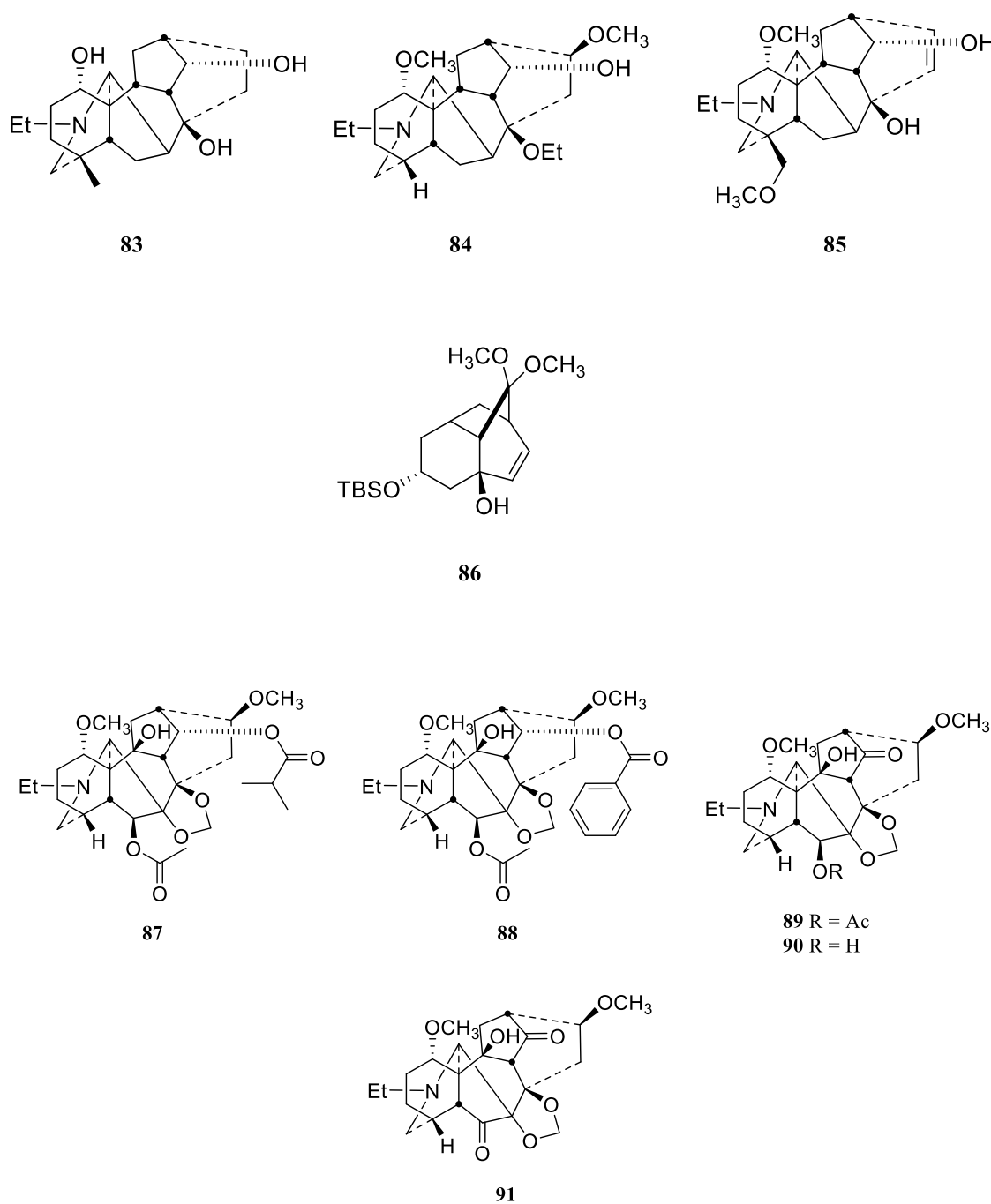


**Figure 12.** NDAs and their construction **83-91**.

Lian et al. reported five new C-18 NDA anthriscifoltines C-G **87-91** from *D. anthriscifolium* var. *majus* (Figure 12) [88]. Song et al. (2018) reported three new C-19 NDA szechenyianine D-F **92-94** from *A. szechenyianum* (Figure 13) [89].

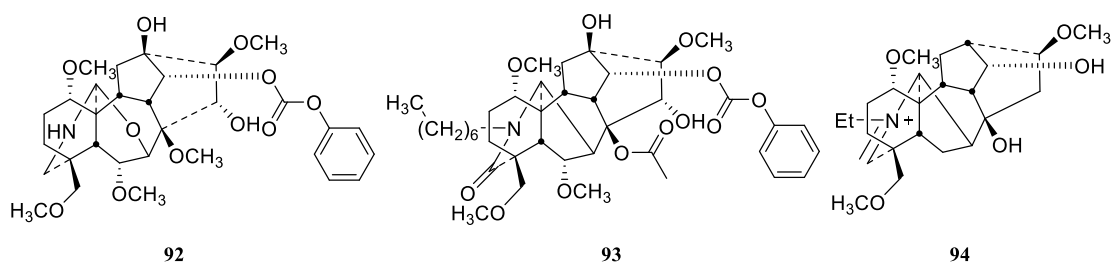


**Figure 13.** NDAs **92-94**.

Another four new C-19 NDA, elapacigine **95**, *N*-deethyl-*N*-formylpaciline **96**, *N*-deethyl-*N*-formylpacinine **97**, and *N*-formyl-4,19-seco-yunnadelphinine **98** (Figure 14), were isolated from *D. elatum* cv. Pacific giant [90].

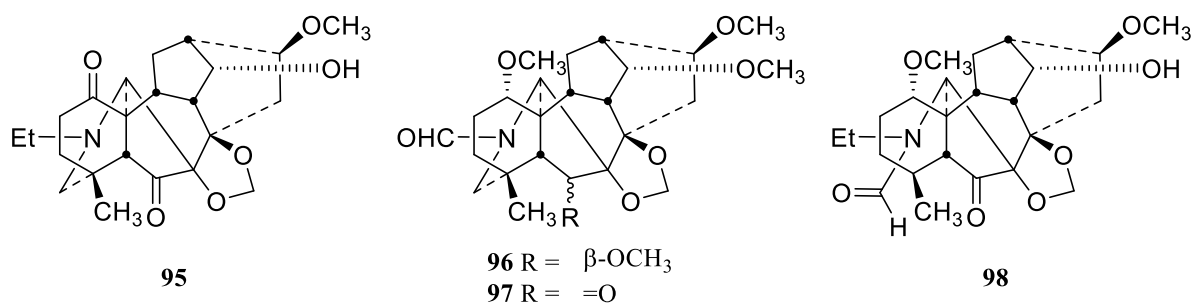


**Figure 14.** NDAs **95-98**.

Yamashita et al. also reported four new C-19 NDA, 14-anisoyllasianine **99**, 14-anisoyl-*N*-deethylaconine **100**, *N*-deethylaljesaconitine A **101**, and *N*-deethylnevadensine **102**, from *A. japonicum* subsp. *subcuneatum* (Nakai) Kadota (Figure 15) [91].

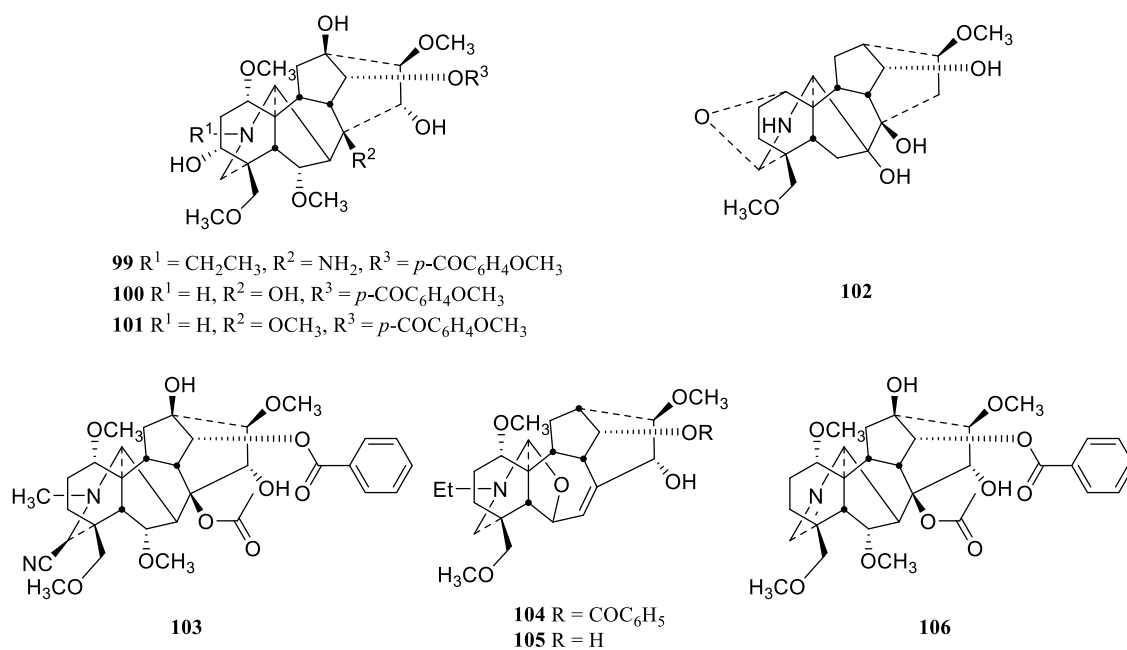


**Figure 15.** NDAs **99-106**.

Li et al. isolated four new C-19 NDA carnichasines A-D **103-106** from *A. carmichaelii* Debeaux (Figure 15) [92]. Extraction of the roots of *Aconitum taronense* Fletcher et Lauener, which has been used in traditional Chinese medicine (TCM) to treat rheumatism and arthritis, yielded 4 new C-19 NDA taronenines A-D **107-110** (Figure 16) [93]; NDA **107**, **108**, and **110** exhibit anti-inflammatory activity when tested in mice cells.

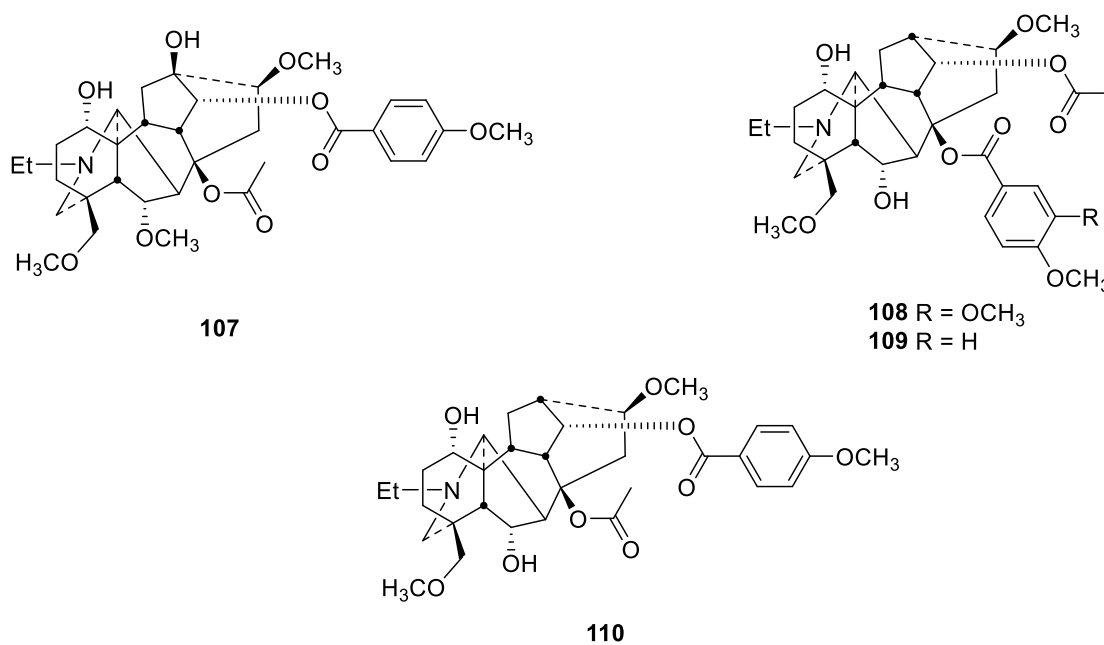


**Figure 16.** NDAs **107-110**.

A study conducted on the *D. pseudoaemulans* C. Y. Yang et B. Wang resulted in the isolation of 8 new C-19 NDA, pseudophnines A–D **111-114**, pseudorenines A–B **115-116**, and pseudonidines A–B **117-118** (Figure 17) [94].

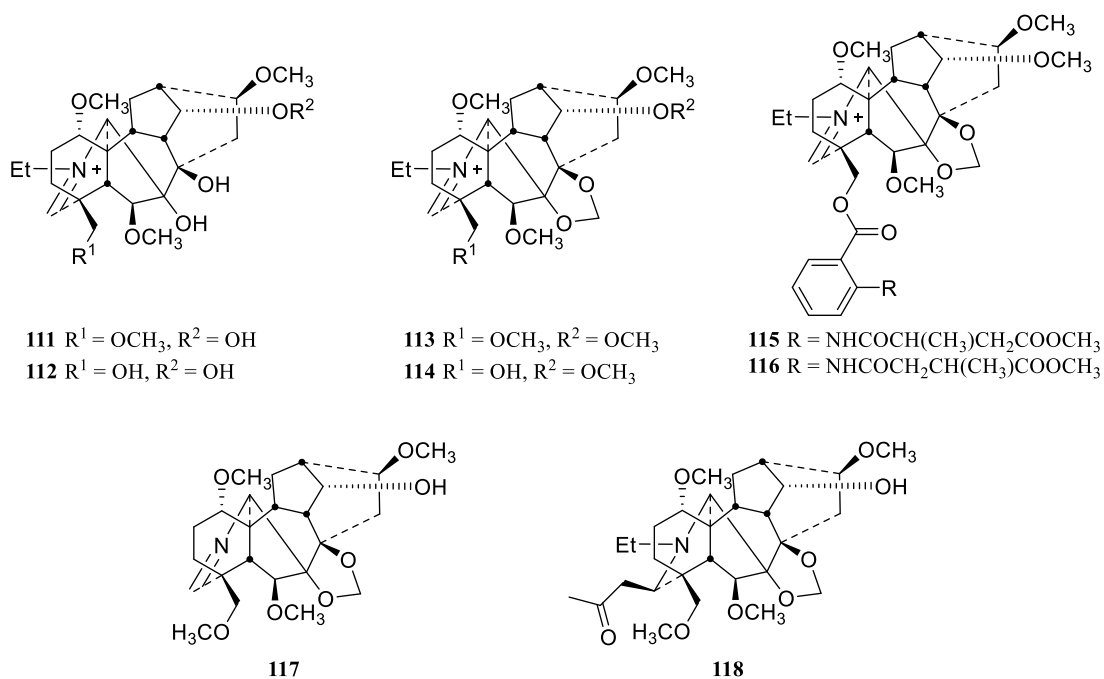


**Figure 17.** NDAs **111-118**.

Ahmad and co-workers reported the isolation of two new C-19 NDAs, jadwarine A–B **119–120** from *D. denudatum* [95]. They also reported a new lycotonine-type C-19 NDA, swatinine C **121** (Figure 18) which showed competitive inhibitory activity on acetylcholinesterase (AChE) and butyrylcholinesterase (BChE) [96].

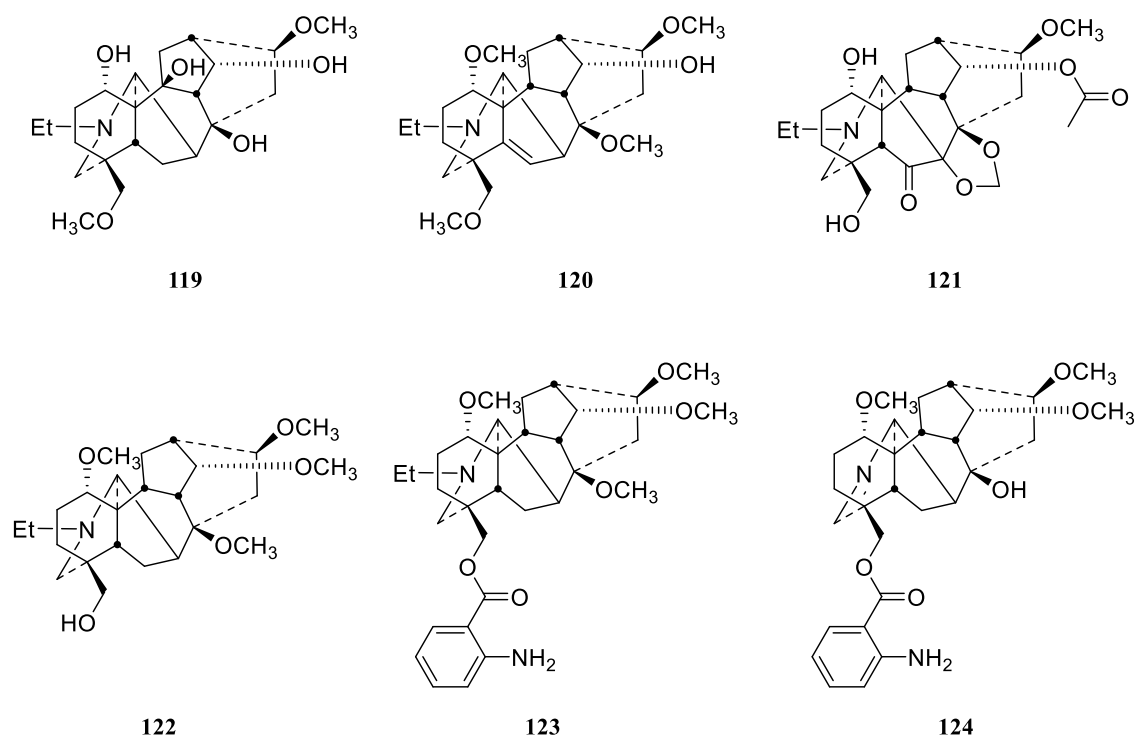


**Figure 18.** NDAs **119-124**.

Extraction of the roots of *A. brevicaratum* led to the isolation of three new C-19 NDAs, brochyponines A–C **122–124** (Figure 18) [97]. Abjalan et al. discovered a new lycoponine-type C-19 NDA, aemulansine **125** from *D. aemulans* Navaski, which showed in vitro cytotoxicity [98]. Two novel 8,15-seco C-19 NDAs, nagarine A **126** and B **127** (Figure 19), were isolated from *A. nagarum* [99].

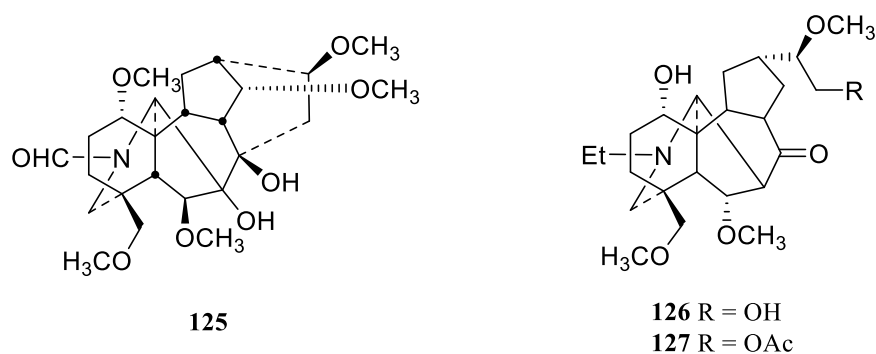


**Figure 19.** NDAs **125-127**.

The variation in pharmacological activities of the NDAs, despite their structural similarities, is an attractive aspect for synthetic chemists to work on to obtain a better understanding of the structure–activity relationships (SAR). Liu et al. reported a total synthesis of the ABCDE system of the C-19 NDAs [100]. Another study reported the construction of the

AEF ring system attached to a phenyl group as an analogue to ring D [101]. The construction of the fused CD-bicycle of aconitine was also achieved [102]. Lv et al. built the hexacyclic ring system of franchetine **128**, a 7,17-seco NDA [103]. The importance of such NDAs continues to attract chemists to attempt to make a total synthesis of them. Progress has been made in the total synthesis of aconitine **12**, but the construction of a pentacyclic system of the aconitine skeleton failed [104]. On the other hand, a total synthesis of talatisamine **129** (Figure 20) has been completed in 33 steps [105]. In addition, the synthesis of a [6-6-6] ABE-tricyclic analogue of MLA **16** has been achieved [106]. A synthetic approach has also been established for the BCD-tricyclic system [107].

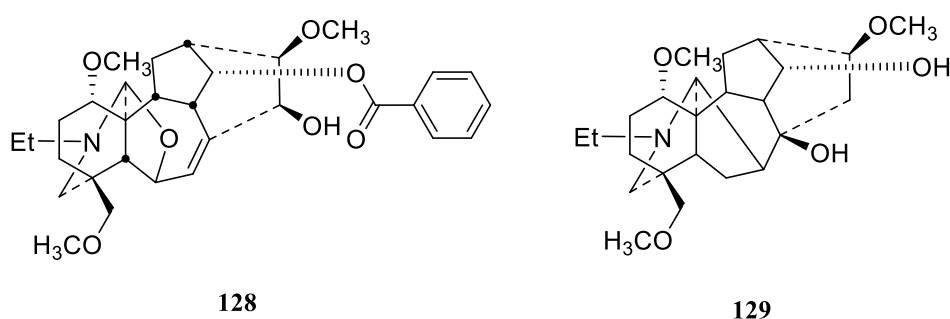


**Figure 20.** NDAs **128** and **129**.

## Conclusions

It is clear that Nature is rich with many examples of plants that can be described as medicinal or poisonous. The poisonous piperidine plants show that dose and mode of pharmacological action are very important. The biodiversity of natural sources of NDA, based upon a substituted piperidine nucleus, are important for continuing to provide leads in drug discovery. NDA from *Aconitum* and *Delphinium* have complex highly oxygenated hexacyclic systems, and as many of them are of pharmacological importance, their structures and 3D configuration are important factors in their actions at various protein targets with respect to medicine and toxicology.

The majority of NDA possess an N-Et group. We have investigated the occurrence count in the SciFinder database for NDA skeletons including in many new NDA. Substitution at position 1 is important to determine the NDA skeleton conformation as ring A in 1-OMe NDA

free bases exists in a twisted-chair conformation. In 1-OH NDA ring A adopts a twisted-boat conformation. In conclusion, screening of NDA for their biological activity has resulted in the discovery of new sets of ligands. These are promising natural compounds that are pharmacologically active, hits potentially eventually becoming selective leads for the treatment of a wide variety of disease states. Where these NDA are new natural products, and if they can be isolated from easy-to-grow *Aconitum* or *Delphinium* plants, then the future is bright for further NDA development based on experimental aspects including phytochemistry leading to SAR studies, and hopefully to new, selective, if not specific, drugs.

## References

1. Vetter, J. Poison hemlock (*Conium maculatum* L.). *Food Chem. Toxicol.* **2004**, *42*, 1373–1382, doi:10.1016/j.fct.2004.04.009.
2. Beers, W.H.; Reich, E. Structure and activity of acetylcholine. *Nature* **1970**, *228*, 917–922, doi:10.1038/228917a0.
3. Schep, L.J.; Slaughter, R.J.; Beasley, D.M.G. Nicotinic plant poisoning. *Clin. Toxicol.* **2009**, *47*, 771–781, doi:10.1080/15563650903252186.
4. Green, B.T.; Lee, S.T.; Welch, K.D.; Panter, K.E. Plant alkaloids that cause developmental defects through the disruption of cholinergic neurotransmission. *Birth Defects Res. Part C - Embryo Today Rev.* **2013**, *99*, 235–246, doi:10.1002/bdrc.21049.
5. Green, B.T.; Welch, K.D.; Panter, K.E.; Lee, S.T. Plant toxins that affect nicotinic acetylcholine receptors: A review. *Chem. Res. Toxicol.* **2013**, *26*, 1129–1138, doi:10.1021/tx400166f.
6. Folquitto, D.G.; Swiech, J.N.D.; Pereira, C.B.; Bobek, V.B.; Halila Possagno, G.C.; Farago, P. V.; Miguel, M.D.; Duarte, J.L.; Miguel, O.G. Biological activity, phytochemistry and traditional uses of genus *Lobelia* (Campanulaceae): A systematic review. *Fitoterapia* **2019**, *134*, 23–38, doi:10.1016/j.fitote.2018.12.021.
7. Felpin, F.-X.; Lebreton, J. History, chemistry and biology of alkaloids from *Lobelia inflata*. *Tetrahedron* **2004**, *60*, 10127–10153, doi:10.1016/j.tet.2004.08.010.

8. Keeler, R.F.; Panter, K.E. Piperidine alkaloid composition and relation to crooked calf disease-inducing potential of *Lupinus formosus*. *Teratology* **1989**, *40*, 423–432, doi:10.1002/tera.1420400503.
9. Green, B.T.; Lee, S.T.; Panter, K.E.; Welch, K.D.; Cook, D.; Pfister, J.A.; Kem, W.R. Actions of piperidine alkaloid teratogens at fetal nicotinic acetylcholine receptors. *Neurotoxicol. Teratol.* **2010**, *32*, 383–390, doi:10.1016/j.ntt.2010.01.011.
10. James, L.F.; Panter, K.E.; Gaffield, W.; Molyneux, R.J. Biomedical applications of poisonous plant research. *J. Agric. Food Chem.* **2004**, *52*, 3211–3230, doi:10.1021/jf0308206.
11. Meghwal, M.; Goswami, T.K. *Piper nigrum* and piperine: An update. *Phytother. Res.* **2013**, *27*, 1121–1130, doi:10.1002/ptr.4972.
12. Smilkov, K.; Ackova, D.G.; Cvetkovski, A.; Ruskovska, T.; Vidovic, B.; Atalay, M. Piperine: Old spice and new nutraceutical? *Curr. Pharm. Des.* **2019**, *25*, 1729–1739, doi:10.2174/1381612825666190701150803.
13. Shityakov, S.; Bigdelian, E.; Hussein, A.A.; Hussain, M.B.; Tripathi, Y.C.; Khan, M.U.; Shariati, M.A. Phytochemical and pharmacological attributes of piperine: A bioactive ingredient of black pepper. *Eur. J. Med. Chem.* **2019**, *176*, 149–161, doi:10.1016/j.ejmech.2019.04.002.
14. Butt, M.S.; Nazir, A.; Sultan, M.T.; Schroën, K. *Morus alba* L. Nature's functional tonic. *Trends Food Sci. Technol.* **2008**, *19*, 505–512, doi:10.1016/j.tifs.2008.06.002.
15. Zhang, W.; Mu, W.; Wu, H.; Liang, Z. An overview of the biological production of 1-deoxynojirimycin: current status and future perspective. *Appl. Microbiol. Biotechnol.* **2019**, *103*, 9335–9344, doi:10.1007/s00253-019-10191-9.
16. Kalant, H. Opium revisited: A brief review of its nature, composition, non-medical use and relative risks. *Addiction* **1997**, *92*, 267–277, doi:10.1111/j.1360-0443.1997.tb03197.x.
17. Frick, S.; Kramell, R.; Schmidt, J.; Fist, A.J.; Kutchan, T.M. Comparative qualitative and quantitative determination of alkaloids in narcotic and condiment *Papaver somniferum* cultivars. *J. Nat. Prod.* **2005**, *68*, 666–673, doi:10.1021/np0496643.



18. Drewes, A.M.; Jensen, R.D.; Nielsen, L.M.; Droney, J.; Christrup, L.L.; Arendt-Nielsen, L.; Riley, J.; Dahan, A. Differences between opioids: Pharmacological, experimental, clinical and economical perspectives. *Br. J. Clin. Pharmacol.* **2013**, *75*, 60–78, doi:10.1111/j.1365-2125.2012.04317.x.
19. Daly, J.W. Nicotinic agonists, antagonists, and modulators from natural sources. *Cell. Mol. Neurobiol.* **2005**, *25*, 513–552, doi:10.1007/s10571-005-3968-4.
20. Keith, L.H.; Pelletier, S.W. The C19-diterpene alkaloids. In *Chemistry of The Alkaloids*; Pelletier, S.W., Ed.; Van Nostrand Reinhold: New York, NY, USA, 1970; pp. 549–590.
21. Dunstan, W.R.; Ince, W.H. Contributions to our knowledge of the aconite alkaloids. Part I. On the crystalline alkaloid of *Aconitum napellus*. *J. Chem. Soc. Trans.* **1891**, *59*, 271–287.
22. Ameri, A. The effects of *Aconitum* alkaloids on the central nervous system. *Prog. Neurobiol.* **1998**, *56*, 211–235, doi:10.1016/S0301-0082(98)00037-9.
23. Wang, F.P.; Chen, Q.H.; Liang, X.T. *Chapter 1. The C18-Diterpenoid Alkaloids*; Elsevier, Amsterdam, The Netherlands, 2009; Vol. 67; ISBN 9780123747853.
24. Sun, W.; Wang, H.; Zhang, S.; Wang, X. Crystal structure of lappaconitine-ium nitrate monohydrate, C<sub>32</sub>H<sub>47</sub>N<sub>3</sub>O<sub>12</sub>. *Zeitschrift fur Krist. - New Cryst. Struct.* **2014**, *229*, 485–487, doi:10.1515/ncrs-2014-0142.
25. Hubschmann, V.F. Ueber *Aconitum lycoctonum* L. *Schweizerische Wochenschrift fur Pharm.* **1865**, *3*, 269–271.
26. Dragendorff, V.G.; Spohn, H. Reviews and bibliographical notices. *Am. J. Pharm.* **1884**, *8*, 44, doi:10.1007/bf02972485.
27. Manske, R.H.F. An alkaloid from *Delphinium brownii* Rydb. . *Can. J. Res.* **1938**, *16b*, 57–60.
28. Goodson, J.A. The alkaloids of the seeds of *Delphinium elatum*, L. *J. Chem. Soc.* **1943**, 139–141.
29. Wonnacott, S.; Albuquerque, E.X.; Bertrand, D. MLA discriminates between nicotinic receptor subclasses. *Methods Neurosci.* **1993**, 263–275.
30. Manners, G.D.; Panter, K.E.; Pelletier, S.W. Structure-activity relationships of

- norditerpenoid alkaloids occurring in toxic larkspur (*Delphinium*) species. *J. Nat. Prod.* **1995**, *58*, 863–869, doi:10.1021/np50120a007.
31. Lakstygai, A.M.; Kolesnikova, T.O.; Khatsko, S.L.; Zabegalov, K.N.; Volgin, A.D.; Demin, K.A.; Shevyrin, V.A.; Wappler-Guzzetta, E.A.; Kalueff, A. V. DARK classics in chemical neuroscience: Atropine, scopolamine, and other anticholinergic deliriant hallucinogens. *ACS Chem. Neurosci.* **2019**, *10*, 2144–2159, doi:10.1021/acchemneuro.8b00615.
  32. Krenzelok, E.P. Aspects of Datura poisoning and treatment. *Clin. Toxicol.* **2010**, *48*, 104–110, doi:10.3109/15563651003630672.
  33. Wang, F.-P.; Chen, Q.-H. The C19-diterpenoid alkaloids. In *The Alkaloids. Chemistry and biology*; Elsevier, Amsterdam, The Netherlands, 2010; *69*, pp. 1–577.
  34. ITIS report: Asteraceae Available online:  
[https://www.itis.gov/servlet/SingleRpt/SingleRpt?search\\_topic=TSN&search\\_value=35420#null](https://www.itis.gov/servlet/SingleRpt/SingleRpt?search_topic=TSN&search_value=35420#null) (accessed on Sep 14, 2022).
  35. ITIS report: Garrya Available online:  
[https://www.itis.gov/servlet/SingleRpt/SingleRpt?search\\_topic=TSN&search\\_value=27826#null](https://www.itis.gov/servlet/SingleRpt/SingleRpt?search_topic=TSN&search_value=27826#null) (accessed on Sep 14, 2022).
  36. ITIS report: Ranunculaceae Available online:  
[https://www.itis.gov/servlet/SingleRpt/SingleRpt?search\\_topic=TSN&search\\_value=18410#null](https://www.itis.gov/servlet/SingleRpt/SingleRpt?search_topic=TSN&search_value=18410#null) (accessed on Sep 14, 2022).
  37. Christenhusz, M.J.M.; Byng, J.W. Phytotaxa. *Phytotaxa* **2016**, *261*, 201–217, doi:10.11646/phytotaxa.261.3.1.
  38. The Plant List: *Delphinium* Available online:  
<http://www.theplantlist.org/browse/A/Ranunculaceae/Delphinium/> (accessed Sep 14, 2022).
  39. The Plant List: *Aconitum* Available online:  
<http://www.theplantlist.org/browse/A/Ranunculaceae/Aconitum/> (accessed Sep 14, 2022).
  40. Hao, D.C.; Xiao, P.G.; Ma, H.Y.; Peng, Y.; He, C.N. Mining chemodiversity from

- biodiversity: Pharmacophylogeny of medicinal plants of Ranunculaceae. *Chin. J. Nat. Med.* **2015**, *13*, 507–520, doi:10.1016/S1875-5364(15)30045-5.
41. ITIS: *Aconitum* Available online:  
[https://www.itis.gov/servlet/SingleRpt/SingleRpt?search\\_topic=TSN&search\\_value=18411#null](https://www.itis.gov/servlet/SingleRpt/SingleRpt?search_topic=TSN&search_value=18411#null) (accessed Sep 14, 2022).
  42. ITIS report: *Delphinium* Available online:  
[https://www.itis.gov/servlet/SingleRpt/SingleRpt?search\\_topic=TSN&search\\_value=18457#null](https://www.itis.gov/servlet/SingleRpt/SingleRpt?search_topic=TSN&search_value=18457#null) (accessed on Sep 14, 2022).
  43. Bisset, N.G. Arrow poisons in China. Part ii. *Aconitum* botany, chemistry, and pharmacology. *J. Ethnopharmacol.* **1981**, *4*, 247–336, doi:10.1016/0378-8741(81)90001-5.
  44. Blanché, C. *Delphinium* L. Subgen. *Delphinium*: origin and evolutionary trends. *Collect. Bot.* **1990**, *19*, 75–96, doi:10.3989/collectbot.1990.v19.118.
  45. Kuder, R.C. Larkspurs, delphiniums, and chemistry. *J. Chem. Educ.* **1947**, *24*, 418–422, doi:10.1021/ed024p418.
  46. Trifonova, V.I. Comparative biomorphological study of the taxonomy and phylogeny of the genera *Consolida* (DC.) S.F. Gray and *Aconitella* spach. *Collect. Botánica* **1990**, *19*, 97–110.
  47. Jabbour, F.; Renner, S.S. A phylogeny of *Delphinieae* (Ranunculaceae) shows that *Aconitum* is nested within *Delphinium* and that Late Miocene transitions to long life cycles in the Himalayas and Southwest China coincide with bursts in diversification. *Mol. Phylogenet. Evol.* **2012**, *62*, 928–942, doi:10.1016/j.ympev.2011.12.005.
  48. Legro, R.A.H. Species hybrids in *Delphinium*. *Euphytica* **1961**, *10*, 1–23, doi:10.1007/BF00037200.
  49. Lawrence, W.J.C. The origin of new forms in *Delphinium*. *Genetica* **1936**, *18*, 109–115.
  50. Dalla Guda, C.; Cervelli, C.; Farina, C. Effects of lighting regimes on flowering of *Delphinium* hybrids “Pacific Giants.” *XXV Int. Hortic. Congr. Part 5 Cult. Tech. with Spec. Emphas. Environ. Implic.* 1998, *515*, 173–178. Publisher: International Society for Horticultural Science, Leuven, Belgium.

51. Nielsen, D.B.; Ralphps, M.H.; Evans, J.O.; Call, C.A. Economic feasibility of controlling tall Larkspur on rangelands. *Rangel. Ecol. Manag. Range Manag. Arch.* **1994**, *47*, 369–372.
52. Panter, K.E.; Manners, G.D.; Stegelmeier, B.L.; Lee, S.; Gardner, D.R.; Ralphps, M.H.; Pfister, J.A.; James, L.F. Larkspur poisoning: Toxicology and alkaloid structure-activity relationships. *Biochem. Syst. Ecol.* **2002**, *30*, 113–128, doi:10.1016/S0305-1978(01)00123-5.
53. Cook, D.; Gardner, D.R.; Lee, S.T.; Stonecipher, C.A.; Pfister, J.A.; Welch, K.D.; Green, B.T. Two *Delphinium ramosum* chemotypes, their biogeographical distribution and potential toxicity. *Biochem. Syst. Ecol.* **2017**, *75*, 1–9, doi:10.1016/j.bse.2017.09.002.
54. Manners, G.D.; Panter, K.E.; Ralphps, M.H.; Pfister, J.A.; Olsen, J.D.; James, L.F. Toxicity and chemical phenology of norditerpenoid alkaloids in the Tall Larkspurs (*Delphinium* species). *J. Agric. Food Chem.* **1993**, *41*, 96–100, doi:10.1021/jf00025a020.
55. Dobelis, P.; Madl, J.E.; Pfister, J.A.; Manners, G.D.; Walrond, J.P. Effects of *Delphinium* alkaloids on neuromuscular transmission. *J. Pharmacol. Exp. Ther.* **1999**, *291*, 538–546.
56. Green, B.T.; Keele, J.W.; Gardner, D.R.; Welch, K.D.; Bennett, G.L.; Cook, D.; Pfister, J.A.; Davis, T.Z.; Stonecipher, C.A.; Lee, S.T.; et al. Sex-dependent differences for larkspur (*Delphinium barbeyi*) toxicosis in yearling Angus cattle. *J. Anim. Sci.* **2019**, *97*, 1424–1432, doi:10.1093/jas/skz002.
57. Green, B.T.; Keele, J.W.; Bennett, G.L.; Gardner, D.R.; Stonecipher, C.A.; Cook, D.; Pfister, J.A. Animal and plant factors which affect larkspur toxicosis in cattle: Sex, age, breed, and plant chemotype. *Toxicon* **2019**, *165*, 31–39, doi:10.1016/j.toxicon.2019.04.013.
58. Welch, K.D.; Green, B.T.; Gardner, D.R.; Cook, D.; Pfister, J.A.; Panter, K.E. The effect of 7, 8-methylenedioxylycoctonine-type diterpenoid alkaloids on the toxicity of tall larkspur (*Delphinium* spp.) in cattle. *J. Anim. Sci.* **2012**, *90*, 2394–2401,

doi:10.2527/jas.2011-4560.

59. Qasem, A.M.A.; Zeng, Z.; Rowan, M.G.; Blagbrough, I.S. Norditerpenoid alkaloids from *Aconitum* and *Delphinium*: structural relevance in medicine, toxicology, and metabolism. *Nat. Prod. Rep.* **2022**, *39*, 460-473. doi:10.1039/d1np00029b.
60. Zeng, Z.; Qasem, A.M.A.; Kociok-Köhn, G.; Rowan, M.G.; Blagbrough, I.S. The 1 $\alpha$ -hydroxy-A-rings of norditerpenoid alkaloids are twisted-boat conformers. *RSC Adv.* **2020**, *10*, 18797–18805. doi:10.1039/D0RA03811C.
61. Zeng, Z.; Qasem, A.M.A.; Woodman, T.J.; Rowan, M.G.; Blagbrough, I.S. Impacts of steric compression, protonation, and intramolecular hydrogen bonding on the 15N NMR spectroscopy of norditerpenoid alkaloids and their piperidine-ring analogues. *ACS Omega* **2020**, *5*, 14116–14122, doi:10.1021/acsomega.0c01648.
62. Chen, L.; Shan, L.; Zhang, J.; Xu, W.; Wu, M.; Huang, S.; Zhou, X. Diterpenoid alkaloids from *Aconitum soongaricum* var. *pubescens*. *Nat. Prod. Commun.* **2015**, *10*, 2063–2065, doi:10.1177/1934578x1501001212.
63. Yin, T.P.; Cai, L.; Fang, H.X.; Fang, Y.S.; Li, Z.J.; Ding, Z.T. Diterpenoid alkaloids from *Aconitum vilmorinianum*. *Phytochemistry* **2015**, *116*, 314–319, doi:10.1016/j.phytochem.2015.05.002.
64. Qin, X.; Yang, S.; Zhao, Y.; Gao, Y.; Ren, F.; Zhang, D.; Wang, F. Five new C19-diterpenoid alkaloids from *Aconitum carmichaeli*. *Phytochem. Lett.* **2015**, *13*, 390–393, doi:10.1016/j.phytol.2015.07.017.
65. Zhao, Q.; Gou, X.J.; Liu, W.; He, G.; Liang, L.; Chen, F.Z. Majusine D: A new C19-diterpenoid alkaloid from *Delphinium majus*. *Nat. Prod. Commun.* **2015**, *10*, 2069–2070, doi:10.1177/1934578x1501001214.
66. Yin, T.P.; Cai, L.; Li, Y.; Fang, Y.S.; Peng, L.; Ding, Z.T. New alkaloids from *Aconitum stapfianum*. *Nat. Products Bioprospect.* **2015**, *5*, 271–275, doi:10.1007/s13659-015-0075-1.
67. Zhao, B.; Usmanova, S.K.; Yili, A.; Kawuli, A.; Abdulla, R.; Aisa, H.A. New C19-norditerpenoid alkaloid from *Delphinium shawurensense*. *Chem. Nat. Compd.* **2015**, *51*, 519–522, doi:10.1007/s10600-015-1328-2.

68. Chen, C.L.; Tan, W.H.; Wang, Y.; Xue, Z.G.; Wan, C.P.; Yang, Z.Y.; Zhou, Z.H.; Ma, X.X. New norditerpenoid alkaloids from *Aconitum vilmorinianum* Komarov. *J. Nat. Med.* **2015**, *69*, 601–607, doi:10.1007/s11418-015-0926-4.
69. Wada, K.; Chiba, R.; Kanazawa, R.; Matsuoka, K.; Suzuki, M.; Ikuta, M.; Goto, M.; Yamashita, H.; Lee, K.H. Six new norditerpenoid alkaloids from *Delphinium elatum*. *Phytochem. Lett.* **2015**, *12*, 79–83, doi:10.1016/j.phytol.2015.02.010.
70. Shan, L.; Zhang, J.; Chen, L.; Wang, J.; Huang, S.; Zhou, X. Two new C18-diterpenoid alkaloids from *Delphinium anthriscifolium*. *Nat. Prod. Commun.* **2015**, *10*, 2067–2068, doi:10.1177/1934578x1501001213.
71. Cai, L.; Fang, H.X.; Yin, T.P.; Yu, J.; Li, Z.J.; Dong, J.W.; Ding, Z.T. Unusual C19-diterpenoid alkaloids from *Aconitum vilmorinianum* var. *patentipilum*. *Phytochem. Lett.* **2015**, *14*, 106–110, doi:10.1016/j.phytol.2015.09.010.
72. Zhang, J. Fa; Dai, R. Yang; Shan, L. Hai; Chen, L.; Xu, L.; Wu, M. Yu; Wang, C. Juan; Huang, S.; Zhou, X. Li Iliensines A and B: Two new C19-diterpenoid alkaloids from *Delphinium iliense*. *Phytochem. Lett.* **2016**, *17*, 299–303, doi:10.1016/j.phytol.2016.08.014.
73. Wada, K.; Asakawa, E.; Tosho, Y.; Nakata, A.; Hasegawa, Y.; Kaneda, K.; Goto, M.; Yamashita, H.; Lee, K.H. Four new diterpenoid alkaloids from *Delphinium elatum*. *Phytochem. Lett.* **2016**, *17*, 190–193, doi:10.1016/j.phytol.2016.06.009.
74. Wang, F.; Yue, Z.; Xie, P.; Zhang, L.; Li, Z.; Song, B.; Tang, Z.; Song, X. C19-norditerpenoid alkaloids from *Aconitum szechenyianum* and their effects on LPS-activated NO production. *Molecules* **2016**, *21*, 4–11, doi:10.3390/molecules21091175.
75. Lin, C.Z.; Liu, Z.J.; Bairi, Z.D.; Zhu, C.C. A new diterpenoid alkaloid isolated from *Delphinium caeruleum*. *Chin. J. Nat. Med.* **2017**, *15*, 45–48, doi:10.1016/S1875-5364(17)30007-9.
76. Chen, N.H.; Zhang, Y.B.; Li, W.; Li, P.; Chen, L.F.; Li, Y.L.; Li, G.Q.; Wang, G.C. Grandiflodines A and B, two novel diterpenoid alkaloids from *Delphinium grandiflorum*. *RSC Adv.* **2017**, *7*, 24129–24132, doi:10.1039/c7ra02869e.
77. Zhao, D.K.; Shi, X.Q.; Zhang, L.M.; Yang, D.Q.; Guo, H.C.; Chen, Y.P.; Shen, Y. Four

- new diterpenoid alkaloids with antitumor effect from *Aconitum nagarum* var. heterotrichum. *Chinese Chem. Lett.* **2017**, *28*, 358–361, doi:10.1016/j.ccllet.2016.09.012.
78. Li, G.Q.; Zhang, L.M.; Zhao, D.K.; Chen, Y.P.; Shen, Y. Two new C19-diterpenoid alkaloids from *Aconitum tsaii*. *J. Asian Nat. Prod. Res.* **2017**, *19*, 457–461, doi:10.1080/10286020.2016.1234457.
79. Shan, L.H.; Zhang, J.F.; Gao, F.; Huang, S.; Zhou, X.L. Diterpenoid alkaloids from *Delphinium anthriscifolium* var. majus. *Sci. Rep.* **2017**, *7*, 6063. doi:10.1038/s41598-017-05372-3.
80. Guo, R.; Guo, C.; He, D.; Zhao, D.; Shen, Y. Two new C19-diterpenoid alkaloids with anti-inflammatory activity from *Aconitum iochanicum*. *Chinese J. Chem.* **2017**, *35*, 1644–1647, doi:10.1002/cjoc.201700401.
81. Liang, X.; Chen, L.; Song, L.; Fei, W.; He, M.; He, C.; Yin, Z. Diterpenoid alkaloids from the root of *Aconitum sinchiangense* W. T. Wang with their antitumor and antibacterial activities. *Nat. Prod. Res.* **2017**, *31*, 2016–2023, doi:10.1080/14786419.2016.1272113.
82. Yang, L.; Zhang, Y.B.; Zhuang, L.; Li, T.; Chen, N.H.; Wu, Z.N.; Li, P.; Li, Y.L.; Wang, G.C. Diterpenoid alkaloids from *Delphinium ajacis* and their anti-RSV activities. *Planta Med.* **2017**, *83*, 111–116, doi:10.1055/s-0042-107252.
83. Meng, X.H.; Guo, Q.L.; Zhu, C.G.; Shi, J.G. Unprecedented C19-diterpenoid alkaloid glycosides from an aqueous extract of “fu zi”: Neoline 14-O-L-arabinosides with four isomeric L-anabinosyls. *Chinese Chem. Lett.* **2017**, *28*, 1705–1710, doi:10.1016/j.ccllet.2017.04.026.
84. Nishiyama, Y.; Yokoshima, S.; Fukuyama, T. Synthesis of cardiopetaline via a Wagner–Meerwein rearrangement without preactivation of the pivotal hydroxy group. *Org. Lett.* **2017**, *19*, 5833–5835, doi:10.1021/acs.orglett.7b02812.
85. Kou, K.G.M.; Kulyk, S.; Marth, C.J.; Lee, J.C.; Doering, N.A.; Li, B.X.; Gallego, G.M.; Lebold, T.P.; Sarpong, R. A unifying synthesis approach to the C18-, C19-, and C20-diterpenoid alkaloids. *J. Am. Chem. Soc.* **2017**, *139*, 13882–13896, doi:10.1021/jacs.7b07706.

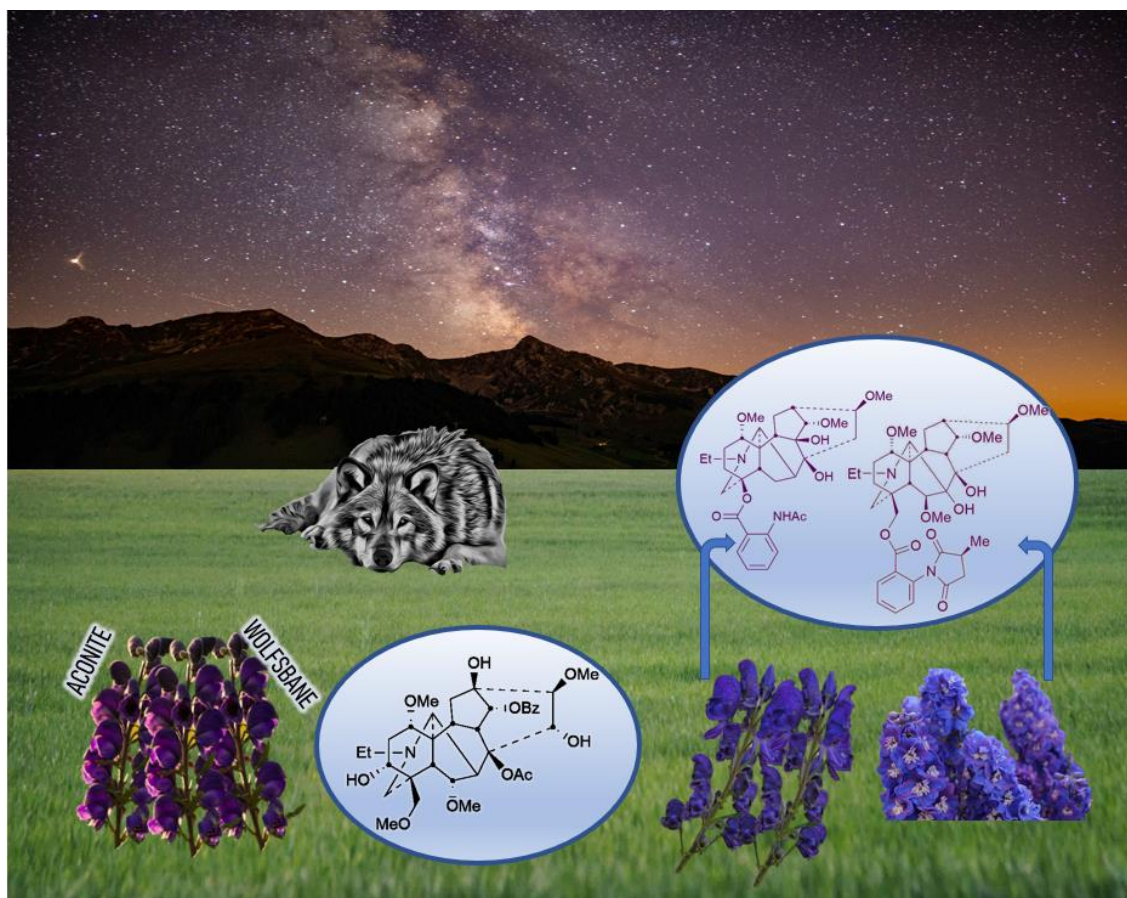
86. Liu, X.-Y.; Qin, Y. Enabling syntheses of diterpenoid alkaloids and related diterpenes by an oxidative dearomatization/Diels-Alder cycloaddition strategy. *Nat. Prod. Rep.* **2017**, *34*, 1044–1050, doi:10.1039/c7np00033b.
87. Yang, X.; Cheng, B.; Cheng, H.; Xu, L.; Wang, J.L. Rapid construction of the unique BCD ring system of tricyclo[6.2.1.0]undecane in the C19-diterpenoid alkaloid aconitine. *Chinese Chem. Lett.* **2017**, *28*, 1788–1792, doi:10.1016/j.ccllet.2017.03.032.
88. Shan, L.H.; Zhang, J.F.; Gao, F.; Huang, S.; Zhou, X.L. C18-Diterpenoid alkaloids from *Delphinium anthriscifolium* var. *majus*. *J. Asian Nat. Prod. Res.* **2018**, *20*, 423–430, doi:10.1080/10286020.2017.1335309.
89. Song, B.; Jin, B.; Li, Y.; Wang, F.; Yang, Y.; Cui, Y.; Song, X.; Yue, Z.; Liu, J. C19-Norditerpenoid alkaloids from *Aconitum szechenyianum*. *Molecules* **2018**, *23*, 1108. doi:10.3390/molecules23051108.
90. Yamashita, H.; Katoh, M.; Kokubun, A.; Uchimura, A.; Mikami, S.; Takeuchi, A.; Kaneda, K.; Suzuki, Y.; Mizukami, M.; Goto, M.; et al. Four new C19-diterpenoid alkaloids from *Delphinium elatum*. *Phytochem. Lett.* **2018**, *24*, 6–9, doi:10.1016/j.phytol.2017.12.013.
91. Yamashita, H.; Takeda, K.; Haraguchi, M.; Abe, Y.; Kuwahara, N.; Suzuki, S.; Terui, A.; Masaka, T.; Munakata, N.; Uchida, M.; et al. Four new diterpenoid alkaloids from *Aconitum japonicum* subsp. *subcuneatum*. *J. Nat. Med.* **2018**, *72*, 230–237, doi:10.1007/s11418-017-1139-9.
92. Li, Y.; Gao, F.; Zhang, J.F.; Zhou, X.L. Four new diterpenoid alkaloids from the roots of *Aconitum carmichaelii*. *Chem. Biodivers.* **2018**, *15*, 1–8, doi:10.1002/cbdv.201800147.
93. Yin, T.; Hu, X.; Mei, R.; Shu, Y.; Gan, D.; Cai, L.; Ding, Z. Four new diterpenoid alkaloids with anti-inflammatory activities from *Aconitum taronense* Fletcher et Lauener. *Phytochem. Lett.* **2018**, *25*, 152–155, doi:10.1016/j.phytol.2018.04.001.
94. Xue, W.J.; Zhao, B.; Ruzi, Z.; Zhao, J.Y.; Aisa, H.A. Norditerpenoid alkaloids from *Delphinium pseudoaemulans* C. Y. Yang et B. Wang. *Phytochemistry* **2018**, *156*, 234–240, doi:10.1016/j.phytochem.2018.09.010.
95. Ahmad, H.; Ahmad, S.; Ali, M.; Latif, A.; Shah, S.A.A.; Naz, H.; ur Rahman, N.;



- Shaheen, F.; Wadood, A.; Khan, H.U.; Ahmad, M. Norditerpenoid alkaloids of *Delphinium denudatum* as cholinesterase inhibitors. *Bioorg. Chem.* **2018**, *78*, 427–435, doi:10.1016/j.bioorg.2018.04.008.
96. Ahmad, H.; Ahmad, S.; Shah, S.A.A.; Khan, H.U.; Khan, F.A.; Ali, M.; Latif, A.; Shaheen, F.; Ahmad, M. Selective dual cholinesterase inhibitors from *Aconitum laeve*. *J. Asian Nat. Prod. Res.* **2018**, *20*, 172–181, doi:10.1080/10286020.2017.1319820.
97. Shu, Y.; Yin, T.P.; Wang, J.P.; Gan, D.; Zhang, Q.Y.; Cai, L.; Ding, Z.T. Three new diterpenoid alkaloids isolated from *Aconitum brevicaratum*. *Chin. J. Nat. Med.* **2018**, *16*, 866–870, doi:10.1016/S1875-5364(18)30128-6.
98. Ablajan, N.; Zhao, B.; Zhao, J.Y.; Kodirova, D.R.; Sagdullaev, S.S.; Aisa, H.A. Alkaloids from *Delphinium aemulans*. *Chem. Nat. Compd.* **2020**, *56*, 836–839, doi:10.1007/s10600-020-03207-8.
99. Yin, T.; Shu, Y.; Zhou, H.; Cai, L.; Ding, Z. Nagarines A and B, two novel 8,15-seco diterpenoid alkaloids from *Aconitum nagarum*. *Fitoterapia* **2019**, *135*, 1–4, doi:10.1016/j.fitote.2019.03.021.
100. Liu, M.; Cheng, C.; Xiong, W.; Cheng, H.; Wang, J.L.; Xu, L. Total synthesis of C19-diterpenoid alkaloid: Construction of a functionalized ABCDE-ring system. *Org. Chem. Front.* **2018**, *5*, 1502–1505, doi:10.1039/c8qo00143j.
101. Doering, N.A.; Kou, K.G.M.; Norseeda, K.; Lee, J.C.; Marth, C.J.; Gallego, G.M.; Sarpong, R. A copper-mediated conjugate addition approach to analogues of aconitine-type diterpenoid alkaloids. *J. Org. Chem.* **2018**, *83*, 12911–12920, doi:10.1021/acs.joc.8b01967.
102. Zhou, X.H.; Liu, Y.; Zhou, R.J.; Song, H.; Liu, X.Y.; Qin, Y. Construction of the highly oxidized bicyclo[3.2.1]octane CD ring system of aconitine via a late stage enyne cycloisomerization. *Chem. Commun.* **2018**, *54*, 12258–12261, doi:10.1039/C8CC06819D.
103. Lv, Z.; Gao, L.; Cheng, C.; Niu, W.; Wang, J.L.; Xu, L. Expedient construction of the hexacycle of franchetine. *Chem. An Asian J.* **2018**, *13*, 955–958, doi:10.1002/asia.201800116.

104. Zhou, R.J.; Dai, G.Y.; Zhou, X.H.; Zhang, M.J.; Wu, P.Z.; Zhang, D.; Song, H.; Liu, X.Y.; Qin, Y. Progress towards the synthesis of aconitine: Construction of the AE fragment and attempts to access the pentacyclic core. *Org. Chem. Front.* **2019**, *6*, 377–382, doi:10.1039/c8qo01228h.
105. Kamakura, D.; Todoroki, H.; Urabe, D.; Hagiwara, K.; Inoue, M. Total synthesis of talatisamine. *Angew. Chemie - Int. Ed.* **2020**, *59*, 479–486, doi:10.1002/anie.201912737.
106. Xiao, D.; Zhao, X.; Lei, J.; Zhu, M.; Xu, L. Synthesis of [6-6-6] ABE tricyclic ring analogues of methyllycaconitine. *Chinese Chem. Lett.* **2021**, *32*, 3031–3033, doi:10.1016/j.ccllet.2021.03.068.
107. Cao, S.Y.; Yue, H.J.; Zhu, M.Q.; Xu, L. Synthesis of tricyclo[7.2.1.09,10]dodecan-11-one core ring systems of norditerpenoid alkaloids and racemulosine. *Org. Chem. Front.* **2020**, *7*, 933–937, doi:10.1039/d0qo00088d.

Selected image as a front cover photo by RSC Natural Products Reports



Qasem, A. M. A., Zeng, Z., Rowan, M.G., Blagbrough, I.S., 2022. Norditerpenoid alkaloids from *Aconitum* and *Delphinium* : structural relevance in medicine, toxicology, and metabolism, *Nat. Prod. Rep.*, **39**, 460-473.

## HIGHLIGHT

### **Norditerpenoid alkaloids from *Aconitum* and *Delphinium*: Structural relevance in medicine, toxicology, and metabolism**

#### Highlight contents

1. Introduction to norditerpenoid alkaloids (NDA)
2. Missing links in NDA biosynthesis
3. Medicinal applications of *Aconitum* and *Delphinium* in current TCM
4. NDA in current medicine and their structure-activity relationship (SAR) studies
  - 4.1 Aconitine type
  - 4.2 Lappaconitine type
  - 4.3 Lycoctonine type
  - 4.4 *Delphinium* (larkspur) toxicity
5. Metabolism of NDA
  - 5.1 Cell-free systems – microsomal studies
  - 5.2 Animal studies
  - 5.3 Human studies
  - 5.4 Metabolic effects on biological activity
6. Analysis of NDA
7. Conclusions and future prospects
8. References

**Aims:** Norditerpenoid alkaloids (NDA), typically *N*-ethylpiperidine containing C19 or C18 natural product diterpenes, are hexacycles with several contiguous often oxygenated stereocentres. As a function of their structural complexity, they display important pharmacological activities. The processed plants are used as important folk drugs and four NDAs have now been clinically approved. Many metabolism studies on *Aconitum* alkaloids have been reported as the understanding of their biotransformation in living systems and in cell-free systems is important for the development of these alkaloids as drugs. This Highlight sets out the missing links in NDA biosynthesis, their biological applications, SAR, toxicity, metabolism, and analytical studies.

<b>This declaration concerns the article entitled:</b>			
Norditerpenoid alkaloids from <i>Aconitum</i> and <i>Delphinium</i> : structural relevance in medicine, toxicology, and metabolism			
<b>Publication status (tick one)</b>			
<b>Draft manuscript</b>	<input type="checkbox"/>	<b>Submitted</b>	<input type="checkbox"/>
		<b>In review</b>	<input type="checkbox"/>
		<b>Accepted</b>	<input type="checkbox"/>
		<b>Published</b>	<input checked="" type="checkbox"/>
<b>Publication details (reference)</b>	Qasem, A. M. A., Zeng, Z., Rowan, M.G., Blagbrough, I.S., 2022. Norditerpenoid alkaloids from <i>Aconitum</i> and <i>Delphinium</i> : structural relevance in medicine, toxicology, and metabolism, <i>Nat. Prod. Rep.</i> , 39, 460-473.		
<b>Copyright status (tick the appropriate statement)</b>			
The material has been published with a CC-BY license		<input checked="" type="checkbox"/>	The publisher has granted permission to replicate the material included here
<b>Candidate's contribution to the paper (provide details, and also indicate as a percentage)</b>		<p><b>Formulation of ideas:</b> The candidate considerably contributed to the formulation of the article ideas to cover SAR of norditerpenoid alkaloids, toxicology, and metabolism (60%)</p> <p><b>Design of methodology:</b> Critical review of the recent literature (50%).</p> <p><b>Experimental work:</b> The candidate considerably contributed to the experimental work using Web of science and SciFinder databases (60%).</p> <p><b>Presentation of data in journal format:</b> The candidate considerably contributed to the data presentation through writing, referencing, and preparing the article figures (70%).</p>	
<b>Statement from Candidate</b>	This paper reports on original research I conducted during the period of my Higher Degree by Research candidature.		
<b>Signed (typed signature)</b>	Ashraf Qasem	<b>Date</b>	21/09/2022

## 1. Introduction to norditerpenoid alkaloids (NDA)

The majority of norditerpenoid alkaloids (NDA, C<sub>18</sub>- or C<sub>19</sub>-diterpenoid alkaloids) are isolated from the genera *Aconitum* and *Delphinium* (larkspur), *Consolida*, and *Spirea*,<sup>1</sup> and the whole plants are lethal, e.g., *Delphinium* has been extensively reported as responsible for poisoning livestock in North America leading to financial losses.<sup>2</sup> NDA display important pharmacological activities. Especially, they have been used as insecticides for two thousand years. At the time of the eruption of Mount Vesuvius covering Pompeii and Herculaneum, Pliny

the Elder reported: *Delphinium* seeds, pounded and extracted into wine (ethanol), rid the head and body of lice.<sup>3</sup> *Delphinium* seeds were even reportedly issued to British soldiers at the battle of Waterloo (still for the treatment of body lice).<sup>4</sup> Therefore, if the NDA dose is appropriately adjusted, it is of no surprise that they have been known to be widely used as folk medicines, not least earning the trivial (?) name Wolf's bane, but perhaps more accurate is the descriptive name Monkshood. They are deadly poisons to mammals, even on simple handling if the skin is broken, e.g., if it has been scratched.

NDA have a complex highly oxygenated hexacyclic structure (Fig. 1A),<sup>5,6</sup> A/B/C/D/E/F rings are 6/7/5/6/6/5-membered rings respectively. The substituent at position 14 is commonly drawn going under the C15-C16 C-C bond, but our single-crystal X-ray diffraction (SXR) data show that in reality it lies above that bond (Fig. 1C), although it is in the  $\alpha$ -orientation.<sup>5</sup> Also, the C7 substituent in the lycoctonine-type NDA is usually assigned in the  $\beta$ -orientation while the SXR shows that it cannot be axially  $\beta$ -orientated like C6 and C8 substituents, but it is equatorial  $\beta$ -orientated and it is better to draw it in the plane of the paper (Fig. 1).<sup>5</sup> This attention to molecular detail is important when considering the drug-like physical and chemical properties of such molecules and their binding modes at their target receptors and ion channels as conformation is an important determinant of biological activity.

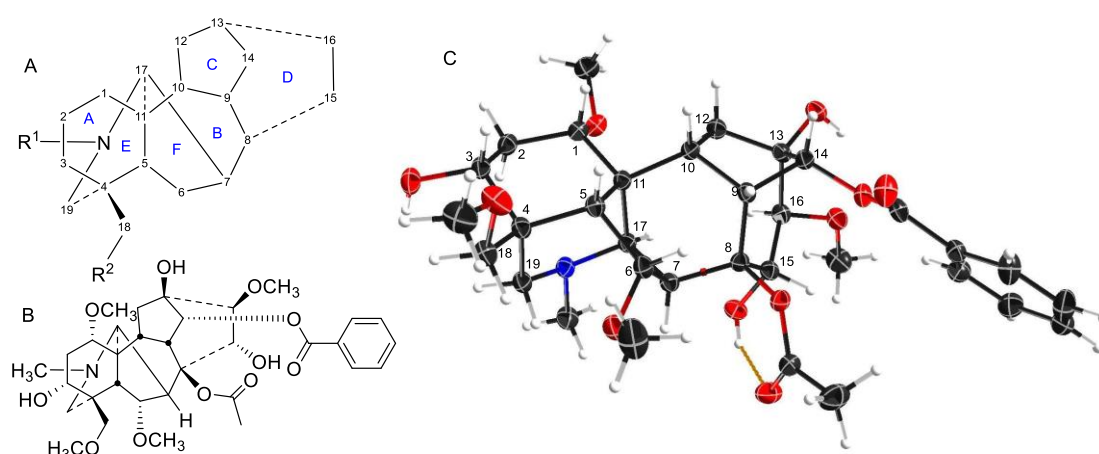


Fig. 1 A. The NDA numbering system; B. mesaconitine (**1**); C. SXR data of mesaconitine (**1**).<sup>5</sup>

## 2. Missing links in NDA biosynthesis

The biosynthesis of C19 and C18 NDA starts from the precursor isopentenyl pyrophosphate (IPP) which is produced from the mevalonate and the methylerythritol (MEP) pathways (Fig. 2). Allylic isomerisation converts IPP into dimethylallyl PP (DMAPP) by isopentenyl diphosphate isomerase (IPP isomerase). Geranylgeranyl pyrophosphate synthase converts DMAPP with 3 IPP units into geranylgeranyl pyrophosphate and then *ent*-copalyl diphosphate is produced from GGPP by *ent*-copalyl diphosphate synthase.<sup>1</sup> *ent*-C<sub>pp</sub> is further cyclised to *ent*-kaurane, which leads into veatchine- and napelline-type alkaloids, and *ent*-atisane which leads into atisine- and denudatine-type alkaloids. *ent*-Kaurane and *ent*-atisane are the only two precursors for the C19 and C18 NDA biosynthesis. *ent*-Kaurene synthase mediates the conversion of *ent*-c<sub>pp</sub> into *ent*-kaurene and then *ent*-kaurenal is produced from *ent*-kaurene by *ent*-kaurene oxidase (KO, CYP701A).<sup>1</sup> Amination by L-serine aminotransferase happens to *ent*-kaurane-type to produce veatchine-type which rearrange to napelline-type. While L-serine aminotransferase amination of *ent*-atisane-type results in atisine-type which rearranged to denudatine-type diterpenoid alkaloids.<sup>1,7</sup>

The production of *ent*-atisane and *ent*-atisanal from *ent*-c<sub>pp</sub> remains unclear. There could be rearrangement between atisine- and veatchine types and between denudatine- and napelline types, but there is no clear evidence for this. The wide distribution of denudatine- and napelline NDA in *Aconitum* species supports their position in the biosynthesis of C19 aconitine type NDA. The C19 lycoctonine type NDA are likely to be formed from protoaconine type rather than by the direct rearrangement of the atisine type.<sup>7</sup> In addition, the high occurrence of ajaconine in *Delphinium* species supports the idea that it could be the most important precursor of the lycoctonine type,<sup>7</sup> where scientific results are still missing. The rearrangement of C20 DA to C19 NDA happens through oxidative cleavage (loss of the *exo*-methylene) and the latter can undergo oxidative loss of one carbon by a different mechanism to generate the C18 NDA (Fig. 2).<sup>1,7</sup> The loss of the C-18 carbon atom from C-4 may indeed follow the established pathway for the removal of one or two methyl groups at C-4 $\alpha$  in ergosterol (ERG) catalysed sequentially by the enzymes ERG25/26/27.

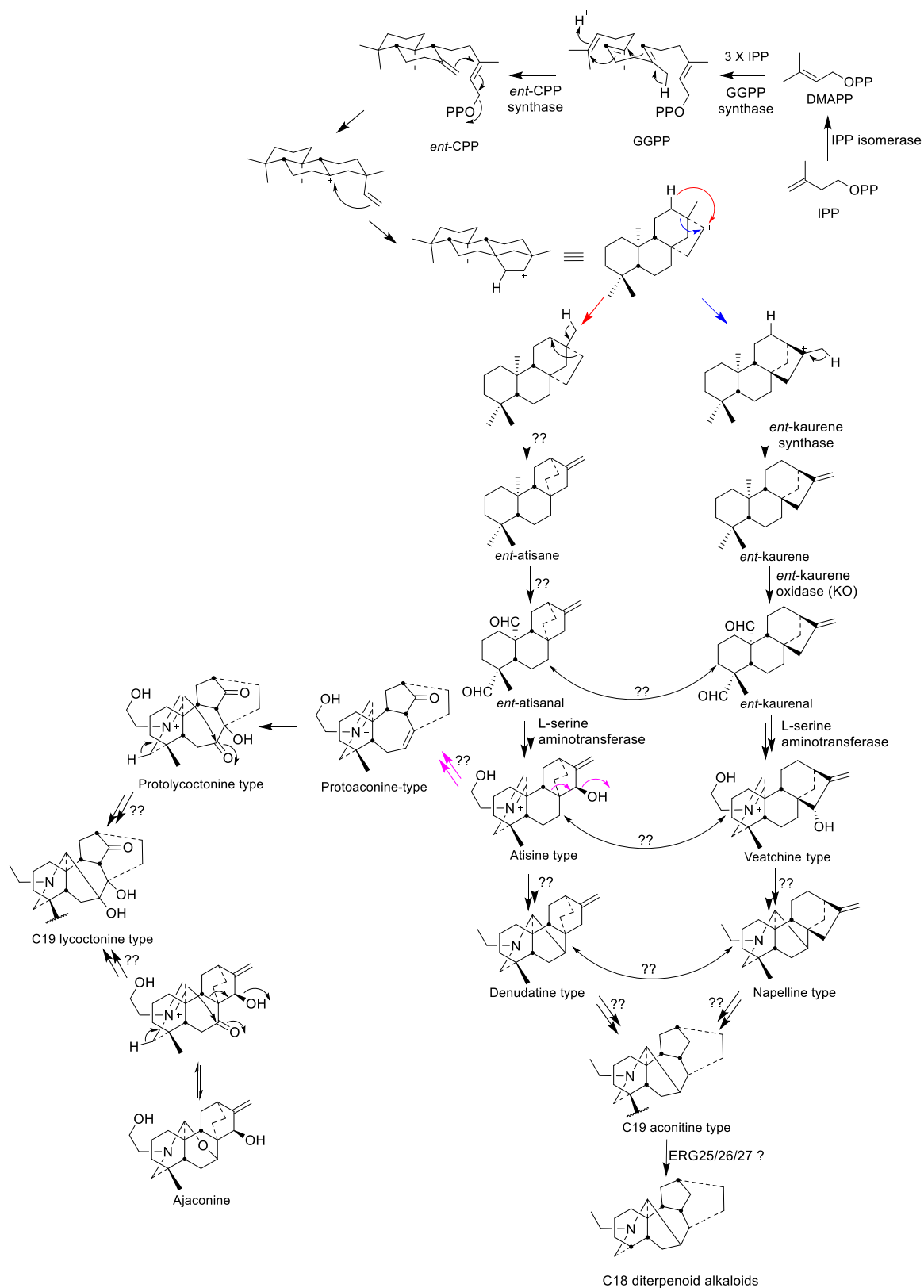


Fig. 2 Biosynthesis of C19 lycoctonine type, C19 aconitine type, and C18 diterpenoid alkaloids.<sup>1,7</sup>



### 3. Medicinal applications of *Aconitum* and *Delphinium* in current TCM

Clinical applications of *Aconitum* in traditional medicinal systems are found worldwide, particularly in Eurasia.<sup>8</sup> In Table 1 are highlighted some Traditional Chinese Medicine (TCM) uses.<sup>9-12</sup> The key processes for the raw dried main roots of *A. carmichaelli* Debx. and *A. kusnezoffii* Reichb. are boiling in water or steaming (usually known as *Pao 'Zhi*), and then slicing. The slices are boiled again thus detoxifying to obtain the decoction, or mixed with excipients, e.g., honey pills for oral use, which are used clinically as an oral analgesic for rheumatism, joint pain, and several other different pains.

In TCM, there are many formulae which are mixtures of *Aconitum* with other plants. Sini decoction is an official formula in the Chinese Pharmacopeia to treat cardiovascular disease and kidney deficiency syndrome. Sini decoction is composed of *A. carmichaelli*, *Glycyrrhiza uralensis*, and *Zingiber officinalis*. The diester NDA are hydrolysed during the decoction process to afford the monoester NDA (*vide infra* 5.2 where metabolism is discussed).

The medicinal application of *Delphinium* is popular in the Unani medicine system, a traditional medicinal system applied across nearly the whole of South and Central Asia, particularly in India and Pakistan. The species *D. denudatum* Wall., known as *Jadwar*, has even been described as one of the most important drugs in the Unani medicine system. Its roots are reported to be used for the treatment of aconite poisoning, brain diseases, fungal infection, piles, and toothache.<sup>13</sup>

Table 1. Medicinal applications of *Aconitum* and *Delphinium* extracts

Plant material	Use	Ref
<i>Aconitum</i> root (tuber) No specific species was mentioned	anti-rheumatic and analgesic	9
<b><i>A. carmichaelli</i> Debx.</b>		
dry main root ( <i>Chuan 'wu</i> )	normally use after processing as analgesic	10
processed main root ( <i>Zhi 'chuan 'wu</i> )	normally used as decoction, as anti-rheumatic and analgesic for joint pain	10

processed side root ( <i>Fu'zi</i> )	normally used as decoction, as analgesic and tonic	10
<b><i>A. kusnezoffii</i> Reichb.</b>		
dry main root ( <i>Cao'wu</i> )	normally use after processing as analgesic	10
	tincture used externally as anti-rheumatic	11
processed main root ( <i>Zhi'cao'wu</i> )	normally used as decoction, as anti-rheumatic and analgesic for joint pain	10
dry leaves ( <i>Cao'wu'ye</i> )	normally used as round pills, used as anti-inflammatory antipyretics, and analgesic; clinically used for abdominal pain, diarrhoea, headache, and toothache	10
<b><i>A. tanguticum</i> (Maxim.) Stapf. and <i>A. naviculare</i> (Bruhl.) Stapf.</b>		
dry whole plant ( <i>Tang'gu'te Wu'tou</i> )	used as anti-inflammatory, antipyretic, and wound-healing-promoting agent; clinically used for fever, hepatitis, cholecystitis, gastritis, skin ulcers and sores, and for bites (by insects, snakes etc.)	12
<b><i>A. flavum</i> Hand.-Mazz. and <i>A. pendulum</i> Busch.</b>		
processed main root ( <i>Tie'bang'chui</i> )	used as anti-inflammatory, analgesic, and sedation; clinically used for skin ulcers and sores, leprosy, and mania	12
dry seedling (seedling of <i>Tie'bang'chui</i> )	used as anti-inflammatory, antipyretic, and analgesic; clinically used for fever, 'flu, skin ulcers, and sores	12
<b><i>D. kamaonense</i> Huth var. <i>glabrescens</i> (W.T.Wang) W. T. Wang</b>		
dry above-ground parts ( <i>Zhan'mao'cui'que</i> )	used as anti-inflammatory and analgesic; clinically used for diarrhoea and dysentery, also externally used on skin ulcers and sores	12

#### 4. NDA in current medicine and their structure-activity relationship (SAR) studies

Despite their similar sounding trivial names and being based on the same hexacyclic skeleton, many NDA do not have the same oxygen substitution pattern and this structural change may be one of the reasons for their different pharmacological properties.

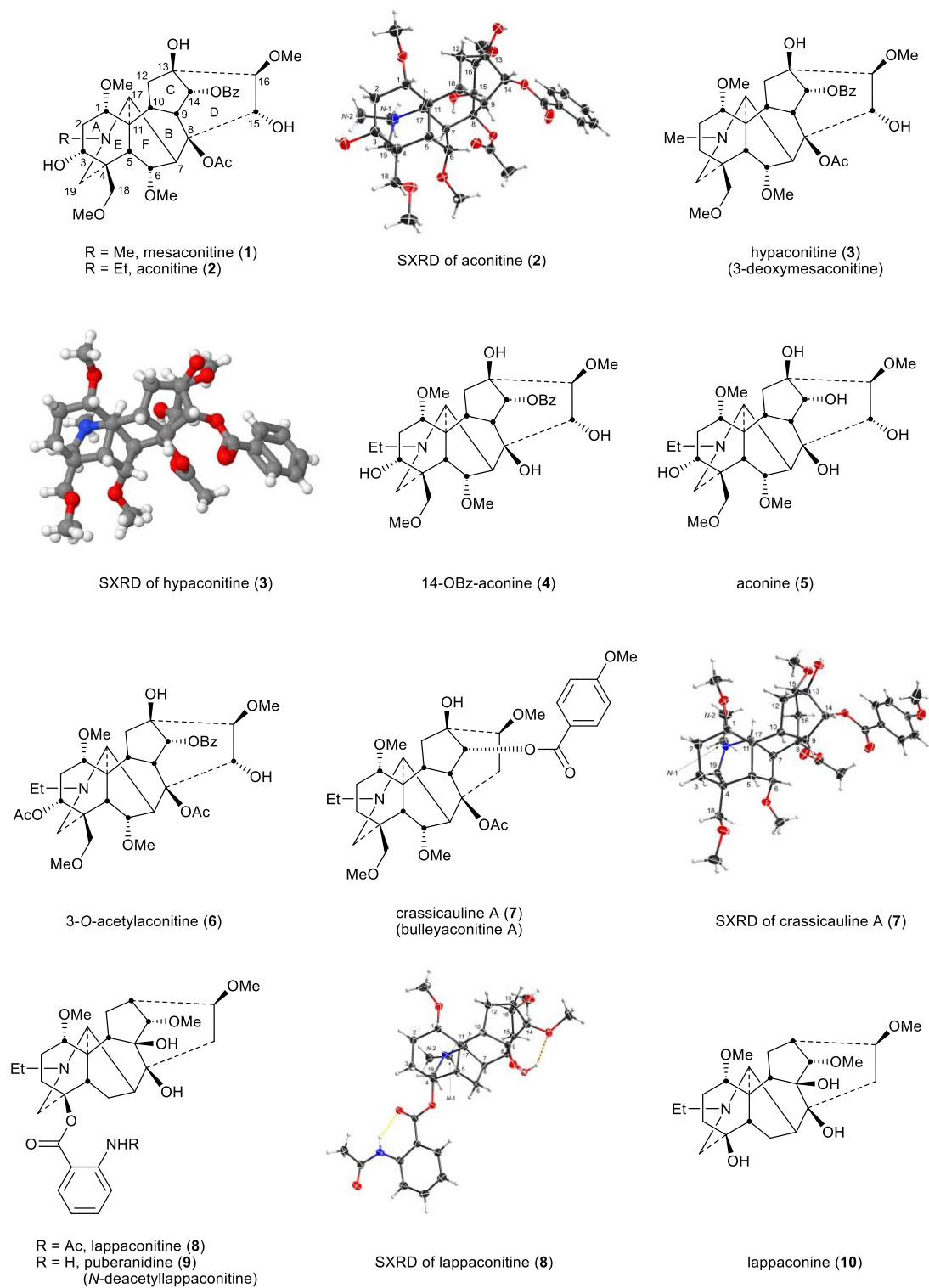


Fig. 3 Mesaconitine (1), aconitine (2), hyaconitine (3), and their related NDA. SXRDS of hyaconitine (3) is reprinted with permission from Ref 14. Copyright 2012 ACS.

#### 4.1 Aconitine type

Mesaconitine (**1**), aconitine (**2**), and hyaconitine (**3**)<sup>14</sup> (Fig. 3) are cardiotoxins,<sup>15,16</sup> interacting with cardiac voltage-sensitive sodium channels (VSSCs) and maintaining them in an open conformation,<sup>15,17,18</sup> introducing arrhythmia,<sup>19,20</sup> whereby these alkaloids are highly toxic, e.g., LD<sub>50</sub> (aconitine **2**, mice, subcutaneous, mg/kg) = 0.12-0.20.<sup>17,21</sup> The potent, indeed lethal cardiotoxin aconitine (**2**) was first discovered in 1833 by P. L. Geiger from *A. napellus*.<sup>22,23</sup> These NDA (**1-3**) act at VSSCs in the central nervous system (CNS) and muscle tissues exhibiting analgesic activity.<sup>24</sup> The NDA (**1-3**) with 8-OAc or other fatty acid ester sidechains are also known as lipo-alkaloids.<sup>25</sup> The primary functional subunit of VSSCs is the  $\alpha$ -subunit, and this subunit contains four domains (I-IV). There are at least five reported toxin binding sites on domain I, and the lipophilic NDA, e.g., mesaconitine (**1**) and aconitine (**2**) that carry ester groups 8-OAc and 14-OBz, can bind on the neurotoxin receptor 2 that is located in the transmembrane region, and this binding leads to VSSCs remaining in the open-state.<sup>26</sup> The boiling process in the preparation of *Aconitum* roots hydrolyses the highly toxic diester NDA, e.g., aconitine **2** to less toxic monoester NDA, e.g., 14-OBz-aconine **4**. Structure-activity relationship (SAR) studies show that further hydrolysis produces alkaloids lacking an ester group and which are even less toxic, e.g., aconine **5**, but the analgesic activities are also lost.<sup>17,18,27</sup> When the NDA bear different oxygenated substituents, e.g. 3-*O*-acetylaconitine (**6**) and crassicauline A (**7**, also known as bulleyaconitine A), they may interact with the different subdomains on the  $\alpha$ -subunit and this results in decreased toxicity as evidenced by LD<sub>50</sub> (mice; subcutaneous; mg/kg) = 0.87-1.40 and 0.92, respectively.<sup>17,19,21</sup> These NDA (**6, 7**) exhibit non-addictive potent analgesic activity ED<sub>50</sub> (mice; hotplate; mg/kg) = 0.16 and 0.087, respectively. Although the clinical use of the lipo-alkaloids as diester (crassicauline A, **7**) or even triesters (3-*O*-acetylaconitine **6**) is debatable as they are toxic,<sup>17</sup> 3-*O*-acetylaconitine (**6**) and crassicauline A (**7**) were introduced in the 1980s into clinical use in China as analgesic agents for long-term treatment.<sup>28-30</sup>

#### 4.2 Lappaconitine type

Lappaconitine (**8**), the first C18 NDA to be reported, was isolated from *A. septentrionale* Koelle by H. V. Rosendahl in 1895.<sup>31</sup> The most successful medical application of an NDA to date is Allapinin, the hydrobromide salt of lappaconitine (**8**) as it is a VSSC blocker.<sup>17,32-34</sup> It has been used clinically in Russia since 1987 as an anti-arrhythmic drug.<sup>35-39</sup> This compound also shows a potent non-addictive analgesic property, and recent studies reported that this bioactivity is related to a decrease of expression and sensitisation of the P2X<sub>3</sub> receptors on mice dorsal root ganglion (DRG) neurons.<sup>40,41</sup> A naturally occurring analogue of lappaconitine (**8**), puberanidine (**9**, *N*-deacetylappaconitine), exhibits similar biological activities. Indeed, it is an *N*-deacetyl metabolite of lappaconitine (**8**) found in the urine of certain drug users.<sup>42</sup> Toxicity studies on these two compounds revealed that their LD<sub>50</sub> (mice; subcutaneous; mg/kg) were 11.7 and 36.4, respectively which, due to their lower toxicity, are significantly higher than that of aconitine (**2**) given above (mice, subcutaneous, mg/kg = 0.12-0.20).<sup>17,21</sup> Structurally, lappaconitine (**8**) and puberanidine (**9**) are monoesters and they have a smaller chance to bind to neurotoxin receptor 2 in the transmembrane region in comparison with more lipophilic aconitine (**2**), thus, these compounds are less toxic. When these NDA lack lipophilic ester groups, their (toxic) activities on VSSCs are less, whereas the analgesic effects on the CNS remain, e.g., as demonstrated by lappaconine (**10**).<sup>34</sup>

#### 4.3 Lycoctonine type

Lycoctonine (**14**) (Fig. 4) was first reported in 1865 isolated from *A. lycoctonum* L.<sup>43</sup> and lycaconitine (**15**) was first reported in 1884 also from *A. lycoctonum* L.<sup>44</sup> Methyllycaconitine (MLA, **11**) was first reported by Manske in 1938 from *D. brownii* Rydb.<sup>45</sup> In 1943, Goodson reported its exact formula (Fig. 3).<sup>46</sup> MLA (**11**) is one of the most potent competitive antagonists of  $\alpha$ 7-nicotinic acetylcholine receptors (nAChRs)<sup>47</sup> with highly selective targeting of the snake venom toxin  $\alpha$ -bungarotoxin ( $\alpha$ -BgTx) binding sites.<sup>48,49</sup>

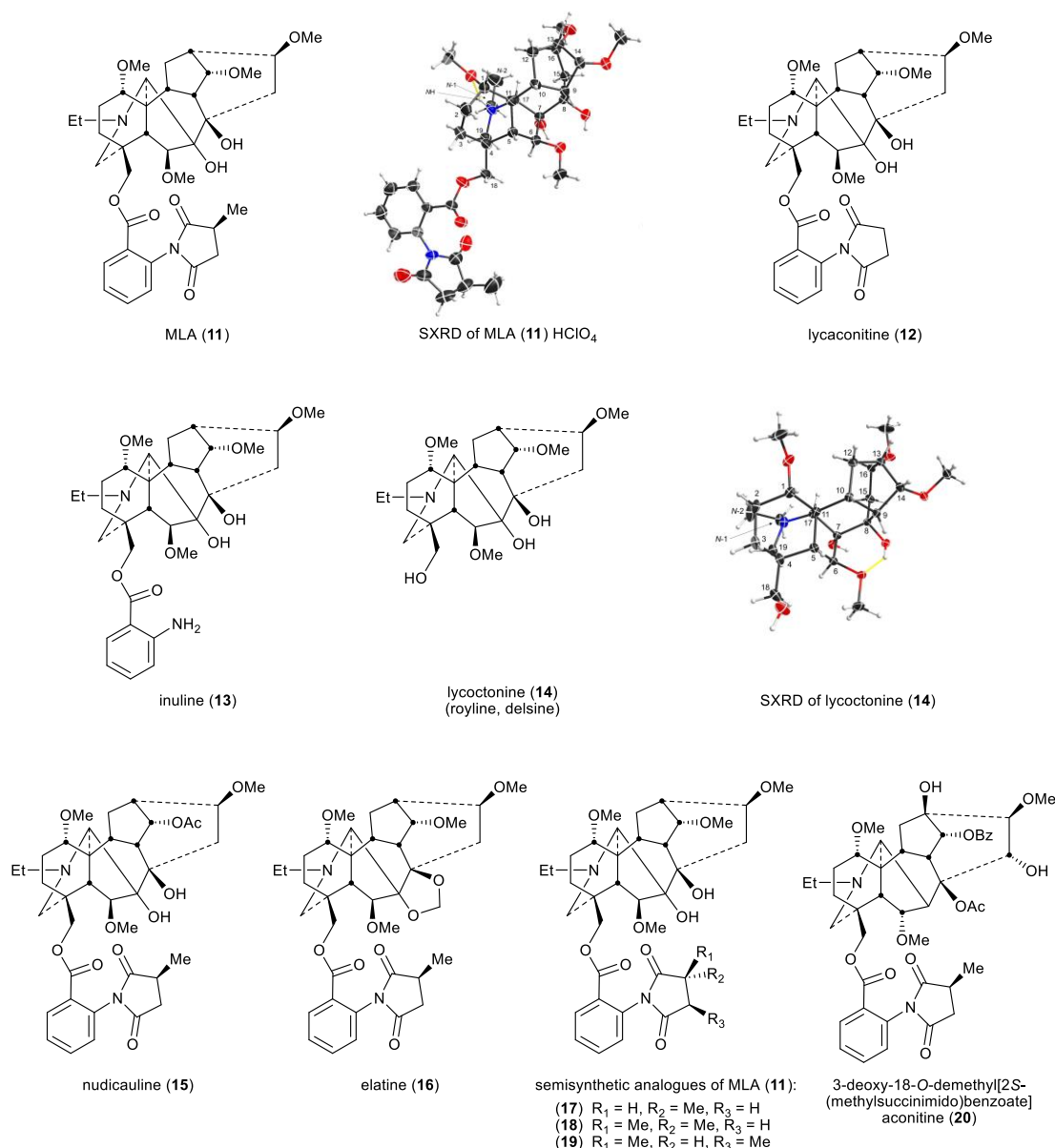


Fig. 4 MLA (11), related NDAs, and their semisynthetic analogues.

A rare pharmaceutical preparation of MLA (11), mellictin, has been reported in clinical use for the treatment of Parkinson's disease and cerebral palsy at least in Uzbekistan and Kyrgyzstan.<sup>36</sup> The 2*S*-(methylsuccinimido)benzoate moiety was the key for this compound to exhibit high affinity. Compared with MLA (11)  $IC_{50} = 7.6 \pm 3.4 \times 10^{-9}$  M (mice brain neuronal  $\alpha 7$  nAChR), the  $IC_{50}$  of lycaconitine (12) on  $\alpha 7$  nAChR was  $6.8 \pm 0.9 \times 10^{-6}$  M as the methyl group on the succinimide is removed, significantly lowering affinity. The  $IC_{50}$  of inuline (13) is similarly modest  $1.6 \pm 0.6 \times 10^{-6}$  M due to the removal of the essential methylsuccinimide group. When the entire (methylsuccinimido)benzoate ester is cleaved, the affinity of lycoctonine (14, which is also known as royline and delsine<sup>50</sup>) has sharply decreased, the  $IC_{50}$  increasing

through the  $\mu\text{M}$  range to  $1.0 \pm 0.1 \times 10^{-5} \text{ M}$ , which indicates that this neopentyl alcohol derived from MLA (**11**) has essentially lost all affinity for the  $\alpha 7$  nAChR.<sup>51</sup> For NDA substituted with 18-*O*-2*S*-(methylsuccinimido)benzoates, e.g., nudicauline (**16**) and elatine (**17**), their  $\text{IC}_{50}$  remained at the nM level as MLA (**11**),  $1.7 \pm 0.7 \times 10^{-9} \text{ M}$  and  $6.1 \pm 1.5 \times 10^{-9} \text{ M}$ , respectively. Also, Carroll and co-workers reported that stereochemical modification on the succinimide ring of MLA (**11**), e.g., changing the chirality of the succinimide methine substituted with a methyl from *S* to *R* decreases the affinity for  $\alpha 7$  nAChR, e.g., semisynthetic analogues (**17-19**).<sup>52</sup>

The pharmacophore in MLA (**11**)<sup>51</sup> for nAChR incorporates the key distance between the *N*-atom of the piperidine E-ring (ring labelling see Fig. 1) and the ester carbonyl of 18-*O*-2*S*-(methylsuccinimido)benzoate. Aconitine (**2**) contains no such distance and therefore it shows only modest affinity for nAChR. However, after the 3-OH and the *O*-methyl of 18-OMe were specifically removed chemically and then 2*S*-(methylsuccinimido)benzoic acid was esterified with the unmasked 18-neopentyl alcohol, the product 3-deoxy-18-*O*-demethyl[2*S*-(methylsuccinimido) benzoate]aconitine (**20**) exhibited high affinity for  $\alpha 7$  nAChR at the same (low) nM level as that of MLA (**11**).<sup>53</sup>

The complex structure of such hexacyclic NDA secondary metabolites make them potential drugs, at an appropriate dose, rather than toxins. Their biophysical properties show that they are well absorbed in mammals and therefore they possess good properties for orally delivered human medicines leading to good distribution in the body. NDA are therefore prime candidates for aspects of computational drug design and development, starting from natural product leads (from sustainable sources) and progressing in particular using computers to assess the (bio)physical properties and data sets, e.g., *Aconitum* and *Delphinium* alkaloids: “Drug-likeness” descriptors related to toxic mode of action.<sup>54</sup> Such QSAR studies of large datasets of NDA aim to discriminate between “drugs” and “non-drugs”. These calculations have been proven to give reliable results on specific NDA as to whether they are more likely to be a poison or a drug. Rasulev and co-workers constructed QSAR models with “drug-likeness” descriptors discussed in terms of the mode of toxic action exhibited by the selected set of 95 NDA.<sup>54</sup> The antiarrhythmic NDA, e.g. lappaconitine (**8**), the curare-like NDA, e.g. MLA (**11**), and aconitine-like NDA were studied using a range of typical “drug-likeness” descriptors. The molecular size

descriptors (differences in positive and negative regression terms of MWt and Ghose-Grippen molar refractivity, MR) were identified as those most related to toxic mode of action.

Preliminary theoretical absorption, distribution, metabolism, and excretion (ADME) properties of the NDA gave promising data. However, NDA showing the higher desirable therapeutic activity are still those of high toxicity. Dose remains crucial and therefore further pharmacological studies should be carried out.

#### *4.4 Delphinium (larkspur) toxicity*

Larkspur toxicity varies as a function of, e.g., species, stage of growth, plant part, environment, and the individual NDA.<sup>55</sup> There are many important structural features contributing to the toxicity of larkspur NDA. The ionized nitrogen plays a major role in the interaction with nAChR. The ester moiety in MLA-type (methylsuccinimidoanthranoyl lycocotinine, MSAL) plays an important role in neuromuscular blockade (at  $\alpha 1$  nAChR). In addition, a C14 substituent has a profound biological effect. This important functionality was reported in many studies which established that the electronic or the stereochemical factors of the C14 substituent affect the affinity for nAChR. The order of activity at C14 was determined to be acetate > hydroxyl > methoxy > carbonyl (C=O). In contrast, the observed effect of substituents at C1 and C16 is: methoxy > hydroxyl > acetate. The opposite biological effects are caused by substituents at C1 and C16, and C14.<sup>55-60</sup>

Livestock intoxication by larkspur is a function of the cattle breed and their genetics also affect the susceptibility to the intoxication. Age is another factor where young heifers are more susceptible than mature cows. Cattle sex is also important. Heifers are more prone to the toxicity than steers and bulls. Of course, the plant plays an important role where the MSAL and non-MSAL alkaloid concentration and composition, which depend on the population, species, climate, and the year, affect the cattle toxicity and the amount needed from the plant to develop clinical signs of toxicity.<sup>61,62</sup> The 7,8-methylenedioxy-NDA are the least toxic alkaloids. The lycocotinine-type is twice as toxic, but is still considered to be of relatively low toxicity. The MSAL alkaloids, e.g. MLA (**11**), are 10-times more toxic than any other tested alkaloid.<sup>56</sup> The MSAL alkaloid concentration in tall larkspur is the major contributor to livestock poisoning. An



investigation of the SAR of NDA toxicity found that 7,8-methylenedioxy-NDA exacerbates the toxicity of the MSAL alkaloids. The exact molecular mechanism of this toxicity is not known, but a possible explanation is that such substituted NDA can act as co-agonists on nAChR, enhancing the activity at the receptors.<sup>63</sup>

## 5. Metabolism of NDA

As set out above, *Aconitum* preparations are widely used in TCM and a few NDA have been clinically approved: 3-*O*-acetylaconitine (**6**), crassicauline A (**7**), lappaconitine (**8**), and MLA (**11**). The metabolism of these alkaloids has been studied extensively in vitro in cell-free systems (microsomes) (Table 2) and in vivo in animals and humans.

### 5.1 Cell-free systems – microsomal studies

Metabolism of aconitine (**2**) in rat liver microsomes (RLM) was studied and it was found to be metabolised through hydrolysis, demethylation, *N*-deethylation, and dehydrogenation. Several CYP450 inhibitors were used to determine which isoform was involved in the metabolism; CYP3A and/or CYP1A1/2 inducers or inhibitors will affect the metabolism of aconitine (**2**).<sup>64</sup> Metabolic studies using human liver microsomes (HLMs), where the liver cells were obtained from donors aged between 21-76, showed that the main metabolic pathways are hydroxylation, dehydrogenation, *O*-demethylation, di-*O*-demethylation and/or *N*-deethylation. CYP3A5 and 2D6 mediate the di-*O*-demethylation and the hydroxylation, CYP3A4/5, 2D6, and 2C9 the *N*-deethylation, and CYP3A4/5 the dehydrogenation.<sup>65</sup>

Metabolism of mesaconitine (**1**) using the above HLM obtained from male donors, was found to be conducted mainly through demethylation, hydroxylation, dehydrogenation, and demethylation-dehydrogenation. It was found that CYP3A4/5, 2C8, and 2D6 mediated the demethylation pathway; CYP3A4/5 the hydroxylation and dehydrogenation; CYP3A4/5, 2C8/9, and 2D6 the demethylation-dehydrogenation.<sup>66</sup>

Metabolism of crassicauline A (bulleyaconitine A, **7**) by RLM results showed that the main metabolic pathways were hydroxylation, deacetylation, *O*-demethylation, di-*O*-demethylation and/or *N*-deethylation, and deacetylation-dehydration. CYP3A and 2C mediated all pathways,

CYP3A, 2C, and 2D contributed to the hydroxylation, CYP3A, 2C and 2E1 the demethylation, CYP3A, 2C, 2D, and 2E1 the *N*-deethylation, deacetylation and deacetylation-dehydration.<sup>67</sup>

The metabolism of *A. carmichaelii* Debx. roots' individual diesters, mesaconitine (1), aconitine (2), and hyaconitine (3), and monoesters, benzoylmesaconine, benzoylaconine, and benzoylhyaconine NDA by HLM and human intestinal microsomes (HIM), obtained from mixed gender donors, was studied. It was found that demethylation and dehydrogenation were the main metabolic pathways, and *N*-deethylation was observed in aconitine (2) and benzoylaconine. Hydroxylation was detected in mesaconitine (1) and hyaconitine (3). Deoxygenation was observed in aconitine (2). Subsequent metabolism was observed in diesters more than monoesters to form, e.g., di-*O*-demethylated, didehydrogenated, and demethylated-dehydrogenated metabolites.<sup>68</sup> The amount/concentration of HLM metabolites were higher than HIM metabolites as HLM catalytic capacity is higher and could be due to other CYPs alongside CYP3A that could play a role in the metabolism which was reported previously.<sup>65,66</sup> Glucuronidation followed phase I metabolism, but no conjugated metabolites were found in HIM and HLM incubations.<sup>68</sup>

Table 2. Metabolism of NDA

<b>NDA</b>	<b>Metabolic Enzymes</b>	<b>Ref</b>
<b>RLM</b>		
aconitine (2)	major CYP3A	64
	minor CYP1A1/2	64
crassicauline A (7)	major CYP3A and 2C	67
	minor CYP2D and 2E1	67
	least CYP1A2	67
<b>HLM</b>		
Aconite diesters	major CYP3A	68
	minor other CYPs	68
mesaconitine (1)	major CYP3A4/5	66
	minor CYP2C8/9, 2D6	66
aconitine (2)	major CYP3A4/5	65
	minor CYP2C8/9, 2D6	65

Metabolism of lappaconitine (**8**) by HLM and RLM showed that *N*-deacetylation, hydroxylation, and *O*-demethylation were the main metabolic pathways whereas *N*-deethylation and hydrolysis contributed to a lesser extent. Subsequent metabolism was observed, and many metabolites of metabolites were generated from combinations of the previously mentioned pathways. The *O*-demethylated metabolites were present in the order 16-*O*-demethyl- > 14-*O*-demethyl- > 1-*O*-demethyl-lappaconitine. It was found that HLM metabolism generated more metabolites than RLM.<sup>69</sup>

## 5.2 Animal studies

A study showed that *G. uralensis* and *Z. officinalis* enhance the absorption of *A. carmichaelii* monoesters and reduce the half-life by increasing the excretion or speeding up the metabolism of other active compounds.<sup>70</sup> In vivo metabolic studies of Sini decoction<sup>70</sup> in rats urine showed that hydrolysis and demethylation were the main metabolic pathways of diterpenoid alkaloids.<sup>71</sup> In vivo study of pure aconitine (**2**) metabolism in rats and rabbits stomach showed that the biotransformation was mainly through oxidation (+16 Da) resulting in hydroxylation, deoxygenation (-16 Da) in dehydroxylation, *O*-demethylation (-14 Da), and di-*O*-demethylation and/or *N*-deethylation (-28 Da). Ester exchange at C8 was also observed as some fatty acyl chains replaced the acetyl moiety to form lipo-aconitines (Fig. 5). The metabolic profile from rats and rabbits stomach is similar, but there are fewer metabolites in rats.<sup>72</sup>

The metabolism of crassicauline A (bulleyaconitine A, **7**) (p.o. and i.v.), which is used clinically in China, has been studied in rat urine and faeces. The amount recovered unchanged was higher in the i.v. group compared to that in the p.o. group.<sup>73</sup> A hydroxylated metabolite was observed in MS (+16 Da). From the fragmentation analysis, it was concluded that the hydroxylation was probably at C15 to give deoxyjesaconitine, but this conclusion requires scientific confirmation.<sup>73</sup>

Qi-Li-Qiang-Xin (QLQX) is a TCM prescription composed of eleven herbal medicines, which can interfere with the metabolism of each other. One of them is Radix Aconiti Lateralis which is also known as fu'zi (the side roots of *A. carmichaelii*). The metabolism of QLQX capsules (p.o.) in rats' plasma, urine, and faeces was studied. Diester NDA were not detected in the preparation and the metabolic pathways according to the metabolites identified mainly in urine and plasma were: hydrolysis, hydroxylation, methylation, *O*-demethylation, dehydrogenation, and dehydration. In addition, no NDA phase II metabolites were detected.<sup>74</sup> Similarly, the pharmacokinetics of multiple NDA, e.g., mesaconitine, aconitine, hypaconitine, and benzoylmesaconitine, have been reported following the administration of the TCM Zhenwu Tang and Radix Aconiti Lateralis Praeparata extracts to rats with quantitative analysis by HPLC-MS/MS.<sup>75</sup> Likewise, the simultaneous determination and the pharmacokinetics of six NDA in rat plasma have been reported following the oral administration of Radix Aconiti extracts.<sup>76</sup> The analytical technique of SPE-HPLC-MS/MS is sensitive and accurate. These results provide a scientific basis for a metabolism study of *Aconitum* NDA in humans. Therefore, they pave the way for studies in to the clinical uses of *Aconitum* NDA and its extracts.

The metabolism of lappaconitine (**8**) HBr (Allapinin) was studied in rats after i.v. administration. Deacetylappaconitine (**9**), 14-*O*-demethyl-deacetylappaconitine, and 16-*O*-demethyl-deacetylappaconitine, were detected in rat urine in addition to unmetabolized drug (**8**). Their ratio was 4:2:3:4 respectively after 24 h. As lappaconitine (**8**) concentration decreased with time, deacetylappaconitine (**9**) increased due to metabolism by *N*-deacetylation. Also, as the amount of deacetylappaconitine (**9**) decreased, 14-*O*-demethyl- and 16-*O*-demethyl-deacetylappaconitine increased (Fig. 5).<sup>77</sup> Another study in rats showed that *N*-deacetylation, *O*-demethylation, and hydroxylation are the main metabolic pathways, where 16-*O*-demethyl-deacetylappaconitine and 5'-OH-lappaconitine are the major metabolites.<sup>69</sup>

### 5.3 Human studies

The metabolism of aconite NDA was studied in the urine of females who had been given p.o. decoctions of a prescription consisting of 10 g Cao'wu (processed roots of *A. kusnezoffii*

Reichb) and 10 g Chuan'wu (processed roots of *A. carmichaelii* Debx.). In addition to the parent alkaloids, mesaconitine (**1**), aconitine (**2**), and hypaconitine (**3**), there were three hydrolysed metabolites, benzoylmesaconine, benzoylaconine, and benzoylhypaconine, and two *O*-demethylated metabolites, which were assigned as 16-*O*-demethylaconitine and 16-*O*-demethylhypaconitine<sup>78</sup> by analogy.<sup>77</sup> The monoesters may not only be derived by metabolism as the processed roots contain substantial amounts of them.

Lappaconitine (**8**) metabolism was studied in the urine of men who had received i.m. injections of lappaconitine (**8**) HBr (Allapinin). In addition to the parent alkaloid, *N*-deacetylappaconitine (**9**) and 16-*O*-demethyl-deacetylappaconitine were detected (Fig. 5). In 24 h collected urine, the ratio of lappaconitine (**8**), the *N*-deacetyl-, and 16-*O*-demethyl-deacetylappaconitine was 160:2:1 respectively,<sup>79</sup> different from the rat metabolism ratio (i.v. administered).<sup>77</sup> The high ratio of lappaconitine (**8**) compared to its metabolites is after i.m. administration which (like i.v.) allows the drug to bypass the liver, thereby avoiding first-pass (through the liver) metabolism. In addition, Allapinin (**8** as an HBr salt) is likely to be more water soluble and potentially rapidly excreted unchanged in the urine. The amounts of lappaconitine (**8**) and its metabolites detected did not show significant difference upon potential hydrolysis after incubation (in vitro) with the enzymes  $\beta$ -glucuronidase and sulfatase. This indicates that conjugation with glucuronic or (PAPS, the biological equivalent precursor for) sulfuric acid was not a major metabolic pathway.<sup>79</sup>

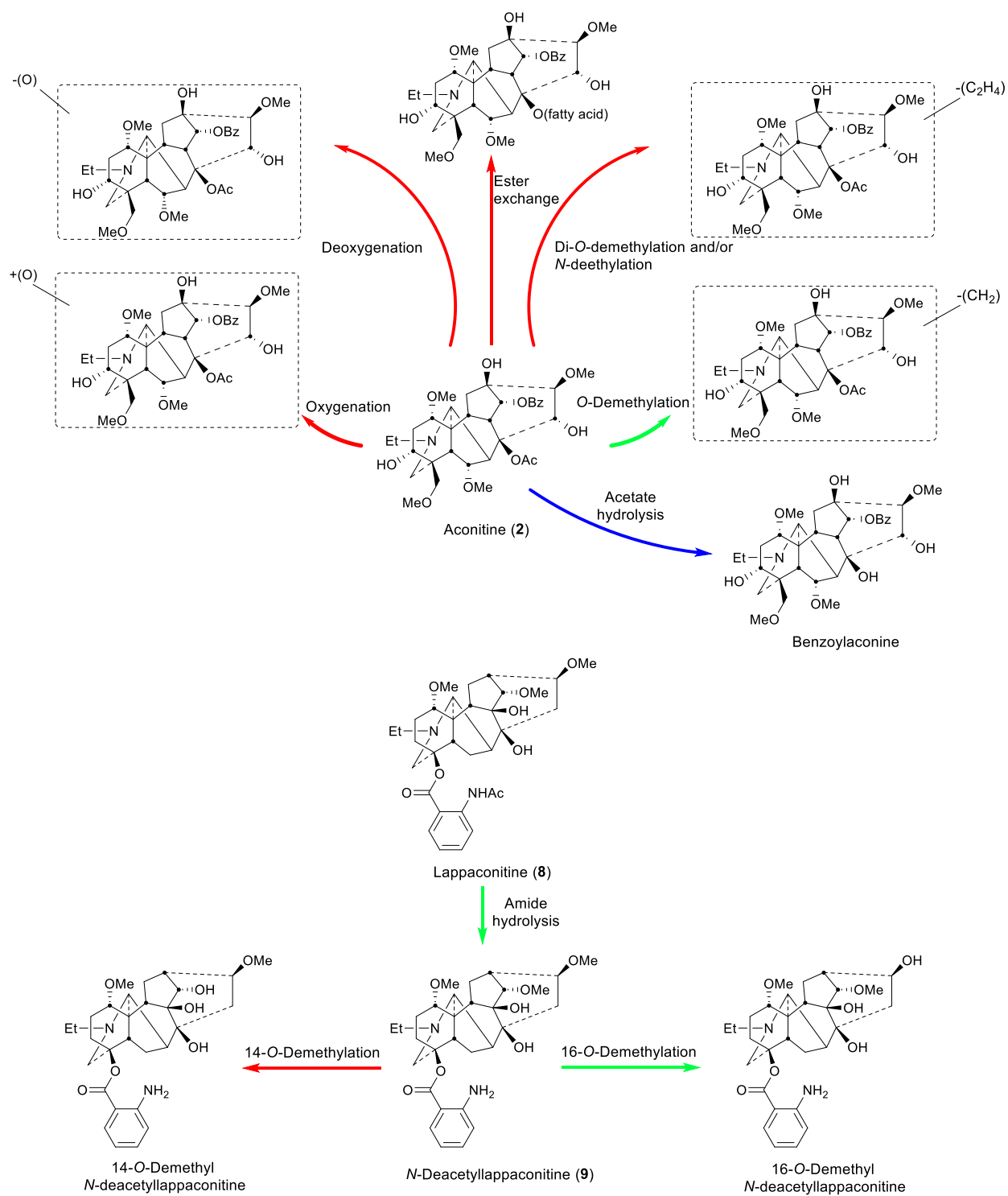


Fig. 5 Metabolism of aconitine (2)<sup>72,78</sup> and lappaconitine (8)<sup>79,81</sup> in humans (blue), animals (red), and pathways common in both (green).

#### 5.4 Metabolic effects on biological activity

The high toxicity of *Aconitum* alkaloids is due mainly to the benzoyl ester at C14 and C8 acetate. C1, C6, C16, C18 methoxyl groups, and C13 hydroxyl also contribute to their toxicity.<sup>17,19</sup> Hydrolysis of *Aconitum* alkaloids results in monoester alkaloids which have lower toxicity. In addition, demethoxylation and dehydration aid in lowering the toxicity. The formation of lipo-aconitines in rat and rabbit stomachs<sup>72</sup> is an important biotransformation as they show an anti-inflammatory effect which is variable according to the length and degree of unsaturation of the fatty acids.<sup>80</sup> The metabolic processes convert *Aconitum* alkaloids into more polar metabolites, and consequently their excretion will be promoted and their retention in the body will be shorter. Such conversion can be considered as a natural response to reduce the toxicity of these alkaloids.<sup>66</sup>

The metabolism of lappaconitine (**8**) is mainly through deacetylation to yield *N*-deacetylappaconitine (**9**) which shows higher biological activity than the parent compound.<sup>18</sup> It has been proposed that lappaconitine (**8**) does not act directly on the CNS, but is converted in vivo into the active metabolite *N*-deacetylappaconitine (**9**),<sup>81</sup> and the activity can be considered as a sum of the parent compound and this metabolite.<sup>82</sup> The number of metabolites of lappaconitine (**8**)<sup>69</sup> was much higher than of mesaconitine (**1**), aconitine (**2**), and hypaconitine (**3**),<sup>64</sup> and the lower toxicity of lappaconitine (**8**) compared with other *Aconitum* alkaloids<sup>17</sup> can be attributed to this extensive metabolism, at least in rats.<sup>69</sup> It is obvious that the liver is the main metabolic site, but the stomach and intestinal metabolism cannot be ignored as sites of metabolic detoxification.

#### 6. Analysis of NDA

*Aconitum* alkaloids vary widely in their chemical structures and substitution patterns as well as being well known for their bioactivity and toxicity. Naturally occurring analogues with closely similar structures or positional isomers are widespread in herbs of the *Aconitum* genus. It is still challenging to identify rapidly unknown compounds by MS, especially positional isomers. MS is also used in the monitoring and detection of NDA metabolites, often achieved using LC-ESI-MS due to its sensitivity. It is important to understand the MS fragmentation of

the parent alkaloids as the metabolites follow them in their fragmentation patterns. The fragmentation ions of aconitine (**2**)<sup>68,72</sup> and lappaconitine (**8**)<sup>69</sup> skeletons (as representative aconitine type and lappaconitine type NDA) show that such NDA undergo cleavage of the benzoate or acetate ester side chain, loss of water, and loss of methanol. These fragmentations involve typically two sequential cleavages of *O*-methyl ethers occurring with one or even two dehydration steps, in either order.

Due to the lack of major MS fragmentations of the NDA skeleton, the actual position of the CYP-catalysed metabolic reactions e.g., *O*-demethylation, hydroxylation, can be difficult to pinpoint. In addition, it is difficult in some cases to determine if there is one metabolic process or a combination of more than one e.g., di-*O*-demethylation vs *N*-deethylation. In such cases, the MS fragment analysis can indicate a metabolic position, but it needs to be confirmed using other analytical techniques.

F. Gao and co-workers continue to report new NDA, most recently from the roots of *A. novoluridum* and from the aerial parts of *A. apetalum*. The former provided 3 novolunines A, B, and C where the structures were established using spectral data analysis.<sup>83</sup> The latter afforded 5 apetalrines A-E based on *N*-acylated 2-aminobenzoyl esters and also structurally identified following detailed spectral analysis.<sup>84</sup> Ablajan et al. reported 5 previously undescribed DA, barpuberudine and barpubesines A-D, and two interesting novel C18 NDA, barpubenines A-B, isolated from the whole plant of *A. barbatum* var. *puberulum* Ledeb. The possible rearrangement of the C18 NDA structures led to a discussion of their probable biosynthetic pathway.<sup>85</sup> The global profiling of NDA in *A. stapfianum* and analysis of the basis of its use for detoxification of fu'zi has been reported.<sup>86</sup> The analysis was performed by UPLC/Q-TOF-(ESI)-MS with fragmentation patterns from MS/MS spectra as this is a method of high sensitivity, selectivity, and analytical speed.<sup>86</sup>

Our double Mannich route<sup>87,88</sup> and the elegant studies of Brimble and co-workers<sup>89-93</sup> afford a rapid and efficient entry to small molecule NDA analogues, i.e., without completing a total or even a formal synthesis of lycoctonine (**14**), inuline (**13**), or MLA (**11**). These studies are an important foundation for the next phase of this research. The regioselective *O*-demethylation of aconitine (**2**)<sup>94</sup> has enabled its regioselective anthranoylation<sup>95</sup> leading to such



NDA analogues and thereby swapping from the VSSC to the nAChR series of important biological activities.<sup>53</sup> Our studies on deuteration<sup>96</sup> led to the tritiation of the key ligand MLA (**11**).<sup>49,97,98</sup> A huge amount of important pharmacology has been uncovered using this biological tool.

The through-space <sup>1</sup>H NMR effect of steric compression by the lone-pair electrons of O- and N-atoms, with an associated deshielding effect, has been shown in synthetic [3.3.1]oxa- and azabicycles.<sup>99</sup> Likewise the relevance of determining the crystal or solution protonated [3.3.1]azabicyclic conformation, true-boat/true-chair conformation in the crystal lattice, but in solution the conformation is true-chair/true-chair.<sup>99</sup>

Moving from bicycles to hexacycles, conformational analyses have very recently been reported of several pharmacologically important NDA in crystal and in solution states.<sup>100</sup> Indeed, crystal data of 8 NDA (4 free bases and 4 salts) were obtained, in which crassicauline A (**7**), aconitine (**2**) HCl, and methyllycaconitine (**11**) HClO<sub>4</sub> have been reported for the first time together with the comprehensive 1D/2D NMR spectroscopies of 7 NDA.<sup>100</sup> The A/E-rings of NDA-free bases exist in twisted-chair/twisted-chair conformations, with examples of the <sup>1</sup>H NMR effect of steric compression shown in the A-ring. The A/E-rings of NDA salts adopt boat/chair crystal conformations, as do the protonated synthetic [3.3.1]azabicyclic. However, in aqueous solutions at physiological pH, this protonated analogue adopts a true chair/true chair conformation where the NDA salts retain their twisted boat/twisted chair.<sup>100</sup>

<sup>15</sup>N NMR analysis showed that the <sup>15</sup>N chemical shift of 1-OMe NDA increases (electron density decreases) upon protonation<sup>6</sup> due to H-bonding between 1-OMe and N-H<sup>+</sup> which stabilize the twisted boat-twisted chair conformation of the AE bicycle.<sup>100</sup> Such an increase in the <sup>15</sup>N chemical shift has been observed in the 1- $\alpha$ OH NDA free bases where ring A adopts a twisted boat conformation due to intramolecular H-bonding.<sup>5,6</sup> These results prove that the analysis of the N-electron density of piperidine containing alkaloids is useful for solution conformational analysis.

## 7. Conclusions and future prospects

Although currently studied and, if starting with Pliny the Elder,<sup>3</sup> now for 2000 years, research in this area of phytochemistry continues apace. New C19 and C18 NDA continue to be discovered and their biosynthesis will be better understood with analysis at the genetic level. These natural products and their analogues and semi-synthetic variants exhibit a wide range of important biological activities. SAR studies have a focus of discovering NDA with low toxicity and a wider therapeutic window. There are many metabolic studies on *Aconitum* alkaloids, but to-date none has been reported on *Delphinium*. NDA are excellent proving grounds for fundamental aspects of analytical chemistry.

All of these continuing studies turn out to be based on the stellar contributions of Professor S. William Pelletier (1924-2004) who thought deeply and published widely in this important research area.

## 8. References

- 1 Y. Shen, W.-J. Liang, Y.-N. Shi, E. J. Kennelly and D.-K. Zhao, *Nat. Prod. Rep.*, 2020, **37**, 763-796.
- 2 D. Cook, J. A. Pfister, J. R. Constantino, J. M. Roper, D. R. Gardner, K. D. Welch, Z. J. Hammond and B. T. Green, *J. Agric. Food Chem.*, 2015, **63**, 1220-1225.
- 3 G. Plinius, *Naturalis Historia*, 77 AD, Book 23/37, Chapter XIII, 426-427.
- 4 M. H. Benn and J. M. Jacyno, in: *Alkaloids: Chemical and Biological Perspectives*, 1983, vol. **1**, pp. 153-210.
- 5 Z. Zeng, A. M. A. Qasem, G. Kociok-Köhn, M. G. Rowan and I. S. Blagbrough, *RSC Advances*, 2020, **10**, 18797-18805 doi 10.1039/d0ra03811c
- 6 Z. Zeng, A. M. A. Qasem, T. J. Woodman, M. G. Rowan and I. S. Blagbrough, *ACS Omega*, 2020, **5**, 14116-14122 doi 10.1021/acsomega.0c01648
- 7 F.-P. Wang and Q.-H. Chen, *The C19-Diterpenoid Alkaloids*, in: *The Alkaloids: Chemistry and Biology*, Ed. G. A. Cordell, Elsevier, 2010, vol. 69, pp. 362-369 and references cited therein.
- 8 G. H. Zhou, L. Y. Tang, X. D. Zhou, T. Wang, Z. Z. Kou and Z. J. Wang, *J. Ethnopharmacol.*, 2015, **160**, 173-193.

- 9 G. Gu, translated A. Dubreuil and X. Dubreuil, *The Divine Farmer's Classic of Materia Medica* (200-250 A.D.), Foreign Languages Press, Beijing, 2015.
- 10 Chinese Pharmacopoeia Commission, *Pharmacopoeia of the People's Republic of China*, vol. 1, China Medical Science Press, Beijing, 2015 edn (in Chinese).
- 11 Chinese Pharmacopoeia Commission, People's Republic of China Ministry of Health, *Drug Standards: Pharmaceutics of Chinese Medicine Prescriptions* (vol. 8), Beijing, 1993 edn (in Chinese).
- 12 Chinese Pharmacopoeia Commission, People's Republic of China Ministry of Health, *Drug Standards: Tibetan Medicine* (vol. 1), Beijing, 1995 edn (in Chinese).
- 13 S. Rahman, R. Ali Khan and A. Kumar, *BMC Complement. Altern. Med.*, 2002, **2**, 6.
- 14 B. Jiang et al., *J. Nat. Prod.*, 2012, **75**, 1145-1159.
- 15 Y. T. Tai, C. P. Lau, K. Young and P. H. But, *Lancet*, 1992, **340**, 1254-1256.
- 16 X.-X. Liu, X.-X. Jian, X.-F. Cai, R.-B. Chao, Q.-H. Chen, D.-L. Chen, X.-L. Wang and F.-P. Wang, *Chem. Pharm. Bull.*, 2012, **60**, 144-149.
- 17 A. Ameri, *Prog. Neurobiol.*, 1998, **56**, 211-235.
- 18 A. Ameri, *Brain Res.*, 1997, **769**, 36-43.
- 19 F. Dzhakhangirov, M. Sultankhodzhaev, B. Tashkhodzhaev and B. Salimov, *Chem. Nat. Compd.*, 1997, **33**, 190-202.
- 20 J. Friese, J. Gleitz, U. T. Gutser, J. F. Heubach, T. Matthiesen, B. Wilffert and N. Selve, *Eur. J. Pharmacol.*, 1997, **337**, 165-174.
- 21 D. Y. Zhu, D. L. Bai and X. C. Tang, *Drug Develop. Res.*, 1996, **39**, 147-157.
- 22 W. R. Dunstan and W. H. Ince, *J. Chem. Soc. Trans.*, 1891, **59**, 271-287.
- 23 L. H. Keith and S. W. Pelletier, in: *Chemistry of the Alkaloids*, ed. S. W. Pelletier, Van Nostrand Reinhold, New York, 1970, pp. 549-590.
- 24 Y. Li, Y. X. Li, M. J. Zhao, A. Yuan, X. H. Gong, M. J. Zhao and C. Peng, *Eur. J. Drug Metab. Pharmacokinet.*, 2017, **42**, 441-451.
- 25 M. Murayama, T. Mori, H. Bando and T. Amiya, *J. Ethnopharmacol.*, 1991, **35**, 159-164.
- 26 M. E. Adams and B. M. Olivera, *Trends Neurosci.*, 1994, **17**, 151-155.
- 27 T. F. Li, N. Gong and Y. X. Wang, *Front. Pharmacol.*, 2016, **7**, 367.
- 28 D. X., Lu, X. Guo and X. C. Tang, *Acta Pharmacol. Sin.*, 1988, **9**, 216-220.
- 29 C. F. Wang, P. Gerner, S. Y. Wang and G. K. Wang, *Anesthesiology*, 2007, **107**, 82-90.

- 30 H. Q. Zhu, J. Xu, K. F. Shen, R. P. Pang, X. H. Wei and X. G., Liu, *Exp. Neurol.*, 2015, **273**, 263-272.
- 31 H. V. Rosendahl, *J. Pharm.*, 1896, **4**, 262-266.
- 32 J. Singhuber, M. Zhu, S. Prinz and B. Kopp, *J. Ethnopharmacol.*, 2009, **126**, 18-30.
- 33 N. Mollov, M. Tada and L. Marion, *Tetrahedron Lett.*, 1969, **10**, 2189-2192
- 34 F.-P. Wang, Q.-H. Chen, X.-T. Liang, in: *The Alkaloids: Chemistry and Biology* (vol. 67), ed. G. A. Cordell, Elsevier, Amsterdam, 2009, ch. 1, pp. 1-73.
- 35 Y. V. Vakhitova, E. I. Farafontova, R. Y. Khisamutdinova, V. M. Yunusov, I. P. Tsypysheva and M. S. Yunusov, *Russ. J. Bioorg. Chem.*, 2013, **39**, 92-101.
- 36 D. E. Zaurov, I. V. Belolipov, A. G. Kurmukov, I. S. Sodobekov, A. A. Akimaliev and S. W. Eisenman, in: *Medicinal Plants of Central Asia: Uzbekistan and Kyrgyzstan*, eds. S. W. Eisenman, D. E. Zaurov and L. Struwe, Springer, New York, 2013, ch. 5, pp. 15-273.
- 37 M. S. Yunusov, *Russ. Chem. Bull.*, 2011, **60**, 633-638,
- 38 T. M. Gabbasov, E. I. Andrianova, S. F. Petrova, S. P. Ivanov, E. M. Tsyrlina, A. Z. Sadikov, S. S. Sagdullaev and M. S. Yunusov, *Chem. Nat. Compd.*, 2020, **56**, 767-770.
- 39 I. B. Chernikova, T. M. Gabbasov, E. M. Tsyrlina and M. S. Yunusov, *Russ. Chem. Bull.*, 2021, **70**, 515-519
- 40 S. Ou, Y. D. Zhao, Z. Xiao, H. Z. Wen, J. Cui and H. Z. Ruan, *Neurochem. Int.*, 2011, **58**, 564-573.
- 41 J. S. S. Quintans, A. R. Antonioli, J. R. G. S. Almeida, V. J. Santana and L. J. Quintans, *Basic Clin. Pharmacol. Toxicol.*, 2014, **114**, 442-450.
- 42 F. M. Xie, H. C. Wang, J. H. Li, H. L. Shu, J. R. Jiang, J. P. Chang and Y. Y. Hsieh, *Biomed. Chromatogr.*, 1990, **4**, 43-46.
- 43 V. F. Hubschmann, *Schweizerische Wochenschrift fur Pharm.*, 1865, **3**, 269-271.
- 44 V. G. Dragendorff and H. Spohn, *Am. J. Pharm.*, 1884, **8**, 44.
- 45 R. H. F. Manske, *Can. J. Res.*, 1938, **16b**, 57-60.
- 46 J. A. Goodson, *J. Chem. Soc.*, 1943, 139-141.
- 47 S. Wonnacott, E. X. Albuquerque and D. Bertrand, *Methods Neurosci.*, 1993, 263-275.
- 48 G. E. Barrantes, A. T. Rogers, J. Lindstrom and S. Wonnacott, *Brain Res.*, 1995, **672**, 228-236.
- 49 A. R. L. Davies, D. J. Hardick, I. S. Blagbrough, B. V. L. Potter, A. J. Wolstenholme and S. Wonnacott, *Neuropharmacology*, 1999, **38**, 679-690.
- 50 O. E. Edwards and L. Marion, *Can. J. Chem.*, 1954, **32**, 1146-1148.

- 51 D. J. Hardick, I. S. Blagbrough, G. Cooper, B. V. L. Potter, T. Critchley and S. Wonnacott, *J. Med. Chem.*, 1996, **39**, 4860-4866.
- 52 F. I. Carroll, W. Ma, H. A. Navarro, P. Abraham, S. A. Wolckenhauer, M. Damaj and B. R., Martin, *Bioorg. Med. Chem.*, 2007, **15**, 678-685.
- 53 D. J. Hardick, G. Cooper, T. Scott-Ward, I. S. Blagbrough, B. V. L. Potter and S. Wonnacott, *FEBS Lett.*, 1995, **365**, 79-82.
- 54 M. A. Turabekova, B. F. Rasulev, F. N. Dzhakhangirov and S. I. Salikhov, *Environ. Toxicol. Pharmacol.*, 2008, **25**, 310-320.
- 55 J. D. Olsen, G. D. Manners and S. W. Pelletier, *Collect. Bot.*, 1990, **19**, 141-152.
- 56 G. D. Manners, K. E. Panter, M. H. Ralphs, J. A. Pfister, J. D. Olsen and L. F. James, *J. Agric. Food Chem.*, 1993, **41**, 96-100.
- 57 C. F. Kukel and K. R. Jennings, *Can. J. Physiol. Pharmacol.*, 1994, **72**, 104-107.
- 58 G. D. Manners, K. E. Panter and S. W. Pelletier, *J. Nat. Prod.*, 1995, **58**, 863-869.
- 59 G. D. Manners, K. E. Panter, J. A. Pfister, M. H. Ralphs and L. F. James, *J. Nat. Prod.*, 1998, **61**, 1086-1089.
- 60 K. E. Panter, G. D. Manners, B. L. Stegelmeier, S. Lee, D. R. Gardner, M. H. Ralphs, J. A. Pfister and L. F. James, *Biochem. Syst. Ecol.*, 2002, **30**, 113-128.
- 61 B. T. Green, J. W. Keele, G. L. Bennett, D. R. Gardner, C. A. Stonecipher, D. Cook and J. A. Pfister, *Toxicol.*, 2019, **165**, 31-39.
- 62 B. T. Green, J. W. Keele, D. R. Gardner, K. D. Welch, G. L. Bennett, D. Cook, J. A. Pfister, T. Z. Davis, C. A. Stonecipher, S. T. Lee and B. L. Stegelmeier, *J. Anim. Sci.*, 2019, **97**, 1424-1432.
- 63 K. D. Welch, B. T. Green, D. R. Gardner, D. Cook, J. A. Pfister and K. E. Panter, *J. Anim. Sci.*, 2012, **90**, 2394-2401.
- 64 Y. Wang, S. Wang, Y. Liu, L. Yan, G. Dou and Y. Gao, *J. Chromatogr. B: Anal. Technol. Biomed. Life Sci.*, 2006, **844**, 292-300.
- 65 L. Tang, L. Ye, C. Lv, Z. Zheng, Y. Gong and Z. Liu, *Toxicol. Lett.*, 2011, **202**, 47-54.
- 66 L. Ye, L. Tang, Y. Gong, C. Lv, Z. Zheng, Z. Jiang and Z. Liu, *Xenobiotica*, 2011, **41**, 46-58.
- 67 Y. Bi, X. Zhuang, H. Zhu, F. Song, Z. Liu and S. Liu, *Biomed. Chromatogr.*, 2015, **29**, 1027-1034.
- 68 M. Zhang, C.-S. Peng and X.-B. Li, *Toxicol. in vitro*, 2017, **45**, 318-333.
- 69 S. Yang, H. Zhang, R. C. Beier, F. Sun, X. Cao, J. Shen, Z. Wang and S. Zhang, *J. Pharm. Biomed. Anal.*, 2015, **110**, 1-11.

- 70 H. Zhang, M. Liu, W. Zhang, J. Chen, Z. Zhu, H. Cao and Y. Chai, *Biomed. Chromatogr.*, 2015, **29**, 1076-1083.
- 71 G. Tan, M. Liu, X. Dong, S. Wu, L. Fan, Y. Qiao, Y. Chai and H. Wu, *J. Pharm. Biomed. Anal.*, 2014, **96**, 187-196.
- 72 Z. Sui, N. Li, Z. Liu, J. Yan and Z. Liu, *Xenobiotica*, 2013, **43**, 628-635.
- 73 X. Fan, S. S. Yin, X. J. Li, K. Yang, L. Xu and K. Lan, *Eur. J. Drug Metab. Pharmacokinet.*, 2017, **42**, 857-869.
- 74 W. J. Yun, Z. H. Yao, C. L. Fan, Z. F. Qin, X. Y. Tang, M. X. Gao, Y. Dai and X. S. Yao, *J. Chromatogr. B: Anal. Technol. Biomed. Life Sci.*, 2018, **1090**, 56-64.
- 75 Y. Liu, H. Sun, C. Li, Z. Pu, Z. Wu, M. Xu, X. Li, Y. Zhang, H. Li, J. Dong, R. Bi, H. Xie and D. Liang, *Xenobiotica*, 2021, **51**, 345-354.
- 76 B. Fan, S. Xu, J. Bi, S. Huang, Z. Zu and C. Qian, *ACS Pharmacol. Transl. Sci.*, 2021, **4**, 118-127.
- 77 F. Xie, H. Wang, H. Shu, J. Li, J. Jiang, J. Chang and Y. Hsieh, *J. Chromatogr. B: Biomed. Sci. Appl.*, 1990, **526**, 109-118.
- 78 H. G. Zhang, Y. Sun, M. Y. Duan, Y. J. Chen, D. F. Zhong and H. Q. Zhang, *Toxicol.*, 2005, **46**, 500-506.
- 79 F. Xie, H. Wang, J.-H. Li, H.-L. Shu, J.-R. Jiang, J.-P. Chang and Y.-Y. Hsieh, *Biomed. Chromatogr.*, 1990, **4**, 43-46.
- 80 B. Borcsa, U. Widowitz, D. Csupor, P. Forgo, R. Bauer and J. Hohmann, *Fitoterapia*, 2011, **82**, 365-368.
- 81 X. Guo and X. C. Tang, *Acta Pharmacol. Sin.*, 1990, **11**, 107-112.
- 82 M. S. Yunusov, *Russ. Chem. Bull.*, 2011, **60**, 633-638.
- 83 J. Lu, J.-B. Xu, X. Li, X.-L. Zhou, C. Zhang and F. Gao, *Chem. Pharm. Bull.*, 2021, **69**, 811-816.
- 84 L.-X. Wan, J.-F. Zhang, Y.-Q. Zhen, L. Zhang, X. Li, F. Gao and X.-L. Zhou, *J. Nat. Prod.*, 2021, **84**, 1067-1077.
- 85 N. Ablajan, B. Zhao, J.-Y. Zhao, B.-L. Wang, S. S. Sagdullaev and H. A. Aisa. *Phytochemistry*, 2021, **181**, 112567. doi: 10.1016/j.phytochem.2020.112567
- 86 S. Liu, C. Lai, Y. Long, W. Yang, Q. Ren, L. Huang and J. Chen, *J. Chromatography A*, 2021, **1652**, 462362.
- 87 P. A. Coates, I. S. Blagbrough, M. G. Rowan, B. V. L. Potter, D. P. J. Pearson and T. Lewis, *Tetrahedron Lett.*, 1994, **35**, 8709-8712.

- 88 G. Grangier, W. J. Trigg, T. Lewis, M. G. Rowan, B. V. L. Potter and I. S. Blagbrough, *Tetrahedron Lett.*, 1998, **39**, 889-892.
- 89 D. Barker, M. A. Brimble, M. McLeod, G. P. Savage and D. J. Wong, *J. Chem. Soc., Perkin Trans. I*, 2002, 924-931.
- 90 C. Brocke, M. A. Brimble, D. S.-H. Lin and M. D. McLeod, *Synlett*, 2004, 2359-2363.
- 91 M. A. Brimble and C. Brocke, *Eur. J. Org. Chem.*, 2005, 2385-2396.
- 92 K. J. Goodall, D. Barker and M. A. Brimble, *Synlett*, 2005, 1809-1827.
- 93 K. J. Goodall, M. A. Brimble and D. Barker, *Magn. Reson. Chem.*, 2006, **44**, 980-983.
- 94 I. S. Blagbrough, D. J. Hardick, S. Wonnacott and B. V. L. Potter, *Tetrahedron Lett.*, 1994, **35**, 3367-3370.
- 95 D. J. Hardick, I. S. Blagbrough, S. Wonnacott and B. V. L. Potter, *Tetrahedron Lett.*, 1994, **35**, 3371-3374.
- 96 D. J. Hardick, I. S. Blagbrough and B. V. L. Potter, *J. Am. Chem. Soc.*, 1996, **118**, 5897-5903.
- 97 P. Whiteaker, A. R. L. Davies, M. J. Marks, I. S. Blagbrough, B. V. L. Potter, A. J. Wolstenholme, A. C. Collins and S. Wonnacott, *Eur. J. Neurosci.*, 1999, **11**, 2689-2696.
- 98 R. J. Lind, D. J. Hardick, I. S. Blagbrough, B. V. L. Potter, A. J. Wolstenholme, A. R. L. Davies, M. S. Clough, F. G. P. Earley, S. E. Reynolds and S. Wonnacott, *Insect Biochem. Mol. Biol.*, 2001, **31**, 533-542.
- 99 Z. Zeng, G. Kociok-Köhn, T. J. Woodman, M. G. Rowan and I. S. Blagbrough, *ACS Omega*, 2021, **6**, 12769-12786.
- 100 Z. Zeng, G. Kociok-Köhn, T. J. Woodman, M. G. Rowan and I. S. Blagbrough, *Eur. J. Org. Chem.*, 2021, 2169-2179.

## Chapter 2

### Isolation of norditerpenoid alkaloids from *Delphinium elatum*

#### INTRODUCTION

Norditerpenoid alkaloids (NDA), the main alkaloid components of *Delphinium* and *Aconitum* plants, are a group of natural products with a complex hexacyclic system which display important and interesting pharmacological activities.<sup>1</sup> *Delphinium* extracts are well known for their pediculicide activity.<sup>2</sup> *D. elatum* is a well-known species that has been investigated extensively to discover new NDA, where recently Wada and co-workers discovered eleven new NDA with the characteristic 7,8-methylenedioxy moiety<sup>3</sup> and methylsuccinimidebenzoate esters of lycoctonine. This study reports the phytochemical investigation of *D. elatum* seeds which resulted in the isolation of four NDA (Fig. 1): methyllycaconitine (MLA) **1**, shawurensine A **2**, shawurensine B **3**. The alkaloids **2** and **3** have been compared to the reported delavaines **4** and delsemines **5**. In addition, this study reports the isolation of delpheline **6**.

MLA **1** was first reported by Manske in 1938 from *D. brownii* Rydb.<sup>4</sup> and Goodson (1943) confirmed the structure of MLA **1**, isolated from *D. elatum* seeds be a 2-*S*-methylsuccinimidobenzoate ester of lycoctonine.<sup>5</sup> MLA **1** is a potent competitive antagonist at  $\alpha 7$  nAChRs<sup>6</sup> where a rare pharmaceutical preparation, mellictin, was reported in a few countries, Uzbekistan and Kyrgyzstan to be used clinically to treat Parkinson's disease (PD) and cerebral palsy.<sup>7</sup> Shawurensine has a similar structure to MLA, but with the imide ring opened with water (hydrolysis) as a side-chain. Isolation of shawurensine A **2** was reported<sup>8</sup> and in this study we report the complete corrected and unambiguous NMR assignments. In addition, an isomer of shawurensine A **2** was isolated and is reported for the first time, shawurensine B **3**. The importance of the open side-chain was reported<sup>9</sup> where it was found that delavaines **4** (LD<sub>50</sub> = 3.3  $\mu$ g/kg) are more potent than MLA **1** (LD<sub>50</sub> = 7.5  $\mu$ g/kg) when tested in mice. Delsemines **5** were found to be slightly less potent than MLA **1** when tested on frog muscles preparation.<sup>9</sup> The activity of delsemines **5** and MLA **1** were also compared on rat brain membranes where



delsemines **5** were less potent by 200-fold than MLA **1**, and in house fly brain membrane by 10-folds.<sup>9</sup> Shawurensine A **2** antifeedant activity was found to be better than MLA **1** against larvae of *Spodoptera exigua* (Hübner).<sup>10</sup>

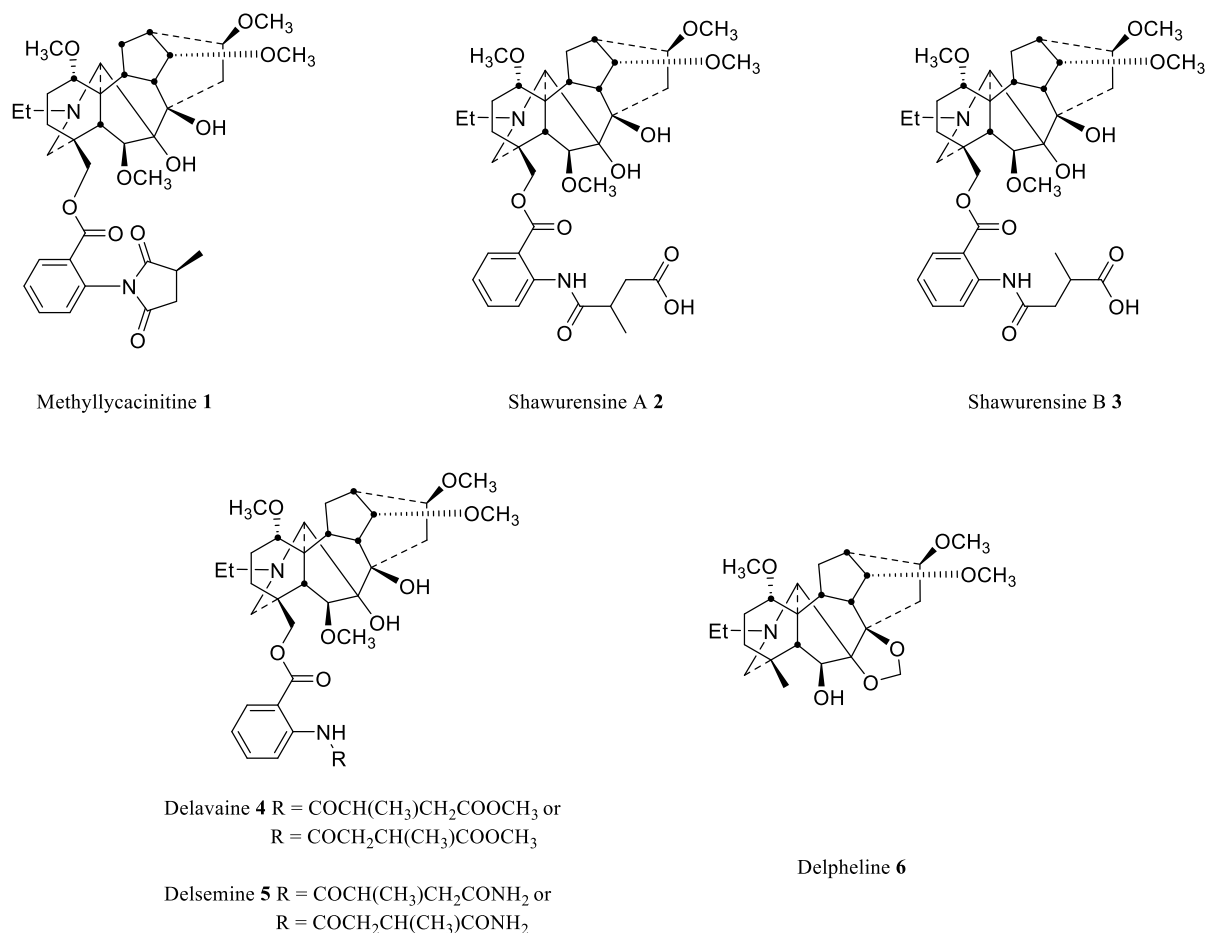


Fig. 1. Selected lycoctonine-type norditerpenoid alkaloids.

## RESULTS and DISCUSSION

### 1. Isolation of methyllycaconitine **1**

HRMS data of MLA **1** [M+H]<sup>+</sup> (C<sub>37</sub>H<sub>51</sub>N<sub>2</sub>O<sub>10</sub>) requires 683.3544 and was found 683.3548.

NMR data and full assignment are listed in Table 1, consistent with the literature.<sup>11</sup> The <sup>1</sup>H

NMR showed the presence of four methoxy groups that have been assigned using 2D NMR at

position 1, 6, 14, and 16. The data also showed the presence of the N-ethyl group. The <sup>1</sup>H-<sup>15</sup>N

HMBC has a correlation between the tertiary nitrogen and the triplet signal of the NCH<sub>2</sub>CH<sub>3</sub>

methyl group, where the tertiary nitrogen resonates at  $\delta_N$  47.00 ppm. The imide nitrogen does not show a correlation in the  $^1\text{H}$ - $^{15}\text{N}$  HMBC to the succinimide protons.

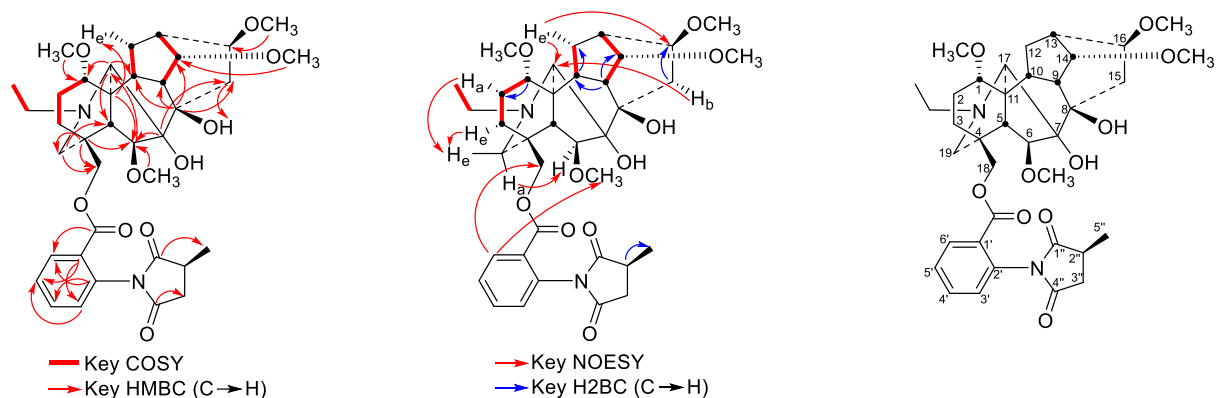


Table 1. NMR assignment of MLA 1

Carbon	$\delta_C$	$\delta_H$ , multiplicity ( $J$ , in Hz; orientation or label*)	key HMBC (C→H)	key NOESY
1	83.86 <sup>[a]</sup>	2.96, d (10.0, 7.3; $\alpha$ , $\beta$ )	-	-
2	26.00	2.06, m ( $\epsilon$ , $\beta$ ) <sup>[a]</sup>	-	-
		2.14, m ( $\alpha$ , $\alpha$ ) <sup>[a]</sup>	-	19- $H_e$
3	31.97	1.52, m ( $\alpha$ , $\beta$ ) <sup>[a]</sup>	-	19- $H_e$
		1.72, m ( $\epsilon$ , $\alpha$ ) <sup>[a]</sup>	-	-
4	37.41	-	6-H, 18-H (A, B), 19-H ( $\alpha$ , $\epsilon$ )	-
5	50.00	1.69, br s ( $\beta$ )	-	-
6	90.67	3.84, s ( $\alpha$ )	17-H	19- $H_a$
7	88.36	-	6-H, 15-H (f, b)	-
8	77.42	-	9-H, 10-H, 14-H, 15-H (f, b)	-
9	43.11	3.03, m ( $\beta$ ) <sup>[a]</sup>	-	-
10	45.96	1.92, dt (12.0, 6.0; $\beta$ )	-	-
11	48.91	-	5-H, 6-H, 12- $H_{e'}$	-
12	28.54	2.43, m ( $\epsilon'$ , $\alpha$ ) <sup>[a]</sup>	-	16-H, 17-H
		1.83, m ( $\alpha'$ , $\beta$ ) <sup>[a]</sup>	-	-
13	37.98	2.31, dd (7.4, 4.6; $\epsilon'$ , $\beta$ )	-	-

14	83.79 <sup>[a]</sup>	3.57, t (4.7; $\beta$ )	-	-
15	33.45	1.65, dd (15.3, 6.9; f, $\beta$ )	8-OH	-
		2.58, dd (15.3, 8.9; b, $\alpha$ )		17-H
16	82.46	3.19, t (7.5; $\alpha$ )	-	12-H <sub>e'</sub>
17	64.35	2.91, br s (e)	1-H, 5-H, 10-H	12-H <sub>e'</sub> , 15-H <sub>b</sub>
18	69.35	4.04, d (11.2, HA)	-	-
		4.10, d (11.2, HB)		6'-H
19	52.19	2.40, d (12.0; a)	5-H, 18-H (A, B)	6-H
		2.68, d (12.0. e)		2-H <sub>a</sub> , 3-H <sub>e</sub>
NCH <sub>2</sub> CH <sub>3</sub>	50.87	2.79, dt (13.0, 7.0; HA)	-	-
		2.90, m (HB) <sup>[a]</sup>		-
NCH <sub>2</sub> CH <sub>3</sub>	13.93	1.03, t (7.1)	-	-
1-OMe	55.67	3.23, d (0.9)	1-H	-
6-OMe	57.99	3.33, br s	6-H	6'-H
14-OMe	57.68	3.38, d (1.1)	14-H	-
16-OMe	56.16	3.32, d (1.0)	16-H	-
OCO	164.00 <sup>[a]</sup>	-	6'-H	-
1'	126.91 <sup>[a]</sup>	-	3'-H, 5'-H	-
2'	132.90	-	4'-H, 6'-H	-
3'	129.91	7.25, d (7.8)	5'-H	-
4'	133.52	7.66, t (7.8)	-	-
5'	129.29	7.52, t (7.8)	-	-
6'	130.93	8.02, d (7.8)	-	18-HB, 6-OMe
1''	179.76	-	5''-CH <sub>3</sub>	-
2''	35.08	3.03, m	-	-
3''	36.88	2.50, m (HA) <sup>[a]</sup>	-	-
		3.07, m (HB) <sup>[a]</sup>		-
4''	175.77	-	3''-H	-
5''	17.81	1.43, m	-	-
8-OH	-	3.99, br s	-	-

\* a: axial, e: equatorial, a': pseudoaxial, e': pseudoequatorial, f: flagpole, b: bowsprit.

[a] The accurate  $\delta_{\text{H}}$  or  $\delta_{\text{C}}$  was recorded from HSQC, HMBC or H2BC as  $^1\text{H}/^{13}\text{C}$  1D spectra signals are overlapped or weak signals.

## 2. Isolation of shawurensine A **2**

HRMS data of shawurensine A **2**  $[\text{M}+\text{H}]^+$  ( $\text{C}_{37}\text{H}_{53}\text{N}_2\text{O}_{11}$ ) requires 701.3649, found 701.3643.

NMR data (Table 2) were very similar to MLA **1**, where 4 methoxy groups were detected and assigned at positions 1, 6, 14, and 16. An N-ethyl group was detected. The aromatic protons where an observed difference compared to MLA **1**, where protons 4', 5', and 6' showed lower chemical shifts compared to those in MLA **1**, while proton 3' is shifted downfield to resonate at 8.70 ppm (the highest aromatic proton) while it was the lowest aromatic proton in MLA **1** (resonates at 7.25 ppm) and that indicates the change of the substitution at position 2' from imide to amide moiety. The amide moiety affects position 3' significantly as the calculated chemical shift <sup>12</sup> puts the carbon at ~112 ppm and the proton ~7.5 ppm and these values are lower than the ones observed.

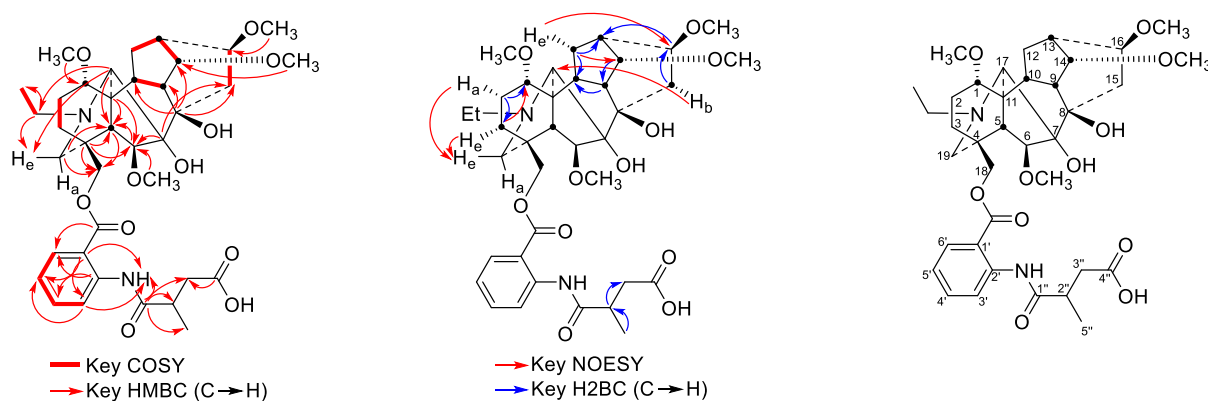


Table 2. NMR assignment of shawurensine A **2**

Carbon	$\delta_{\text{C}}$	$\delta_{\text{H}}$ , multiplicity ( $J$ , in Hz; orientation or label*)	key HMBC (C→H)	key NOESY
1	83.83 <sup>[a]</sup>	3.01, m (a, $\beta$ ) <sup>[a]</sup>	-	3- $\text{H}_{\text{a}}$
2	25.94	2.09, m (e, $\beta$ ) <sup>[a]</sup>	-	-

		2.16, m (a, $\alpha$ ) <sup>[a]</sup>		19-He
3	31.97	1.53, m (a, $\beta$ ) <sup>[a]</sup>	-	H-1
		1.81, m (e, $\alpha$ ) <sup>[a]</sup>		19-He
4	37.48	-	5-H, 6-H, 18-H (A, B)	-
5	50.26	1.72, br s ( $\beta$ )	18-H (A, B)	-
6	90.78	3.92, s ( $\alpha$ )	5-H	-
7	88.41	-	15-H (f, b)	-
8	77.55	-	9-H, 10-H, 14-H, 15-H (f, b)	-
9	43.18	3.08, dd (7.2, 4.6; $\beta$ )	-	-
10	45.97	1.96, m ( $\beta$ ) <sup>[a]</sup>	-	-
11	49.02	-	5-H, 6-H	-
12	28.65	2.45, m (e', $\alpha$ ) <sup>[a]</sup>	-	16-H
		1.86, m (a', $\beta$ ) <sup>[a]</sup>		14-H
13	38.00	2.34, dd (7.6, 4.6; e', $\beta$ )	-	-
14	83.80 <sup>[a]</sup>	3.61, t (4.6; $\beta$ )	-	12-H <sub>a'</sub>
15	33.58	1.68, dd (15.2, 7.0; f, $\beta$ )	-	-
		2.61, dd (15.2, 8.8; b, $\alpha$ )		17-H
16	82.50	3.22, t (8.0; $\alpha$ )	-	12-He'
17	64.45	2.96, m (e) <sup>[a]</sup>	5-H, 19-He, NCH <sub>2</sub> CH <sub>3</sub>	15-H <sub>b</sub>
18	69.73	4.17, d (11.2, HA)	-	-
		4.21, d (11.2, HB)		-
19	52.39	2.48, m (a) <sup>[a]</sup>	5-H, 18-H (A, B)	2-H <sub>a</sub> , 3-He
		2.76, d (11.4; e)		-
NCH <sub>2</sub> CH <sub>3</sub>	50.96	2.83, m (HA) <sup>[a]</sup>	19-He, NCH <sub>2</sub> CH <sub>3</sub>	-
		2.95, m (HB) <sup>[a]</sup>		-
NCH <sub>2</sub> CH <sub>3</sub>	13.97	1.07, t (7.2)	-	-
1-OMe	55.79	3.26, s	1-H	-
6-OMe	58.04	3.38, s	6-H	-
14-OMe	57.77	3.41, s	14-H	-
16-OMe	56.26	3.34, s	16-H	-
OCO	167.87	-	6'-H	-
1'	114.78	-	NHCO, 3'-H, 5'-H	-
2'	141.83	-	4'-H, 6'-H	-

3'	120.65	8.70, d (8.0)	NHCO, 5'-H	-
4'	134.72	7.54, td (8.0, 1.6)	-	-
5'	122.41	7.10, t (8.0)	-	-
6'	130.21	7.96, dd (8.0, 1.6)	-	-
NHCO	-	11.14, s	-	-
1''	174.96	-	NHCO, 2''-H, 3''-H (A, B), 5''-H	-
2''	39.35	2.96, m [a]	-	-
3''	38.66[a]	2.46, m (HA) [a] 2.82, m (HB) [a]	-	-
4''	175.91[a]	-	3''-H (A, B)	-
5''	17.85	1.33, d (7.1)	-	-

\* a: axial, e: equatorial, a': pseudoaxial, e': pseudoequatorial, f: flagpole, b: bowsprit.

[a] The accurate  $\delta_{\text{H}}$  or  $\delta_{\text{C}}$  was recorded from HSQC, HMBC or H2BC as  $^1\text{H}/^{13}\text{C}$  1D spectra signals are overlapped or weak signals.

The assignment reported in this study corrects some signals reported by Gu et al. (2007) as carbon 5 and 9 were reported<sup>8</sup> at 43.3 and 50.4 ppm respectively while based on 2D NMR, they should be swapped and carbon 5 resonates at 50.26 ppm based on the HMBC correlation to the protons at position 18 and correlation from adjacent carbons to the proton at position 5 (Fig. 2 upper). Carbon 9 assigned at 43.18 ppm based on the COSY correlation of 9-H with 10-H (Fig. 2 lower) and the H2BC correlation from carbon 14 to 9-H and from carbon 9 to 10-H (see blue arrows above Table 2). Carbon 10 and 13 were reported at 38.4 and 45.9 ppm and based on 2D NMR, they should be swapped based on COSY (Fig. 2 lower) and H2BC correlations as reported in Table 2. The carbon signals of 6-OMe and 14-OMe are very close where Gu et al. (2007)<sup>8</sup> assign 6-OMe as the lower value while the HMBC spectrum showed that 14-OMe comes at 57.77 ppm followed by 6-OMe at 58.04 ppm (Fig. 2 upper). The aromatic protons were assigned in the wrong order<sup>8</sup> ( $4' < 5' < 3' < 6'$ ) and they have been corrected based on HSQC, HMBC, and COSY spectra to be  $5' < 4' < 6' < 3'$  (Fig. 2).

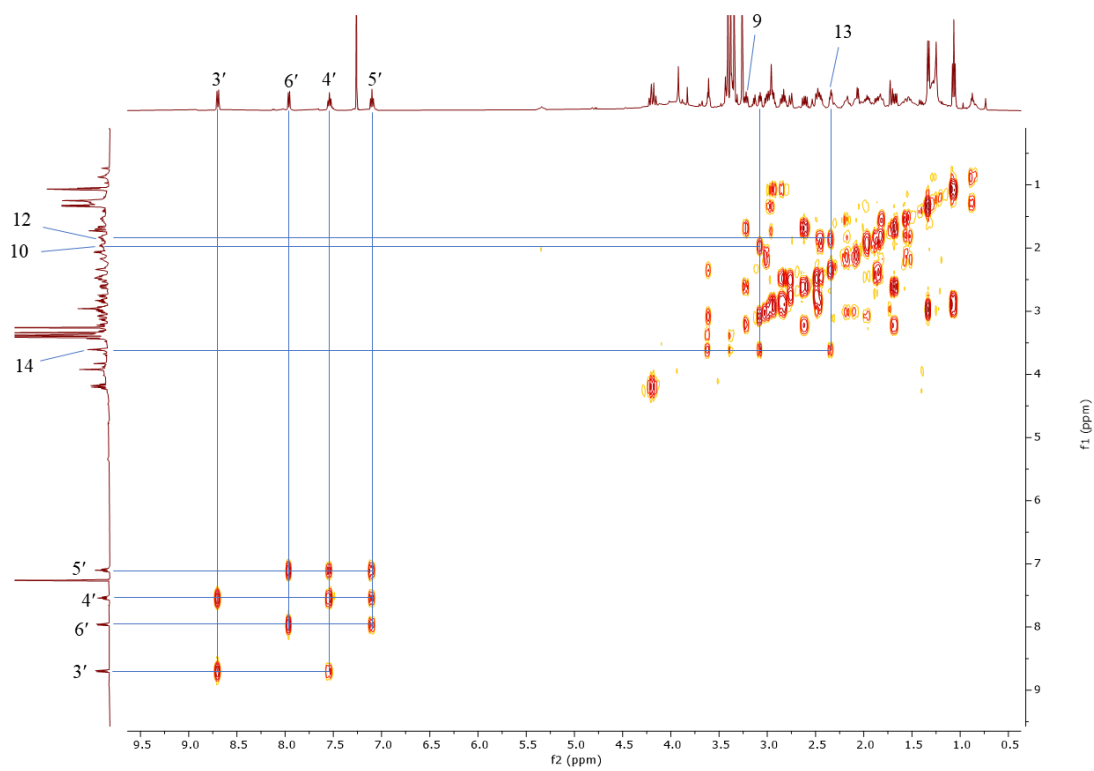
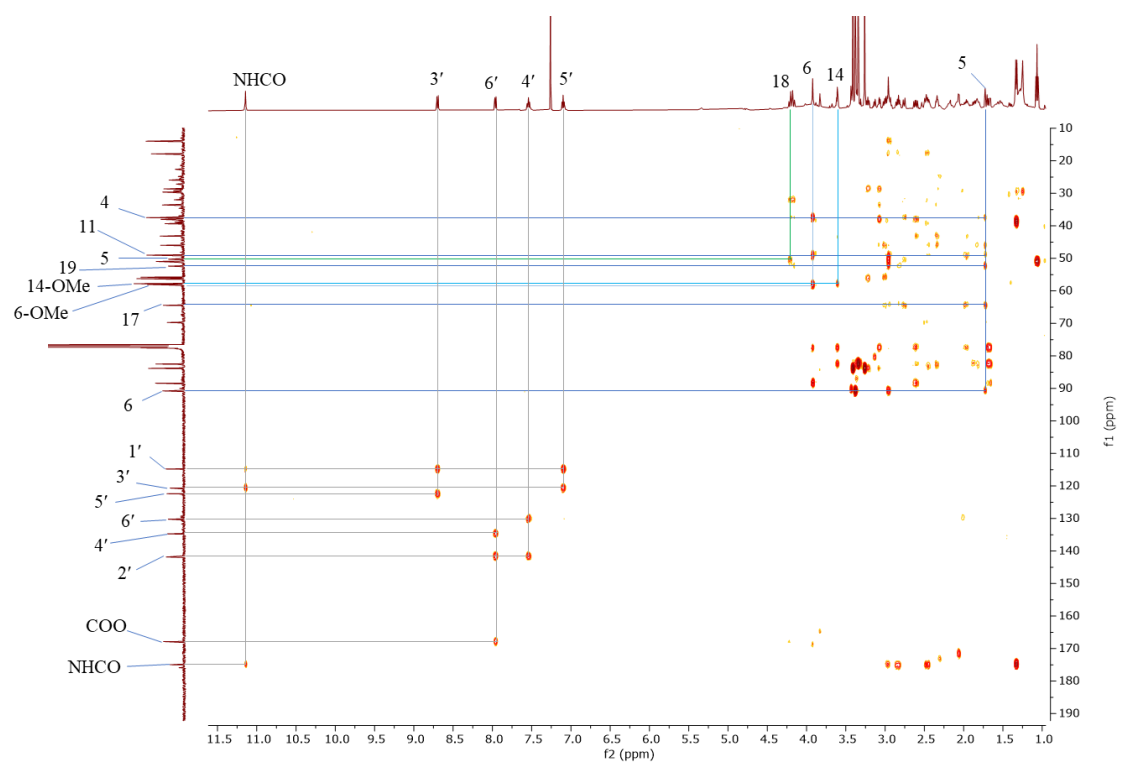


Fig. 2. HMBC (upper) and COSY (lower) of shawurensine A 2

The amide NH signal has correlation in the  $^1\text{H}$ - $^{15}\text{N}$  HMBC (Fig. 3) with a nitrogen at  $\delta_{\text{N}}$  137.30 which is an atypical value for secondary amides and that suggests that MLA **1** side chain has been opened to give Shawurensine A **2**. The spectrum below shows a one bond coupling for the N-H correlation and appeared as a doublet ( $J = 90$  Hz). In addition, the tertiary nitrogen shows correlation with the triplet signal of the  $\text{NCH}_2\text{CH}_3$  methyl group (Fig. 3) and resonates at  $\delta_{\text{N}}$  48.00 ppm.

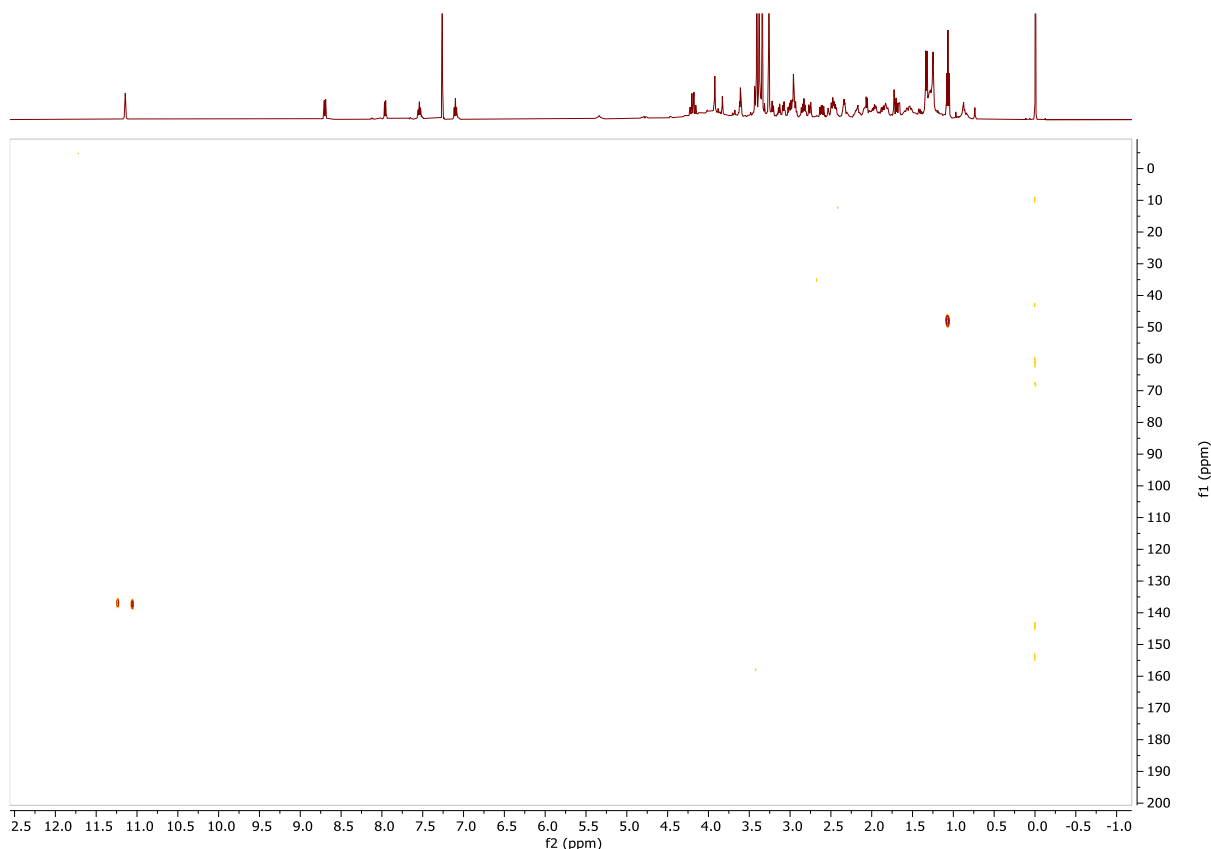


Fig. 3. The  $^1\text{H}$ - $^{15}\text{N}$  HMBC spectrum of shawurensine A **2**.

### 3. Isolation of shawurensine B **3**

HRMS data of shawurensine B **3**  $[\text{M}+\text{H}]^+$  ( $\text{C}_{37}\text{H}_{53}\text{N}_2\text{O}_{11}$ ) requires 701.3649 and was found 701.3644. NMR data (Table 3) are very similar to shawurensine A **2**, where the chemical shift of the protons at positions 1, 3, 17, 18 and the methylene of the N-ethyl group has increased compared to shawurensine A **2**. The carbon signal of carbons 1'' and 4'' were almost overlapped. The amide NH signal has a correlation in the  $^1\text{H}$ - $^{15}\text{N}$  HMBC with a nitrogen at  $\delta_{\text{N}}$  137.27 and showed a one bond coupling for the N-H correlation and appeared as a doublet ( $J = 90$  Hz). In



addition, the tertiary nitrogen correlates with the triplet signal of the  $NCH_2CH_3$  methyl group and resonates at  $\delta_N$  49.44 ppm.

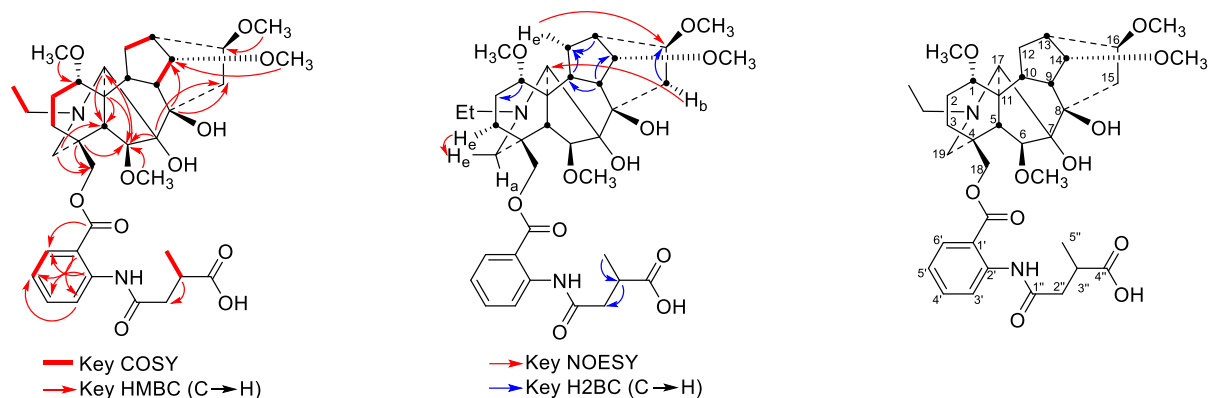


Table 3. NMR assignment of shawurensine B 3

Carbon	$\delta_C$	$\delta_H$ , multiplicity ( $J$ , in Hz; orientation or label*)	key HMBC (C→H)	key NOESY
1	83.31 <sup>[a]</sup>	3.10, m (a, $\beta$ ) <sup>[a]</sup>	-	-
2	25.31	2.10-2.22, m	-	-
3	31.97	1.60, m (a, $\beta$ ) <sup>[a]</sup>	-	19-H <sub>e</sub>
		1.87, m (e, $\alpha$ ) <sup>[a]</sup>	-	-
4	37.52	-	6-H, 18-H (A, B)	-
5	50.26	1.77, br s ( $\beta$ )	-	-
6	90.67	3.96, m ( $\alpha$ ) <sup>[a]</sup>	17-H	-
7	88.17	-	6-H, 15-H (f, b)	-
8	77.77	-	14-H, 15-H (f, b)	-
9	43.23	3.08, m ( $\beta$ ) <sup>[a]</sup>	-	-
10	45.78	2.02, m ( $\beta$ ) <sup>[a]</sup>	-	-
11	49.24	-	5-H, 6-H	-
		2.29, m (e', $\alpha$ ) <sup>[a]</sup>	-	16-H
12	28.88	1.89, m (a', $\beta$ ) <sup>[a]</sup>	-	-
		2.29, m (e', $\alpha$ ) <sup>[a]</sup>	-	16-H
13	38.03	2.37, t (6.0; e', $\beta$ )	-	-
14	83.87 <sup>[a]</sup>	3.62, t (4.6; $\beta$ )	-	-
15	33.62	1.72, dd (15.2, 7.1; f, $\beta$ )	-	-
		2.62, m (b, $\alpha$ )	-	17-H

16	82.52	3.21, t (8.0; $\alpha$ )	-	12-He'
17	64.13	3.04, br s (e)	5-H	15-H <sub>b</sub>
18	69.65	4.16, d (11.1, HA)	-	-
		4.30, d (11.1, HB)		-
19	53.00	2.59, m <sup>[a]</sup>	5-H, 18-H (A, B)	-
NCH <sub>2</sub> CH <sub>3</sub>	51.10	2.98, m (HA) <sup>[a]</sup>	-	-
		3.09, m (HB) <sup>[a]</sup>		-
NCH <sub>2</sub> CH <sub>3</sub>	13.45 <sup>[a]</sup>	1.13, t (7.2)	-	-
1-OMe	55.89	3.29, s	1-H	-
6-OMe	58.17	3.39, s	6-H	-
14-OMe	57.84	3.41, s	14-H	-
16-OMe	56.35	3.35, s	16-H	-
OCO	167.95	-	6'-H	-
1'	115.00	-	3'-H, 5'-H	-
2'	141.53	-	4'-H, 6'-H	-
3'	120.86	8.68, d (8.4)	5'-H	-
4'	134.86	7.55, ddd (8.4, 7.3, 1.6)	-	-
5'	122.75	7.11, ddd (8.4, 7.3, 1.6)	-	-
6'	130.26	7.95, dd (8.4, 1.6)	-	-
NHCO	-	11.11, s	-	-
1''	174.65 <sup>[a]</sup>	-	-	-
2''	38.89	2.51, dd (16.7, 5.0; HA)	3''-H	-
		2.85, dd (16.7, 8.4; HB)		-
3''	37.80 <sup>[a]</sup>	2.97, m <sup>[a]</sup>	-	-
4''	174.68 <sup>[a]</sup>	-	-	-
5''	17.81	1.34, d (7.1)	-	-

\* a: axial, e: equatorial, a': pseudoaxial, e': pseudoequatorial, f: flagpole, b: bowsprit.

[a] The accurate  $\delta_{\text{H}}$  or  $\delta_{\text{C}}$  was recorded from HSQC, HMBC or H2BC as <sup>1</sup>H/<sup>13</sup>C 1D spectra signals are overlapped or weak signals.

It was reported in delavaines **5** and delsemines **6** that moving the methyl group in the side chain from position 2'' to 3'' will decrease the chemical shift of carbon 3'' due to shielding effect from the electron donating methyl group<sup>13</sup>. Carbon 3'' in shawurensine B **3** has lower chemical shift than that in shawurensine A **2** but an increase in 2'' was not observed.

The ESI-MS/MS fragmentation of shawurensine A and B shows characteristic fragments (Fig. 4). Shawurensine A **2** showed a 701 molecular peak  $[M+H]^+$  (84 %) while the base peak (100 %) corresponds to 699 which indicates a loss of a proton which could possibly be the acidic proton of the side-chain. Shawurensine B **3** showed a 701 molecular peak  $[M+H]^+$  (100 %) and 699 peak as second most abundant (95 %). Both compounds showed fragmentation of the ester side-chain (466). The fragmentation of amide linkage was quite different between both compounds as shawurensine A **2** showed higher fragment intensity and that indicates that the free radical intermediate is more stabilized due to the presence of two adjacent electron donating groups. The loss of the carboxylic acid moiety (655) was observed in shawurensine B **3** only (1%).

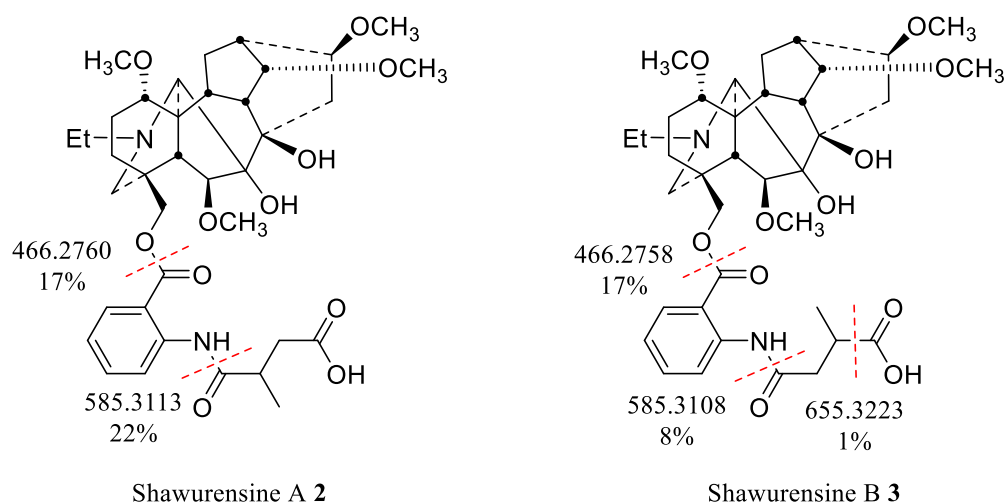


Fig. 4. Fragments of shawurensine A **2** and B **3** using ESI-MS/MS.

The observed differences in NMR and MS/MS fragmentation of shawurensine A **2** and B **3** suggests that carbon 5'' is next to the carboxylic acid end in shawurensine B **3**.

#### 4. Isolation of delpheline **6**

Delpheline **6** has a characteristic 7,8-methylenedioxy moiety where it was first isolated by Goodson (1943) using *D. elatum* seeds<sup>14</sup>. This study reports the X-ray crystal characterisation of delpheline **6** free base for the first time.

HRMS data of delpheline **6**  $[M+H]^+$  ( $C_{25}H_{40}NO_6$ ) requires 450.2856 and was found 450.2856. NMR data (Table 4) is consistent with the reported assignment<sup>15</sup> where it shows N-ethyl group and three methoxy groups at positions 1, 14, and 16. Two singlets appear 5.05 and 5.13 ppm corresponding to the methylenedioxy protons. The tertiary nitrogen shows correlation with the triplet signal of the  $NCH_2CH_3$  methyl group and resonates at 51.22 ppm.

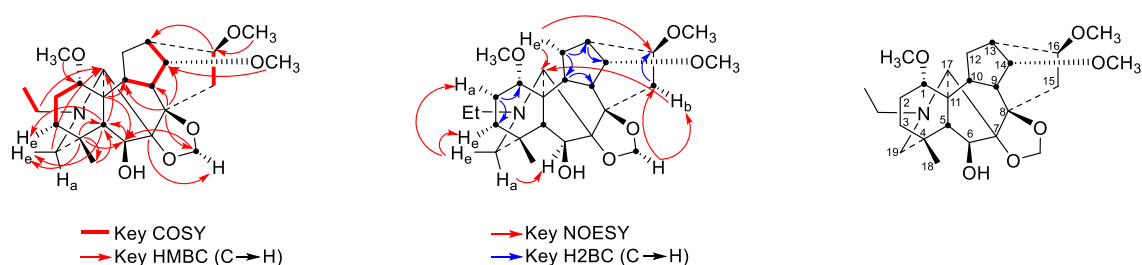


Table 3. NMR assignment of delpheline **6**

Carbon	$\delta_c$	$\delta_H$ , multiplicity ( $J$ , in Hz; orientation or label*)	key HMBC (C→H)	key NOESY
1	82.87 <sup>[a]</sup>	3.02, dd (10.0, 7.3; $\alpha$ , $\beta$ )	-	-
2	26.93	1.98-2.07, m ( $e$ , $\beta$ )	-	19- $H_e$
		2.14, m ( $\alpha$ , $\alpha$ ) <sup>[a]</sup>		
3	36.90	1.16-1.20, m ( $\alpha$ , $\beta$ )	-	19- $H_e$
		1.59, ddd (15.3, 5.2, 2.5; $e$ , $\alpha$ )		
4	33.88	-	5-H, 6-H, 18- $CH_3$ ,	-
		-	19- $H_e$	
5	56.71	1.21, s ( $\beta$ )	3- $H_e$ , 17-H, 19- $H_e$	-
6	79.25	4.2, s ( $\alpha$ )	5-H	19- $H_a$
7	92.72 <sup>[a]</sup>	-	$OCH_2O$ ( $\alpha$ )	-
8	84.07	-	9-H, 10-H, 14-H,	-
		-	$OCH_2O$ ( $\beta$ )	

9	40.40	3.64, dd (7.4, 5.1; $\beta$ )	-	-
10	47.85	2.12, m ( $\beta$ ) <sup>[a]</sup>	-	-
11	50.39 <sup>[a]</sup>	-	6-H, 10-H	-
12	28.09	2.56, dd (14.7, 4.9; e', $\alpha$ )	-	16-H, 17-H
		1.80, m (a', $\beta$ ) <sup>[a]</sup>		-
13	37.78	2.37, dd (7.3, 4.9; e', $\beta$ )	-	-
14	83.06 <sup>[a]</sup>	3.68, t (4.9; $\beta$ )	-	-
15	33.36	1.82, m (f, $\beta$ ) <sup>[a]</sup>	-	OCH <sub>2</sub> O ( $\alpha$ )
		2.49, dd (14.9, 8.9; b, $\alpha$ )		OCH <sub>2</sub> O ( $\alpha$ )
16	81.82	3.23, m ( $\alpha$ ) <sup>[a]</sup>	13-H	12-H <sub>e</sub> '
17	63.65	3.06, d (2.1; e)	-	12-H <sub>e</sub> '
18	25.35	0.92, s	5-H	-
19	57.29	2.24, dd (11.3, 2.1; a)	17-H	2-H <sub>a</sub> , 3-H <sub>e</sub>
		2.60-2.68, m (e)		6-H
NCH <sub>2</sub> CH <sub>3</sub>	50.57 <sup>[a]</sup>	2.60-2.68, m (HA)	-	-
		2.73-2.80, m (HB)		-
NCH <sub>2</sub> CH <sub>3</sub>	13.97	1.04, t (7.2)	-	-
1-OMe	55.56	3.26, s	1-H	-
16-OMe	56.26	3.35, s	16-H	-
14-OMe	57.82	3.43, s	14-H	-
OCH <sub>2</sub> O	92.87 <sup>[a]</sup>	5.05, s ( $\alpha$ )	-	15-H (f, b)
		5.13, s ( $\beta$ )		-
6-OH	-	3.37, s	-	-

\* a: axial, e: equatorial, a': pseudoaxial, e': pseudoequatorial, f: flagpole, b: bowsprit.

[a] The accurate  $\delta_{\text{H}}$  or  $\delta_{\text{C}}$  was recorded from HSQC, HMBC or H2BC as <sup>1</sup>H/<sup>13</sup>C 1D spectra signals are overlapped or weak signals.

In the NMR reported for delpheline **6** by Pelletier and co-workers<sup>15</sup>, the  $\beta$  proton of the methylenedioxy was assigned as the upfield one (5.02 ppm compared to 5.10 ppm of the  $\alpha$  proton). However, the NOE correlation reported here showed that of the methylenedioxy signals, the  $\alpha$  proton resonated with the lower chemical shift at 5.05 ppm and therefore the  $\beta$  is at 5.13 ppm (Fig. 5).

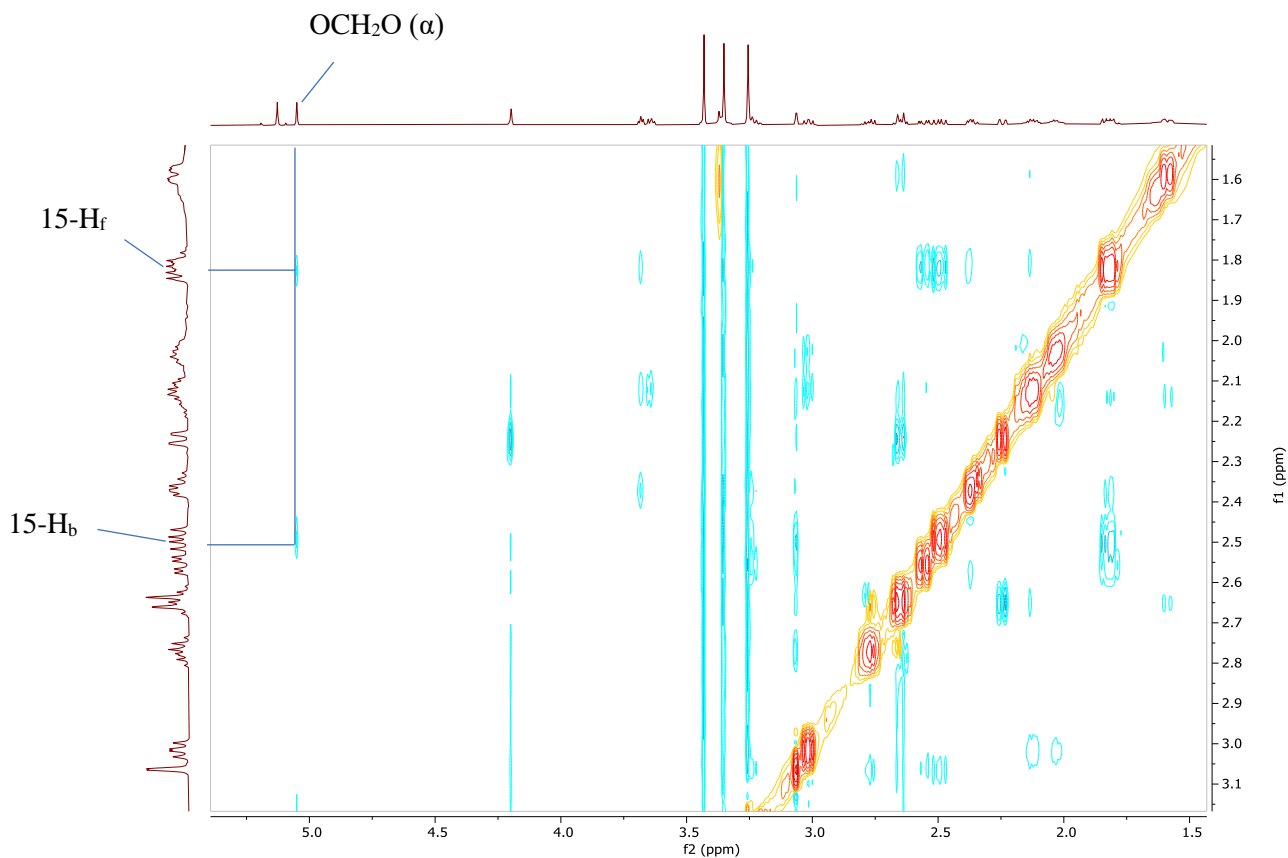


Fig. 5. NOE correlation between alpha proton of delpheline methylenedioxy group and 15-H (f, b)

The X-ray single crystal, which is the first reported for delpheline **6** free base, shows the proximity of the  $\alpha$ -proton of the methylenedioxy and protons at position 15 (Fig. 6).

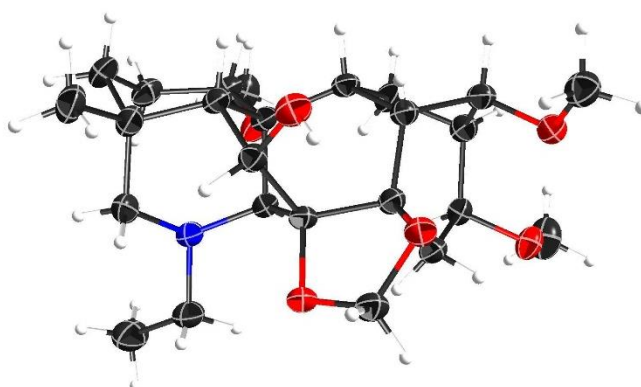


Fig. 6. X-ray of delpheline **6** free base.

## Experimental

### General Methods

*Chemicals and Materials.* *D. elatum* seeds were purchased from Thompson and Morgan company. Chloroform-d (99.8% D atom, CDCl<sub>3</sub>) was used for NMR experiments purchased from Cambridge Isotope Laboratories (U.S.A.). All other solvents were of HPLC grade, ≥99.9% purity (Fisher Scientific, U.K. and VWR, U.K.).

*Instrumentation.* Analytical thin layer chromatography (TLC) was performed using aluminium backed sheets of precoated silica gel plates (Merck Kieselgel 60 F254). Compounds were visualized by staining with iodine vapour, and Dragendorff solution (stock solution prepared by mixing bismuth subnitrate (1.7 g) with water (80 ml) and glacial acetic acid (20 ml). Potassium iodide solution (50% w/v, 100 ml) was added then and stirred until dissolved. The solution is kept in an amber bottle. The working solution is prepared by mixing the stock solution (100 ml) with glacial acetic acid (200 ml) and make up to volume (1 litre) with distilled water and stored in an amber bottle). Flash column chromatography Column chromatography was performed on RediSep prepacked columns with a Teledyne Isco CombiFlash instrument. The fragmentation study for shawurensine A and B was done using LC-MS analyses were performed using an Agilent QTOF 6545 with Jetstream ESI spray source coupled to an Agilent 1260 Infinity II Quat pump HPLC with 1260 autosampler, column oven compartment and variable wavelength detector (VWD). The MS was operated in positive ionization mode with the gas temperature at 250 °C, the drying gas at 12 L/min and the nebulizer gas at 45 psi (3.10 bar). The sheath gas temperature and flow were set to 350 °C and 12 L/min, respectively. The MS was calibrated using reference calibrant introduced from the independent ESI reference sprayer. The VCap, Fragmentor and Skimmer was set to 3500, 100 and 45 respectively. The MS was operated in all-ions mode with 3 collision energy scan segments at 0, 20 and 40 V. Data were compared at collision induced dissociation (CID) of 40 V. Chromatographic separation of a 5 µL sample injection was performed on a InfinityLab Poroshell 120 EC-C18 (3.0 x 50 mm, 2.7 µm) column using H<sub>2</sub>O (Merck, LC-MS grade) with 0.1 % formic acid (FA, Fluka) v/v and methanol (MeOH, VWR, HiPerSolv) with 0.1% FA v/v as mobile phase A and B, respectively. The column was operated at flow rate of 0.3 mL/min at 40°C starting with 1 % mobile phase B for 3

min, thereafter the gradient was initiated and ran for 2 min to a final 100% B, held at 100% B for 3 min then returned to 1% B, held for re-equilibration for 3.9 min in a total 12 min run time. The VWD was set to collect 254 and 320 nm wavelengths at 2.5 Hz. Data processing was automated in Qual B 07.00 with a Find by formula matching tolerance of 10 ppm. <sup>1</sup>H NMR spectra were recorded with a Bruker Avance III (500 MHz) spectrometer at 25 °C. Chemical shifts are given in parts per million (ppm) referenced to the residual solvent peak, and reported as position ( $\delta$ ), multiplicity (s = singlet, br = broad, d = doublet, dd = doublet of doublets, t = triplet, dt = doublet of triplets, td = triplet of doublet, m = multiplet), relative integral, assignment and coupling constant ( $J$  in Hz). <sup>1</sup>H-<sup>15</sup>N HMBC spectra were recorded on a Bruker Avance III (<sup>15</sup>N Larmor precession frequency 51 MHz) spectrometer at 25 °C. The spectra were externally calibrated with a MeNO<sub>2</sub> solution (50% in CDCl<sub>3</sub>, v/v), recorded, and set at  $\delta_N$  379.8 ppm, and the correction factor is measured as -511.72 on our spectrometer. High Resolution Time-of-Flight (HR TOF) mass spectra were obtained on a Bruker Daltonics "microTOF" mass spectrometer using electrospray ionisation (ESI) (loop injection +ve ion mode). The crystal was mounted onto a goniometer head and cooled to 150 K with an Oxford Cryosystem. Intensity data for s22phar2 were collected on a SuperNova, Dual, Cu at zero, EosS2 using a Cu microfocus source ( $\lambda = 1.54184$ ) Å. Unit cell determination, data collection, data reduction and a symmetry-related (multi-scan) absorption correction were performed using the CrysAlisPro software

The structure was solved with SHELXT and refined by a full-matrix least-squares procedure based on F (Shelxl-2018/3). All non-hydrogen atoms were refined anisotropically. Hydrogen atoms were placed onto calculated positions and refined using a riding model except for the OH hydrogen atoms which have been located in the difference Fourier map and were refined freely.

#### Extraction of *D. elatum* seeds

*D. elatum* seeds (500 g) were ground macerated for two days in isopropanol (3 L). This step was repeated five times and each extract was evaporated to dryness under reduced pressure at <45 °C using a vacuum rotary evaporator. Each extract was tested for the presence of alkaloids using Dragendorff reagent. The combined crude extract was accurately weighed (110 g). The extract



was suspended in water and extracted with petroleum ether (6 x 300 mL) to yield 78 g fraction. The extract then extracted with dichloromethane (8 x 300 mL) until the last extract showed negative result with Dragendorff reagent to yield around 30 gm fraction. The petroleum ether fraction and the dichloromethane fraction were partitioned between 0.1M aq. HCl (200 mL) and dichloromethane (400 mL). The organic layer was further extracted with aq. HCl (3 x 200 mL) until the last extract showed a negative result with Dragendorff's reagent. The combined aq. Layers were collected and made alkaline using saturated aq. sodium carbonate solution then partitioned against dichloromethane (6 x 300 mL) and the combined organic layers were dried (MgSO<sub>4</sub>), filtered, and then concentrated in vacuo to yield the extracts of (25 g) and (6 g) respectively.

The total alkaloid extract from the dichloromethane extract, was purified by column chromatography using silica gel and mobile phase dichloromethane: methanol (9.8:0.2) to (9:1) gradually in order of increasing polarity. five fractions were obtained, fraction 1 (150 mg) was identified as methyllycaconitine **1** ( $R_f = 0.27$  5% DCM / MeOH). Fraction 4 (30 mg) was identified as shawurensine A **2** ( $R_f = 0.55$  20% DCM / MeOH). Fraction 5 was purified by column chromatography and yield shawurensine B **3** (10 mg) ( $R_f = 0.60$  20% DCM / MeOH).

Total alkaloidal extract from the petroleum ether extract, was purified by column chromatography using silica gel and mobile phase dichloromethane: methanol (9.8:0.2) to (9:1) gradually in order of increasing polarity and yield delpheline 4 (60 mg) ( $R_f = 0.42$  5% DCM / MeOH).

**Table 5. Crystal data and structure refinement for delpheline 4 (s22phar2).**

Identification code	s22phar2
Empirical formula	C <sub>25</sub> H <sub>39</sub> N O <sub>6</sub>
Formula weight	449.57
Temperature	150.01(10) K
Wavelength	1.54184 Å
Crystal system	Orthorhombic
Space group	P212121

Unit cell dimensions	a = 11.98820(9) Å	a = 90°.
	b = 13.21037(11) Å	b = 90°.
	c = 14.32101(13) Å	g = 90°.
Volume	2268.00(3) Å <sup>3</sup>	
Z	4	
Density (calculated)	1.317 Mg/m <sup>3</sup>	
Absorption coefficient	0.753 mm <sup>-1</sup>	
F(000)	976	
Crystal size	0.308 x 0.189 x 0.172 mm <sup>3</sup>	
Theta range for data collection	4.554 to 72.911°.	
Index ranges	-14<=h<=14, -16<=k<=16, -16<=l<=17	
Reflections collected	49710	
Independent reflections	4522 [R(int) = 0.0268]	
Completeness to theta = 67.684°	100.0 %	
Absorption correction	Semi-empirical from equivalents	
Max. and min. transmission	1.00000 and 0.86657	
Refinement method	Full-matrix least-squares on F <sup>2</sup>	
Data / restraints / parameters	4522 / 0 / 298	
Goodness-of-fit on F <sup>2</sup>	1.102	
Final R indices [I>2sigma(I)]	R1 = 0.0397, wR2 = 0.1109	
R indices (all data)	R1 = 0.0398, wR2 = 0.1110	
Absolute structure parameter	0.01(3)	
Extinction coefficient	n/a	
Largest diff. peak and hole	0.565 and -0.291 e.Å <sup>-3</sup>	

## Conclusions

This study reports the isolation of methyllycaconitine **1**, shawurensine A **2**, shwurensine B **3**, and delpheline **6** from *Delphinium elatum* seeds. The NMR analysis is in agreement with the literature. The reported NMR assignment of shawurensine A **2** has been corrected in this study based on 2D NMR. This study reports the isolation of shwurensine isomer for the first time, shwurensine B **3**. The NMR analysis alongside the MS/MS fragmentation study suggests that the methyl group of the open side chain has moved to be next to the carboxylic acid end. The isolation of delpheline **6** has been accomplished and based on NOESY spectrum, the reported NMR assignment of the methylenedioxy protons has been reversed where the  $\beta$  proton resonates downfield to the  $\alpha$  proton. This study shows the X-ray crystal structure of delpheline **6** free base for the first time.

## References

- (1) Shen, Y.; Liang, W. J.; Shi, Y. N.; Kennelly, E. J.; Zhao, D. K. Structural Diversity, Bioactivities, and Biosynthesis of Natural Diterpenoid Alkaloids†. *Nat. Prod. Rep.* **2020**, *37* (6), 763–796. <https://doi.org/10.1039/d0np00002g>.
- (2) Kuder, R. C. Larkspurs, *Delphiniums*, and Chemistry. *J. Chem. Educ.* **1947**, *24* (9), 418–422. <https://doi.org/10.1021/ed024p418>.
- (3) Yamashita, H.; Doi, N.; Hanawa, N.; Itoh, M.; Nakano, W.; Takahashi, E.; Mizukami, M.; Kaneda, K.; Suzuki, Y.; Goto, M.; Lee, K. H.; Wada, K. Eleven New C19-Diterpenoid Alkaloids from *Delphinium Elatum* Cv. Pacific Giant. *J. Nat. Med.* **2022**, *76* (1), 161–170. <https://doi.org/10.1007/s11418-021-01569-z>.
- (4) Manske, R. H. F. An Alkaloid From *Delphinium Brownii* Rydb. . *Canadian Journal of Research.* 1938, pp 57–60. <https://doi.org/10.1139/cjr38b-007>.
- (5) Goodson, J. A. The Alkaloids of the Seeds of *Delphinium Elatum*, L. *J. Chem. Soc.* **1943**, 139–141. <https://doi.org/10.1039/jr9430000139>.
- (6) Wonnacott, S.; Albuquerque, E. X.; Bertrand, D. MLA Discriminate between Nicotinic Receptor Subclasses. *Methods Neurosci.* **1993**, 263–275.
- (7) Qasem, A. M. A.; Zeng, Z.; Rowan, M. G.; Blagbrough, I. S. Norditerpenoid Alkaloids

- from *Aconitum* and *Delphinium* : Structural Relevance in Medicine, Toxicology, and Metabolism. *Nat. Prod. Rep.* **2022**, *39* (3), 460–473.  
<https://doi.org/10.1039/D1NP00029B>.
- (8) Gu, D. Y.; Aisa, H. A.; Usmanova, S. K. Shawurensine, a New C19-Diterpenoid Alkaloid from *Delphinium* Shawurense. *Chem. Nat. Compd.* **2007**, *43* (3), 298–301.  
<https://doi.org/10.1007/s10600-007-0109-y>.
- (9) Manners, G. D.; Panter, K. E.; Pelletier, S. W. Structure-Activity Relationships of Norditerpenoid Alkaloids Occurring in Toxic Larkspur (*Delphinium*) Species. *J. Nat. Prod.* **1995**, *58* (6), 863–869. <https://doi.org/10.1021/np50120a007>.
- (10) Shan, L.; Chen, L.; Gao, F.; Zhou, X. Diterpenoid Alkaloids from *Delphinium* Naviculare Var. Lasiocarpum with Their Antifeedant Activity on Spodoptera Exigua. *Nat. Prod. Res.* **2019**, *33* (22), 3254–3259.  
<https://doi.org/10.1080/14786419.2018.1475382>.
- (11) Zeng, Z.; Kociok-Köhn, G.; Woodman, T. J.; Rowan, M. G.; Blagbrough, I. S. Structural Studies of Norditerpenoid Alkaloids: Conformation Analysis in Crystal and in Solution States. *European J. Org. Chem.* **2021**, *2021* (15), 2169–2179.  
<https://doi.org/10.1002/ejoc.202100179>.
- (12) Fleming, I.; Williams, D. *Spectroscopic Methods in Organic Chemistry*, 7th ed.; Spinger Nature : Cham, Switzerland, 2019. <https://doi.org/10.1007/978-3-030-18252-6>.
- (13) Pelletier, S. W.; Harraz, F. M.; Badawi, M. M.; Tantiraksachai, S.; Wang, F.; Chen, S. The Diterpenoid Alkaloids of *Delphinium* Delavayi Franch Var. Pogonanthum (H.-M.) Wang. *Heterocycles* **1986**, *24* (7), 1853–1865.
- (14) Goodson, J. A. *Delphinium* Alkaloids. Part III. Delpheline. *J. Chem. Soc.* **1944**, 665.  
<https://doi.org/10.1039/jr9440000665>.
- (15) Joshi, B. S.; Pelletier, S. W.; Zhang, X.; Snyder, J. K. Proton and Carbon-13 NMR Studies of Delpheline, 8,9-Methylenedioxyappaconitine and Dictyzine. *Tetrahedron* **1991**, *47* (25), 4299–4316. [https://doi.org/10.1016/S0040-4020\(01\)87100-3](https://doi.org/10.1016/S0040-4020(01)87100-3).

## Chapter 3

### Quantification and chemical profiling of TCM *Aconitum* preparations using LC-ESI-MS/MS

#### Introduction

According to *Shen'nong'ben'cao'jing*,<sup>1</sup> the application of *Aconitum* plants as analgesics in TCM, especially for the treatment of rheumatism, is known since 200–250 A.D. Thus, there is no doubt that *Aconitum* is useful in the clinical treatment. However, in terms of modern pharmacology, the key to the application of medicine is dose, especially for those with an unclear boundary between the potent activity and toxicity. Indeed, poisoning by clinical use of *Aconitum* plants is widely reported.<sup>2</sup> Furthermore, aconitine (**1**, C<sub>19</sub>-diterpenoid alkaloid, Fig. 1), which is the first isolated diterpenoid alkaloid and thus it is named after this plant,<sup>3</sup> is one of the main toxicological components of many species of *Aconitum*, and this natural product is known to be one of the most toxic chemicals in the world.<sup>4</sup>

The bioactivities of *Aconitum* alkaloids vary, for instance, aconitine can induce arrhythmia as it maintains cardiac voltage-sensitive sodium channels (VSSCs) in an open-state, thus it could be lethal (depending upon dose),<sup>4,5</sup> however, its derivative, 3-*O*-acetylaconitine **2**, is less toxic and is allowed to be clinically used as an analgesic in China.<sup>5,6</sup> Moreover, C<sub>18</sub>-diterpenoid alkaloid analogue lappaconitine **3** isolated from *Aconitum* plants even displays antiarrhythmic activity by the blockade of VSSCs, and its HBr salt, allapinin is used as an antiarrhythmic agent in China and Russia.<sup>7,8</sup> The development and use of medicines of single component of NDA would be much safer than using plant preparations which contains mixture of components and require quality control of the preparation method. For the safe clinical administration of *Aconitum* in modern TCM, the total amount of both di- and monoester-type diterpenoid alkaloids is limited in the current Chinese Pharmacopeia.<sup>9</sup> Indeed, due to the various bioactivities of *Aconitum* alkaloids, it is essential to understand the amount of certain key components in detail. Thus, the quantitative analysis on both toxic and pharmacologically active

components of *Aconitum* product should be investigated in-depth, for discovering a safe and effective dose of medicinal application of TCM.

The processed roots of *Aconitum carmichaelii* Debx. (Family Ranunculaceae) are used in the clinic as analgesic, tonic, and anti-rheumatic.<sup>10</sup> The processed main roots are called Zhi'chuan'wu while the side roots (*Aconiti Lateralis Radix Praeparata*) are called Fu'zi. There are five different methods of Fu'zi processing in the Chinese Pharmacopeia and result in five different preparations: Yan'fu'zi (salted Fu'zi), Dan'fu'pian (slight salted Fu'zi slice), Hei'shun'pian (Black glossy Fu'zi slice), Bai'fu'pian (White Fu'zi slice), and Pao'fu'pian (Roasted Fu'zi slice). The main medical application of Fu'zi. Preparations as analgesic and tonic. On the other hand, the processed main roots of *A. kusnezoffii* Reichb. (Zhi'cao'wu) are used in clinic as analgesic and anti-rheumatic.<sup>10</sup> Diester norditerpenoid alkaloids DDA (mainly aconitine **1**, mesaconitine **4**, and hypaconitine **5**) pose cardiac and analgesic activities,<sup>5</sup> but due to their high toxicity, these herbal preparations are used after processing to convert DDA into monoester alkaloids MDA (benzoylaconine **6**, benzoylmesaconine **7**, and benzoylhypaconine **8**) which are less toxic but still active. Therefore, these 6 alkaloids have been chosen (Fig. 1) as the target compounds for the quality control of *Aconitum* preparations. As many cases are being reported due to *Aconitum* poisoning,<sup>2</sup> these preparations must be analysed and quantified to ensure its content. According to Chinese Pharmacopeia, the total amount of the DDA in the main root preparations (Zhi'chuan'wu and Zhi'cao'wu) must be less than 0.04% (400 µg/g) and total MDA must be in the range 0.07-0.15% (700-1500 µg/g).<sup>9,11</sup> For side root preparations (Bai'fu'pian, Yan'fu'zi, and Hei'shun'pian), total DDA must be less than 0.02% (200 µg/g) and total MDA must be higher than 0.01% (100 µg/g)<sup>9,12</sup>. In this study, we analyse and quantify five *Aconitum* preparations using LC/MS-ESI: Zhi'cao'wu, Zhi'chuan'wu, Yan'fu'zi, Bai'fu'pian, and, Hei'shun'pian (Fig. 2) obtained from a pharmacy in China to ensure that the DDA and MDA levels comply with the Chinese Pharmacopeia limits, and also to chemically profile these preparations to identify the markers related to each of them and help assess the quality of them Table 1 explains the processing method for each of the five TCM preparations.

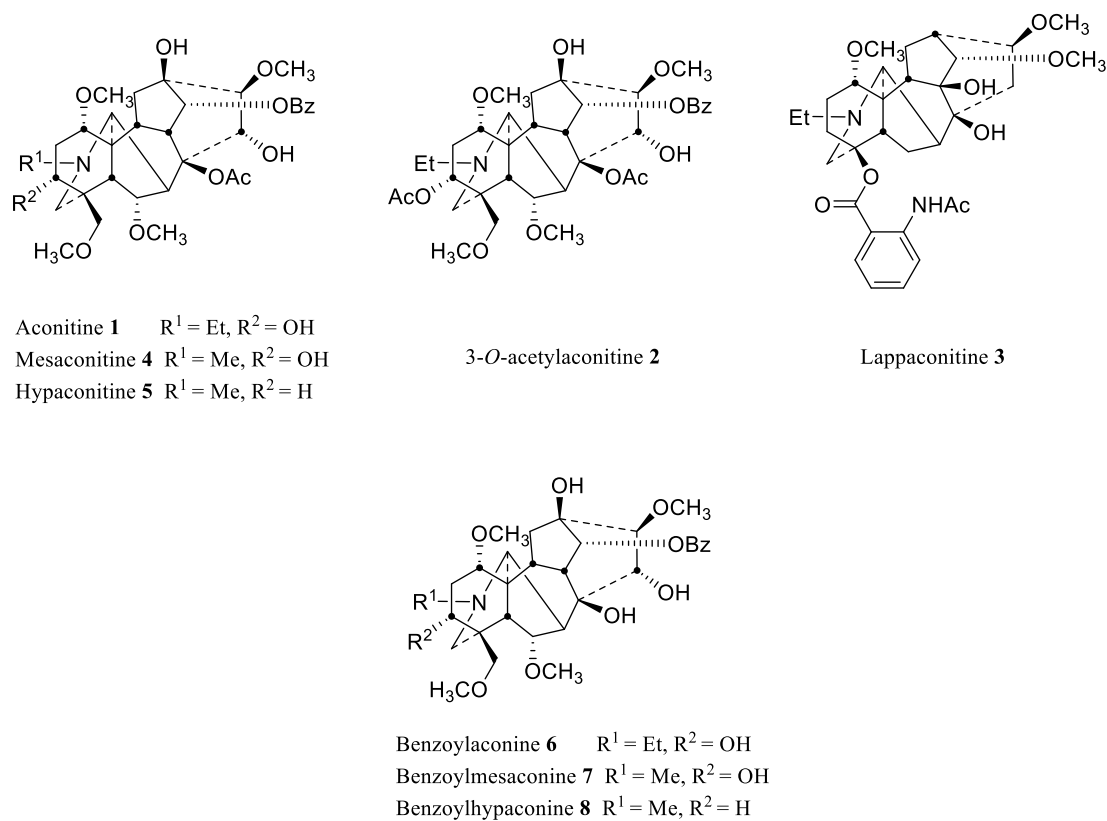


Fig. 1. Selected *Aconitum* norditerpenoid alkaloids

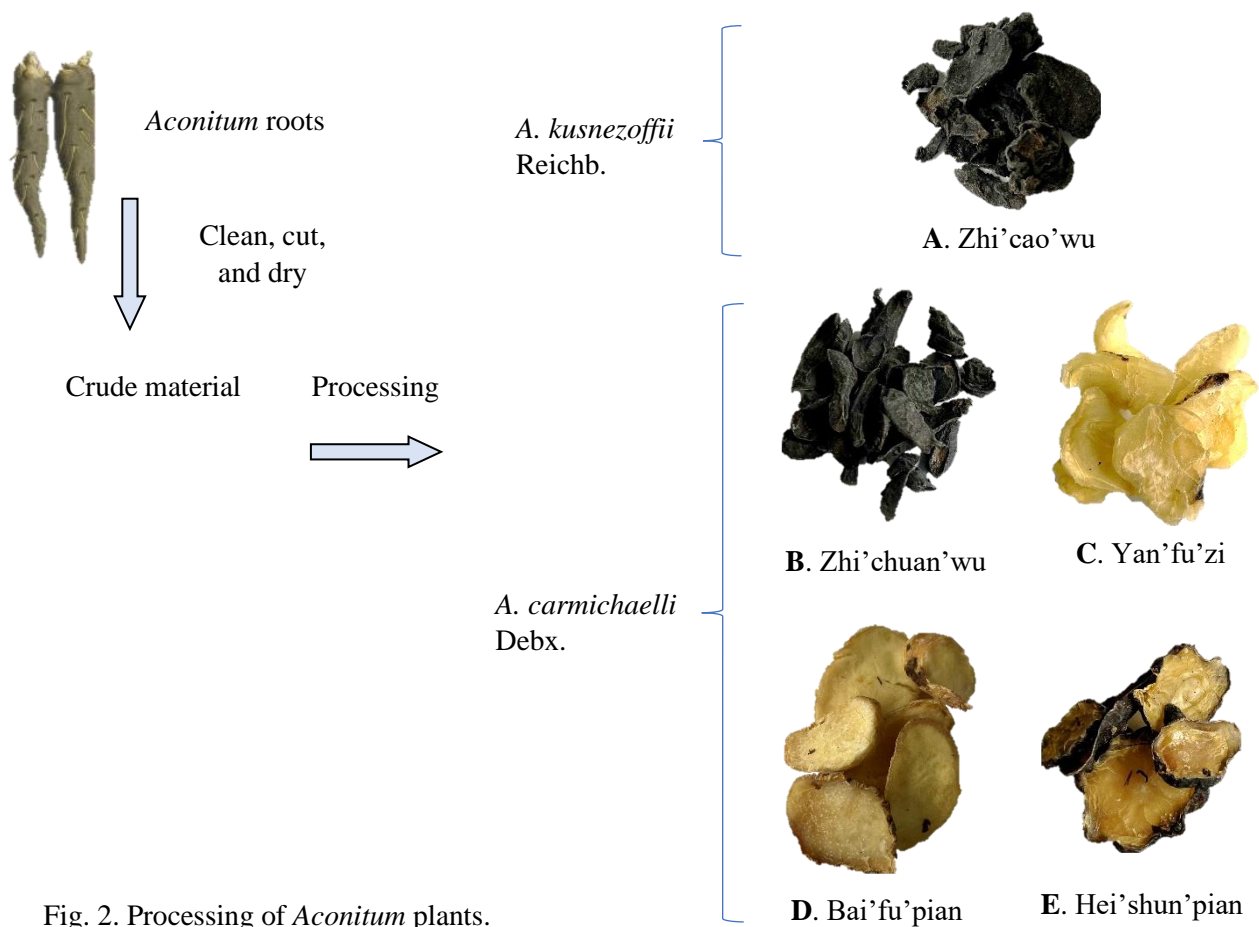


Fig. 2. Processing of *Aconitum* plants.

Table 1. Processing method of the TCM preparations.

<b>Preparation</b>	<b>Source</b>	<b>Processing method</b>
<b>A.</b> Zhi'cao'wu	processed dry main root of <i>A.</i> <i>kusnezoffii</i>	soaked and boiled in water until no "white part" is displayed on the vertical section.
<b>B.</b> Zhi'chuan'wu	processed dry main root of <i>A.</i> <i>carmichaelli</i>	soaked in cold water then boiled in fresh water for 4-8 hours until no "white part" is displayed on the vertical section.
<b>C.</b> Yan'fu'zi	processed dry side root of <i>A.</i> <i>carmichaelli</i>	soaked in an aqueous solution of "Danba"* overnight, then dried. This process repeated till until it is hardened and plenty of salt is crystallized on its surface.
<b>D.</b> Bai'fu'pian	processed dry side root of <i>A.</i> <i>carmichaelli</i>	soaked in an aqueous solution of "Danba"* for several days, and then it is boiled thoroughly in the solution. Then sliced, washed with water, and The slices are steamed thoroughly then dried in sunlight.
<b>E.</b> Hei'shun'pian	processed dry side root of <i>A.</i> <i>carmichaelli</i>	soaked in an aqueous solution of "Danba"* for several days, and then it is thoroughly boiled in the solution. Then sliced, washed with water, and these brown coloured slices are then steamed until the surface is glossy followed by oven drying.

\* "Danba" is the crystals from the dried mother liquor of sea water or water from salt lakes that are used for salt production, which mainly consists of magnesium chloride and sodium chloride.



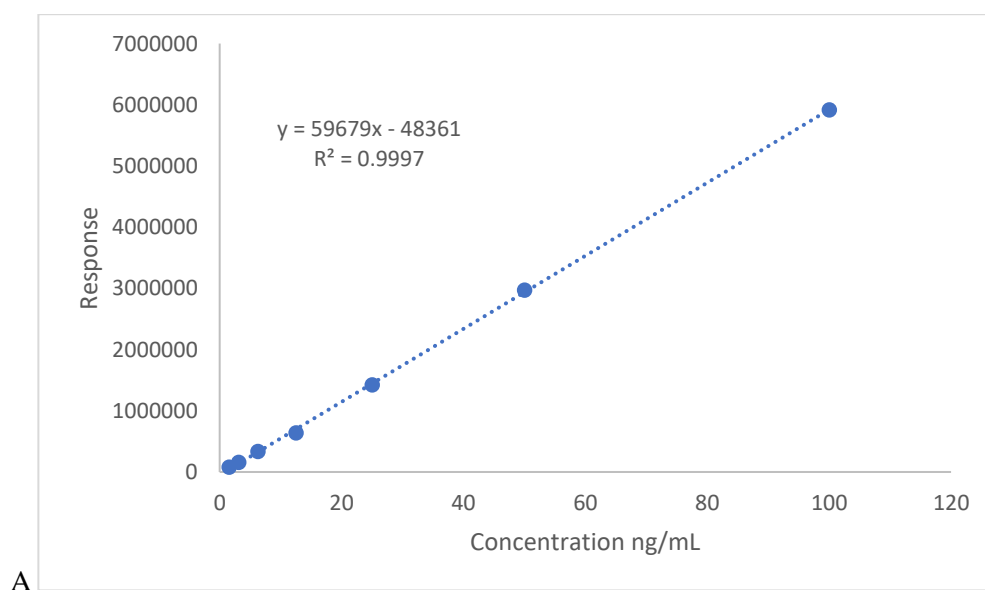
## Results and Discussion

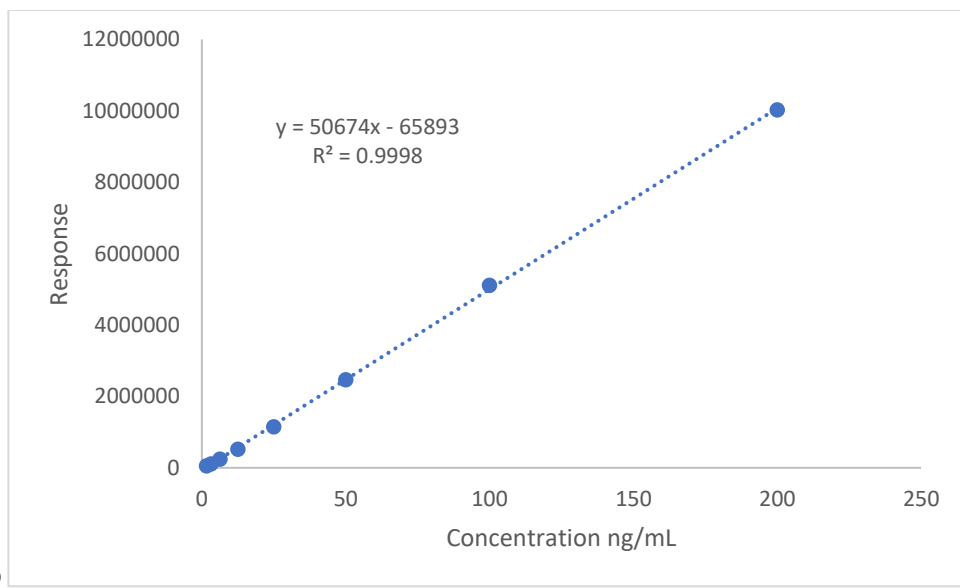
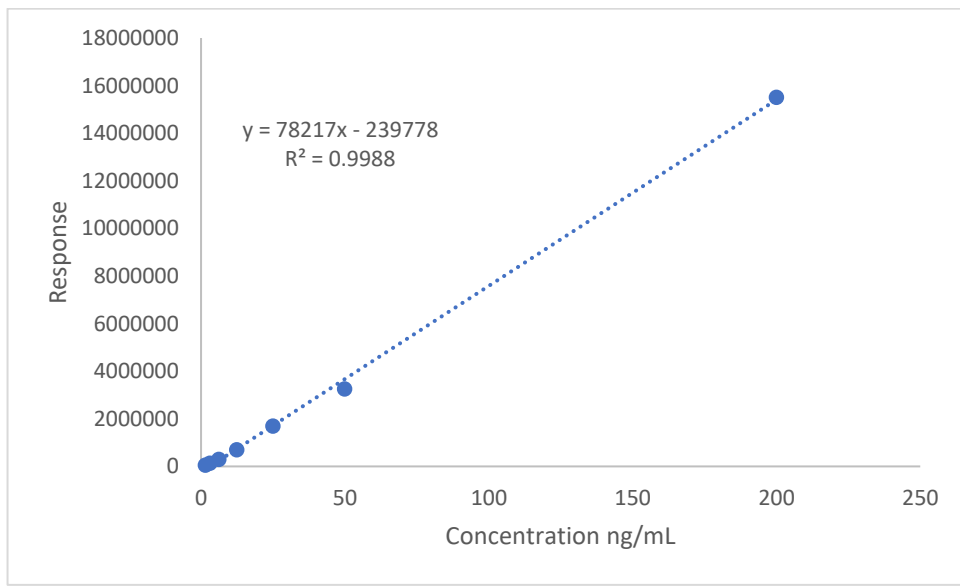
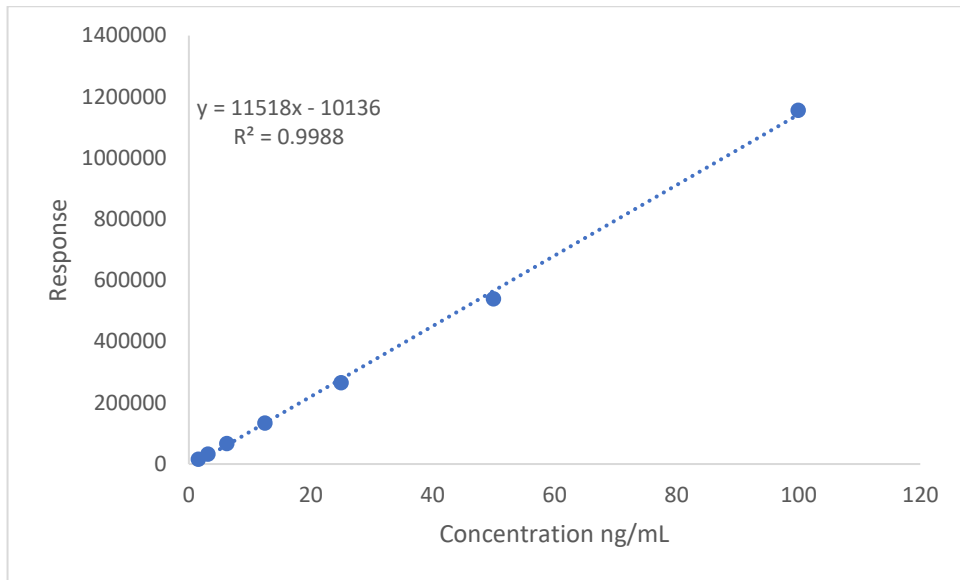
### 1. Optimization of the alkaloid's extraction

In order to optimize the extraction process, six alkaloids markers (Table 2) have been quantified in *Aconitum carmichaelii* seeds, and Fig. 3 shows the plotting charts. The seeds were extracted using seven different solvents mixtures: methanol (MeOH), ethanol (EtOH), EtOH: water (1:1), water, isopropanol (IPA), IPA: ethyl acetate (EtOAc) 1:1, and chloroform (Table 3). The six alkaloids markers have been quantified to choose the best extracting solvent (Fig. 4).

Table 2. Calibration curve data of NDAs

	equation	R <sup>2</sup>	Linear range ng/mL
Aconitine	59679x - 48361	0.999	1.5625-100
Mesaconitine	11518x - 10136	0.999	1.5625-100
Hypaconitine	78217x - 239778	0.997	1.5625-200
Benzoylaconine	50674x - 65893	0.999	1.5625-200
Benzoylmesaconine	104029x - 95453	0.999	1.5625-100
Benzoylhypaconine	51569x - 113881	0.999	1.5625-200





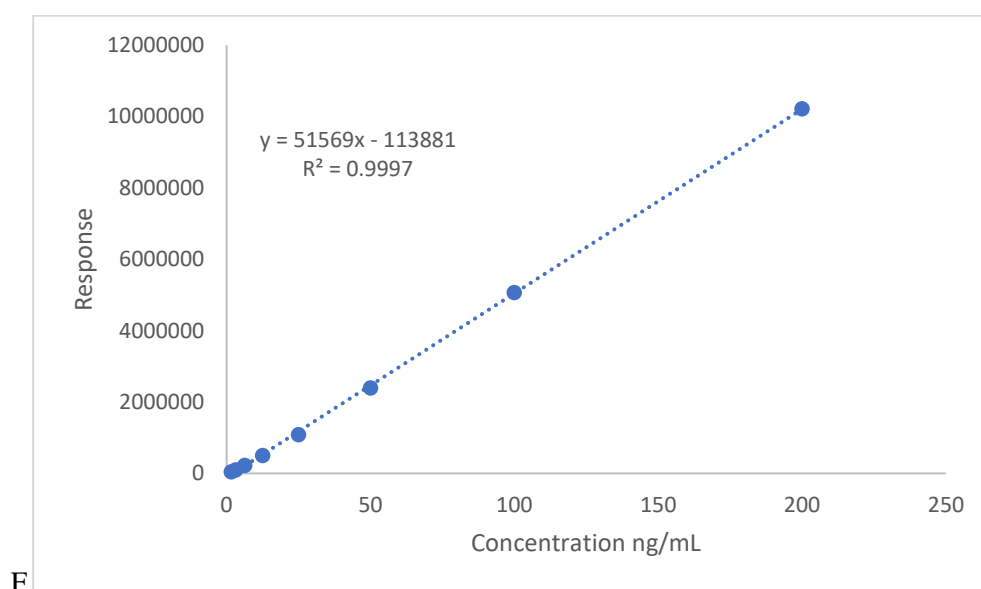
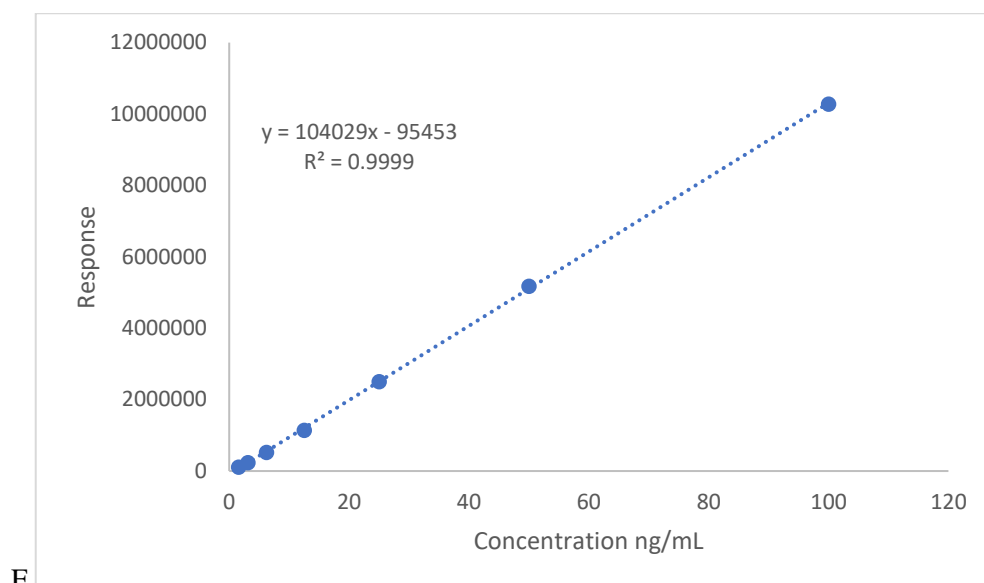


Fig. 3. Calibration curves A-F for aconitine, mesaconitine, hypaconitine, benzoylaconine, benzylmesaconine, and benzoylhypaconine respectively.

Table 3. Quantification of NDAs using different extraction solvents

	Ac μg/g	Mes μg/g	Hyp μg/g	BAc μg/g	BMes μg/g	BHyp μg/g
MeOH	0.18	1.22	0.58	0.18	0.57	0.28
EtOH	2.31	2.32	0.61	2.8	11.00	0.92
EtOH:H <sub>2</sub> O (1:1)	1.92	2.3	0.95	1.64	6.02	0.61

H <sub>2</sub> O	0.01	0.01	0.02	0.13	3.54	0.13
Isopropanol (IPA)	3.29	1.8	2.54	1.41	4.54	0.32
IPA:EtOAc (1:1)	1.48	1.22	0.86	1.48	5.51	0.35
CHCl <sub>3</sub>	0.05	0.05	0.04	0.13	2.05	0.12

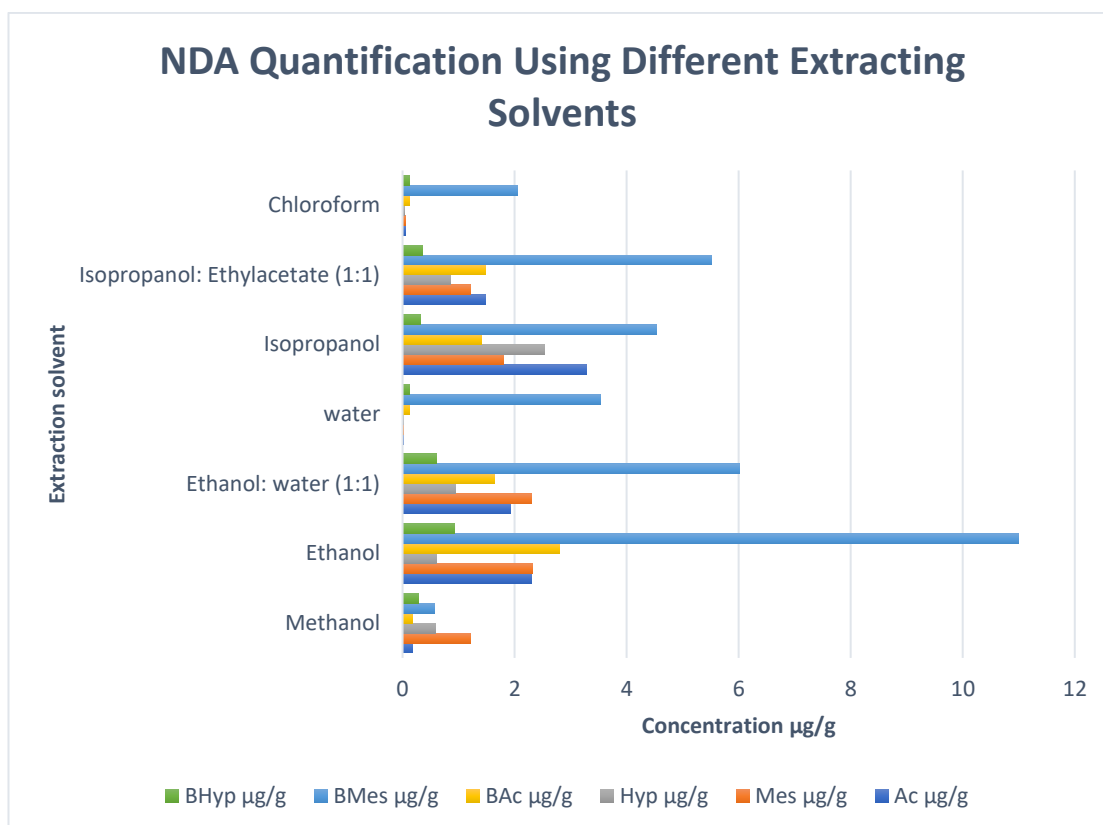


Fig. 4. NDAs quantities in different solvent (Chart)

Based on the quantification results, it was found that IPA, EtOH and MeOH were the best extracting conditions. It was reported that protic solvents but due to the stability concerns of diester NDAs in MeOH and EtOH.<sup>13</sup> IPA was chosen for the extraction of the TCM preparations as IPA showed good stability toward the DDA.<sup>14,15</sup>

## 2. TCM quantification

The chromatography retention time of the six markers standards were compared to those in the TCM samples where hei'shun'pian and yan'fu'zi were taken as examples (Table 4). Fig. 5 shows the markers chromatogram in a standard mixture and TCM preparations.

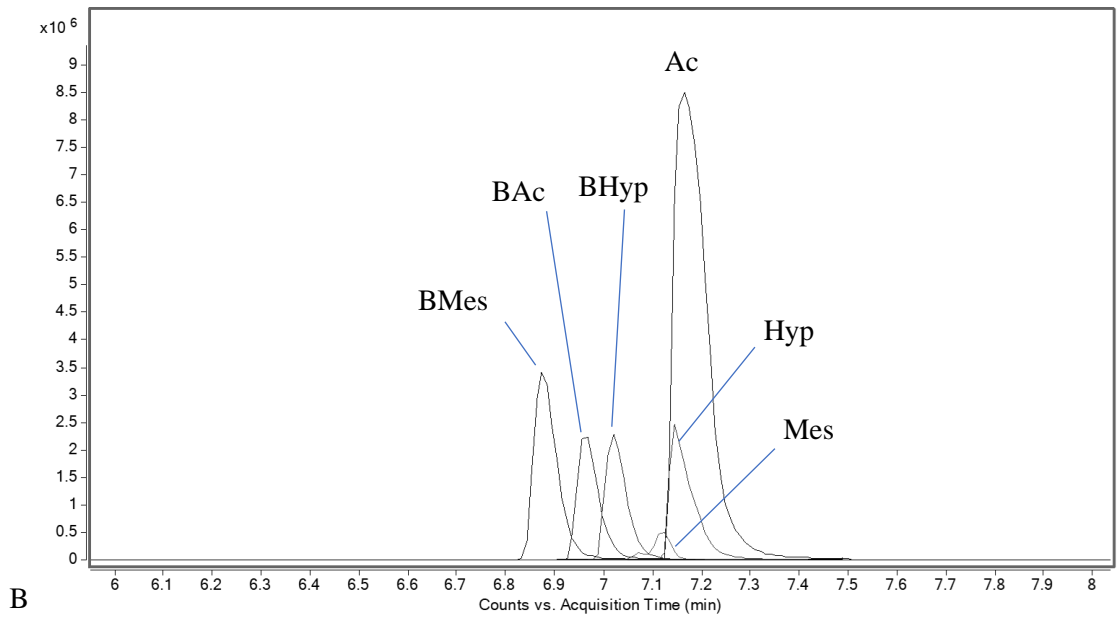
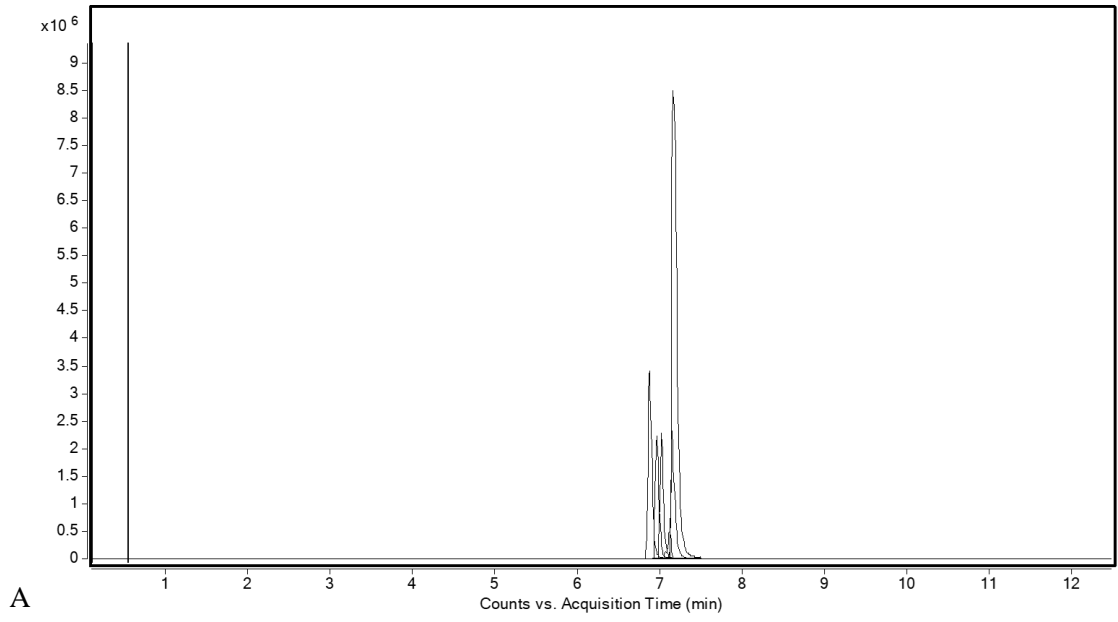
Table 4. Retention time of the six markers in a standard mixture, Hei'shun'pian extract, and Yan'fu'zi extract.

	Molecular formula	Required m/z	Observed m/z	Std RT	Hei'shun'pian RT	Yan'fu'zi RT
Ac	C <sub>34</sub> H <sub>47</sub> NO <sub>11</sub>	646.3227	646.3217	7.172	7.174	7.166
Hyp	C <sub>33</sub> H <sub>45</sub> NO <sub>10</sub>	616.3122	616.3126	7.152	7.163	7.155
Mes	C <sub>33</sub> H <sub>45</sub> NO <sub>11</sub>	632.3071	632.3079	7.120	7.122	7.124
BAC	C <sub>32</sub> H <sub>45</sub> NO <sub>10</sub>	604.3122	604.3131	6.964	6.965	6.957
BHyp	C <sub>31</sub> H <sub>43</sub> NO <sub>9</sub>	574.3016	574.3024	7.020	7.017	7.020
BMes	C <sub>31</sub> H <sub>43</sub> NO <sub>10</sub>	590.2965	590.2977	6.880	6.871	6.863

The five *Aconitum* preparations were extracted using isopropanol and the six markers were quantified. Table 5 summarize the quantification results.

Table 5. Quantification of Aconitine Ac, Mesaconitine Mes, Hypaconitine Hyp, benzoyleaconine BAc, benzoylmesaconine BMes, benzoylhypaconine, in five TCM preparations.

	Ac µg/g	Mes µg/g	Hyp µg/g	BAC µg/g	BMes µg/g	BHyp µg/g
Zhi'cao'wu	123.90	5.08	3.41	556.51	8.49	10.93
Zhi'chuan'wu	1.02	9.29	6.11	7.24	15.13	11.98
Yan'fu'zi	0.36	5.34	1.63	1.02	7.92	8.47
Bai'fu'pian	0.04	0.09	0.10	0.10	0.09	0.14
Hei'shun'pian	0.96	6.90	0.27	2.82	10.32	1.69



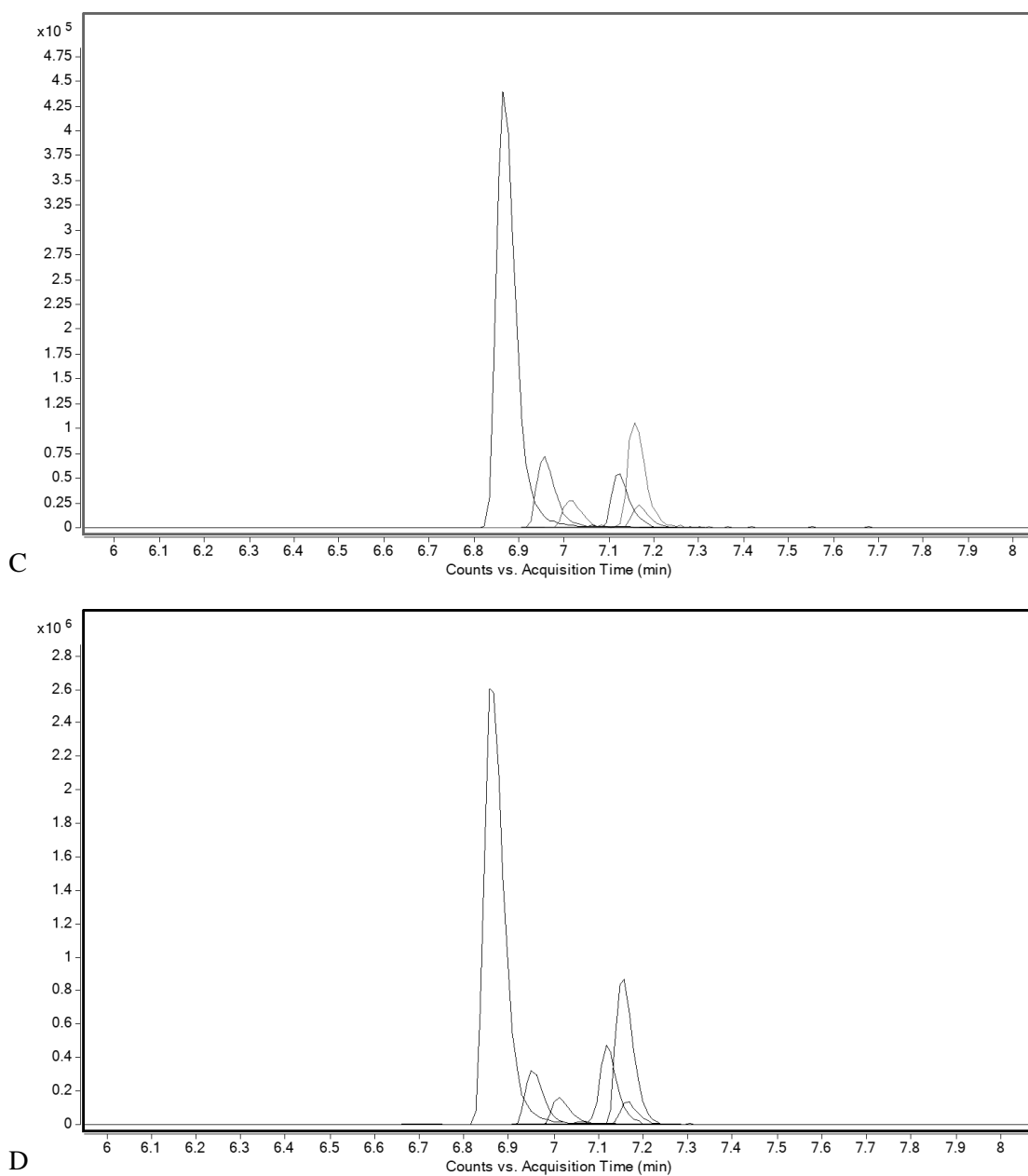


Fig. 5. LC-MS chromatograms of the six markers. A. Standards mixture, B. Standards mixture expansion, C. Hei'shun'pian extract, D. Yan'fu'zi extract.

The quantification results of the main roots preparations, Zhi'chuan'wu and Zhi'cao'wu, indicated that the total DDA (aconitine **1**, mesaconitine **4**, and hypaconitine **5**) amount is around 16 and 132.39  $\mu\text{g/g}$  respectively and that's comply the pharmacopeia limit which is 400  $\mu\text{g/g}$ . The total amount of the MDA markers (benzoulaconine **6**, benzoylmesaconine **7**, and benzoylhypaconine **8**) is around 34  $\mu\text{g/g}$  in Zhi'chuan'wu and that is lower than the Chinese

Pharmacopeia range (700-1500  $\mu\text{g/g}$ ) which means lower efficacy of this sample. The total MDA in Zhi'cao'wu is around 576  $\mu\text{g/g}$  which fits in the specified range.

The Bai'fu'pian sample was found to have lower concentration of the DDA and MDA compared to other samples, and the assay was repeated twice. The total DDA in Bai'fu'pian is around 0.23  $\mu\text{g/g}$  which is within the limit ( $< 200 \mu\text{g/g}$ ), and the total MDA is around 0.33  $\mu\text{g/g}$  which is much lower than the specified range ( $> 100 \mu\text{g/g}$ ).

The total DDA amount in Yan'fu'zi and Hei'shun'pian is 7.33 and 8.13  $\mu\text{g/g}$  respectively, which fit within the limit ( $< 200 \mu\text{g/g}$ ) while the total MDA amount (17.41 and 14.83  $\mu\text{g/g}$  respectively) is out of the Chinese Pharmacopeia range ( $> 100 \mu\text{g/g}$ ).

Among the tested TCM preparations, only Zhi'cao'wu fits within the pharmacopeia limit for DDA which ensures the safety, and also MDA limit which guarantee the efficacy. The other four preparations comply with DDA ranges and that means they will be safe to consume. On the other hand, the total MDA amount in them is much lower than the specified range and that does not lead to the desired therapeutic effect.

### 3. Chemical profiling

In *Aconitum* species, diterpenoid alkaloids are the major alkaloidal group and responsible of their activities. The main concerns in the TCM application are the toxicity and adulterants. The chemical profiling of the TCM preparations contribute to identify the markers related to each of them and help assess the quality of these preparations.

The chromatograms of the five preparations were obtained using HPLC and the peaks were identified using ESI-MS/MS where the accurate masses along with their fragments and retention times were used to identify these compounds and compare it with the literature.<sup>12,16-18</sup>

A summary of the identified *Aconitum* alkaloids in this study is reported in Table 6 with retention time of each marker, accurate masses of molecular ions with mass error (ppm), and the major fragments. The losses of  $\text{H}_2\text{O}$ ,  $\text{CH}_2\text{O}$ ,  $\text{CH}_3\text{OH}$ , and  $\text{CH}_3\text{COOH}$  are the main fragmentation pathways.



The amount of the identified diterpenoid alkaloids in the main root preparations, Zhi'chuan'wu and Zhi'cao'wu, is much more compared to the lateral roots preparations and the total ion chromatograms shown below in Fig. 6 explain the difference in complexity between the main roots and the side roots sample, Hei'shun'pian.

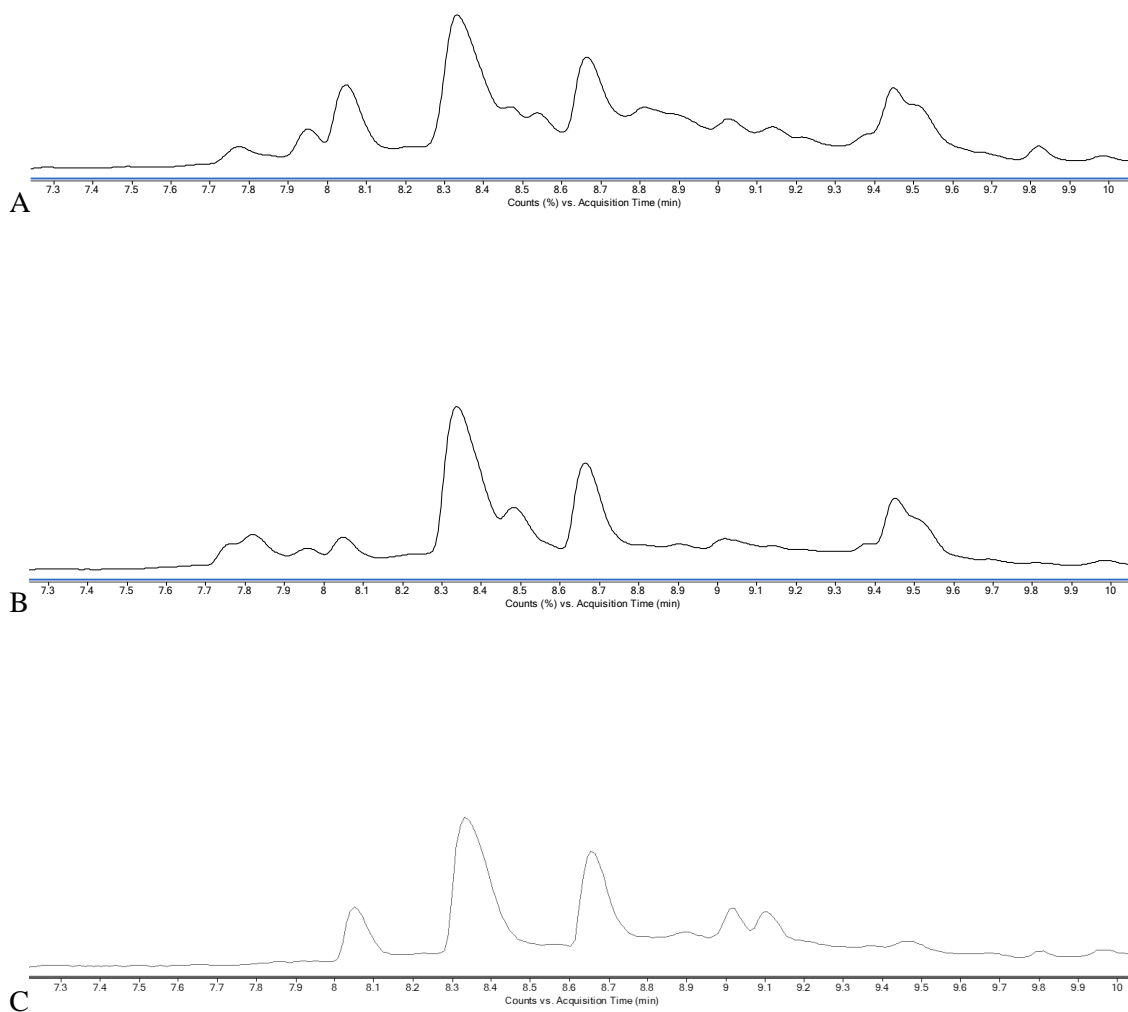


Fig. 6. Total ion chromatograms (TIC) of A. Zhi'chuan'wu, B. Zhi'cao'wu, and C. Hei'shun'pian.

Table 6. Summary of the identified markers in the TCM preparations

No.	Retention time (min)	Molecular formula	[M+H] <sup>+</sup> (mass error, ppm)			Fragment ions	Identification	Structure type *	Detected in **
			Detected	Expected	Error (ppm)				
1	7.27	C <sub>22</sub> H <sub>35</sub> NO <sub>5</sub>	394.2583	394.2593	-2.54	376.2477 [M+H-H <sub>2</sub> O] <sup>+</sup> , 358.2366 [M+H-2H <sub>2</sub> O] <sup>+</sup> , 340.2261 [M+H-3H <sub>2</sub> O] <sup>+</sup> , 344.2212 [M+H-H <sub>2</sub> O-CH <sub>3</sub> OH] <sup>+</sup> .	Kalacolidine	C19 NDA	A, B, C, D, E
2	7.68	C <sub>23</sub> H <sub>37</sub> NO <sub>6</sub>	424.2691	424.2699	-1.89	394.2584 [M+H-CH <sub>2</sub> O] <sup>+</sup> , 392.2426 [M+H-CH <sub>3</sub> OH] <sup>+</sup> , 374.2322 [M+H-H <sub>2</sub> O-CH <sub>3</sub> OH] <sup>+</sup> , 360.2528 [M+H-H <sub>2</sub> O-HCOOH] <sup>+</sup> , 356.2211 [M+H-2H <sub>2</sub> O-CH <sub>3</sub> OH] <sup>+</sup> .	Senbusine A	C19 NDA	A, B, D
3	7.73	C <sub>22</sub> H <sub>35</sub> NO <sub>5</sub>	394.2583	394.2593	-2.54	376.2477 [M+H-H <sub>2</sub> O] <sup>+</sup> , 358.2366 [M+H-2H <sub>2</sub> O] <sup>+</sup> , 340.2261 [M+H-	Chuanfumine	C20 DA	A, B, C, D, E

						3H <sub>2</sub> O) <sup>+</sup> , 328.2255 [M+H-2H <sub>2</sub> O-CH <sub>2</sub> O) <sup>+</sup> , 322.2156 [M+H-4H <sub>2</sub> O) <sup>+</sup> .			
4	7.74	C <sub>24</sub> H <sub>39</sub> NO <sub>9</sub>	486.2694	486.2703	-1.85	468.2581 [M+H-H <sub>2</sub> O) <sup>+</sup> , 454.2417 [M+H-CH <sub>3</sub> OH) <sup>+</sup> , 436.2329 [M+H-H <sub>2</sub> O-CH <sub>3</sub> OH) <sup>+</sup> , 422.2161 [M+H-2CH <sub>3</sub> OH) <sup>+</sup> , 404.2061[M+H-H <sub>2</sub> O-2CH <sub>3</sub> OH) <sup>+</sup> .	Mesaconine	C19 NDA	A, B
5	7.75	C <sub>22</sub> H <sub>31</sub> NO <sub>3</sub>	358.2375	358.2382	-1.95	340.2268 [M+H-H <sub>2</sub> O) <sup>+</sup> , 322.2157 [M+H-2H <sub>2</sub> O) <sup>+</sup> .	Songorine	C20 DA	A, B, D, E
6	7.76	C <sub>23</sub> H <sub>37</sub> NO <sub>6</sub>	424.2691	424.2699	-1.89	394.2584 [M+H-CH <sub>2</sub> O) <sup>+</sup> , 392.2426 [M+H-CH <sub>3</sub> OH) <sup>+</sup> , 374.2322 [M+H-H <sub>2</sub> O-CH <sub>3</sub> OH) <sup>+</sup> , 360.2528 [M+H-H <sub>2</sub> O-HCOOH) <sup>+</sup> , 356.2211 [M+H-2H <sub>2</sub> O-CH <sub>3</sub> OH) <sup>+</sup> .	Senbusine B	C19 NDA	A, B, D
7	7.77	C <sub>22</sub> H <sub>35</sub> NO <sub>4</sub>	378.2636	378.2644	-2.12	360.2529 [M+H-H <sub>2</sub> O) <sup>+</sup> , 346.2371 [M+H-CH <sub>3</sub> OH) <sup>+</sup> .	Karacoline	C19 NDA	A

8	7.78	$C_{23}H_{37}NO_5$	408.2745	408.2750	-1.22	378.2638 [M+H-CH <sub>2</sub> O] <sup>+</sup> , 360.2532 [M+H-CH <sub>3</sub> OH] <sup>+</sup> , 342.2421 [M+H-2H <sub>2</sub> O-CH <sub>2</sub> O] <sup>+</sup> .	Isotalatizidine	C19 NDA	A, B
9	7.82	$C_{25}H_{41}NO_8$	484.2898	484.2910	-2.48	438.2852 [M+H-HCOOH] <sup>+</sup> , 408.2742 [M+H-HCOOH-CH <sub>2</sub> O] <sup>+</sup> , 378.2258 [M+H-C <sub>2</sub> H <sub>5</sub> OH-CH <sub>3</sub> COOH] <sup>+</sup> , 360.2534 [M+H-CH <sub>3</sub> OH-2CH <sub>2</sub> O <sub>2</sub> ] <sup>+</sup> .	Preudoaconine	C19 NDA	A
10	7.83	$C_{25}H_{41}NO_9$	500.2853	500.2860	-1.40	482.2742 [M+H-H <sub>2</sub> O] <sup>+</sup> , 468.2581 [M+H-CH <sub>3</sub> OH] <sup>+</sup> , 450.2848 [M+H-H <sub>2</sub> O-CH <sub>3</sub> OH] <sup>+</sup> , 436.2330 [M+H-2CH <sub>3</sub> OH] <sup>+</sup> .	Aconine	C19 NDA	A, B
11	7.89	$C_{24}H_{39}NO_8$	470.2744	470.2754	-2.13	452.2275 [M+H-H <sub>2</sub> O] <sup>+</sup> , 438.2425 [M+H-CH <sub>3</sub> OH] <sup>+</sup> , 420.2742 [M+H-H <sub>2</sub> O-CH <sub>3</sub> OH] <sup>+</sup> , 406.2584 [M+H-2CH <sub>3</sub> OH] <sup>+</sup> .	Hypaconine	C19 NDA	B

12	7.94	$C_{24}H_{39}NO_7$	454.2799	454.2805	-1.32	436.2688 [M+H-H <sub>2</sub> O] <sup>+</sup> , 422.2533 [M+H-CH <sub>3</sub> OH] <sup>+</sup> , 408.2745 [M+H-CH <sub>3</sub> CH <sub>2</sub> OH] <sup>+</sup> , 404.2426 [M+H-H <sub>2</sub> O-CH <sub>3</sub> OH] <sup>+</sup> .	Fuziline	C19 NDA	A, B, C, E
13	7.94	$C_{24}H_{39}NO_5$	422.2902	422.2906	-1.42	404.2674 [M+H-H <sub>2</sub> O] <sup>+</sup> , 392.2790 [M+H-CH <sub>2</sub> O] <sup>+</sup> , 390.2639 [M+H-CH <sub>3</sub> OH] <sup>+</sup> , 372.2525 [M+H-H <sub>2</sub> O-CH <sub>3</sub> OH] <sup>+</sup> , 360.2528 [M+H-CH <sub>2</sub> O-CH <sub>3</sub> OH] <sup>+</sup> , 358.2375 [M+H-2CH <sub>3</sub> OH] <sup>+</sup> , 326.1417 [M+H-3CH <sub>3</sub> OH] <sup>+</sup> .	Talatisamine	C19 NDA	A, B, C, D
14	7.96	$C_{24}H_{39}NO_6$	438.2844	438.2856	-2.74	420.2734 [M+H-H <sub>2</sub> O] <sup>+</sup> , 402.2573 [M+H-2H <sub>2</sub> O] <sup>+</sup> , 388.2477 [M+H-H <sub>2</sub> O-CH <sub>3</sub> OH] <sup>+</sup> , 374.2322 [M+H-2CH <sub>3</sub> OH] <sup>+</sup> , 370.2311 [M+H-2H <sub>2</sub> O-CH <sub>3</sub> OH] <sup>+</sup> .	Neoline	C19 NDA	A, B, C, D, E

15	8.03	C <sub>25</sub> H <sub>41</sub> NO <sub>6</sub>	452.3005	452.3012	-1.55	422.2899 [M+H-CH <sub>2</sub> O] <sup>+</sup> , 420.2742 [M+H-CH <sub>3</sub> OH] <sup>+</sup> .	8- dehydroxybikhaconine	C19 NDA	B
16	8.07	C <sub>26</sub> H <sub>41</sub> NO <sub>6</sub>	464.3006	464.3012	-1.29	434.2891 [M+H-CH <sub>2</sub> O] <sup>+</sup> , 402.2629 [M+H-CH <sub>2</sub> O-CH <sub>3</sub> OH] <sup>+</sup> , 386.2369 [M+H-H <sub>2</sub> O-CH <sub>3</sub> COOH] <sup>+</sup> .	14-Acetyltalatisamine	C19 MDA	B
17	8.28	C <sub>30</sub> H <sub>41</sub> NO <sub>8</sub>	544.2910	544.2910	0.00	526.2775 [M+H-H <sub>2</sub> O] <sup>+</sup> , 514.2796 [M+H-CH <sub>2</sub> O] <sup>+</sup> .	Straconitine B	C19 MDA	B, D
18	8.29	C <sub>31</sub> H <sub>43</sub> NO <sub>10</sub>	590.2966	590.2965	0.17	558.2686 [M+H-CH <sub>3</sub> OH] <sup>+</sup> , 540.2596 [M+H-H <sub>2</sub> O-CH <sub>3</sub> OH] <sup>+</sup> , 526.2438 [M+H-2CH <sub>3</sub> OH] <sup>+</sup> , 508.2329 [M+H- H <sub>2</sub> O-2CH <sub>3</sub> OH] <sup>+</sup> .	Benzoylmesaconine	C19 MDA	A, B, C, D, E
19	8.34	C <sub>32</sub> H <sub>45</sub> NO <sub>10</sub>	604.3115	604.3122	1.16	586.3006 [M+H-H <sub>2</sub> O] <sup>+</sup> , 572.2854 [M+H-CH <sub>3</sub> OH] <sup>+</sup> , 554.2749 [M+H- H <sub>2</sub> O-CH <sub>3</sub> OH] <sup>+</sup> , 540.2596 [M+H- 2CH <sub>3</sub> OH] <sup>+</sup> , 522.2488 [M+H-H <sub>2</sub> O-	Benzoylaconine	C19 MDA	A, B, C, D, E

						2CH <sub>3</sub> OH] <sup>+</sup> , 462.2617 [M+H-CH <sub>2</sub> O-CH <sub>3</sub> OH] <sup>+</sup> .			
20	8.38	C <sub>31</sub> H <sub>43</sub> NO <sub>9</sub>	574.3014	574.3016	0.35	542.2740 [M+H-CH <sub>3</sub> OH] <sup>+</sup> , 524.2644 [M+H-H <sub>2</sub> O-CH <sub>3</sub> OH] <sup>+</sup> , 510.2473 [M+H-2CH <sub>3</sub> OH] <sup>+</sup> , 492.2383 [M+H-H <sub>2</sub> O-2CH <sub>3</sub> OH] <sup>+</sup> .	Benzoylhypaconine	C19 MDA	A, B, C, D, E
21	8.39	C <sub>35</sub> H <sub>49</sub> NO <sub>12</sub>	676.3325	676.3333	-1.18	644.3068 [M+H-CH <sub>3</sub> OH] <sup>+</sup> , 554.3109 [M+H-CH <sub>2</sub> O-2HCOOH] <sup>+</sup> .	Transaconitine B	C19 DDA	A
22	8.41	C <sub>33</sub> H <sub>45</sub> NO <sub>12</sub>	648.3033	648.3020	2.01	616.2755 [M+H-CH <sub>3</sub> OH] <sup>+</sup> , 558 3062 [M+H-CO <sub>2</sub> -HCOOH] <sup>+</sup> .	Beiwutine	C19 DDA	B, E
23	8.42	C <sub>35</sub> H <sub>49</sub> NO <sub>11</sub>	660.3374	660.3384	-1.51	600.3160 [M+H-CH <sub>3</sub> COOH] <sup>+</sup> , 584.3197 [M+H-CO <sub>2</sub> -CH <sub>3</sub> OH] <sup>+</sup> .	Yunaconitine	C19 DDA	A
24	8.43	C <sub>33</sub> H <sub>45</sub> NO <sub>11</sub>	632.3073	632.3071	0.32	600.2800 [M+H-CH <sub>3</sub> OH] <sup>+</sup> , 572.2854 [M+H-AcOH] <sup>+</sup> , 540.2596 [M+H-AcOH-CH <sub>3</sub> OH] <sup>+</sup> .	Mesaconitine	C19 DDA	A, B, C, D, E

25	8.44	C <sub>32</sub> H <sub>43</sub> NO <sub>9</sub>	586.3008	586.3016	-1.36	568.2905 [M+H-H <sub>2</sub> O] <sup>+</sup> .	Negaconitine B	C19 MDA	B
26	8.45	C <sub>31</sub> H <sub>43</sub> NO <sub>8</sub>	558.3063	558.3067	-0.72	540.2946 [M+H-H <sub>2</sub> O] <sup>+</sup> .	Straconitine A	C19 MDA	C
27	8.47	C <sub>30</sub> H <sub>43</sub> NO <sub>7</sub>	530.3112	530.3118	-1.13	512.3025 [M+H-H <sub>2</sub> O] <sup>+</sup> , 494.2886 [M+H-2H <sub>2</sub> O] <sup>+</sup> .	Carmichaeline D	C19 DDA	B
28	8.47	C <sub>33</sub> H <sub>45</sub> NO <sub>10</sub>	616.3120	616.3116	0.65	584.2855 [M+H-CH <sub>3</sub> OH] <sup>+</sup> , 556.2906 [M+H-AcOH] <sup>+</sup> , 524.2644 [M+H- AcOH-CH <sub>3</sub> OH] <sup>+</sup> , 492.2383 [M+H- AcOH-2CH <sub>3</sub> OH] <sup>+</sup> .	Hypaconitine	C19 DDA	A, B, C, D, E
29	8.48	C <sub>34</sub> H <sub>47</sub> NO <sub>11</sub>	646.3220	646.3221	-0.15	600.3166 [M+H-HCOOH] <sup>+</sup> , 586.3006 [M+H-AcOH] <sup>+</sup> , 572.3216 [M+H-CO <sub>2</sub> -CH <sub>2</sub> O] <sup>+</sup> , 568.2905 [M+H-H <sub>2</sub> O-AcOH] <sup>+</sup> , 554.2749 [M+H-AcOH-CH <sub>3</sub> OH] <sup>+</sup> .	Aconitine	C19 DDA	A, B, C, D, E



30	8.50	$C_{33}H_{45}NO_9$	600.3165	600.3173	-1.33	582.3165 $[M+H-H_2O]^+$ , 568.2903 $[M+H-CH_3OH]^+$ , 564.2954 $[M+H-2H_2O]^+$ .	Ducloudine A	C19 DDA	A, C, D, E
31	8.51	$C_{34}H_{47}NO_{10}$	630.3266	630.3261	0.79	600.3166 $[M+H-CH_2O]^+$ , 570.3064 $[M+H-AcOH]^+$ , 538.2796 $[M+H-AcOH-CH_3OH]^+$ , 506.2534 $[M+H-AcOH-2CH_3OH]^+$ .	Deoxyaconitine	C19 DDA	A, B, C, D, E

\* DA: Diterpenoid alkaloid, NDA: non-ester DA, MDA: mono-ester DA, DDA: di-ester DA.

\*\* A: Zhi'cao'wu, B: Zhi'chuan'wu, C: Yan'fu'zi, D: Bai'fu'pian, E: Hei'shun'pian.

## Conclusions

The safety and effectiveness have been assessed for five *Aconitum* TCM preparations through the quantification of six norditerpenoid markers. It was found that the total DDA amount is within the pharmacopeia limit and therefore they can be safely used. On the other hand, only Zhi'cao'wu met the pharmacopeia limit for the total MDA amount which ensures the preparation efficacy, while the others do not contain enough amount to show the expected therapeutic activity. These results highlight the importance of quality control studies on TCM preparations to ensure their effectiveness and safety. In addition to the safety and effectiveness of TCM, adulteration is a main concern where it is important to identify preparations markers to assess their quality. Therefore, chemical profiling of the selected TCM preparations was accomplished where compounds were identified based on their fragments with comparison to databases.

## Experimental

### General Methods

*Chemicals and Materials.* Aconitine **1** was purchased from Sigma-Aldrich (U.K.), mesaconitine **4** was extracted and then purified by sulfuric acid acid-base cycling from the ground roots of *Aconitum napellus*. After column chromatography to homogeneity, it was indistinguishable from a commercial sample (Sigma-Aldrich, U.K.). Hypaconitine **5**, benzoyleaconine **6**, Benzoylhypaconine **7**, benzoulmesaconine **8** were purchased from Carbosynth Ltd. (U.K.). All other solvents were of HPLC grade,  $\geq 99.9\%$  purity (Fisher Scientific, U.K. and VWR, U.K.).

*Instrumentation.* The quantification was done using LC-MS analyses and performed using an Agilent QTOF 6545 with Jetstream ESI spray source coupled to an Agilent 1260 Infinity II Quat pump HPLC with 1260 autosampler, column oven compartment and variable wavelength detector (VWD). The MS was operated in separate injections in either positive or negative ionization mode with the gas temperature at 250°C, the drying gas at 12 L/min and the nebulizer gas at 45 psi (3.10 bar). The sheath gas temperature and flow were set to 350 °C and 12 L/min, respectively. The MS was calibrated using reference calibrant introduced from the independent ESI reference sprayer. The VCap, Fragmentor and Skimmer was set to 3500, 125 and 45 V

respectively. The MS was operated in all-ions mode with 3 collision energy scan segments at 0, 20 and 40 eV. Chromatographic separation of a 5  $\mu$ L sample injection was performed on a InfinityLab Poroshell 120 EC-C18 (3.0 x 50 mm, 2.7  $\mu$ m) column using H<sub>2</sub>O (Merck, LC-MS grade) with 0.1 % formic acid (FA, Fluka) v/v and methanol (MeOH, VWR, HiPerSolv) with 0.1 % FA v/v as mobile phase A and B, respectively. The column was operated at flow rate of 0.4 mL/min at 50°C starting with 5 % mobile phase B up to 95 % at 5 min and then back to 5% after 7 min, the process repeated as a dual wash procedure. The VWD was set to detect at 254 and 320 nm wavelengths at a frequency of 2.5 Hz. Data processing was automated in Qual 10 with molecular feature extraction set to the largest 20 compounds for [M+H]<sup>+</sup>, [M-H]<sup>-</sup> and [M+HCOO]<sup>-</sup> ions.

The chemical profiling was done using LC-MS analyses performed using an Agilent QTOF 6545 with Jetstream ESI spray source coupled to an Agilent 1260 Infinity II Quat pump HPLC with 1260 autosampler, column oven compartment, and variable wavelength detector (VWD). The MS was operated in positive-ion mode with the gas temperature at 250 °C, the drying gas at 12 L/min and the nebulizer gas at 45 psi (3.10 bar). The sheath gas temperature and flow were set to 350 °C and 12 L/min, respectively. The MS was calibrated using a reference calibrant introduced from the independent ESI reference sprayer. The VCap, Fragmentor, and Skimmer were set to 3500, 100, and 45 respectively. The MS was operated in all-ions mode with 3 collision energy scan segments at 0, 20 and 40 eV. Chromatographic separation of a 5  $\mu$ L sample injection was performed on a InfinityLab Poroshell 120 EC-C18 (3.0 x 50 mm, 2.7  $\mu$ m) column using H<sub>2</sub>O (Merck, LC-MS grade) with 0.1 % formic acid (FA, Fluka) v/v and methanol (MeOH, VWR, HiPerSolv) with 0.1% FA v/v as mobile phase A and B, respectively. The column was operated at a flow rate of 0.3 mL/min at 40°C starting with 1 % mobile phase B for 3 min, thereafter the gradient was initiated and ran for 2 min to a final 100% B, held at 100% B for 3 min then returned to 1% B, held for re-equilibration for 3.9 min in a total run time of 12 min. The VWD was set to collect 254 and 320 nm wavelengths at 2.5 Hz. Data processing was automated in Qual B 07.00 with a Find by formula matching tolerance of 10 ppm.

## References

- (1) Gu, G.; Dubreuil, A.; Dubreuil, X. *The Divine Farmer's Classic of Materia Medica*; Foreign Languages Press: Beijing, 2015.
- (2) Chan, T. Y. K. *Aconitum* Alkaloid Poisoning Because of Contamination of Herbs by Aconite Roots. *Phyther. Res.* **2016**, *30* (1), 3–8. <https://doi.org/10.1002/ptr.5495>.
- (3) Nyirimigabo, E.; Xu, Y.; Li, Y.; Wang, Y.; Agyemang, K.; Zhang, Y. A Review on Phytochemistry, Pharmacology and Toxicology Studies of *Aconitum*. *J. Pharm. Pharmacol.* **2015**, *67* (1), 1–19. <https://doi.org/10.1111/jphp.12310>.
- (4) Lamanna, C. The Most Poisonous Poison. *Science.* **1959**, *130* (3378), 763–772. <https://doi.org/10.1126/science.130.3378.763>.
- (5) Ameri, A. The Effects of *Aconitum* Alkaloids on the Central Nervous System. *Prog. Neurobiol.* **1998**, *56* (2), 211–235. [https://doi.org/10.1016/S0301-0082\(98\)00037-9](https://doi.org/10.1016/S0301-0082(98)00037-9).
- (6) Dzhakhangirov, F. N.; Sultankhodzhaev, M. N.; Tashkhodzhaev, B.; Salimov, B. T. Diterpenoid Alkaloids as a New Class of Antiarrhythmic Agents. Structure Activity Relationship. **1997**, *33* (2), 190–202.
- (7) Vakhitova, Y. V.; Farafontova, E. I.; Khisamutdinova, R. Y.; Yunusov, V. M.; Tsypysheva, I. P.; Yunusov, M. S. A Study of the Mechanism of the Antiarrhythmic Action of Allapinin. *Russ. J. Bioorganic Chem.* **2013**, *39* (1), 92–101. <https://doi.org/10.1134/S1068162013010111>.
- (8) Marion, L.; Fonzes, L.; Wilkins Jr., C. K.; Boca, J. P.; Sandberg, F.; Thorsén, R.; Lindén, E. The Alkaloids of *Aconitum Septentrionale* Koelle. *Can. J. Chem.* **1967**, *45* (9), 969–973. <https://doi.org/10.1139/v67-161>.
- (9) Chinese Pharmacopoeia Commission. *Pharmacopoeia of the People's Republic of China*; Medical Science Press: Beijing, 2020.
- (10) Qasem, A. M. A.; Zeng, Z.; Rowan, M. G.; Blagbrough, I. S. Norditerpenoid Alkaloids from *Aconitum* and *Delphinium*: Structural Relevance in Medicine, Toxicology, and Metabolism. *Nat. Prod. Rep.* **2022**, *39* (3), 460–473. <https://doi.org/10.1039/D1NP00029B>.
- (11) Li, H. Q.; Xu, J. Y.; Fan, X. H.; Wu, S. S. Optimization of the Traditional Processing

- Method for Precision Detoxification of CaoWu through Biomimetic Linking Kinetics and Human Toxicokinetics of Aconitine as Toxic Target Marker. *J. Ethnopharmacol.* **2019**, *242* (83), 112053. <https://doi.org/10.1016/j.jep.2019.112053>.
- (12) Shi, Y.; Zhao, Y.; Qian, J.; Dong, Z.; Wen, G.; Zhao, D.; Kennelly, E. J. *Aconitum* Diterpenoid Alkaloid Profiling to Distinguish between the Official Traditional Chinese Medicine (TCM) Fuzi and Adulterant Species Using LC-QToF-MS with Chemometrics. *J. Nat. Prod.* **2021**, *84* (3), 570–587. <https://doi.org/10.1021/acs.jnatprod.0c00851>.
- (13) Yue, H.; Pi, Z. F.; Li, H. L.; Song, F. R.; Liu, Z. Q.; Liu, S. Y. Studies on the Stability of Diester-Diterpenoid Alkaloids from the Genus *Aconitum* L. by High Performance Liquid Chromatography Combined with Electrospray Ionisation Tandem Mass Spectrometry (HPLC/ESI/MS<sup>n</sup>). *Phytochem. Anal.* **2008**, *19* (2), 141–147.
- (14) He, F.; Wang, C. J.; Xie, Y.; Cheng, C. S.; Liu, Z. Q.; Liu, L.; Zhou, H. Simultaneous Quantification of Nine *Aconitum* Alkaloids in *Aconiti Lateralis Radix Praeparata* and Related Products Using UHPLC-QQQ-MS/MS. *Sci. Rep.* **2017**, *7* (1), 1–12.
- (15) Tarbe, M.; de Pomyers, H.; Mugnier, L.; Bertin, D.; Ibragimov, T.; Gignes, D.; Mabrouk, K. Gram-Scale Purification of Aconitine and Identification of Lappaconitine in *Aconitum Karacolicum*. *Fitoterapia* **2017**, *120* (May), 85–92.
- (16) Tan, G.; Lou, Z.; Jing, J.; Li, W.; Zhu, Z.; Zhao, L.; Zhang, G.; Chai, Y. Screening and Analysis of *Aconitum* Alkaloids and Their Metabolites in Rat Urine after Oral Administration of Aconite Roots Extract Using LC-TOFMS-Based Metabolomics. *Biomed. Chromatogr.* **2011**, *25* (12), 1343–1351. <https://doi.org/10.1002/bmc.1607>.
- (17) Zhang, M.; Peng, C. sheng; Li, X. bo. Human Intestine and Liver Microsomal Metabolic Differences between C19-Diester and Monoester Diterpenoid Alkaloids from the Roots of *Aconitum Carmichaelii* Debx. *Toxicol. Vitr.* **2017**, *45*, 318–333. <https://doi.org/10.1016/j.tiv.2017.09.011>.
- (18) Yang, Z.; Lin, Y.; Gao, L.; Zhou, Z.; Wang, S.; Dong, D.; Wu, B. Circadian Clock Regulates Metabolism and Toxicity of Fuzi (Lateral Root of *Aconitum Carmichaeli* Debx) in Mice. *Phytomedicine* **2020**, *67*, 153161. <https://doi.org/10.1016/j.phymed.2019.153161>.

## Chapter 4

### **The 1 $\alpha$ -Hydroxy-A-rings of norditerpenoid alkaloids are twisted-boat conformers**

**Aims:** The skeletal conformations of naturally occurring norditerpenoid alkaloids fix their substituent functional groups in space, thereby directing their bioactivities. Solution conformations of the A-rings of 4 selected norditerpenoid alkaloid free bases: mesaconitine, karacoline (karakoline), condelphine, and neoline (bullatine B), were analysed by NMR spectroscopy and single-crystal X-ray crystallography. They adopt twisted-chair, twisted-boat, twisted-boat, twisted-boat conformations, respectively. That the A-ring is stabilised in a boat conformer by an intramolecular H-bond from 1 $\alpha$ -OH to the *N*-ethyl tertiary amine is also confirmed in the condelphine single crystal data. The conformations are a result of through-space repulsion between 12-H<sub>e</sub> and atoms attached to C1 (in the equatorial positions). This causes the A-rings with 1 $\alpha$ -OR always to be twisted whether in a chair or a boat conformation. The impact of these studies is in providing a detailed understanding of the shape of the A-ring of these important biologically active natural product alkaloids.

<b>This declaration concerns the article entitled:</b>			
The 1 $\alpha$ -hydroxy-A-rings of norditerpenoid alkaloids are twisted-boat conformers			
<b>Publication status (tick one)</b>			
<b>Draft manuscript</b>	<input type="checkbox"/>	<b>Submitted</b>	<input type="checkbox"/>
		<b>In review</b>	<input type="checkbox"/>
		<b>Accepted</b>	<input type="checkbox"/>
		<b>Published</b>	<input checked="" type="checkbox"/>
<b>Publication details (reference)</b>	Zeng, Z., Qasem, A. M. A., Kociok-Köhn, G., Rowan, M. G., and Blagbrough, I. S., 2020. The 1 $\alpha$ -hydroxy-A-rings of norditerpenoid alkaloids are twisted-boat conformers. <i>RSC Advances</i> , <b>10</b> , 18797-18805.		
<b>Copyright status (tick the appropriate statement)</b>			
The material has been published with a CC-BY license		<input checked="" type="checkbox"/>	The publisher has granted permission to replicate the material included here
		<input type="checkbox"/>	
<b>Candidate's contribution to the paper (provide details, and also indicate as a percentage)</b>	<p><b>Formulation of ideas:</b> The candidate contributed to the formulation of the article ideas (60%)</p> <p><b>Design of methodology:</b> The candidate contributed to design the study of ring A conformation in selected 1-OH and 1-OMe NDA using NMR and X-ray crystallography (60%)</p> <p><b>Experimental work:</b> The candidate contributed to the analysis of the selected NDA crystallization of mesaconitine and condelphine (60%).</p> <p><b>Presentation of data in journal format:</b> The candidate contributed to the paper writing and figures presentation (60%)</p>		
<b>Statement from Candidate</b>	This paper reports on original research I conducted during the period of my Higher Degree by Research candidature.		
<b>Signed (typed signature)</b>	Ashraf Qasem	<b>Date</b>	21/09/2022

## Introduction

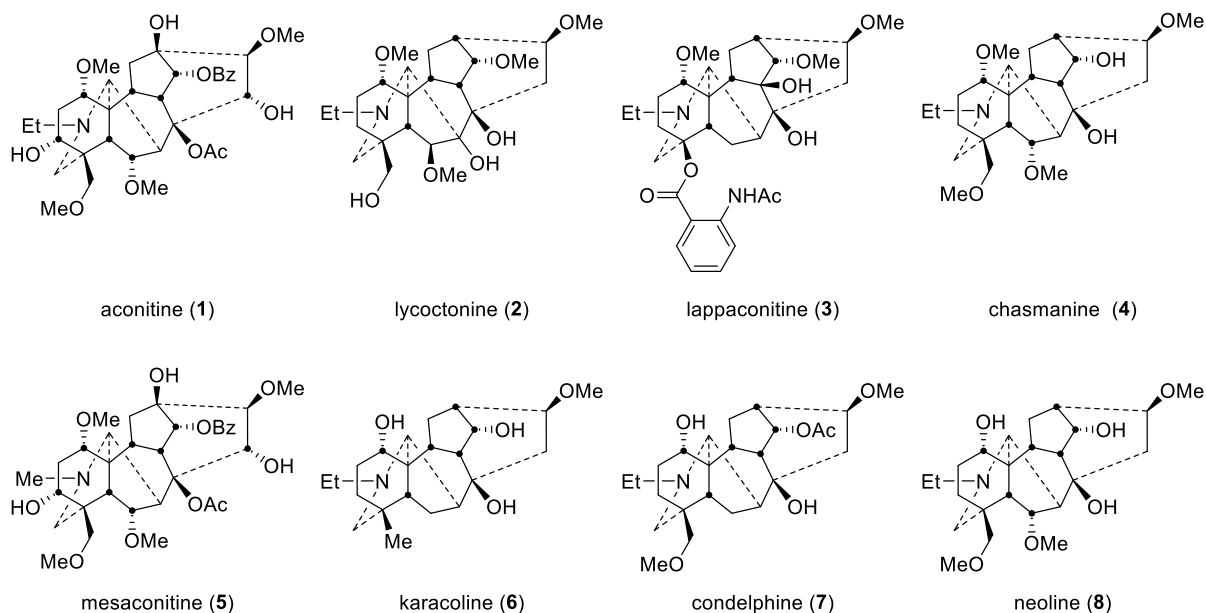


**Figure 1.** Selected norditerpenoid alkaloids

The unambiguous structural identification of naturally occurring norditerpenoid alkaloids with 6 fused and bridged rings is complicated. Evaluation of their structure in terms of both conformation and configuration is important as 3D orientation is a key parameter for controlling biological activity. The positions of certain functional groups were not initially assigned accurately.<sup>1-4</sup> With application of single crystal X-ray diffraction (SXRD), several important norditerpenoid alkaloids were eventually evaluated, e.g. aconitine (**1**, Fig. 1) was first reported in 1833,<sup>5</sup> and its structure was confirmed in 1959;<sup>6,7</sup> lycoctonine (**2**) was first reported in 1865,<sup>8</sup> and its structure was confirmed in 1956;<sup>9</sup> lappaconitine (**3**) was first reported in 1895,<sup>10,11</sup> and its structure was confirmed in 1969.<sup>12,13</sup> The orientational assignments of oxygenated groups attached to C1 of several norditerpenoid alkaloids were revised unambiguously using SXRD data, e.g. aconitine (**1**), lycoctonine (**2**), and chasmanine (**4**).<sup>14-20</sup> Solution conformation studies can provide detail of the bioactive conformations in biological fluids of these pharmacologically important norditerpenoid alkaloids. Specifically, we are studying the effects of the C1- $\alpha$ -oxygenated substituents on the A-rings in four selected norditerpenoid alkaloids.



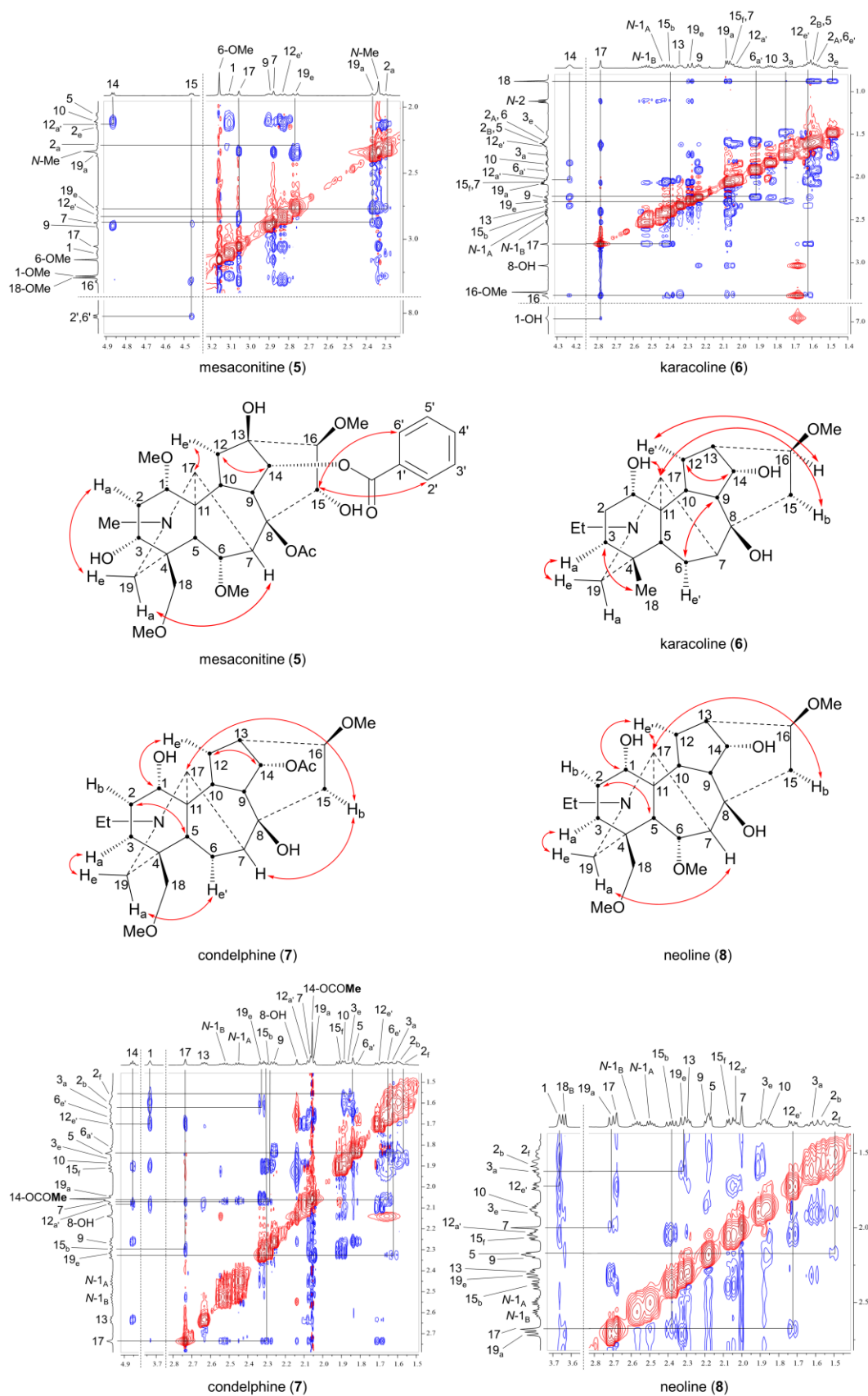


**Figure 2.** Key NOESY correlations of the selected norditerpenoid alkaloids. Orientation label: a = axial, e = equatorial, b = bowsprit, f = flagpole, a' = pseudo-axial, e' = pseudo-equatorial.

## Results and Discussion

Complete and unambiguous NMR spectroscopic data of mesaconitine (**5**, Fig. 1), karacoline (**6**, karakoline), condelphine (**7**), and neoline (**8**, bullatine B) were obtained. Some literature assignments of  $^{13}\text{C}$  NMR signals of mesaconitine (**5**) and condelphine (**7**) have been revised supported by 2D NMR data. Due to repulsion between  $1\alpha\text{-OMe}$  (in the equatorial position)/ $12\text{-H}_e$  proposed by Pelletier and co-workers,<sup>13,21,22</sup> the A-ring of norditerpenoid alkaloid free bases with  $1\alpha\text{-OMe}$  adopting chair conformations are twisted. This significant proximity decreases when the A-rings adopt boat conformations as the *O*-atom flips to the axial position and therefore away from  $12\text{-H}_e$ , e.g. norditerpenoid alkaloid (with  $1\alpha\text{-OMe/OH}$ ) salts and norditerpenoid alkaloid free bases with  $1\alpha\text{-OH}$ , which may lead to the A-rings adopting true-boat (not twisted) conformations.

Mesaconitine (**5**) with  $1\alpha\text{-OMe}$ , having an A-ring in the chair conformation proven by NOESY correlation  $2\text{-H}_a/19\text{-H}_e$  (Fig. 2) and SXRDR data (Fig. 3, torsion angle  $\theta_{\text{C1-C11-C4-C3}} = 9.28^\circ > 4^\circ$ , details of SXRDR data are reported in Tables S5-S6). It is highlighted that  $\delta(2\text{-H}_a) = 2.31$  ppm is unusually larger than  $\delta(2\text{-H}_a) = 2.14$  ppm by 0.17 ppm. The chemical shift of the axial proton of cyclohexane is normally larger than that of the geminal equatorial proton by  $\sim 0.5$  ppm due to magnetic anisotropic effect.<sup>23,24</sup> As the lone-pair electrons of the tertiary amine *N*-atom sterically compress  $2\text{-H}_a$  in the half-cage A/E-[3.3.1]azabicyclo,  $2\text{-H}_a$  is therefore deshielded and its chemical shift becomes larger than that of  $2\text{-H}_e$ .<sup>25,26</sup> In detail,  $1\text{-H}_a$  (Fig. 4) of mesaconitine (**5**) resonates as a dd peak ( $\delta = 3.11$  ppm,  $^3J_{aa} = 9.0$  Hz,  $^3J_{ae} = 6.2$  Hz, Fig. 5) confirms that the A-ring adopts a chair conformation,<sup>22</sup> and the smaller  $^3J_{aa} = 9.0$  Hz (normally found in the range 12-14 Hz) indicates that this chair conformation is twisted as explained by Eliel.<sup>27,28</sup>

The A-rings of the selected  $1\alpha\text{-OH}$  alkaloids, karacoline (**6**), condelphine (**7**), and neoline (**8**), adopt boat conformations stabilized by an H-bond between the tertiary amine and  $1\alpha\text{-OH}$ ,<sup>21,29,30</sup> and they are proven to be in a twisted-boat conformation. For instance, the A-ring of neoline (**8**) adopts a boat conformation confirmed by NOESY correlation  $2\text{-H}_f/5\text{-H}$ , and  $1\text{-H}_e$  resonates as a narrow t peak ( $\delta = 3.66$  ppm,  $^3J_{be} = ^3J_{ef} = 3.3$  Hz, proton labelling is shown in Fig. 4). It is notable that  $^3J_{ef} = 3.3$  Hz of this  $1\text{-H}_e$  of neoline (**8**) is different from  $^3J_{ef} = 5.3$  Hz of  $3\text{-H}_e$

that displays in the signal of 2-H<sub>f</sub> ( $\delta = 1.49$  ppm, tdd,  $^2J_{\text{gem}} = ^3J_{\text{af}} = 14.0$  Hz,  $^3J_{\text{ef}} = 5.3$  Hz,  $^3J_{\text{ef}} = 3.3$  Hz) determining that the boat-conformer A-ring of neoline (**8**) is twisted, as  $^3J_{\text{ef}} = 5.3$  Hz (3-H<sub>e</sub>)  $>$   $^3J_{\text{ef}} = 3.3$  Hz (1-H<sub>e</sub>) indicates dihedral angle  $\angle(1\text{-H}_e)\text{-C1-C2-(2-H}_f) <$   $\angle(2\text{-H}_f)\text{-C2-C3-(3-H}_e)$  according to the Karplus relationship.<sup>31</sup>

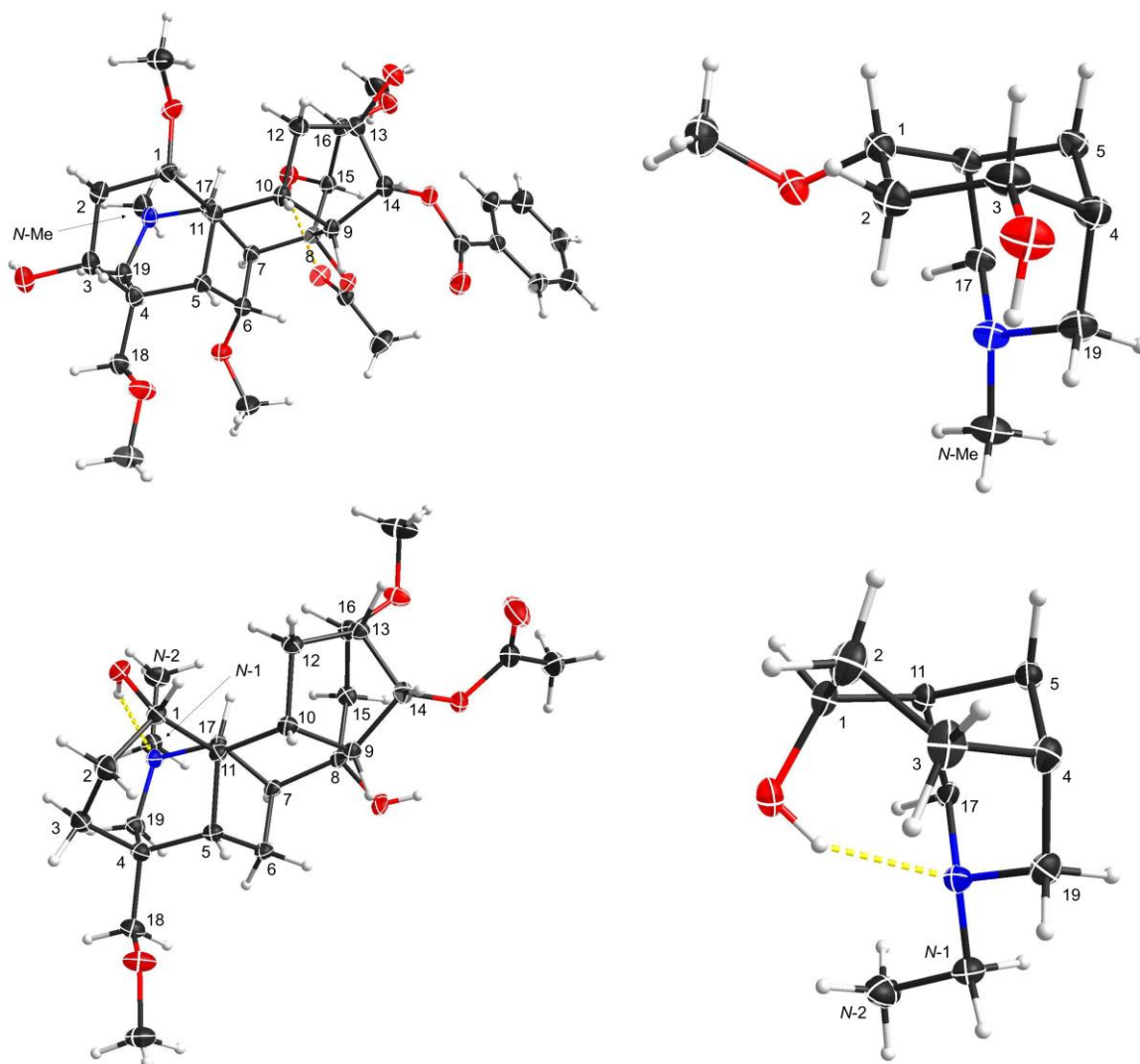


**Figure 3.** SXR D data of mesaconitine (**5**, upper) and condelphine (**7**, lower), and their A/E-[3.3.1]azabicyclic frames. ORTEP presentations of the crystal structures show the atom position with a 50% probability for each ellipsoid.

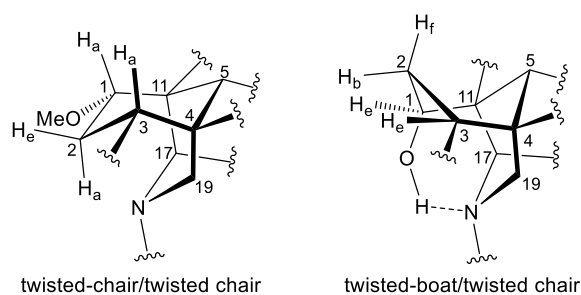


**Figure 4.** Conformations of A/E-[3.3.1]azabicycles of norditerpenoid alkaloids

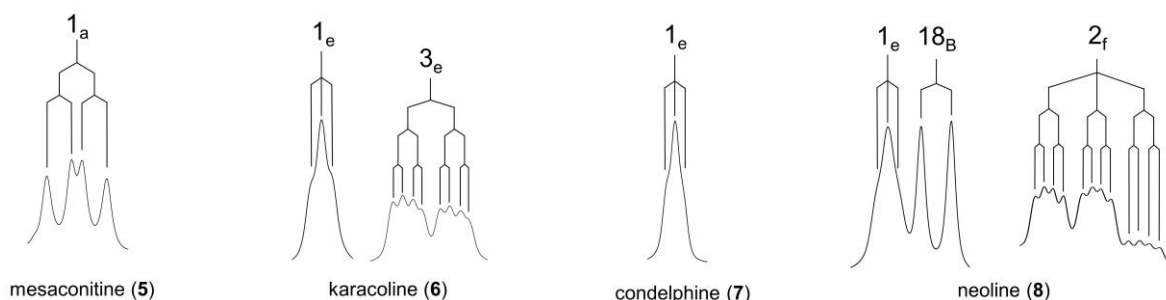


**Figure 5.** Coupling patterns of key  $^1\text{H}$  NMR signals of the selected norditerpenoid alkaloids

This result reveals that the through-space repulsion between 1- $\text{H}_e$  and 12- $\text{H}_e'$  is twisting the A-ring in a boat conformation.<sup>21,22</sup> Similar broad triplets of 1- $\text{H}_e$  with small  $^3J_{ef} \sim 3$  Hz were observed in  $^1\text{H}$  NMR spectra of karacoline (**6**) ( $\delta = 3.71$  ppm,  $^3J_{be} = ^3J_{ef} = 3.0$  Hz) and condelphine (**7**) ( $\delta = 3.73$  ppm,  $^3J_{be} = ^3J_{ef} = 3.0$  Hz). In addition, 3- $\text{H}_e$  of karacoline (**6**) resonates as a ddd peak ( $\delta = 1.48$  ppm,  $^2J_{gem} = 13.5$  Hz,  $^3J_{ef} = 5.8$  Hz,  $^3J_{be} = 3.0$  Hz). Its  $^3J_{ef}$  (5.8 Hz) of 3- $\text{H}_e$  is significantly different from the  $^3J_{ef}$  (3.0 Hz) of 1- $\text{H}_e$  which supports the conclusion that the boat-like A-rings of these  $1\alpha$ -OH alkaloids are twisted. This conclusion that the A-rings of  $1\alpha$ -OH norditerpenoid alkaloids adopt twisted-boat conformations are supported by SXR D data of condelphine (**7**) free base (Fig. 3), in which the A-ring clearly adopts a twisted-boat conformer (torsion angle  $\theta_{\text{C1-C11-C4-C3}} = 6.81^\circ > 4^\circ$ ), and is stabilized by an H-bond between 1-OH and the tertiary N-atom.

As there is proximity between  $6\alpha$ - $\text{H}_e'$  (or  $6\alpha$ -OMe) and 19- $\text{H}_a$ , e.g. in the NOESY correlation  $6\alpha$ - $\text{H}_e'/19$ - $\text{H}_a$  of condelphine (**7**) (Fig. 2), the N-substituted piperidine E-rings of norditerpenoid alkaloids always adopt twisted-chair conformations.<sup>21,22</sup> This conclusion of the E-ring adopting twisted-chair conformations is supported by the SXR D data of both mesaconitine (**5**) and condelphine (**7**) (torsion angles  $\theta_{\text{C19-C4-C11-C17}}$  are  $13.60^\circ$  and  $11.32^\circ$ , respectively,  $> 4^\circ$ ). Thus,

the conformations of the A/E-[3.3.1]azabicycles of norditerpenoid alkaloids bearing 1 $\alpha$ -OR are always twisted (Fig. 4).

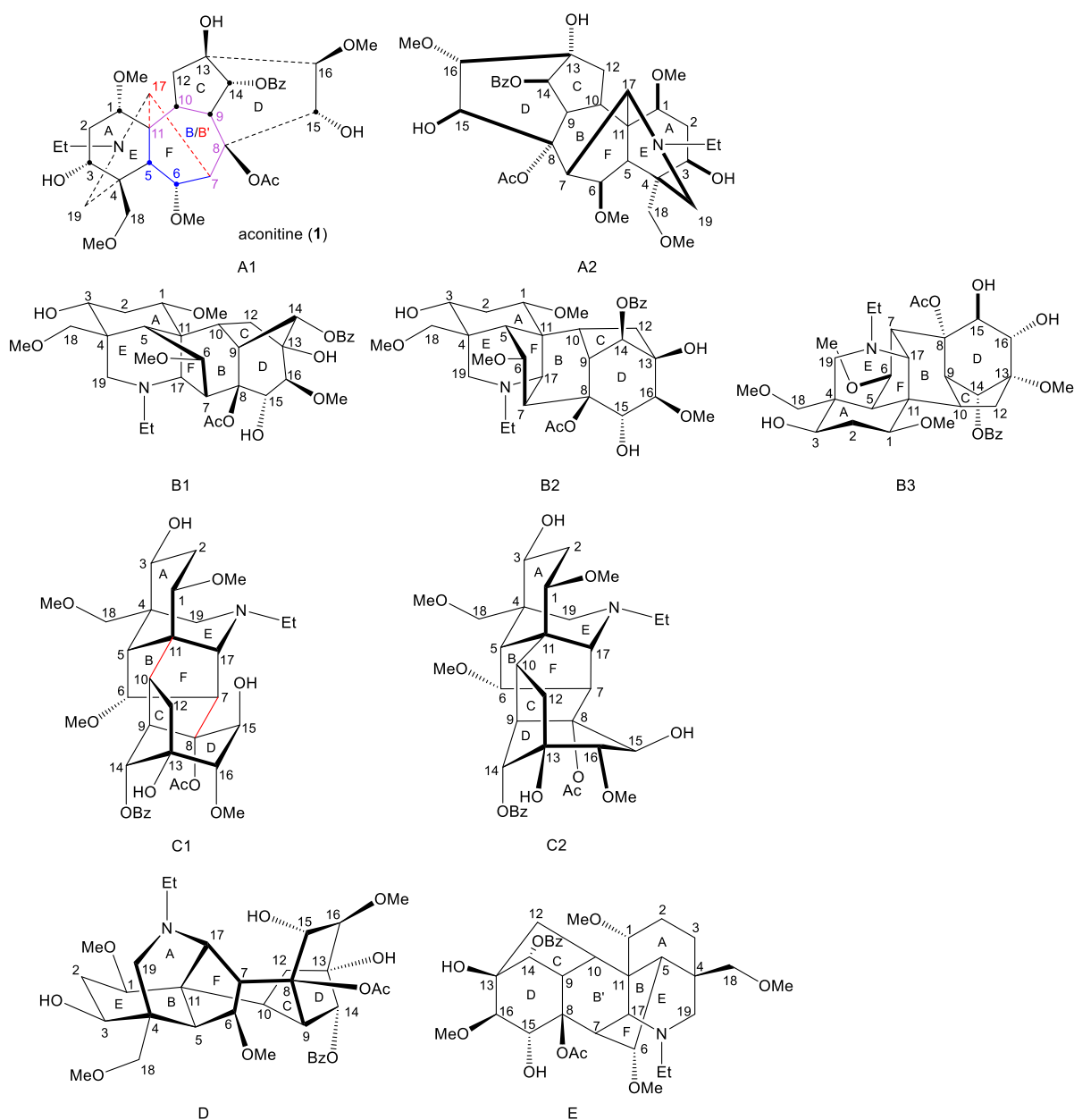


**Figure 6.** Aconitine (**1**) free base shown in different literature depictions

For any research purpose in studies of norditerpenoid alkaloids, certain depictions must be employed to present structures of these polycyclic natural products, and a suitable depiction displaying favourable stereochemical information helps to achieve those specific goals. Such an understanding may possibly inspire research in various related areas, e.g. phytochemistry, organic synthesis, and structure-activity relationship (SAR) studies of biological activity. Several

different reported depictions of norditerpenoid alkaloids are shown (Fig. 6) using aconitine (**1**) free base as an example.

The depiction A1 is currently the most popular reported in the field of phytochemistry.<sup>32-36</sup> The depiction clearly displays three rings, A-, B- and C-ring, in suitable shapes. However, the conformations of some rings, e.g. A-, B-, and D-ring, are difficult to determine from this depiction. Through-space distances between some atoms are not favoured, e.g. C15 and C17 are actually close in space, but they are shown away in depiction A1. Also, some bonds have to be depicted with a particularly long length, e.g. C7–C17. In some reported studies, especially in crystallographic studies,<sup>9,37,38</sup> the 7-membered B-ring (C5–C11) refers to a 6-membered ring (B'-ring = C7–C8–C9–C10–C11–C17). Depiction A2 which is viewing depiction A1 from the other face (it is not the enantiomer) was also employed in order to present the D-, E- or F-ring on the  $\beta$ -face that might be beneficial for retrosynthetic analysis.<sup>39-41</sup>

Depictions B1 and B2 are also popularly used.<sup>42,43</sup> Generally, these depictions B1 and B2 allow almost all the rings to be shown in the correct conformation, with well-balanced bond lengths (not of extreme length), and reasonable orientations of substituted functional groups. Specifically, depiction B1 shows the D-ring in the correct mono-flattened conformation. Depiction B2 allows space for the highly bridged B-ring, which brings benefit to any essential expansion of functional groups attached to the B-ring. However, depiction B2 cannot show the conformation of the D-ring, and therefore the orientations of the atoms/functional groups attached to this ring are ambiguously presented. Depictions B1 and B2 are widely employed by organic synthetic chemists for various reasons, e.g. B-ring with the largest number of bridgeheads displayed in the front may benefit retrosynthetic analysis,<sup>44,45</sup> and it is also useful for designing disconnections of C-, D- and F-rings as these drawings correctly express the conformations.<sup>46,47</sup> A rotated depiction of B2 (depiction B3, Fig. 6) was used for designing synthetic approaches starting with analogues of C/D-rings.<sup>48</sup> Apart from the popular drawings A and B, an uncommon depiction C1 was also used,<sup>49,50</sup> in which the relationship between the A/E/F-tricycle and C/D-bicycle are distinctly expressed, and these two cycles are clearly linked by bond C7–C8 and bond C10–C11 perhaps motivating retrosynthetic analysis. As the D-ring adopts a mono-flattened boat conformation with C14 at the flap, thus depiction C1 is slightly revised to C2. It is notable that

only the A-ring has 3 flexible C-atoms (C1-C3) that allow the conformation of the A-ring to flip; all other rings only have one or two flexible atoms in their skeleta. Therefore, conformations of these rings are inflexible, and the D-ring thereby adopts a fixed mono-flattened boat conformation. Furthermore, rare depictions D and E were also reported in older studies. Depiction D presents similar ideals to those of depiction C1,<sup>51</sup> and depiction E was also shown in some crystallographic studies displaying piperidine E-, B'-, and D-rings in essentially ideal shapes.<sup>9,20,37</sup>

In order to compare these depictions of norditerpenoid alkaloid, key NOESY correlations of mesaconitine (**5**), karacoline (**6**), condelphine (**7**), and neoline (**8**) are shown in depiction B1 (B1') and C2 (C2') (Fig. 7a and Fig. 7b) in comparison with those in depiction A1 (Fig. 6).

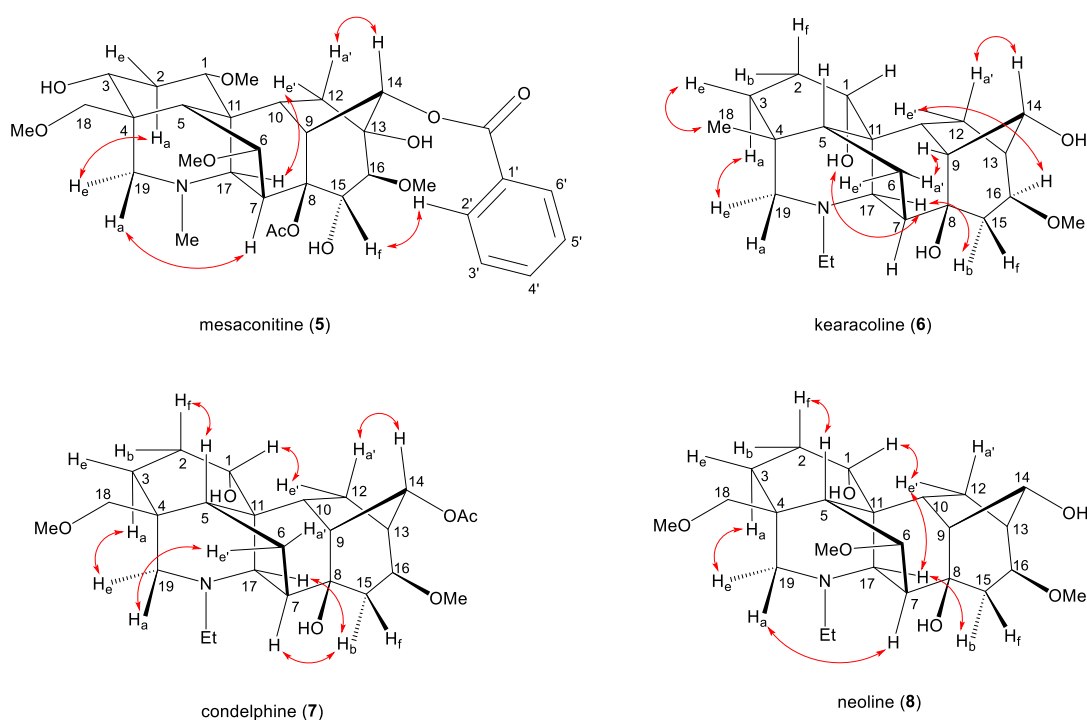


**Figure 7a.** Key NOESY correlations of the selected norditerpenoid alkaloids in depiction B1 (B1'). Depiction B1 shows the A-ring in chair conformation and depiction B1' shows the A-ring in boat conformation

The A-rings of karacoline (**6**), condelphine (**7**), and neoline (**8**) adopt boat conformation proven by NOESY correlation 2-H<sub>f</sub>/5-H; however, this evidence cannot be unambiguously presented by depiction A1 as the conformation of the A-ring is hard to display in this depiction (Fig. 7). Moreover, some atoms that are close in space are not able to be displayed in this depiction, e.g. 7-H/19-H<sub>a</sub>, 15-H<sub>b</sub>/17-H (both on the  $\alpha$ -face).

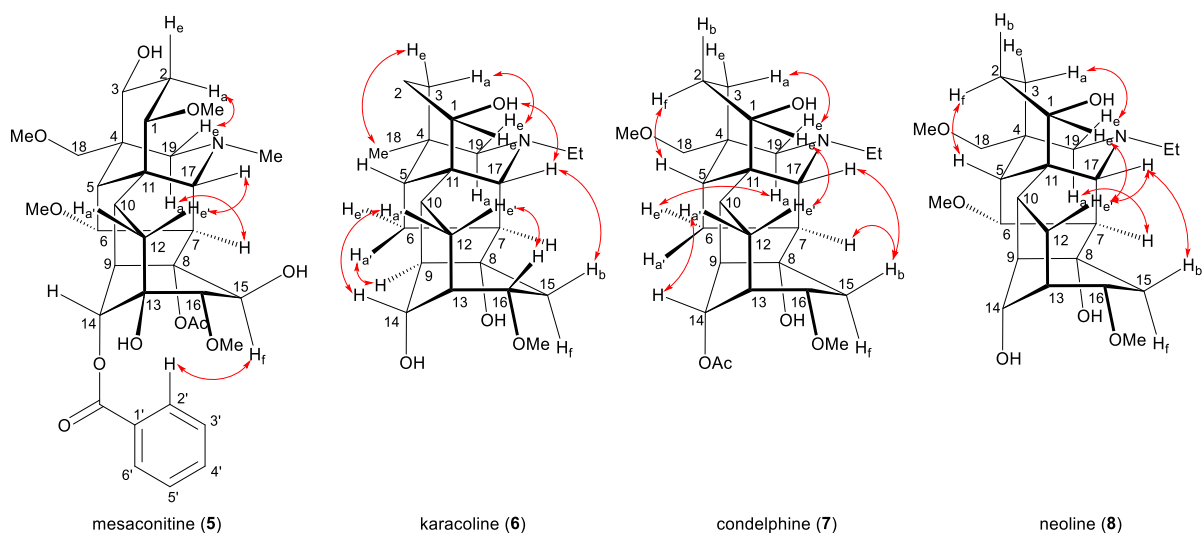


**Figure 7b.** Key NOESY correlations of the selected norditerpenoid alkaloids in depiction C2 (C2'). Depiction C2 shows the A-ring in chair conformation and depiction C2' shows the A-ring in boat conformation

Depictions B1 (B1') and C2 (C2') indicate the conformations of the A-rings (Fig. 7a and Fig. 7b). However, some atoms that are close in space are separated from each other in depiction C2, e.g. 6-H<sub>c</sub>/19-H<sub>a</sub> of condelphine (7) and 15-H<sub>b</sub>/17-H of neoline (8). Besides, the internal space of depiction C2 is too narrow to allow the essential expansion of certain C–H bonds, e.g. protons attached to C1 and C12. Depiction B1 (B1') almost ideally displays the distances between atoms in space except 7-H/19-H<sub>a</sub>, and the internal space of the B-ring of this depiction is narrow, in which some C–H bonds are hard to be shown clearly, e.g. protons attached to C6 and C9. According to the SXRD data of mesaconitine (5) and condelphine (7) (Fig. 8) and a report by Marion and co-workers,<sup>43</sup> depiction B1 (B1') is slightly modified to afford depiction B4 (B4') (Fig. 7c), in which through-space distances between atoms are well-balanced and that aspect is favoured for the investigation of the stereochemistry of these norditerpenoid alkaloids.



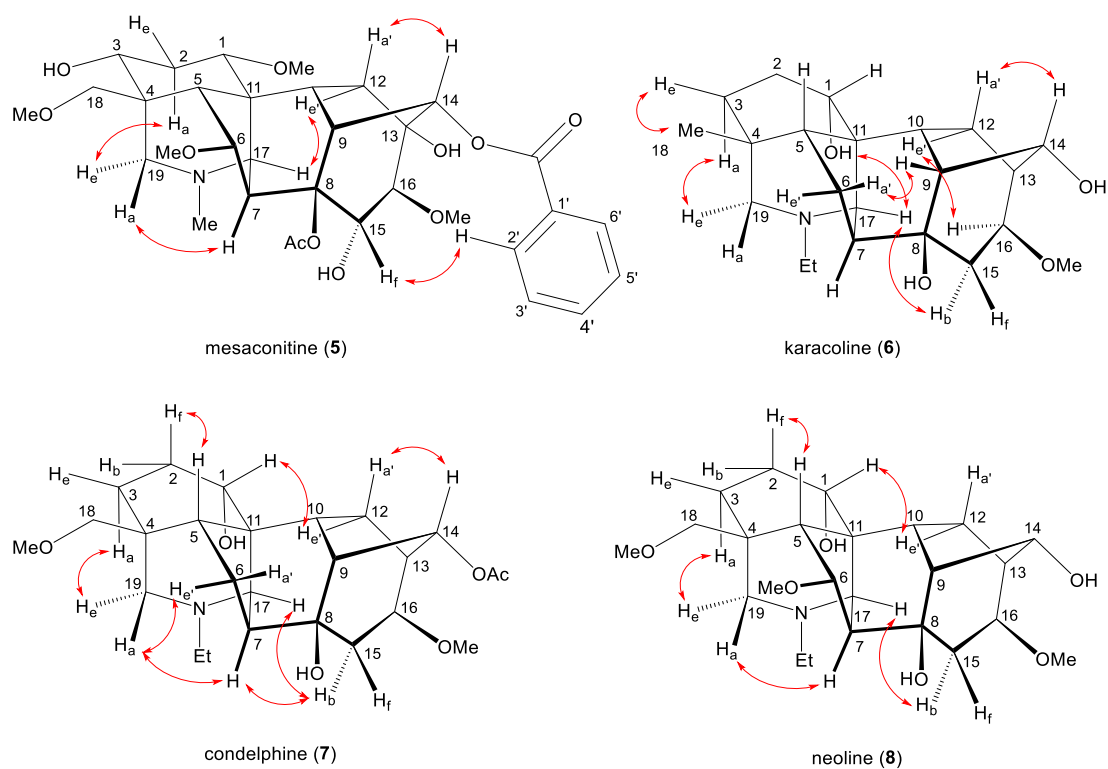


**Figure 7c.** Key NOESY correlations of the selected norditerpenoid alkaloids in depiction B4 (B4'). Depiction B4 shows the A-ring in chair conformation and depiction B4' shows the A-ring in boat conformation

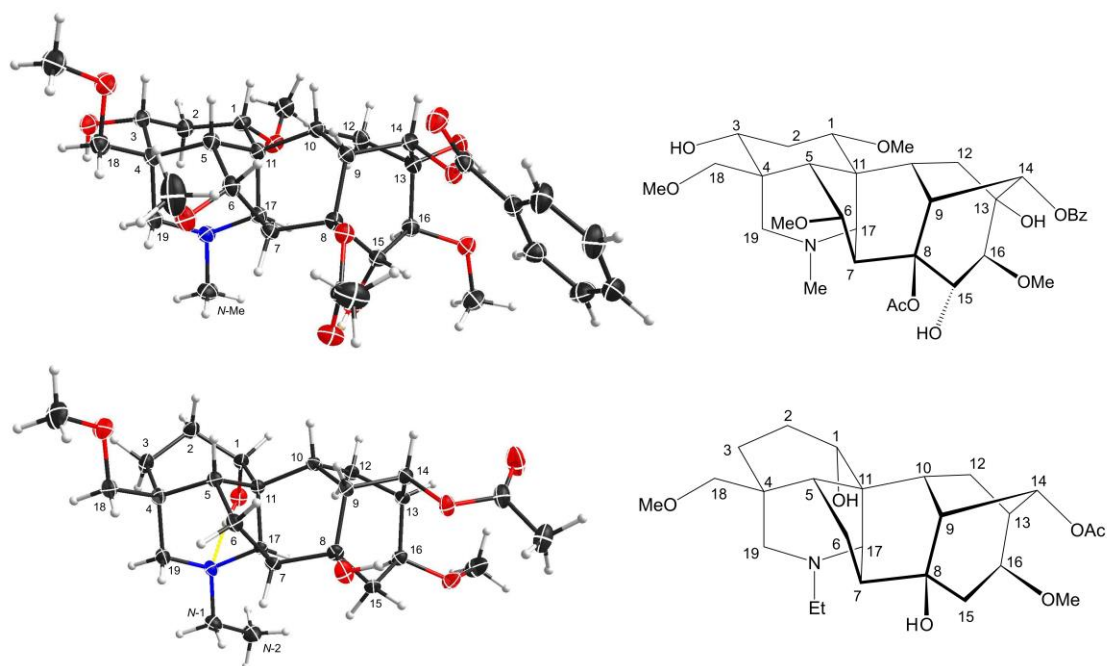


**Figure 8.** Depiction B4 (B4') according to SXRD data of mesaconitine (5, upper) and condolphine (7, lower)

## Orientation of 7-H/OR

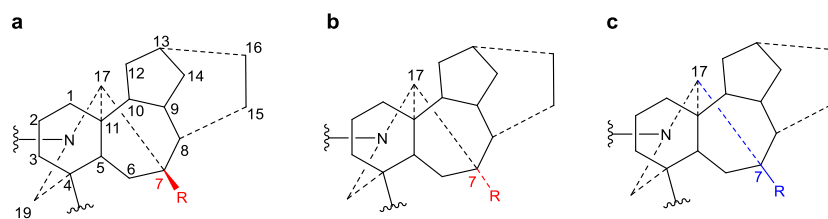


**Figure 9.** Skeleta of norditerpenoid alkaloids in depiction A1

7-OR is the signature of the lycoctonine-subtype  $C_{19}$ -diterpenoid alkaloids.<sup>18</sup> In norditerpenoid alkaloids presented in depiction A1, 7-H/7-OR is popularly assigned as  $\beta$ -orientated (Fig. 9a).<sup>32,33,36</sup> However, 7-H displayed in the SXR data of mesaconitine (**5**) and condelphine (**7**) shown in an angle imitating depiction A1 do not show a typical  $\beta$ -orientation (Fig. 3). Moreover, NOESY correlations of 7-H/19- $H_a$  of mesaconitine (**5**), condelphine (**7**), and neoline (**8**) were observed in this work, which proves that this 7-H cannot be  $\beta$ -orientated as typically drawn. In fact, a few uncommon assignments of  $7\alpha$ -OH of lycoctonine-type alkaloids have been reported (Fig. 9b),<sup>37,52</sup> but they are not favoured as bond C7–C17 must be on the  $\alpha$ -face. These 7-H/7-OR are equatorial  $\beta$ -orientated rather than typically axial  $\beta$ -orientated like protons or functional groups attached to C8 (Fig. 8), therefore, it is more appropriate and precise to draw the 7-H/7-OR in the plane of the paper if depiction A1 is employed for emphasizing this orientational feature of 7-H/7-OR, which has also been used in previous publications (Fig. 9c).<sup>18,34,35</sup>

## Conclusions

A rare  $^1H$  NMR effect of steric compression is demonstrated in the A/E-[3.3.1]azabicyclic of mesaconitine (**5**), in which the lone-pair electrons of the tertiary amine *N*-atom compress 2- $H_a$  through space and therefore they deshield this proton. The A-rings of norditerpenoid alkaloids substituted at C1 with  $\alpha$ -orientated oxygenated functional groups adopt twisted conformers due to the repulsion between atoms attached to C1 (*H*- or *O*-atoms in the equatorial position) and 12- $H_e$ , no matter whether the A-rings are in chair or boat conformations. Different reported depictions of norditerpenoid alkaloids are compared according to the clarity of understanding for

key NOESY correlations of the 4 selected alkaloid free bases, and the depiction B4 modified from depictions B1 and B2 is favoured to represent these natural products in publications as B4 expresses all the necessary information on conformation and orientation. 7-H/OR of norditerpenoid alkaloids is equatorially  $\beta$ -orientated, thus 7-H/7-OR is best drawn in the plane of the paper to distinguish its orientation from those typically axially  $\beta$ -orientated functional groups, e.g. 8-H/OR.

### Acknowledgements

We thank Carbosynth Ltd. (UK) for the donated condelphine (**7**).

*RSC Advances*, **2020**, *10*, 18797-18805. doi 10.1039/d0ra03811c

Crystallographic data from the structural analysis have been deposited with CCDC no. 1990874 for mesaconitine (**5**) and 1990875 for condelphine (**7**) at the Cambridge Crystallographic Data Center (CCDC). Copies of this information may be obtained free of charge from the website: [www.ccdc.cam.ac.uk](http://www.ccdc.cam.ac.uk).

### References

- 1 K. Wiesner, M. Gotz, D. L. Simmons, L. R. Fowler, F. W. Bachelor, R. F. C. Brown and G. Buchi, *Tetrahedron Lett.*, 1959, **1**, 15-24.
- 2 L. Marion and R. H. F. Manske, *Can. J. Res.*, 1946, **24b**, 1-4.
- 3 O. E. Edwards and L. Marion, *Can. J. Chem.*, 1952, **30**, 627-645.
- 4 O. E. Edwards and L. Marion, *Can. J. Chem.*, 1954, **32**, 195-213.
- 5 E. Nyirimigabo, Y. Y. Xu, Y. B. Li, Y. M. Wang, K. Agyemang and Y. J. Zhang, *J. Pharm. Pharmacol.*, 2015, **67**, 1-19.
- 6 M. Przybylska and L. Marion, *Can. J. Chem.*, 1959, **37**, 1116-1118.
- 7 K. Wiesner, D. L. Simmons and L. R. Fowler, *Tetrahedron Lett.*, 1959, **1**, 1-4.
- 8 E. S. Stern in: *The Alkaloids* (Eds.: R. H. F. Manske and H. L. Holmes), Academic Press, New York, 1954, vol. 4, ch. 37, pp. 275-333.
- 9 M. Przybylska and L. Marion, *Can. J. Chem.*, 1956, **34**, 185-187.

- 10 L. Marion, L. Fonzes, C. K. Wilkins, J. P. Boca, F. Sandberg, R. Thorsen and E. Linden, *Can. J. Chem.*, 1967, **45**, 969-973.
- 11 N. Mollov, M. Tada and L. Marion, *Tetrahedron Lett.*, 1969, **10**, 2189-2192.
- 12 G. I. Birnbaum, *Tetrahedron Lett.*, 1969, **10**, 2193-2194.
- 13 G. I. Birnbaum, *Acta Crystallogr. B*, 1970, **26**, 755-765.
- 14 K. B. Birnbaum, K. Wiesner, E. W. K. Jay and L. Jay, *Tetrahedron Lett.*, 1971, **12**, 867-870.
- 15 S. W. Pelletier, Z. Djarmati and S. Lajsic, *J. Am. Chem. Soc.*, 1974, **96**, 7817-7818.
- 16 S. W. Pelletier, W. H. De Camp and Z. Djarmati, *J. Chem. Soc., Chem. Commun.*, 1976, 253-254.
- 17 W. H. De Camp and S. W. Pelletier, *Acta Crystallogr. B*, 1977, **33**, 722-727.
- 18 S. W. Pelletier, N. V. Mody, K. I. Varughese, J. A. Maddry and H. K. Desai, *J. Am. Chem. Soc.*, 1981, **103**, 6536-6538.
- 19 O. E. Edwards and M. Przybylska, *Can. J. Chem.*, 1982, **60**, 2661-2667.
- 20 M. Cygler, M. Przybylska and O. E. Edwards, *Acta Crystallogr. B*, 1982, **38**, 479-482.
- 21 S. W. Pelletier, Z. Djarmati, S. Lajsic and W. H. De Camp, *J. Am. Chem. Soc.*, 1976, **98**, 2617-2625.
- 22 S. W. Pelletier and Z. Djarmati, *J. Am. Chem. Soc.*, 1976, **98**, 2626-2636.
- 23 E. W. Garbisch and M. G. Griffith, *J. Am. Chem. Soc.*, 1968, **90**, 6543-6544.
- 24 D. H. Williams and I. Fleming, *Spectroscopic Methods in Organic Chemistry*, McGraw-Hill, London, 6th edn., 2008.
- 25 S. Winstein, P. Carter, F. A. L. Anet and A. J. R. Bourn, *J. Am. Chem. Soc.*, 1965, **87**, 5247-5249.
- 26 E. Vogel, U. Brocker and H. Junglas, *Angew. Chem., Int. Ed. Engl.*, 1980, **19**, 1015-1016.
- 27 E. L. Eliel and S. M. C. Knoeber, *J. Am. Chem. Soc.*, 1968, **90**, 3444-3458.
- 28 E. L. Eliel, *Acc. Chem. Res.*, 1970, **3**, 1-8.
- 29 Z.-Q. Mu, H. Gao, Z.-Y. Huang, X.-L. Feng and X.-S. Yao, *Org. Lett.*, 2012, **14**, 2758-2761.
- 30 Z.-T. Zhang, L. Wang, Q.-F. Chen, Q.-H. Chen, D.-L. Chen, X.-Y. Liu and F.-P. Wang, *Tetrahedron*, 2013, **69**, 5859-5866.
- 31 M. Karplus, *J. Am. Chem. Soc.*, 1963, **85**, 2870-2871.
- 32 S. W. Pelletier and S. W. Page, *Nat. Prod. Rep.*, 1984, **1**, 375-386.
- 33 S. W. Pelletier and S. W. Page, *Nat. Prod. Rep.*, 1986, **3**, 451-464.
- 34 M. S. Yunusov, *Nat. Prod. Rep.*, 1991, **8**, 499-526.
- 35 M. S. Yunusov, *Nat. Prod. Rep.*, 1993, **10**, 471-486.
- 36 F.-P. Wang, Q.-H. Chen and X.-Y. Liu, *Nat. Prod. Rep.*, 2010, **27**, 529-570.

- 37 M. Przybylska, *Acta Crystallogr.*, 1961, **14**, 424-429.
- 38 P. W. Codding, *Acta Crystallogr. B*, 1982, **38**, 2519-2522.
- 39 K. Wiesner, T. Y. R. Tsai, K. Huber, S. E. Bolton and R. Vlahov, *J. Am. Chem. Soc.*, 1974, **96**, 4990-4992.
- 40 T. Tabuchi, D. Urabe and M. Inoue, *J. Org. Chem.*, 2016, **81**, 10204-10213.
- 41 D. Kamakura, H. Todoroki, D. Urabe, K. Hagiwara and M. Inoue, *Angew. Chem. Int. Ed.*, 2020, **59**, 479-486.
- 42 L. H. Keith and S. W. Pelletier in *Chemistry of The Alkaloids* (Ed.: S. W. Pelletier), Van Nostrand Reinhold, New York, 1970, ch. 18, pp. 549-590.
- 43 O. E. Edwards, L. Fonzes and L. Marion, *Can. J. Chem.*, 1966, **44**, 583-589.
- 44 C. J. Marth, G. M. Gallego, J. C. Lee, T. P. Lebold, S. Kulyk, K. G. M. Kou, J. Qin, R. Lilien and R. Sarpong, *Nature*, 2015, **528**, 493-498.
- 45 K. G. M. Kou, S. Kulyk, C. J. Marth, J. C. Lee, N. A. Doering, B. X. Li, G. M. Gallego, T. P. Lebold and R. Sarpong, *J. Am. Chem. Soc.*, 2017, **139**, 13882-13896.
- 46 N. A. Doering, K. G. M. Kou, K. Norseeda, J. C. Lee, C. J. Marth, G. M. Gallego and R. Sarpong, *J. Org. Chem.*, 2018, **83**, 12911-12920.
- 47 X.-H. Zhou, Y. Liu, R.-J. Zhou, H. Song, X.-Y. Liu and Y. Qin, *Chem. Commun.*, 2018, **54**, 12258-12261.
- 48 R. M. Conrad and J. Du Bois, *Org. Lett.*, 2007, **9**, 5465-5468.
- 49 Y. Shi, J. T. Wilmot, L. U. Nordstrøm, D. S. Tan and D. Y. Gin, *J. Am. Chem. Soc.*, 2013, **135**, 14313-14320.
- 50 X. Y. Liu and D. Y. Chen, *Angew. Chem. Int. Ed.*, 2014, **53**, 924-926.
- 51 W. Schneider and H. Tausend, *Liebigs Ann.*, 1959, **628**, 114-122.
- 52 O. E. Edwards, M. Los and L. Marion, *Can. J. Chem.*, 1959, **37**, 1996-2006.

## Chapter 5

### **Impacts of steric compression, protonation, and intramolecular hydrogen-bonding on the $^{15}\text{N}$ NMR spectroscopy of norditerpenoid alkaloids and their piperidine-ring Analogues**

**Aims:**  $^1\text{H}$ - $^{15}\text{N}$  HMBC spectra of norditerpenoid alkaloids and their synthetic azabicyclic analogues were obtained in order to investigate the impacts caused by the through-space effect of steric compression, protonation, and the formation of intramolecular hydrogen-bonding on the  $^{15}\text{N}$  NMR spectroscopy of these natural products and their piperidine containing analogues. A rare  $^{15}\text{N}$  NMR effect of steric compression is demonstrated in half-cage A/E-rings of norditerpenoid alkaloid free bases and their synthetic azabicyclic analogues, in which the distribution of the lone-pair electrons of the tertiary amine *N*-atom is sterically restricted by bridged cycloalkanes, e.g. cyclopentane, cyclohexane, and cycloheptane rings. This results in significant changes in the  $^{15}\text{N}$  chemical shift, typically by at least  $\sim 10$  ppm. The lone-pair electrons of the *N*-atom in the piperidine ring are sterically compressed whether the bridged cyclohexane ring adopts a chair or boat conformation. The  $^{15}\text{N}$  chemical shifts of  $1\alpha$ -OMe norditerpenoid alkaloid free bases significantly increase ( $\Delta\delta_{\text{N}} \geq 15.6$  ppm) on alkaloid protonation and thence the formation of an intramolecular hydrogen bond between  $\text{N}^+\text{-H}$  and  $1\alpha$ -OMe. The intramolecular hydrogen bonds between the *N*-atom and  $1\alpha$ -OH of  $1\alpha$ -OH norditerpenoid alkaloid free bases, karacoline, condelphine, and neoline, stabilize their A-rings adopting an unusual twisted boat conformation, and they also significantly increase  $\delta_{\text{N}}$  of the tertiary amine *N*-atom.

*ACS Omega*, **2020**, *5*, 14116-14122. doi 10.1021/acsomega.0c01648

<b>This declaration concerns the article entitled:</b>			
Impacts of Steric Compression, Protonation, and Intramolecular Hydrogen Bonding on the <sup>15</sup> N NMR Spectroscopy of Norditerpenoid Alkaloids and Their Piperidine-Ring Analogues			
<b>Publication status (tick one)</b>			
<b>Draft manuscript</b>	<input type="checkbox"/>	<b>Submitted</b>	<input type="checkbox"/>
		<b>In review</b>	<input type="checkbox"/>
		<b>Accepted</b>	<input type="checkbox"/>
		<b>Published</b>	<input checked="" type="checkbox"/>
<b>Publication details (reference)</b>	Zeng, Z., Qasem, A. M. A., Woodman, T. J., Rowan, M. G., and Blagbrough, I. S., 2020. Impacts of Steric Compression, Protonation, and Intramolecular Hydrogen Bonding on the <sup>15</sup> N NMR Spectroscopy of Norditerpenoid Alkaloids and Their Piperidine-Ring Analogues. <i>ACS Omega</i> , <b>5</b> , 14116-14122.		
<b>Copyright status (tick the appropriate statement)</b>			
The material has been published with a CC-BY license		<input checked="" type="checkbox"/>	The publisher has granted permission to replicate the material included here
		<input type="checkbox"/>	
<b>Candidate's contribution to the paper (provide details, and also indicate as a percentage)</b>	<p><b>Formulation of ideas:</b> The candidate contributed to the formulation of the article ideas (60%)</p> <p><b>Design of methodology:</b> The candidate contributed to design the study of various factors on the chemical shift of the nitrogen in NDA and their analogues (60%).</p> <p><b>Experimental work:</b> The candidate contributed to the analysis of the NDA and the analogues analysis (60%)</p> <p><b>Presentation of data in journal format:</b> The candidate contributed to the paper writing and figures presentation (60%)</p>		
<b>Statement from Candidate</b>	This paper reports on original research I conducted during the period of my Higher Degree by Research candidature.		
<b>Signed (typed signature)</b>	Ashraf Qasem	<b>Date</b>	21/09/2022

## INTRODUCTION

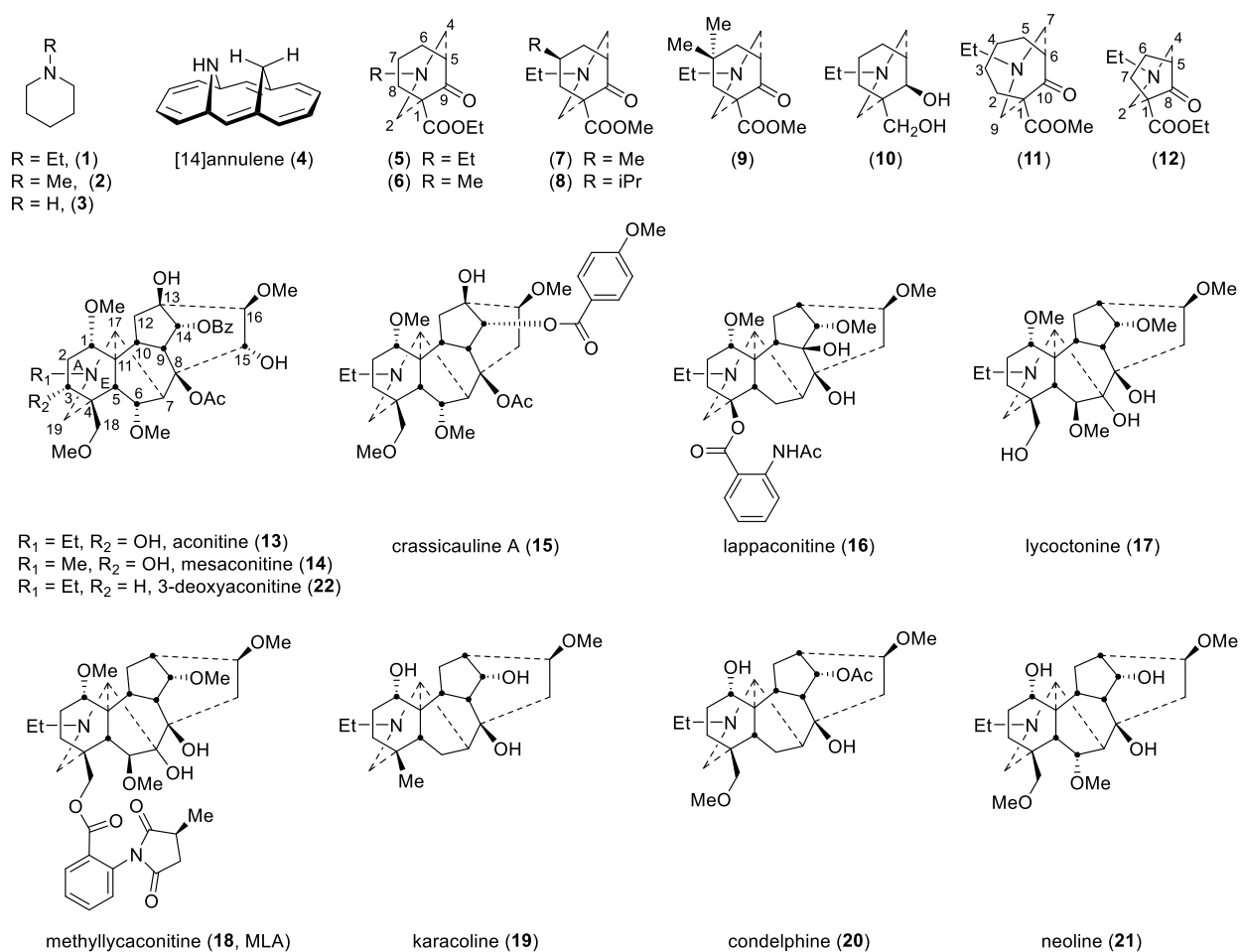


**Figure 1.** [14]Annulene (4), synthetic azabicycles (5-12), and norditerpenoid alkaloids (13-22).

For non-isotopically enriched samples, the sensitivity of  $^{15}\text{N}$  NMR is limited by the low natural abundance of  $^{15}\text{N}$  nuclei (0.36%,  $I = 1/2$ ) and its intrinsic low receptivity. Typically, compared with the  $^1\text{H}$  signals in a sample, the signal to noise will be of the order of  $10^4$  smaller. This essentially precludes direct measurement without recourse to extended acquisition times or extremely concentrated samples. These limitations can be overcome through judicious use of inverse-detected  $^{15}\text{N}$  NMR experiments, e.g.  $^1\text{H}$ - $^{15}\text{N}$  heteronuclear multiple-bond correlation ( $^1\text{H}$ - $^{15}\text{N}$  HMBC) spectroscopy.<sup>1,2</sup> Chemical shifts of  $^{15}\text{N}$  nuclei ( $\delta_{\text{N}}$ ) in simple aliphatic amines, e.g. *N*-Et- (1), *N*-Me- (2), and *N*-H-piperidine (3), have been reported,<sup>3-6</sup> and steric and electronic effects of  $N\alpha$ - and  $N\beta$ -substituents on  $\delta_{\text{N}}$  have also been investigated.<sup>6,7</sup> A rare, indeed possibly the only case that has demonstrated the through-space  $^1\text{H}$  NMR effect of steric compression caused by a secondary amine deshielding a proton that is close to the *N*-atom in space has been reported for



imino[14]annulene (**4**, Fig. 1).<sup>8</sup> We are investigating the effects of such steric compression in the synthetic azabicycles (**5-12**) and their related norditerpenoid alkaloids (**13-21**),<sup>9,10</sup> and how such steric interactions impact the tertiary amine using <sup>1</sup>H-<sup>15</sup>N HMBC spectroscopy to report on the environment of the *N*-atom.

## RESULTS AND DISCUSSION

<sup>1</sup>H-<sup>15</sup>N HMBC spectroscopic experiments were carried out on three sample piperidines (**1-3**, Table 1), synthetic azabicycles (**5-12**, Table 2), and their related norditerpenoid alkaloids (Table 3), aconitine (**13**), mesaconitine (**14**), crassicauline A (**15**), lappaconitine (**16**), lycoctonine (**17**), methyllycaconitine (**18**, MLA), karacoline (**19**), condelphine (**20**), and neoline (**21**). In addition, several protonated forms of these compounds (**1'-3'**, **13'**, **15'-17'**) have been studied. All the <sup>1</sup>H-<sup>15</sup>N HMBC spectra were externally calibrated with a MeNO<sub>2</sub> solution (50% in CDCl<sub>3</sub>, v/v) following IUPAC guidelines.<sup>11,12</sup>

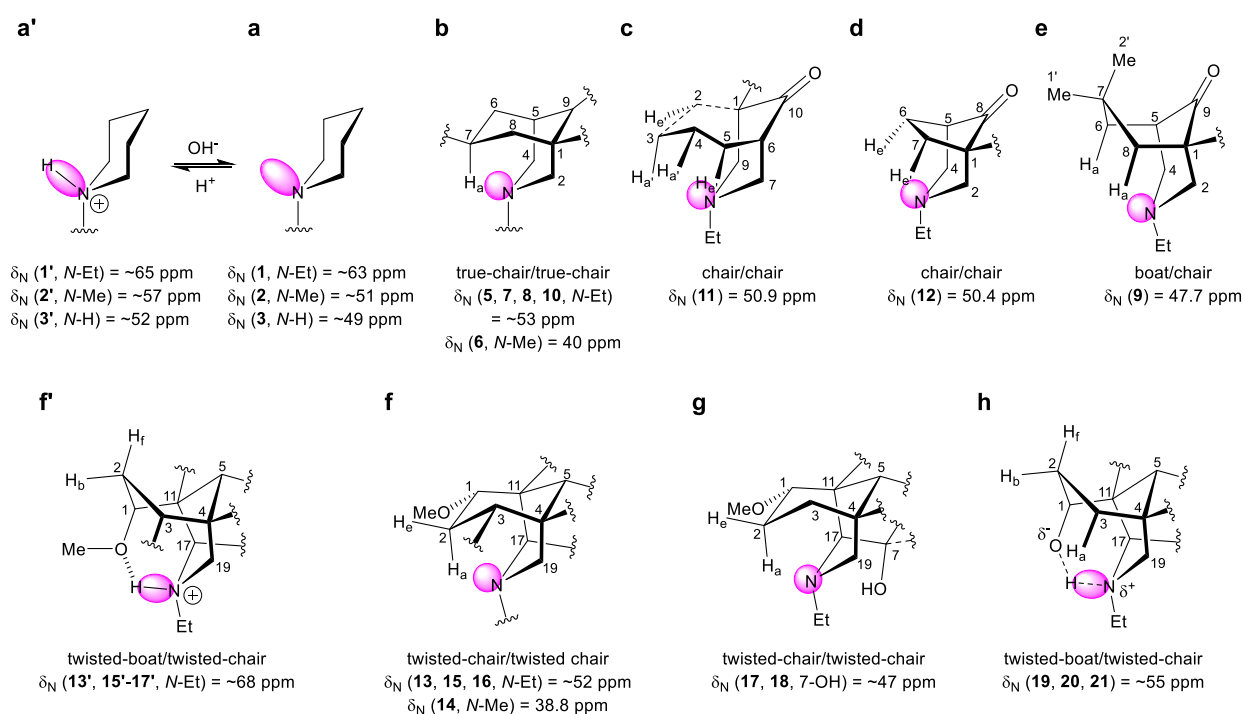


**Figure 2.** A/E-[3.3.1]azabicyclic frames of norditerpenoid alkaloids and their analogues. Pink: lone-pair electrons of the *N*-atom.

**Table 1.**  $\delta_N$  of piperidines ( $\delta$  in ppm)

Compound	Solvent	$\delta_N$	Compound	Solvent	$\delta_N$
<i>N</i> -Et piperidine ( <b>1</b> )	CDCl <sub>3</sub>	64.1	<i>N</i> -Me piperidine ( <b>2</b> )	CDCl <sub>3</sub>	51.3
	CD <sub>3</sub> OD	63.0		D <sub>2</sub> O <sup>a</sup> , D <sub>2</sub> O <sup>a,b</sup>	51.2
	<i>d</i> <sub>6</sub> -DMSO	62.3	<i>N</i> -Me piperidine HCl salt ( <b>2'</b> )	CDCl <sub>3</sub>	57.8
	D <sub>2</sub> O <sup>a</sup>	62.7		D <sub>2</sub> O	54.7
	D <sub>2</sub> O <sup>a,b</sup>	62.6		CDCl <sub>3</sub>	49.8
<i>N</i> -Et piperidine HCl salt ( <b>1'</b> )	CDCl <sub>3</sub>	65.5	<i>N</i> -H piperidine ( <b>3</b> )	D <sub>2</sub> O	49.0
	CD <sub>3</sub> OD	64.5		D <sub>2</sub> O <sup>b</sup>	48.5
	<i>d</i> <sub>6</sub> -DMSO	64.4	<i>N</i> -H piperidine HCl salt ( <b>3'</b> )	CDCl <sub>3</sub> <sup>a</sup>	53.9
	D <sub>2</sub> O	64.3		D <sub>2</sub> O	48.6

<sup>a</sup> with additional 2 drops of *d*<sub>6</sub>-DMSO.

<sup>b</sup> with additional drops of NaOD solution (30% in D<sub>2</sub>O, w/w), pD ~13.

**Table 2.** Key NMR data of synthetic [3.3.1]azabicycles ( $\delta$  in ppm)

Compound	Solvent	$\delta_N$	$\Delta\delta_{7-H}$	$\delta$ (7-H) <sup>a</sup>	
				a ( <i>endo</i> )	e ( <i>exo</i> )
A/E-[3.3.1]azabicyclic diol ( <b>5</b> , <i>N</i> -Et)	CDCl <sub>3</sub>	51.5	1.33	2.86	1.53
A/E-[3.3.1]azabicyclic diol ( <b>6</b> , <i>N</i> -Me)	CDCl <sub>3</sub>	39.7	1.29	2.84	1.55
7-Me A/E-[3.3.1]azabicyclic diol ( <b>7</b> )	CDCl <sub>3</sub>	52.0	-	3.42	-
7- <i>i</i> Pr A/E-[3.3.1]azabicyclic diol ( <b>8</b> )	CDCl <sub>3</sub>	52.0	-	3.02	-
7,7-diMe A/E-[3.3.1]azabicyclic diol ( <b>9</b> )	CDCl <sub>3</sub>	47.7	-	-	-
A/E-[3.3.1]azabicyclic diol ( <b>10</b> )	CDCl <sub>3</sub>	53.6	1.11	2.59	1.48
	CD <sub>3</sub> OD	53.2	1.16	2.58	1.42
	<i>d</i> <sub>6</sub> -DMSO	53.7	1.18	2.47	1.29
	D <sub>2</sub> O <sup>b</sup>	55.3	0.45	2.04	1.59
[4.3.1]azabicyclic diol ( <b>11</b> )	CDCl <sub>3</sub>	50.9	$\Delta\delta_{3-H} = 0.68$	$\delta$ (3-H <sub>a</sub> ) = 2.04	$\delta$ (3-H <sub>e</sub> ) = 1.36
			$\Delta\delta_{4-H} = 0.45$	$\delta$ (4-H <sub>a</sub> ) = 1.96	$\delta$ (4-H <sub>e</sub> ) = 1.51
[3.2.1]azabicyclic diol ( <b>12</b> )	CDCl <sub>3</sub>	50.4	$\Delta\delta_{6-H} = 0.00$	$\delta$ (6-H <sub>a</sub> ) = $\delta$ (6-H <sub>e</sub> ) = 1.95	
			$\Delta\delta_{7-H} = 0.13$	$\delta$ (7-H <sub>e</sub> ) = 2.38	$\delta$ (7-H <sub>a</sub> ) = 2.25

<sup>a</sup> Orientation label: a = axial, e = equatorial, a' = pseudo-axial, e' = pseudo-equatorial. Chemical shifts of overlapping signals were extracted from HSQC.

<sup>b</sup> with additional 2 drops of *d*<sub>6</sub>-DMSO.

**Table 3.** Key NMR data of the selected norditerpenoid alkaloids ( $\delta$  in ppm)

Compound	Solvent	$\delta_N$ (amine)	$\Delta\delta_{2-H}$	$\delta$ (2-H) <sup>a</sup>		
				a (b)	e (f)	
1 $\alpha$ -OMe	aconitine ( <b>13</b> )	CDCl <sub>3</sub>	52.9	0.37	2.38	2.01
	aconitine HCl salt ( <b>13'</b> )	D <sub>2</sub> O <sup>b</sup>	70.3	0.63	2.32	1.69
	mesaconitine ( <b>14</b> )	CDCl <sub>3</sub>	38.8	0.17	2.31	2.14
	crassicauline A ( <b>15</b> )	CDCl <sub>3</sub>	50.7	0.34	2.29	1.95
	crassicauline A HCl salt ( <b>15'</b> )	D <sub>2</sub> O	67.0	0.33	1.98	1.65
	lappaconitine ( <b>16</b> )	CDCl <sub>3</sub>	52.3	0.12	2.23	2.11
	lappaconitine HBr salt ( <b>16'</b> )	D <sub>2</sub> O <sup>b</sup>	67.9	0.27	2.17	1.90
	lycoctonine ( <b>17</b> )	CDCl <sub>3</sub>	47.3	0.07	2.15 <sup>d</sup>	2.08
	lycoctonine HCl salt ( <b>17'</b> )	D <sub>2</sub> O <sup>b,c</sup>	67.2	0.61	2.02	1.41
	MLA ( <b>18</b> )	CDCl <sub>3</sub>	46.9	0.08	2.10	2.02
1 $\alpha$ -OH	karacoline ( <b>19</b> )	CDCl <sub>3</sub>	56.1	0.04	1.62, 1.58 <sup>e</sup>	
	condelphine ( <b>20</b> )	CDCl <sub>3</sub>	54.2	0.04	1.60	1.56
	neoline ( <b>21</b> )	CDCl <sub>3</sub>	54.5	0.07	1.56	1.49
		CDCl <sub>3</sub> <sup>f</sup>	54.5	0.07	1.56	1.49
	CDCl <sub>3</sub> <sup>g</sup>	54.3	0.06	1.55	1.49	

<sup>a</sup> Orientation label: a = axial, e = equatorial in a chair conformation; b = bowsprit, f = flagpole in a boat conformation. Chemical shifts of overlapping signals were extracted from HSQC.

<sup>b</sup> with additional 2 drops of *d*<sub>6</sub>-DMSO.

<sup>c</sup> with additional drops of DCl (35% in D<sub>2</sub>O), pD ~2.

<sup>d</sup> Chemical shift of this overlapping signal were extracted from COSY.

<sup>e</sup> no evidence was obtained to identify the orientation of these protons unambiguously.

<sup>f</sup> with additional 2 drops of *d*<sub>5</sub>-pyridine.

<sup>g</sup> with additional 2 drops of *d*<sub>5</sub>-pyridine and 2 drops of NaOD solution (30% in D<sub>2</sub>O, w/w).

### 1. Steric compression

In CDCl<sub>3</sub>, synthetic A/E-[3.3.1]azabicyclic free bases (**5-8**, **10**) and their relative 1 $\alpha$ -OMe norditerpenoid alkaloid free bases (**13-18**) show the rare NMR effect of steric compression on 7-H<sub>a</sub> (2-H<sub>a</sub>) as the chemical shifts of 7-H<sub>a</sub> (2-H<sub>a</sub>) are larger than those of 7-H<sub>e</sub> (2-H<sub>e</sub>). The chemical

shift of an axial proton (~1.1 ppm) attached to cyclohexane is normally at higher field than that of its geminal equatorial proton (1.6 ppm) by ~0.5 ppm due to the magnetic anisotropic effect,<sup>13,14</sup> and the reversed order of chemical shifts that are observed in [3.3.1]azabicyclic compounds (**5-8**, **10**, **13-18**) is indicative of the electron cloud of 7-H<sub>a</sub> (2-H<sub>a</sub>) being repulsed by the lone-pair electrons of the tertiary amine *N*-atoms in such half-cage [3.3.1]azabicycles. Therefore, these 7-H<sub>a</sub> (2-H<sub>a</sub>) are deshielded and their chemical shifts increase.<sup>15</sup> Similar effects are displayed in [4.3.1]- and [3.2.1]azabicycles (**11**, **12**).<sup>9</sup>  $\Delta\delta_{7-H}$  of synthetic [3.3.1]azabicyclic free bases (**5-8**, **10**,  $\geq 1.11$  ppm) are significantly larger than  $\Delta\delta_{2-H}$  of natural alkaloid free bases (**13-18**,  $\leq 0.37$  ppm), as the synthetic [3.3.1]azabicycles (**5-8**, **10**) adopt true-chair/true-chair conformations, and the A/E-[3.3.1]azabicycles of the natural norditerpenoid alkaloid free bases (**13-18**) are in twisted-chair/twisted-chair conformations due to through-space repulsion between 12-H<sub>e</sub>/*O*-atom of 1 $\alpha$ -OMe acting on the A-rings and 19-H<sub>a</sub>/6 $\alpha$ -H<sub>e</sub> (6 $\alpha$ -OMe) acting on the E-rings.<sup>10,16</sup>

It is notable that the chemical shifts for *N*-Et, *N*-Me, and *N*-H piperidine (**1-3**) occur at 64.1, 51.3, 49.8 ppm (in CDCl<sub>3</sub>, Table 1), respectively. Likewise, similar differences for  $\delta_N$  between *N*-Et (**5**, **7**, **8**, **10**) and *N*-Me (**6**) bicyclic piperidine analogues were obtained. Shifts of synthetic *N*-Et [3.3.1]azabicyclic free bases (**5**, **7**, **8**, **10**) (in CDCl<sub>3</sub>, Table 2) and *N*-Et 1 $\alpha$ -OMe-norditerpenoid alkaloid free bases (**13**, **15-18**) are found at ~50 ppm (in CDCl<sub>3</sub>, Table 3), and those of *N*-Me [3.3.1]azabicyclic free bases (**6**) and *N*-Me mesaconitine (**14**) resonate at ~39 ppm (in CDCl<sub>3</sub>). Thus, the *N*-alkyl substituents (Et, Me, H) sensitively influence  $\delta_N$  in a simple piperidine. In the half-cage molecules, the typical <sup>15</sup>N shift is reduced by ~12 ppm when compared with such piperidines. This could be a result of the deformation in size and hybridization of the orbitals for the lone-pair electrons of the tertiary amine *N*-atoms.<sup>3</sup>

In order to investigate solvent effects on chemical shift, the <sup>15</sup>N shifts for *N*-Et piperidine (**1**) were recorded in CDCl<sub>3</sub>, CD<sub>3</sub>OD, *d*<sub>6</sub>-DMSO, D<sub>2</sub>O, NaOD solution (in D<sub>2</sub>O, pD ~13) resulting in a value of ~63 ppm, thus showing negligible differences. Similarly, the <sup>15</sup>N shifts of diol (**10**) were obtained from solutions in: CDCl<sub>3</sub>, CD<sub>3</sub>OD, *d*<sub>6</sub>-DMSO, D<sub>2</sub>O, and are typically ~54 ppm. Therefore, the difference of  $\delta_N$  between simple piperidines (**1-3**) and [3.3.1]azabicycles (**5-8**, **10**, **13-18**) is not caused by solvent effects.

The distribution of the *N*-atom lone-pair electrons in piperidines (**1-3**) is not restricted by the steric hindrance caused by bridged cyclohexane rings (Fig. 2a), but those in the half-cage [3.3.1]azabicycles adopting chair/chair conformations are restricted by 7-H<sub>a</sub> (2-H<sub>a</sub>) (Fig. 2b, 2f), and therefore the distribution of the *N*-atom lone-pair electrons are concentrated around the *N*-atom increasing the electron density and decreasing the  $\delta_N$  by ~10 ppm.

Similar results of  $\delta_N$  were observed in synthetic [4.3.1]- and [3.2.1]azabicycles (**11**, **12**), which resonate at 50.9 and 50.4 ppm (Table 2), respectively; these results show that the amine *N*-atoms are shielded by *endo* protons attached to C3 and C4 of [4.3.1]azabicycles (**11**, Fig. 2c) and *endo* protons attached to C6 and C7 of [3.2.1]azabicycles (**12**, Fig. 2d).

*N*-Et 7,7-diMe [3.3.1]azabicyclic (**9**) adopts a boat/chair conformation,<sup>9</sup> and its  $\delta_N$  is smaller than those of *N*-Et [3.3.1]azabicycles (**5**, **7**, **8**, **10**) which adopt chair/chair conformations. The lone-pair electrons of 7,7-diMe [3.3.1]azabicyclic (**9**) are restricted by 6-H<sub>a</sub> and 8-H<sub>a</sub> (Fig. 2e),<sup>17</sup> thus the electron density of the *N*-atom of 7,7-diMe [3.3.1]azabicyclic (**9**) is more concentrated in comparison with those of [3.3.1]azabicycles (**5**, **7**, **8**, **10**). That such <sup>15</sup>N shift effects can be larger has been previously reported by Roberts and co-workers.<sup>3</sup> From our studies, we conclude that the <sup>15</sup>N shift effects makes them useful reporter nuclei of the substitution pattern. Indeed, a possible reason is the difference in size and hybridization of the orbitals for the unshared electrons in such tertiary amines,<sup>4</sup> and whether the substituents adopt axial or equatorial positions.<sup>3</sup>

Due to the proximity in space between 7-OH and the *N*-atom (Fig. 2g), the amine  $\delta_N$  of norditerpenoid alkaloid free bases with *N*-Et and 7-OH (**17**, **18**) resonate at ~47 ppm, slightly lower than those of alkaloid free bases with *N*-Et and 7-H, (**13**, **15**, **16**) which resonate at ~52 ppm.

## 2. Protonation

$\delta_N$  of *N*-Et piperidine (**1**) resonates at ~63 ppm (in CDCl<sub>3</sub>, CD<sub>3</sub>OD, *d*<sub>6</sub>-DMSO, and D<sub>2</sub>O) showing only a small difference<sup>4</sup> from its HCl salt (**1'**) resonating at ~65 ppm (in CDCl<sub>3</sub>, CD<sub>3</sub>OD, *d*<sub>6</sub>-DMSO, and D<sub>2</sub>O).  $\delta_N$  of *N*-Et (**1**), *N*-Me (**2**), and *N*-H free bases (**3**) were also measured in NaOD solutions (in D<sub>2</sub>O, pD ~13), and these  $\delta_N$  have no significant difference from those of their corresponding free bases (**1-3**) obtained in D<sub>2</sub>O.

The A/E-[3.3.1]azabicyclic rings of protonated 1 $\alpha$ -OMe norditerpenoid alkaloid salts (**13'**, **15'-17'**) adopt twisted-boat/twisted-chair conformations, which are stabilized by hydrogen bonds between  $N^+$ -H and 1 $\alpha$ -OMe (Fig. 2f).<sup>10,16</sup>  $\delta_N$  of norditerpenoid alkaloid free bases (**13**, **15-17**; resonating at 52.9, 50.7, 52.3, and 47.3 ppm, respectively; in CDCl<sub>3</sub>) are at higher field than those of their protonated forms (**13'**, **15'-17'**; 70.3, 67.0, 67.9, and 67.2 ppm, respectively; in D<sub>2</sub>O), and the  $\delta_N$  of these natural products (**13**, **15-17**) increase by 17.4, 16.3, 15.6, 19.9 ppm, respectively on protonation. The  $\Delta\delta_N$  ( $\geq 15.6$  ppm) between norditerpenoid alkaloids (**13**, **15-17**) and their salts (**13'**, **15'-17'**) are further supported by the recently reported  $\Delta\delta_N = 18.0$  ppm between 3-deoxyaconitine (**22**) ( $\delta_N = 40.7$  ppm, in *d*<sub>6</sub>-acetone) and its trifluoroacetate salt ( $\delta_N = 58.7$  ppm, in *d*<sub>6</sub>-acetone).<sup>18</sup>

The space that the lone-pair electrons of the  $N$ -atoms in piperidines (**1-3**) occupy (Fig. 2a) is similar to that of their HCl salts (**1'-3'**) (fixed in the  $N^+$ -H bonds, Fig. 2a'), hence  $\delta_N$  of simple piperidines (**1-3**) show only a small change on protonation. The distribution of the lone-pair electrons of the  $N$ -atoms in norditerpenoid alkaloid free bases (**13**, **15-17**) are restricted by 2-H<sub>a</sub> through space (Fig. 2f), which is near the  $N$ -atoms, and these electrons are fixed by  $N^+$ -H bonds and are away from the  $N$ -atom (Fig. 2f') leading to a decrease in the electron density when the alkaloids (**13**, **15-17**) are protonated.

### 3. Intramolecular hydrogen bonding

The A-ring of 1 $\alpha$ -OH norditerpenoid alkaloid free bases adopt twisted-boat conformations stabilized by H-bonds between tertiary amine  $N$ -atom and 1 $\alpha$ -OH (Fig. 2h).<sup>19,20</sup> Compared with  $\delta_N$  (47.7 ppm, in CDCl<sub>3</sub>) of 7,7-diMe [3.3.1]azabicyclic (**9**), which adopts a boat/chair conformation,  $\delta_N$  of 1 $\alpha$ -OH norditerpenoid alkaloid free bases (**19-21**) are higher field, resonating at ~55 ppm for all three. The lone-pair electrons of the  $N$ -atom in 7,7-diMe [3.3.1]azabicyclic (**9**) are significantly compressed by 6-H<sub>a</sub> and 8-H<sub>a</sub> through space (Fig. 2e). The lone-pair electrons of the  $N$ -atom in 1 $\alpha$ -OH natural alkaloids (**19-21**) are shared and fixed by intramolecular H-bond to 1 $\alpha$ -OH. Thus the the electrons are distributed away from the  $N$ -atom, leading to an increase of  $\delta_N$  (Fig. 2h), typically of 6-8 ppm compared with  $\delta_N$  of boat/chair analogue (**9**). Neoline (**21**) in CDCl<sub>3</sub> was treated with additional *d*<sub>5</sub>-pyridine and NaOD solution (30% in D<sub>2</sub>O, w/w)

successively for cleaving the intramolecular H-bond. In comparison with those of neoline (**21**) in CDCl<sub>3</sub>, no notable change was observed in the <sup>1</sup>H NMR and <sup>1</sup>H-<sup>15</sup>N HMBC spectra of neoline (**21**) in basified CDCl<sub>3</sub>, demonstrating that this intramolecular H-bond is stable, and it holds the A-ring in a twisted-boat conformation.

## CONCLUSIONS

A rare <sup>15</sup>N NMR spectroscopic effect of steric compression has been demonstrated in the A/E-rings of several norditerpenoid alkaloid free bases and their synthetic azabicyclic analogues using <sup>1</sup>H-<sup>15</sup>N HMBC spectroscopy. The distribution of the tertiary amine *N*-atom lone-pair electrons is restricted in the half-cage azabicycles, and therefore the electron density of the *N*-atom increases and its  $\delta_N$  decreases.  $\delta_N$  of norditerpenoid alkaloids bearing 1 $\alpha$ -OMe significantly increase on protonation. The intramolecular hydrogen bonds between the *N*-atom and 1 $\alpha$ -OH of 1 $\alpha$ -OH norditerpenoid alkaloid free bases not only stabilize the A-rings, adopting twisted-boat conformation, but they also increase the  $\delta_N$  of the tertiary amine *N*-atom. Thus, <sup>1</sup>H-<sup>15</sup>N HMBC spectroscopy has been demonstrated to be an excellent reporter for the analysis of the electron density of substituted piperidine alkaloids. It is particularly useful for certain norditerpenoid alkaloids with complex substitution patterns and half-cage skeleta.

## ACKNOWLEDGEMENTS

We thank Carbosynth Ltd. (UK) for the donated condelphine (**20**).

## REFERENCES

- (1) Mueller, L. Sensitivity enhanced detection of weak nuclei using heteronuclear multiple quantum coherence. *J. Am. Chem. Soc.* **1979**, *101*, 4481-4484.
- (2) Köck, M.; Junker, J.; Lindel, T. Impact of the <sup>1</sup>H, <sup>15</sup>N-HMBC experiment on the constitutional analysis of alkaloids. *Org. Lett.* **1999**, *1*, 2041-2044.
- (3) Duthaler, R. O.; Williamson, K. L.; Giannini, D. D.; Bearden, W. H.; Roberts, J. D. Natural-abundance nitrogen-15 nuclear magnetic resonance spectroscopy. Steric and electronic effects on nitrogen-15 chemical shifts of piperidines and decahydroquinolines. *J. Am. Chem. Soc.* **1977**, *99*, 8406-8412.

- (4) Duthaler, R. O.; Roberts, J. D. Steric and electronic effects on  $^{15}\text{N}$  chemical shifts of piperidine and decahydroquinoline hydrochlorides. *J. Am. Chem. Soc.* **1978**, *100*, 3882-3889.
- (5) Duthaler, R. O.; Roberts, J. D. Steric and electronic effects on  $^{15}\text{N}$  chemical shifts of saturated aliphatic amines and their hydrochlorides. *J. Am. Chem. Soc.* **1978**, *100*, 3889-3895.
- (6) Wong, T. C.; Collazo, L. R.; Guziec, Jr, F. S.  $^{14}\text{N}$  and  $^{15}\text{N}$  NMR studies of highly sterically hindered tertiary amines. *Tetrahedron* **1995**, *51*, 649-656.
- (7) Pace, V.; Holzer, W.; Ielo, L.; Shi, S.; Meng, G.; Hanna, M.; Szostak, R.; Szostak, M.  $^{17}\text{O}$  NMR and  $^{15}\text{N}$  NMR chemical shifts of sterically-hindered amides: ground-state destabilization in amide electrophilicity. *Chem. Commun.* **2019**, *55*, 4423-4426.
- (8) Vogel, E.; Brocker, U.; Junglas, H. *syn*-1,6-Imino-8,13-methano[14]annulene. *Angew. Chem., Int. Ed. Engl.* **1980**, *19*, 1015-1016.
- (9) Zeng, Z.; Kociok-Köhn, G.; Woodman, T. J.; Rowan, M. G.; Blagbrough, I. S. The rare  $^1\text{H}$  NMR spectroscopic effect of steric compression is found in [3.3.1]azabicycles and their analogues. *J. Org. Chem.* **2020**, submitted.
- (10) Zeng, Z.; Kociok-Köhn, G.; Woodman, T. J.; Rowan, M. G.; Blagbrough, I. S. Structural studies of norditerpenoid alkaloids: conformation analysis in crystal and in solution states. *Org. Biomol. Chem.* **2020**, submitted.
- (11) Witanowski, M. Nitrogen n.m.r. spectroscopy. *Pure Appl. Chem.* **1974**, *37*, 225-233.
- (12) Harris, R. K.; Becker, E. D.; De Menezes, S. M. C.; Goodfellow, R.; Granger, P. NMR nomenclature. Nuclear spin properties and conventions for chemical shifts (IUPAC Recommendations 2001). *Pure Appl. Chem.* **2001**, *73*, 1795-1818.
- (13) Garbisch, E. W.; Griffith, M. G. Proton couplings in cyclohexane. *J. Am. Chem. Soc.* **1968**, *90*, 6543-6544.
- (14) Williams, D. H.; Fleming, I. *Spectroscopic Methods in Organic Chemistry*, 6th edn.; McGraw-Hill: London, 2008; p 165.
- (15) Winstein, S.; Carter, P.; Anet, F. A. L.; Bourn, A. J. R. The effects of steric compression on chemical shifts in half-cage and related molecules. *J. Am. Chem. Soc.* **1965**, *87*, 5247-5249.
- (16) Pelletier, S. W.; Djarmati, Z. Carbon-13 nuclear magnetic resonance: aconitine-type diterpenoid alkaloids from *Aconitum* and *Delphinium* species. *J. Am. Chem. Soc.* **1976**, *98*, 2626-2636.



- (17) Malpass, J. R.; Belkacemi, D.; Russell, D. R. Studies of stereoselectivity in cycloaddition of cyclic dienes to 2-azabicyclo[2.2.2]octene derivatives; through-space effects on  $^{15}\text{N}$  NMR shifts of bicyclic amines and lactams. *Tetrahedron* **2002**, *58*, 197-204.
- (18) Wang, F.-P.; Chen, D.-L.; Deng, H.-Y.; Chen, Q.-H.; Liu X.-Y.; Jian, X. X. Further revisions on the diterpenoid alkaloids reported in a JNP paper (**2012**, *75*, 1145-1159). *Tetrahedron* **2014**, *70*, 2582-2590.
- (19) Pelletier, S. W.; Djarmati, Z.; Lajsic, S.; De Camp, W. H. Alkaloids of *Delphinium staphisagria*. The structure and stereochemistry of delphisine, neoline, chasmanine, and homochasmanine. *J. Am. Chem. Soc.* **1976**, *98*, 2617-2625.
- (20) Mu, Z.-Q.; Gao, H.; Huang, Z.-Y.; Feng, X.-L.; Yao, X.-S. Puberunine and puberudine, two new  $\text{C}_{18}$ -diterpenoid alkaloids from *Aconitum barbatum* var. *puberulum*. *Org. Lett.* **2012**, *14*, 2758-2761.

## Chapter 6

### Conformational analysis of 1 $\alpha$ -methoxy and 1 $\alpha$ -hydroxy norditerpenoid alkaloids

**Aims:** The conformations of the naturally occurring norditerpenoid alkaloids (NDA) affect their bioactivities. Solution conformations of ring A of four selected NDA free bases: 3-deoxyaconitine **1**, hypaconitine **2**, delsoline (belsoline) **3**, and fuziline **4** were analysed using NMR spectroscopy. Their full NMR assignments are reported for the first time. Each ring A adopts twisted chair, twisted chair, twisted boat, and twisted boat respectively. Steric interactions have been reported at various positions as they affect  $^1\text{H}$  and  $^{15}\text{N}$  chemical shifts. The intramolecular H-bond between 1- $\alpha\text{OH}$  and the tertiary N-atom in delsoline **3** and fuziline **4** results in a significant increase in the  $\delta_{\text{N}}$ . These studies provide detailed analysis of these pharmacologically important NDA and that leads to a better understanding of their possible bioactive conformations.

<b>This declaration concerns the article entitled:</b>			
Conformational analysis of 1 $\alpha$ -methoxy and 1 $\alpha$ -hydroxy norditerpenoid alkaloids			
<b>Publication status (tick one)</b>			
Draft manuscript	<input type="checkbox"/>	Submitted	<input type="checkbox"/>
In review	<input checked="" type="checkbox"/>	Accepted	<input type="checkbox"/>
Published	<input type="checkbox"/>		
<b>Publication details (reference)</b>			
<b>Copyright status (tick the appropriate statement)</b>			
The material has been published with a CC-BY license	<input type="checkbox"/>	The publisher has granted permission to replicate the material included here	<input type="checkbox"/>
<b>Candidate's contribution to the paper (provide details, and also indicate as a percentage)</b>	<p><b>Formulation of ideas:</b> The candidate contributed to the formulation of the article ideas (60%)</p> <p><b>Design of methodology:</b> The candidate contributed to design the study of ring A conformation in selected 1-OH and 1-OMe NDA using NMR and how the nitrogen chemical shift affected based on that (60%)</p> <p><b>Experimental work:</b> The candidate contributed to the analysis of the selected NDA with full assignment, determine the conformation based on <sup>1</sup>H NMR and NOESY spectra, and correlate it with the nitrogen chemical environment based on <sup>1</sup>H-<sup>15</sup>N HMBC (60%).</p> <p><b>Presentation of data in journal format:</b> The candidate contributed to the paper writing and figures presentation (60%)</p>		
<b>Statement from Candidate</b>	This paper reports on original research I conducted during the period of my Higher Degree by Research candidature.		
<b>Signed (typed signature)</b>	Ashraf Qasem	<b>Date</b>	21/09/2022

## 1. Introduction

The naturally occurring norditerpenoid alkaloids (NDA) have bridged highly oxygenated hexacyclic skeleta.<sup>1-4</sup> The analysis of their structures is important to determine their conformation and solution studies of these alkaloids using NMR spectroscopy leads to a better understanding of their possible 3D-conformations in biological fluids as several of these alkaloids are of pharmacological and even clinical importance. The structures of NDA show through-space steric compression in <sup>1</sup>H NMR<sup>5-7</sup>, and <sup>1</sup>H-<sup>15</sup>N HMBC has overcome the limitation of the <sup>15</sup>N low sensitivity and shows how such interactions affect the tertiary amine in these alkaloids.<sup>5</sup> We are investigating the effect of C1- $\alpha$  substituents on the conformation of ring A in four selected NDA, 3-deoxyaconitine **1**, hyaconitine **2**, delsoline **3**, and fuziline **4**, and studying the through-space interactions and how they affect the N and H chemical shifts at various positions. 3-Deoxyaconitine **1** was prepared chemically from aconitine **5** in 1962.<sup>8</sup> It was isolated from *Aconitum kusenoffi* in 1980,<sup>9</sup> and its crystal structure was reported in 2010<sup>10</sup> and 2014.<sup>11</sup> Hyaconitine **2** was first isolated from *A. senanense* Nakai in 1929<sup>12</sup>, and its crystal structure was reported in 2010<sup>13</sup> and 2012.<sup>14</sup> Delsoline (also known as belsoline) **3** was first isolated from *Delphinium consolida* in 1924<sup>15</sup> and its crystal structure was reported in 1992.<sup>16</sup> Fuziline **4** has been isolated from fu'zi (the processed lateral roots of *A. carmichaelii* Debx.) and its crystal structure was reported in 1982.<sup>17</sup>

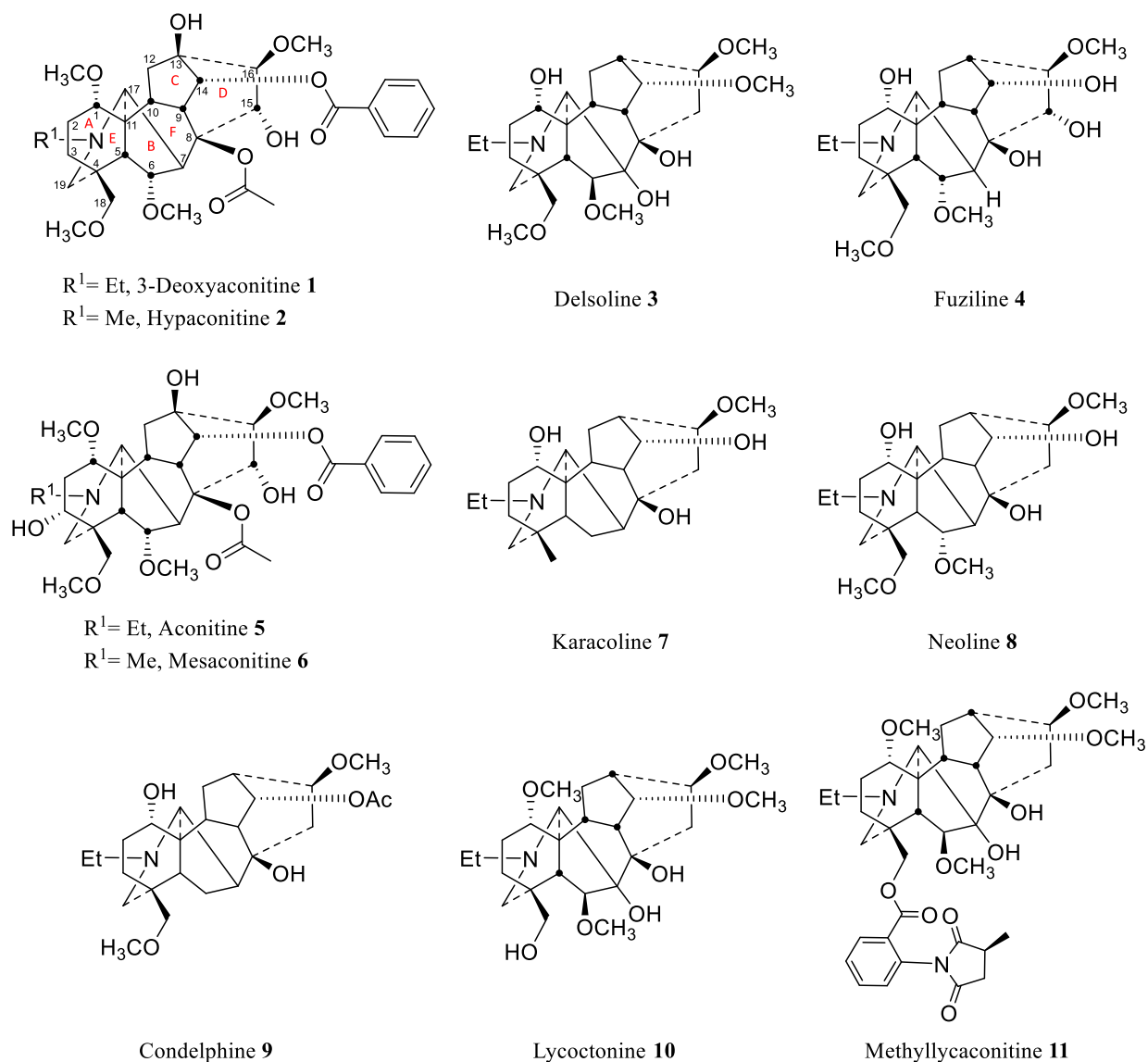


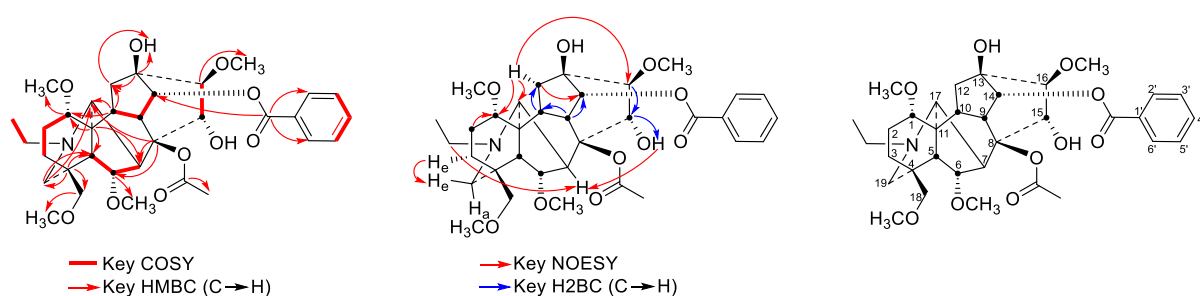
Fig. 1 Selected 1-OMe and 1-OH NDA.

## 2. Results and discussion

Detailed NMR assignments assisted by 2D NMR have been undertaken for 3-deoxyaconitine **1** (Table 1), hyaconitine **2** (Table 2), delsoline (belsoline) **3** (Table 3), and fuziline **4** (Table 4). The  $^{13}\text{C}$  NMR of 3-deoxyaconitine **1** was reported<sup>18</sup> and the literature  $^{13}\text{C}$  NMR assignments for hyaconitine **2** and fuziline **4** have been corrected with the assistance of 2D NMR.<sup>19</sup> This is the first complete and unambiguous report of the NMR assignments of these four NDA. The 1-OH  $^1\text{H}$  NMR signal in delsoline **3** and fuziline **4** resonates at  $\sim 7.5$  ppm compared to other hydroxyl groups which resonate between  $\sim 2.50$ - $4.10$  ppm, and this difference is due to the intramolecular H-bond between  $1\alpha\text{-OH}$  and the N-atom. In delsoline **3**, DEPT135 used to determine carbons 4

and 13 as they resonate close to each other, and to differentiate between carbon 19 and 16-OMe. In 3-deoxyaconitine **1**, DEPT135 helps to differentiate between carbon 5 and methylene carbon in *N*-ethyl side chain (*NCH*<sub>2</sub>CH<sub>3</sub>), and between C-17 and 16-OMe. In 3-deoxyaconitine **1** and hypaconitine **2** there was a <sup>1</sup>H-<sup>15</sup>N HMBC correlation with H-17 and H-19. In these four alkaloids, HSQC, HMBC, and H2BC spectroscopy were used to assign carbons which resonate close to each other and where DEPT cannot be helpful. HSQC was used to determine the exact chemical shifts of proton signals overlapped with others.

Table 1. 3-Deoxyaconitine **1**

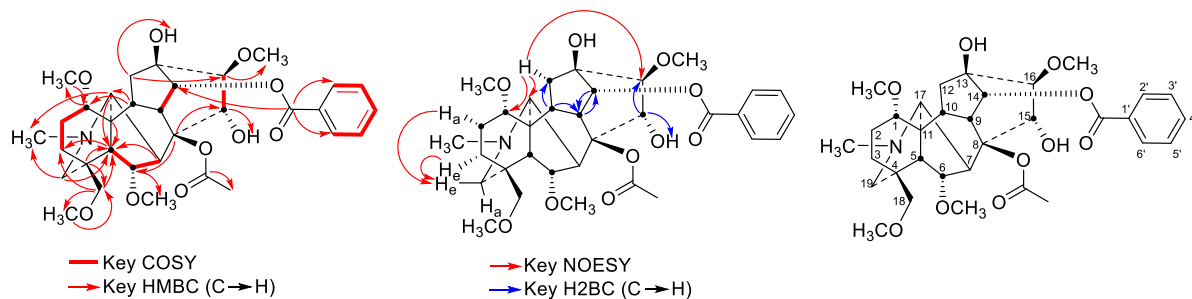


Carbon	$\delta_c$	$\delta_H$ , multiplicity ( <i>J</i> , in Hz; orientation or label*)	key HMBC (C→H)	key NOESY
1	85.27	3.04, dd (10.6, 6.5; $\alpha$ , $\beta$ )	1-OMe	-
2	26.39	1.95, ddd (14.8, 7.0, 4.3; $\epsilon$ , $\beta$ ) 2.32-2.42, m ( $\alpha$ , $\alpha$ )	-	1-H ( $\beta$ )
3	35.27	1.60-1.66, m	-	19- $H_e$
4	39.08	-	5-H, 18 (HA, HB), 19-H	-
5	49.05	2.10, m ( $\beta$ )	-	-
6	83.27	3.98, d (7.5; $\beta$ )	6-OMe	-
7	45.14	2.85, br s	-	-
8	92.12	-	6-H, 7-H, 17-H	-
9	44.61	2.90, m ( $\beta$ )	-	-
10	41.00	2.12, m ( $\beta$ )	1-H, 12-H ( $\alpha'$ , $\epsilon'$ ), 17-H	-
11	49.95	-	1-H, 5-H, 7-H	-
12	36.66	2.93, m ( $\epsilon'$ , $\alpha$ ) 2.15, m ( $\alpha'$ , $\beta$ )	13-OH	1-H, 16-H, 17-H 14-H ( $\beta$ )
13	74.14	-	12-H ( $\alpha'$ , $\epsilon'$ ), 13-OH	-
14	79.00	4.88, d (5.0; $\beta$ )	-	-
15	78.86	4.46, dd (5.3, 2.8; $\epsilon$ , $\beta$ )	-	-
16	90.17	3.33, d (5.3; $\alpha$ )	16-OMe	-
17	61.42	3.14, m	-	-
18	80.30	3.11, d (8.3; HA)	18-OMe	-

		3.63, d (8.3; HB)		
19	53.15	2.48, br s	5-H, 17-H	3-H <sub>e</sub>
<i>N</i> CH <sub>2</sub> CH <sub>3</sub>	49.23	2.74, dq (12.3, 7.4; HA)	-	7-H
		2.32-2.42, m (HB)		
<i>N</i> CH <sub>2</sub> CH <sub>3</sub>	13.45	1.07, t (7.2)	-	-
1-OMe	56.29	3.26, s		
6-OMe	58.01	3.15, s	-	-
16-OMe	61.03	3.73, s	-	-
18-OMe	59.07	3.30, s	-	-
OCOMe	21.43	1.37, s	-	-
OCOMe	172.42	-	OCOMe	-
OCOPh	166.16	-	2'-H, 6'-H, 14-H	-
1'	129.88	-	-	-
2', 6'	129.62	8.03, d (7.4)	-	-
3', 5'	128.63	7.45, t (7.4)	-	-
4'	133.23	7.57, t (7.4)	-	-
13-OH	-	3.90, s	-	-
15-OH	-	4.37, d (2.7)	-	7-H

\* a: axial, e: equatorial, a': pseudoaxial, e': pseudoequatorial, f: flagpole, b: bowsprit.

Table 2. Hypaconitine **2**

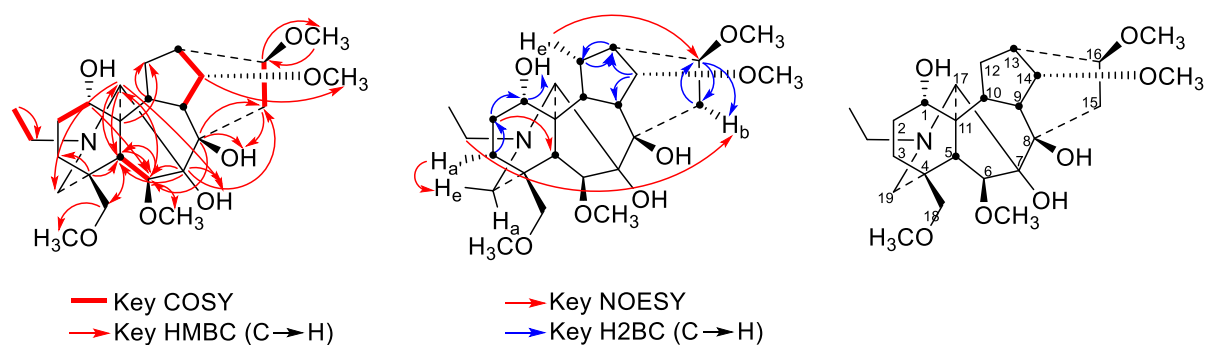


Carbon	$\delta_c$	$\delta_H$ , multiplicity ( <i>J</i> , in Hz; orientation or label*)	key HMBC (C→H)	key NOESY
1	85.10	3.04, dd (10.0, 6.5; a, $\beta$ )	1-OMe	-
2	26.40	2.00, ddt (12.0, 6.5, 4.0; e, $\beta$ ) 2.24, ddt (15.0, 10.0, 8.6; a, $\alpha$ )	-	19-H <sub>e</sub>
3	34.90	1.60-1.66, m	-	19-H <sub>e</sub>
4	39.28	-	18 (HA, HB), 5-H	-
5	48.19	2.09, d (6.9; $\beta$ )	3-H	-
6	83.16	3.97, d (6.9; $\beta$ )	6-OMe	-
7	43.85	2.88, br s	5-H	-
8	91.96	-	6-H, 15-H	-
9	44.55	2.90, m ( $\beta$ )	-	-
10	41.10	2.13, m ( $\beta$ )	1-H, 17-H	-
11	49.94	-	5-H	-

12	36.27	2.14, m (a', $\beta$ ) 2.93, m (e', $\alpha$ )	13-OH, 16-H	1-H, 16-H, 17-H -
13	74.14	-	-	-
14	78.94	4.88, d (5.0; $\beta$ )	-	-
15	78.85	4.46, dd (5.3, 2.9; f, $\beta$ )	15-OH	-
16	90.14	3.33, d (5.3; $\alpha$ )	16-OMe	-
17	62.18	3.08, br s	NCH <sub>3</sub> , 5-H	-
18	80.17	3.11, d (8.4; HA) 3.62, d (8.3; HB)	3-H, 5-H, 18-OMe	-
19	56.00	2.36, d (11.1; e) 2.55, d (11.1; a)	5-H, NCH <sub>3</sub>	2-H <sub>a</sub> ( $\alpha$ ), 3-H <sub>e</sub>
NCH <sub>3</sub>	42.62	2.34, s	-	-
1-OMe	56.62	3.28, s	1-H	-
6-OMe	57.97	3.15, s	-	-
16-OMe	60.99	3.73, s	-	-
18-OMe	59.06	3.27, s	18-H	-
OCOMe	21.42	1.37, s	-	-
OCOMe	172.43	-	OCOMe	-
OCOPh	166.14	-	2'-H, 6'-H, 14-H	-
1'	129.85	-	-	-
2', 6'	129.61	8.03, dd (7.9, 1.3)	-	-
3', 5'	128.63	7.45, t (7.9)	-	-
4'	133.24	7.57, tt (7.9, 1.3)	-	-
13-OH	-	3.91, s	-	-
15-OH	-	4.35, d (2.9)	-	-

\* a: axial, e: equatorial, a': pseudoaxial, e': pseudoequatorial, f: flagpole, b: bowsprit.

Table 3. Delsoline **3**



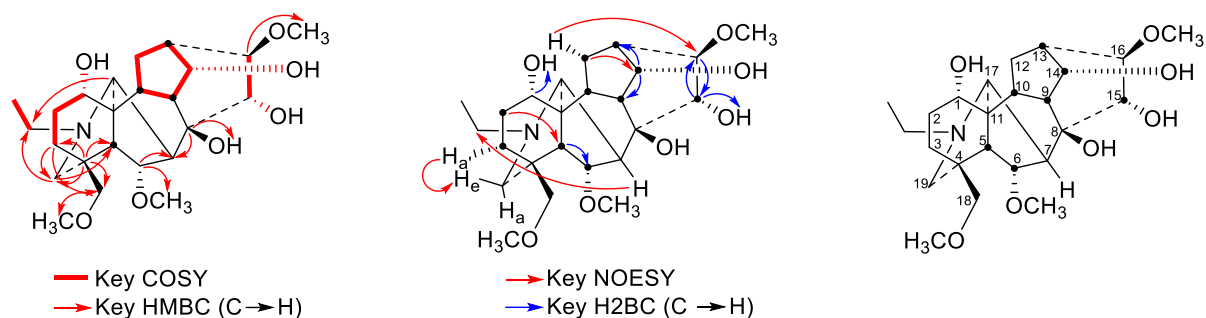
Carbon	$\delta_c$	$\delta_H$ , multiplicity ( $J$ , in Hz; orientation or label*)	key HMBC (C → H)	key NOESY
1	72.68	3.68, dt (9.0, 3.2; e', $\beta$ )	6-H	-
2	29.39	1.46, tdd (14.5, 7.5, 3.2; f, $\beta$ ) 1.60, m (b, $\alpha$ )	-	5-H ( $\beta$ ) -
3	27.22	1.63, m (a', $\alpha$ )	-	19-H <sub>eq</sub>



		2.00, m (e', $\beta$ )		-
4	37.68	-	3-H ( $\alpha$ , $\beta$ ), 5-H	-
5	44.99	1.88, br s ( $\beta$ )	6-H, 17-H, 18 (HA, HB)	-
6	90.45	4.00, s ( $\alpha$ )	5-H, 17-H, 6-OMe	-
7	87.80	-	15-H ( $\alpha$ , $\beta$ ), 5-H, 6-H, 7-OH	-
8	78.51	-	6-H, 8-OH, 15-H ( $\alpha$ , $\beta$ ), 17-H	-
9	43.37	2.92-2.98, m ( $\beta$ )	-	-
10	43.95	1.94, m ( $\beta$ )	12-H ( $\alpha$ , $\beta$ )	-
11	49.33	-	12-H ( $\alpha$ , $\beta$ )	-
12	30.56	1.68, m (e', $\alpha$ ) 2.05, m (a', $\beta$ )	-	16-H -
13	37.47	2.41, m ( $\beta$ )	-	-
14	84.52	3.63, t (4.6; $\beta$ )	14-OMe	-
15	33.49	1.74, m (f, $\beta$ ) 2.62, dd (14.6, 8.8; b, $\alpha$ )	8-OH	-
16	82.93	3.29, t (8.8; $\alpha$ )	16-OMe	-
17	66.01	2.77-2.85, m	H-19, H-5, 7-OH	-
18	77.34	3.01, d (9.4; HA) 3.40, d (9.4; HB)	18-OMe	-
19	57.27	2.44, m	-	-
<i>NCH<sub>2</sub>CH<sub>3</sub></i>	50.28	2.77-2.85, m (HA) 2.92-2.98, m (HB)	-	- 15-H <sub>b</sub> ( $\alpha$ )
<i>NCH<sub>2</sub>CH<sub>3</sub></i>	13.58	1.10, t (7.0)	<i>NCH<sub>2</sub>CH<sub>3</sub></i>	-
6-OMe	57.28	3.36, s	-	-
14-OMe	57.70	3.42, s	-	-
16-OMe	56.29	3.36, s	16-H	-
18-OMe	59.08	3.34, s	-	-
1-OH	-	7.51, d (9.0)	-	-
7-OH	-	3.34, s	-	-
8-OH	-	4.05, s	-	-

\* a: axial, e: equatorial, a': pseudoaxial, e': pseudoequatorial, f: flagpole, b: bowsprit.

Table 4. Fuziline 4



Carbon	$\delta_c$	$\delta_H$ , multiplicity ( $J$ , in Hz; orientation or label*)	key HMBC (C→H)	key NOESY
1	72.15	3.65, m (e', $\beta$ )	-	-
2	30.10	1.49, tdd (14.3, 6.3, 3.1; f, $\beta$ )	-	5-H ( $\beta$ )
		1.58, m (b, $\alpha$ )	-	-
3	29.46	1.63, m (a', $\alpha$ )	18 (HA, HB), 19- $H_e$	19- $H_e$
		1.89, m (e', $\beta$ )		-
4	38.08	-	3-H (a', e'), 18 (HA, HB), 19 ( $H_a$ , $H_e$ ), 5-H	-
5	48.81	2.16, m ( $\beta$ )	-	-
6	84.12	4.14, m ( $\beta$ )	7-H, 6-OMe	-
7	46.33	2.32, br s	-	$NCH_2CH_3$ (HA)
8	78.86	-	7-H, 8-OH	-
9	43.82	2.17, m ( $\beta$ )	-	-
10	44.09	1.87, m ( $\beta$ )	-	-
11	49.39	-	-	-
12	30.56	1.84, m (e', $\alpha$ )	-	16-H ( $\alpha$ )
		2.05, ddd (13.3, 10.6, 7.2; a', $\beta$ )	-	14-H ( $\beta$ )
13	40.67	2.28, m ( $\beta$ )	-	-
14	76.25	4.16, m ( $\beta$ )	-	-
15	79.98	4.41, dd (6.7, 4.1; f, $\beta$ )	-	-
16	90.08	3.17, d (6.7; $\alpha$ )	16-OMe	-
17	62.77	2.68-2.76, m	$NCH_2CH_3$ (HA)	-
18	80.23	3.19, d (8.1; $H_A$ )	18-OMe	-
		3.67, m ( $H_B$ )		-
19	56.75	2.26, m (e)	$NCH_2CH_3$ (HA), 5-H	-
		2.68-2.76, m (a)		-
$NCH_2CH_3$	48.53	2.42, dq (12.5, 6.9; HA)	-	-
		2.68-2.76, m (HB)	-	-
$NCH_2CH_3$	13.15	1.11, t (7.5)	-	-
6-OMe	58.01	3.35, s	-	-
16-OMe	57.42	3.45, s	-	-
18-OMe	59.18	3.33, s	-	-
1-OH	-	7.57, br s	-	-
8-OH	-	2.78, br s	-	-

14-OH	-	2.55, br s	-	-
15-OH	-	2.78, br s	-	-

\* a: axial, e: equatorial, a': pseudoaxial, e': pseudoequatorial, f: flagpole, b: bowsprit.

It was proven that the A ring of 1-OMe NDAs free bases adopt a twisted-chair conformation (Fig. 2A) as the 12-H<sub>e</sub> (α) repulsion with the 1-OMe leads to this twist.<sup>20</sup> Such through space proximity has been observed in the NOE between 12-H<sub>e</sub> (α) and 1β-H in 3-deoxyaconitine **1** and hypaconitine **2**. The NOE also showed correlation between 3-H<sub>e</sub> (α) and 19-H<sub>e</sub>, and between 2-H<sub>e</sub> (β) and 1-H<sub>a</sub> (β) in 3-deoxyaconitine **1**, and showed correlation between 2-H<sub>a</sub> (α) and 19-H<sub>e</sub> in hypaconitine **2** (Fig. 3). These results support the conclusion that ring A in 1α-OMe alkaloids adopts a twisted-chair confirmation.

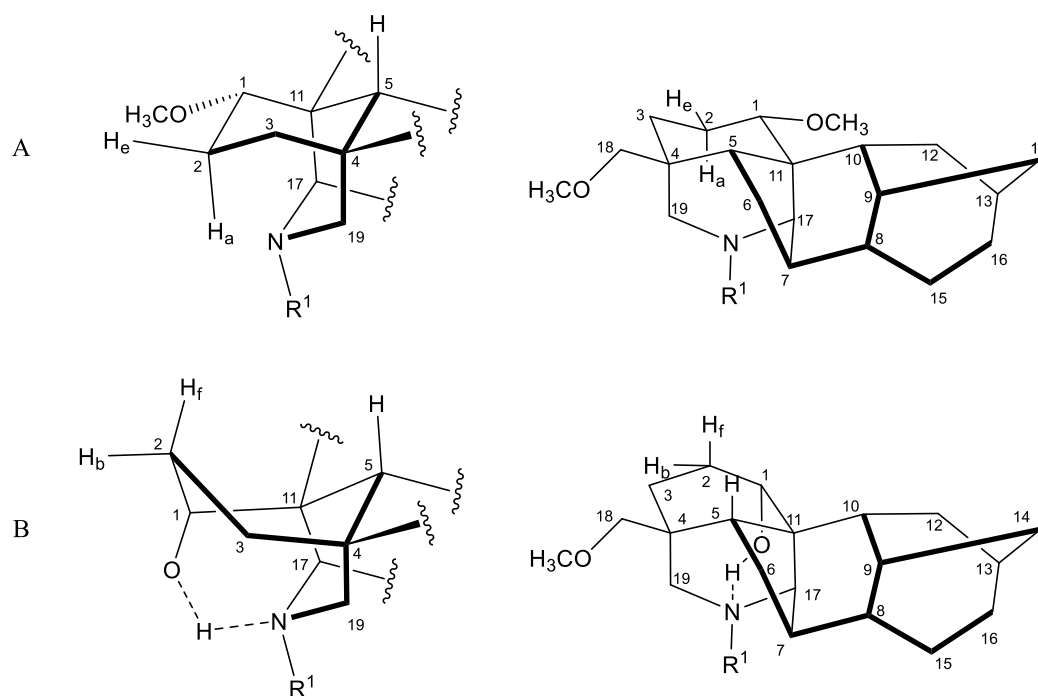
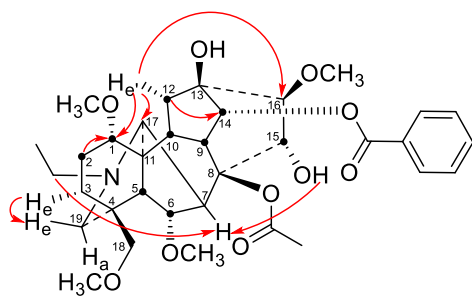
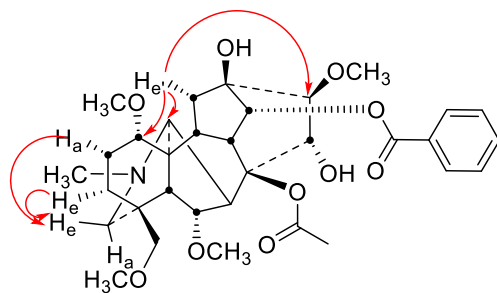
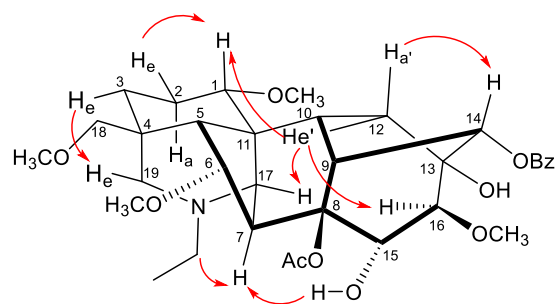


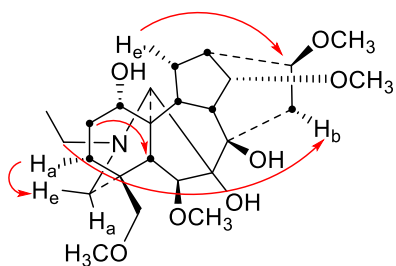
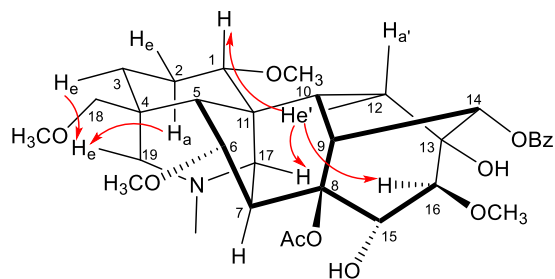
Fig. 2 A (Upper) Ring A in a twisted-chair conformation in 1-OMe NDA; B (Lower) Ring A in a twisted-boat conformation due to the intramolecular H-bond. a: axial, e: equatorial, f: flagpole, b: bowsprit.



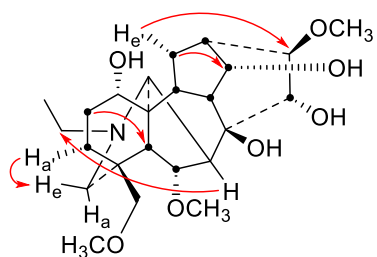
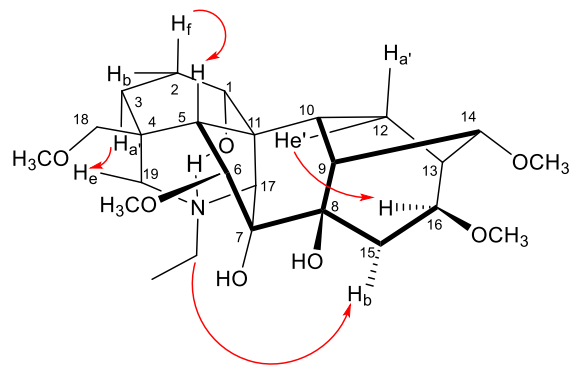
3-Deoxyaconitine



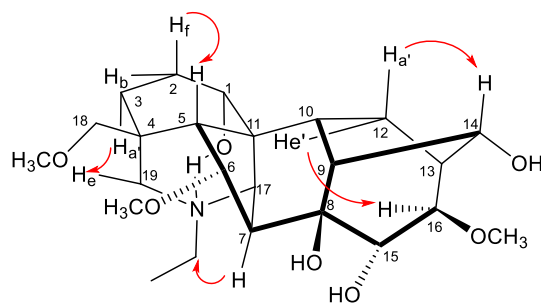
Hypaconitine



Delsoline



Fuziline



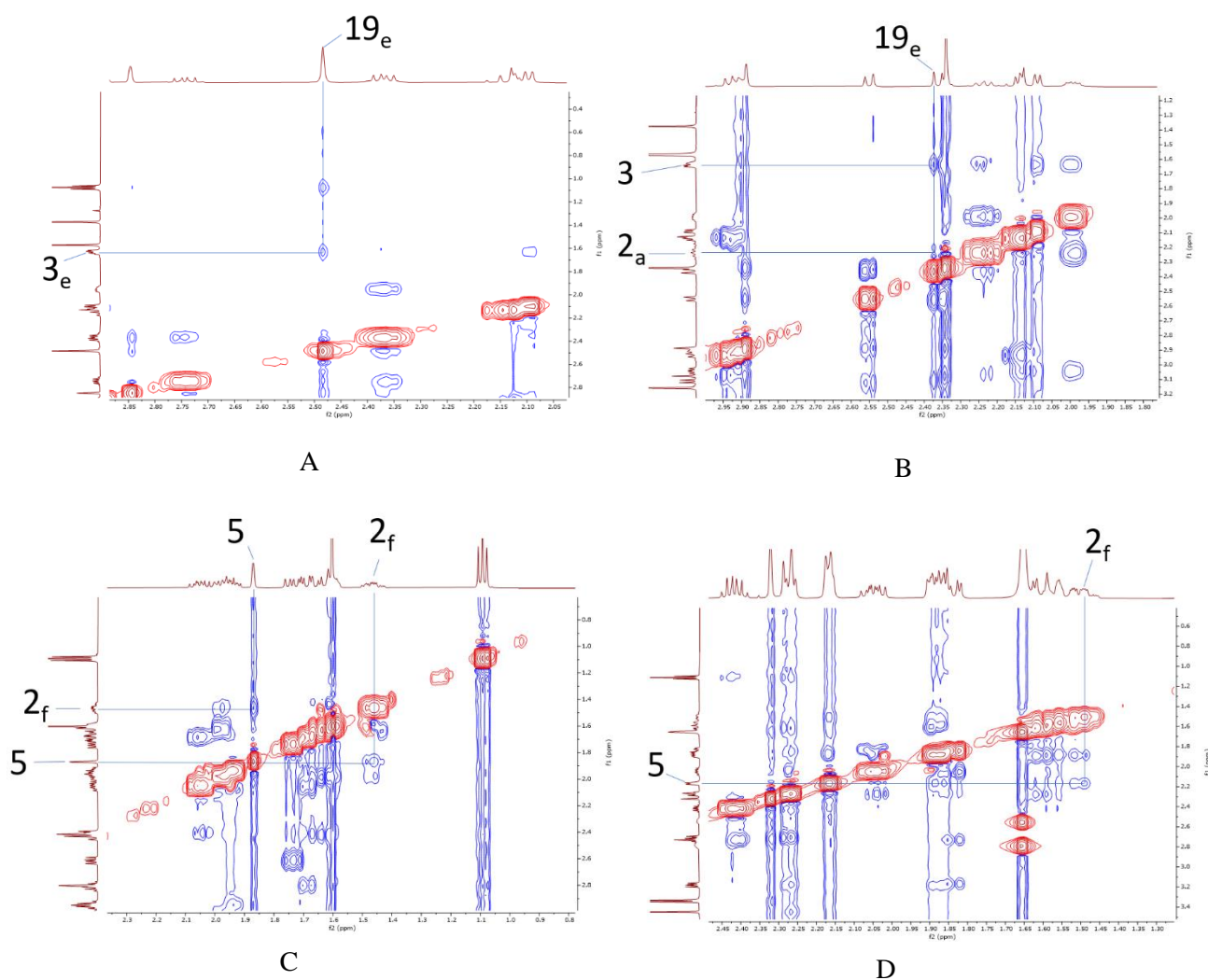


Fig. 3 NOESY correlation in A 3-deoxyaconitine **1** (19- $H_e$  to 3- $H_e$ ); B hyptaconitine **2** (19- $H_e$  to 2- $H_a$ -( $\alpha$ )); C delsolone **3** (5-H to 2- $H_f$  ( $\beta$ )); and D fuziline **4** (5-H to 2- $H_f$  ( $\beta$ )). a: axial, e: equatorial, a': pseudoaxial, e': pseudoequatorial, f: flagpole, b: bowsprit.

In 3-deoxyaconitine **1**, the 1- $H_a$  ( $\beta$ ) resonates at 3.04 ppm (dd,  $^3J_{aa} = 10.6$  Hz,  $^3J_{ae} = 6.5$  Hz) and in hyptaconitine **2**, the 1- $H_a$  ( $\beta$ ) also resonates at 3.04 ppm (dd,  $^3J_{aa} = 10.0$  Hz,  $^3J_{ae} = 6.5$  Hz). This supports the conclusion that ring A adopts a chair conformation in both compounds. In a true chair,  $^3J_{aa}$  is typically between 12-14 Hz, but as it is a slightly smaller value (10.0-10.6 Hz), this indicates that it is a twisted chair ring.<sup>6,7</sup>

In 1-OH NDA, an intramolecular hydrogen bond exists between 1- $\alpha$ OH and the piperidine tertiary amine, resulting in a boat conformation of ring A (Fig. 2B).<sup>20,21</sup> The NOE showed correlation between 2- $H_f$  and 5-H and that supports ring A adopting a boat

conformation in both of them (Fig. 3). In delsoline **3**, the 1-H<sub>e'</sub> (β) resonates at 3.68 ppm (dt,  $^3J_{e'f} = ^3J_{e'b} = 3.2$  Hz,  $^3J = 9.0$  Hz (through the hydrogen bonded oxygen)). H-2<sub>f</sub> (β) resonates at 1.46 ppm (tdd,  $^2J_{gem} = ^3J_{af} = 14.5$  Hz,  $^3J_{e'f} = 7.5$  Hz,  $^3J_{e'f} = 3.2$  Hz) (Fig. 4) and this indicates a twisted ring as the  $^3J_{e'f} = 3.2$  Hz (with 1-H<sub>e'</sub>) <  $^3J_{e'f} = 7.5$  Hz (3-H<sub>e'</sub>) which means that the dihedral angle  $\angle((1-H_{e'})-C1-C2-(2-H_f))$  is larger than  $\angle((2-H_f)-C2-C3-(3-H_{e'}))$  according to the Karplus equation. The dihedral angle dependence of the magnitude of vicinal couplings results from molecular orbital overlap, where maximum orbital overlap occurs when the dihedral angle is 0° and 180° ( $^3J_{HH}$  is large) and the orbital overlap is minimal when the dihedral angle is 90° ( $^3J_{HH}$  is small).<sup>22</sup> In fuziline **4**, 2-H<sub>f</sub> resonates at 1.49 ppm (tdd,  $^2J_{gem} = ^3J_{af} = 14.3$  Hz,  $^3J_{ef} = 6.3$  Hz,  $^3J_{ef} = 3.1$  Hz) (Fig. 4), and it also indicates a twist in ring A; 1-H<sub>e'</sub> and 3-H<sub>e'</sub> signals were overlapped with other signals.

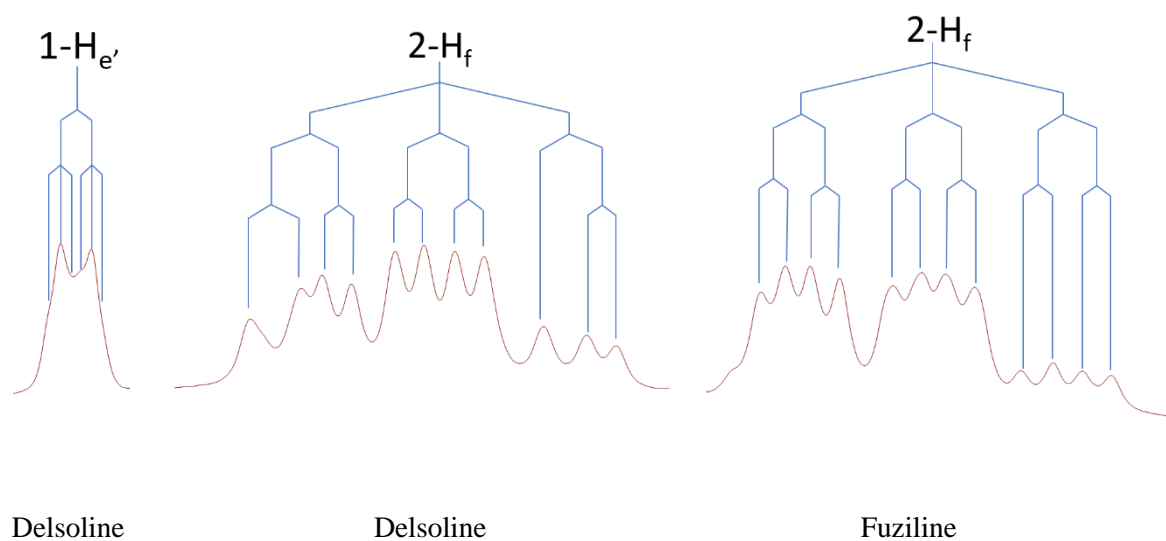


Fig. 4 <sup>1</sup>H NMR coupling pattern of key signals in delsoline **3** (1-H<sub>e'</sub> centred around 3.68 ppm and 2-H<sub>f</sub> centred around 1.46 ppm) and fuziline **4** (2-H<sub>f</sub> centred around 1.49 ppm).

## 2.1. Steric compression

Through-space steric interactions have been reported in NDA and their synthetic analogues.<sup>5,7</sup> Such an effect can be observed on 2-H in 1-OMe NDA as the tertiary amine causes steric compression deshielding the axial proton to resonate downfield of the equatorial proton. In 3-

deoxyaconitine **1**, 2-H<sub>a</sub> resonated at 2.24 ppm compared to 1.95 ppm for 2-H<sub>e</sub>. In hyaconitine **2**, 2-H<sub>a</sub> resonated at 2.24 ppm compared to 2.00 ppm for 2-H<sub>e</sub>. This difference is unusual as the equatorial protons of such 6-membered rings are usually found at a higher chemical shift compared to the axial protons due to the anisotropic effect, but the lone pair of the tertiary *N*-atom pushes the electrons around 2-H<sub>a</sub> ( $\alpha$ ) and results in this deshielding (Fig. 5A).<sup>20</sup> In 1-OH alkaloids as the hydrogen-bonded ring A adopts a boat conformation, the protons are no longer close to the *N*-atom and 2-H<sub>b</sub> ( $\alpha$ ) chemical shift is higher than 2-H<sub>f</sub> ( $\beta$ ) with a difference of 0.14 ppm in delsoleine **3** and 0.09 ppm in fuziline **4** (Fig. 5B).

At position 19, it was observed that in NDA that have a 3-OH substituent ( $\epsilon$ ,  $\alpha$ ) like aconitine **5** and mesaconitine **6**, the hydroxyl group causes deshielding on 19-H<sub>e</sub>. 19-H<sub>e</sub> resonated downfield by ~0.5 ppm in aconitine **5**<sup>6</sup> and by ~0.4 ppm in mesaconitine **6**<sup>20</sup>, compared to 19-H<sub>a</sub>. Such difference has diminished in 3-deoxyaconitine **1** as both the axial and the equatorial protons resonate together as broad singlet (br s). In hyaconitine **2**, 19-H<sub>a</sub> chemical shift was higher compared to 19-H<sub>e</sub> by ~0.2 ppm which could be due to steric compression from 6-OMe ( $\alpha$ ) (Fig. 5A). In fuziline **4**, the same effect was observed as 19-H<sub>a</sub> chemical shift was higher than 19-H<sub>e</sub> by ~0.5 ppm and that supports the idea of the 6-OMe ( $\alpha$ ) compression of 19-H<sub>a</sub> (Fig. 5A). In delsoleine **3**, the 6-OMe is in a  $\beta$ -configuration, but still the steric effect on 19-H<sub>a</sub> is observed as both protons resonate together, possibly due to an effect from 7-OH.

At position 18, it was observed that 6 $\alpha$ -OMe in 3-deoxyaconitine **1**, hyaconitine **2**, and fuziline **4** resulted in a deshielding effect on 18-H<sub>A,B</sub>, where the chemical shift was higher by ~0.2 ppm, compared to the 6 $\beta$ -OMe in delsoleine **3** (Fig. 5C).

At position 12, it was observed in 3-deoxyaconitine **1** and hyaconitine **2** that 1-OMe sterically compresses 12-H<sub>e'</sub> ( $\alpha$ ) and it resonates downfield compared to 12-H<sub>a'</sub> ( $\beta$ ) by ~0.8 ppm (Fig. 5A). Such an effect was not observed in delsoleine **3** and fuziline **4** as the 1-OH group flipped to the axial position away from 12-H<sub>e'</sub> ( $\alpha$ ) due to the intramolecular H-bond with the *N*-atom (Fig. 5B), and the difference between both protons was reduced to ~0.2 ppm. These results are consistent with the NMR data of mesaconitine **6**, karacoline **7**, neoline **8**, and condelphine **9**.<sup>20</sup> In addition, it was observed that the difference in aconitine **5** was ~0.6 ppm and that

difference reduced to  $\sim 0.4$  ppm in aconitine **5** HCl (pseudoaxial  $\delta$  was higher) as ring A flipped into a boat conformation due to the intramolecular H-bond with the *N*-alkylpiperidine N-atom.<sup>6</sup>

It was also observed that 7-OH caused a steric effect on the methylene protons of the *N*-ethyl side-chain (Fig. 5A). The chemical shift in delso-line **3** was higher by  $\sim 0.4$  ppm compared to 3-deoxyaconitine **1**, hyaconitine **2**, and fuziline **4**. Such an effect can also be detected in previously reported lycoc-tonine **10** and methyllycaconitine (MLA) **11**.<sup>6</sup> Another comparison at position 7 is between fuziline (15 $\alpha$ -hydroxyneoline) **4** and neoline **8**, where a steric effect was observed from the 15-OH (b,  $\alpha$ ) on 7-H (Fig. 5C) which results in an increase in the  $\delta_{7H}$  by  $\sim 0.3$  ppm in fuziline **4** compared to neoline **8**.<sup>20</sup>

It has previously been reported that the tertiary nitrogen in 1-OH NDA is affected by the intramolecular H-bonding and that results in higher chemical shifts compared to 1-OMe NDA (Fig. 5A, 5B).<sup>5</sup> In this study, the data are consistent with what has been reported as the nitrogen chemical shifts ( $\delta_N$ ) of delso-line **3** and fuziline **4** were 54.2 and 55.4 ppm respectively, compared to 51.7 and 38.4 ppm for 3-deoxyaconitine **1** and hyaconitine **2** respectively.

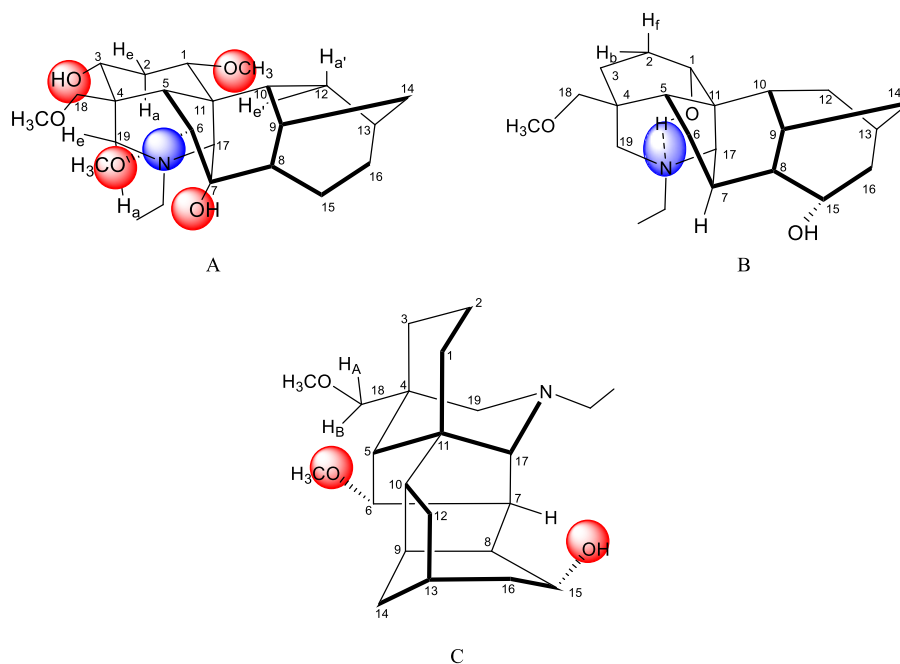


Fig. 5 Steric compression effects seen within 1-OMe and 1-OH NDA. A Effect on 12- $H_e$ , 2- $H_a$ , 19-H (a,e), and  $NCH_2CH_3$ . B Effect on the N-atom due to the intramolecular H-bond in 1-OH NDA. C Effect on 18-H and 7-H.



### 3. Conclusions

The full NMR assignment of four NDA (3-deoxyaconitine **1**, hyaconitine **2**, delsoline **3**, and fuziline **4**) is reported in this study for the first time. The effect of C1 substituent on the conformation of ring A was accomplished in these four NDA, where it was found that ring A adopts a twisted chair conformation in 1-OMe NDA (3-deoxyaconitine **1** and hyaconitine **2**) while it adopts a twisted boat conformation in 1-OH NDA (delsoline **3**, and fuziline **4**) due to an intramolecular H-bonding between the tertiary nitrogen and the hydroxy group at position 1. Such a conformational difference affects the through space steric interactions at various positions and affects chemical environment around the nitrogen where the nitrogen chemical shifts ( $\delta_N$ ) was higher in 1-OH NDA compared to 1-OMe NDA.

### 4. Experimental

**General Methods. Chemicals and Materials.** 3-Deoxyaconitine **1** (98%), delsoline (belsoline) **3** (98%), and fuziline **4** (98%) were donated by Carbosynth Ltd. (U.K.). Hyaconitine **2** (98%) was purchased from Carbosynth Ltd. (U.K.). All other chemicals were purchased from Sigma-Aldrich (U.K.) and used as received. Chloroform-d (99.8% D atom,  $\text{CDCl}_3$ ) was used for NMR experiments purchased from Cambridge Isotope Laboratories (U.S.A.).

**Instrumentation.**  $^1\text{H}$  NMR spectra were recorded on a Bruker Avance III ( $^1\text{H}$  Larmor precession frequency 500 MHz) spectrometer at 25 °C. Chemical shifts were expressed in parts per million (ppm) and residual (protio) solvent peak ( $\text{CHCl}_3$ ) was used as the internal standard (7.26 ppm). Chemical shifts  $\delta_H$  (ppm) were reported as position (accurate  $\delta_H$  of overlapping signals were extracted from two-dimensional (2D) NMR spectra, e.g., HSQC, COSY, and NOESY), expressed in ppm, relative integral, multiplicity, and assignment. Multiplicity was abbreviated: s = singlet, d = doublet, t = triplet, q = quartet, m = multiplet; br = broad. Coupling constants ( $J$ ) are line separations (absolute values expressed in hertz, Hz), rounded and rationalized to 0.1 Hz.  $^{13}\text{C}$  NMR spectra were recorded with complete proton decoupling on a Bruker Avance III ( $^{13}\text{C}$  Larmor precession frequency 125 MHz) spectrometer at 25 °C as well as 2D NMR experiments including HSQC, HMBC, and H2BC. The  $\text{CDCl}_3$  signal was used as the internal standard (77.0 ppm), and  $\delta_C$  (ppm) were reported as position, number of attached protons ( $\text{CH}_3$ ,  $\text{CH}_2$ , CH, quat

= quaternary), and assignment.  $^1\text{H}$ - $^{15}\text{N}$  HMBC spectra were recorded on a Bruker Avance III ( $^{15}\text{N}$  Larmor precession frequency 51 MHz) spectrometer at 25 °C. The spectra were externally calibrated with a MeNO<sub>2</sub> solution (50% in CDCl<sub>3</sub>, v/v), recorded, and set at  $\delta_{\text{N}}$  379.8 ppm, and the correction factor is measured as -511.72 on our spectrometer. Positive-ion [M+H]<sup>+</sup> mode mass spectrometry was performed on samples dissolved in methanol, using an Agilent ESI-Q-TOF mass spectrometer. High-resolution mass spectrometry (HR-MS) data were within 5 ppm error. 3-Deoxyaconitine **1**:  $m/z$  calcd. for C<sub>34</sub>H<sub>48</sub>NO<sub>10</sub> 630.3278, found 630.3275 [M+H]<sup>+</sup>. Hypaconitine **2**:  $m/z$  calcd. for C<sub>33</sub>H<sub>46</sub>NO<sub>10</sub> 616.3122, found 616.3122 [M+H]<sup>+</sup>. Delsoline **3**:  $m/z$  calcd. for C<sub>25</sub>H<sub>42</sub>NO<sub>7</sub> 468.2961, found 468.2963 [M+H]<sup>+</sup>. Fuziline **4**:  $m/z$  calcd. for C<sub>24</sub>H<sub>40</sub>NO<sub>7</sub> 454.2805, found 454.2808 [M+H]<sup>+</sup>.

### Acknowledgements

We thank Carbosynth Ltd. (U.K.) for the donated 3-deoxyaconitine, delsoline (belsoline), and fuziline. We acknowledge Dr Bruce Rogers at Carbosynth Ltd. for his interest in these studies.

### References

- 1 M. S. Yunusov, *Nat. Prod. Rep.*, 1991, **8**, 499–526.
- 2 M. S. Yunusov, *Nat. Prod. Rep.*, 1993, **10**, 471–486.
- 3 Y. Shen, W. J. Liang, Y. N. Shi, E. J. Kennelly and D. K. Zhao, *Nat. Prod. Rep.*, 2020, **37**, 763–796.
- 4 A. M. A. Qasem, Z. Zeng, M. G. Rowan and I. S. Blagbrough, *Nat. Prod. Rep.*, 2021, **38**, in press DOI:10.1039/d1np00029b.
- 5 Z. Zeng, A. M. A. Qasem, T. J. Woodman, M. G. Rowan and I. S. Blagbrough, *ACS Omega*, 2020, **5**, 14116–14122.
- 6 Z. Zeng, G. Kociok-Köhn, T. J. Woodman, M. G. Rowan and I. S. Blagbrough, *Europ. J. Org. Chem.*, 2021, 2169–2179.
- 7 Z. Zeng, G. Kociok-Köhn, T. J. Woodman, M. G. Rowan and I. S. Blagbrough, *ACS Omega*, 2021, **6**, 12769–12786.
- 8 R. E. Gilman and L. Marion, *Can. J. Chem.*, 1962, **40**, 1713–1716.

- 9 Y. G. Wang, Y. L. Zhu, R. H. Zhu, *Yaoxue Xuebao, Acta Pharmaceutica Sinica*, 1980, **15**, 526–531.
- 10 F. Gao, S.-A. Zhu and S.-J. Xiong, *Acta Crystallogr. Sect. E Struct. Reports Online*, 2010, **66**, o1342–o1342.
- 11 T.-P. Yin, L. Cai, H. Zhou, X.-F. Zhu, Y. Chen and Z.-T. Ding, *Nat. Prod. Res.*, 2014, **28**, 1649–1654.
- 12 S.-I. Majima, Riko; Morio, *Justus Liebigs Ann. Chem.*, 1929, **476**, 171–181.
- 13 L.-L. Zheng, Y. Li, T.-Y. Zi and M.-Y. Yuan, *Acta Crystallogr. Sect. E Struct. Reports Online*, 2010, **66**, o2787–o2788.
- 14 B. Jiang, S. Lin, C. Zhu, S. Wang, Y. Wang, M. Chen, J. Zhang, J. Hu, N. Chen, Y. Yang and J. Shi, *J. Nat. Prod.*, 2012, **75**, 1145–1159.
- 15 L. N. Markwood, *J. Am. Pharm. Assoc.*, 1924, **13**, 696–702.
- 16 B. S. Joshi, H. K. Desai, S. W. Pelletier and M. G. Newton, *J. Crystallogr. Spectrosc. Res.*, 1992, **22**, 477–483.
- 17 S. W. Pelletier, N. V. Mody, K. I. Varughese and C. Szu-Ying, *Heterocycles*, 1982, **18**, 47–49.
- 18 S. W. Pelletier and Z. Djarmati, *J. Am. Chem. Soc.*, 1976, **98**, 2626–2636.
- 19 H. S. Sang, S. K. Ju, S. K. Sam, H. S. Kun and K. H. Bae, *Arch. Pharm. Res.*, 2003, **26**, 709–715.
- 20 Z. Zeng, A. M. A. Qasem, G. Kociok-Köhn, M. G. Rowan and I. S. Blagbrough, *RSC Adv.*, 2020, **10**, 18797–18805.
- 21 S. W. Pelletier, Z. Djarmati, S. Lajsic and W. H. De Camp, *J. Am. Chem. Soc.*, 1976, **98**, 2617–2625.
- 22 I. Fleming and D. Williams, *Spectroscopic Methods in Organic Chemistry*, Springer Nature Switzerland, 7th edn., 2019, pp. 192–193.

## Chapter 7

### Effect of position 1 substituent and configuration on APCI-MS fragmentation of norditerpenoid alkaloids including 1-*epi*-condelphine

#### AIMS

Norditerpenoid alkaloids (NDA) are hexacyclic highly oxygenated compounds and the analysis of their 3D configuration is important as it helps to interpret their bioactive conformations. High performance liquid chromatography/ atmospheric pressure chemical ionization mass spectrometry (LC/MS-APCI) is a promising technique to investigate NDA stereochemistry. The effect of the alpha ( $\alpha$ )-substituent at carbon 1 and its configuration on the stability of NDA in the mass spectrometer was studied. It was observed that 1-OH NDA are more stable compared to 1-OMe NDA due to the intramolecular H-bonding that exists in 1-OH NDA. In addition, 1-*epi*-condelphine **9** was found to be less stable in the mass spectrometer compared to condelphine **7** as the nitrogen is no longer hydrogen bonded to the  $\beta$ -hydroxyl at position 1 which highlights the importance of the substituent configuration at carbon 1.

<b>This declaration concerns the article entitled:</b>			
Effect of Position 1 Substituent and Configuration on APCI-MS Fragmentation of Norditerpenoid Alkaloids Including 1- <i>epi</i> -Condelphine			
<b>Publication status (tick one)</b>			
<b>Draft manuscript</b>	<input type="checkbox"/>	<b>Submitted</b>	<input type="checkbox"/>
		<b>In review</b>	<input type="checkbox"/>
		<b>Accepted</b>	<input type="checkbox"/>
		<b>Published</b>	<input checked="" type="checkbox"/>
<b>Publication details (reference)</b>	Qasem, A. M. A., Rowan, M. G., and Blagbrough, I. S., 2022. Effect of Position 1 Substituent and Configuration on APCI-MS Fragmentation of Norditerpenoid Alkaloids Including 1- <i>epi</i> -Condelphine. <i>ACS Omega ASAP</i> .		
<b>Copyright status (tick the appropriate statement)</b>			
The material has been published with a CC-BY license		<input checked="" type="checkbox"/>	The publisher has granted permission to replicate the material included here
<b>Candidate's contribution to the paper (provide details, and also indicate as a percentage)</b>		<p><b>Formulation of ideas:</b> The candidate contributed to the formulation of the article ideas (70%)</p> <p><b>Design of methodology:</b> The candidate contributed to design the study to correlate the effect of position 1 substituent on the alkaloids skeleton stability using APCI-MS and also to study how the substituent configuration affect NDA fragmentation (70%).</p> <p><b>Experimental work:</b> The candidate contributed to the analysis of selected 1-OMe and 1-OH NDA using APCI-MS and also the synthesis and analysis of 1-<i>epi</i>-condelphine (80%).</p> <p><b>Presentation of data in journal format:</b> The candidate contributed to the paper writing and figures presentation (60%)</p>	
<b>Statement from Candidate</b>	This paper reports on original research I conducted during the period of my Higher Degree by Research candidature.		
<b>Signed (typed signature)</b>	Ashraf Qasem	<b>Date</b>	21/09/2022

## INTRODUCTION

The structural investigation and elucidation of natural products is one of the major applications of mass spectrometry. The fragmentation pattern of the analytes is sensitive to the experimental conditions of ionization.<sup>1</sup> Therefore, several analytical methods have been developed to control the amount of energy used to fragment the precursor ion with regards to the fragment ion.<sup>1,2</sup> Several studies have been reported on the application of electrospray ionization tandem mass spectrometry (ESI-MS/MS) to differentiate stereoisomers of different alkaloids groups like indole alkaloids,<sup>3</sup> indoloquinolizidine alkaloids,<sup>4</sup> and matrine-type alkaloids.<sup>5</sup> Electron impact-mass spectrometry (EI-MS) has been applied to study the structural effect on fragmentation, for example to study the effect of stereoisomerism on EI fragmentation of eburnane-type alkaloids.<sup>6</sup> In addition, EI-MS was applied to study the effect of the substituent configuration at position 1 of norditerpenoid alkaloids (NDA) where it was found the intensity of the fragment peak  $[M-15]^+$  was higher for 1- $\beta$ -OH NDA compared to 1- $\alpha$ -OH NDA where the intensity of the  $[M-OH]^+$  was higher with 1- $\alpha$ -OH NDA compared to 1- $\beta$ -OH NDA.<sup>7,8</sup>

There are only a few reports on the usage of high-performance liquid chromatography-atmospheric pressure chemical ionization mass spectrometry (HPLC-APCI-MS), which is a promising technique to investigate the effect of substituents' configuration on the NDA skeleton fragmentation.<sup>9-11</sup> APCI works on the analyte in the gas-phase through nebulization (aerosol generation) by high speed gas and then desolvation of the droplets in the vaporization chamber. After that, ionization of the analyte happens in the gas-phase through corona discharge which is produced through a high voltage needle. The CI reagent gas in APCI is the LC mobile phase (or analyte solvent) where the vaporized solvent forms several adduct ions through the reaction with electrons from corona discharge. In positive-ion mode, proton transfer occurs from the adducts to the analyte. In negative-ion mode, proton subtraction produces the molecular ion.<sup>12</sup>

The advantage of using APCI is that ionization occurs in the gaseous state compared to in the liquid state in ESI, and that enables APCI to work with non-polar solvents, also APCI is less susceptible to matrix effects (including ion suppression) compared to ESI and therefore APCI can be considered for a wide range of applications including non-polar analytes.<sup>11</sup>

Although APCI uses high collision frequency which results in more fragments in the ionizer chamber compared to ESI (harder ionization),<sup>13,14</sup> it is still considered a soft ionization method as the rapid desolvation reduces the thermal degradation considerably and that results in fewer fragmentations compared to hard ionization methods.<sup>14</sup>

It was demonstrated that using APCI ionization, the major fragmentation of the NDA skeleton occurs at position 8 where NDA with 8-OH, 8-OCH<sub>3</sub>, and 8-OAc fragment with the loss of 18 Da, 32 Da, and 60 Da respectively.<sup>10</sup> It was also demonstrated using deuterium labelling that the fragmentation at position 8 starts from the nitrogen where it was shown that the deuterium atom introduced on the nitrogen atom is in the leaving fragment (loss of 20 Da with 8-OH NDA, and loss of 62 Da with 8-OAc NDA).<sup>10</sup> Figure 1A shows the fragmentation at position 8 starting from the nitrogen atom.

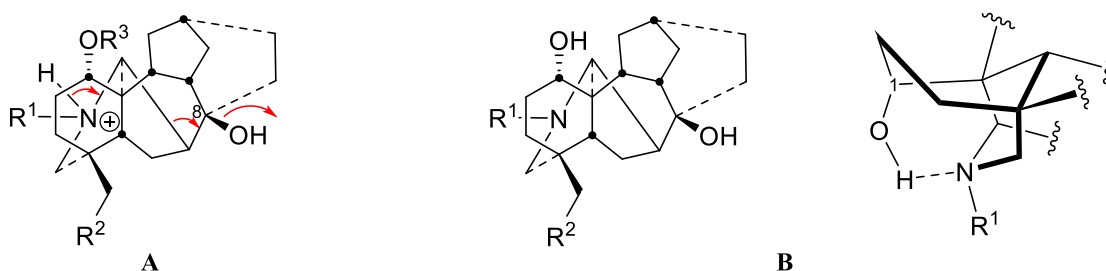


**Figure 1.** A. Fragmentation of NDA skeleton at position 8 using APCI. B. Intramolecular H-bond in 1-OH NDA where the secondary alcohol is axial.

The influence of substitution at position 1 was reported where it was observed that the presence of  $\alpha$ -OH at position 1 results in stabilization and lower fragmentation compared to 1-OMe NDA. It was proposed that the stabilization occurs due to intramolecular H-bonding (Figure 1B).<sup>10</sup> In this study, the APCI fragmentation results of a series of 1-OMe and 1-OH NDA are reported showing the effect of ring A conformation on the mass spectral fragmentation pattern. Also highlighting the importance of the substituent configuration at position 1 on the stabilization of the NDA skeleton.

## RESULTS and DISCUSSION

### 1. Effect of carbon 1 substituent on NDA stability in APCI mass spectrometry.

To study the effect of position 1 substituent on the stability of the NDA skeleton, 8 compounds were chosen (Figure 2) where all of them possess a hydroxy group at position 8 (the initial fragmentation position). The APCI-MS method was applied to investigate the stereochemical effect of the carbon 1 substituent on the stability of alkaloids **1-8**. The APCI mass spectra were simple and showed the  $[M+H]^+$  parent ion alongside the major fragment ion  $[M+H-H_2O]^+$ . The detected signals and their relative abundance (I%) are given in Table 1.

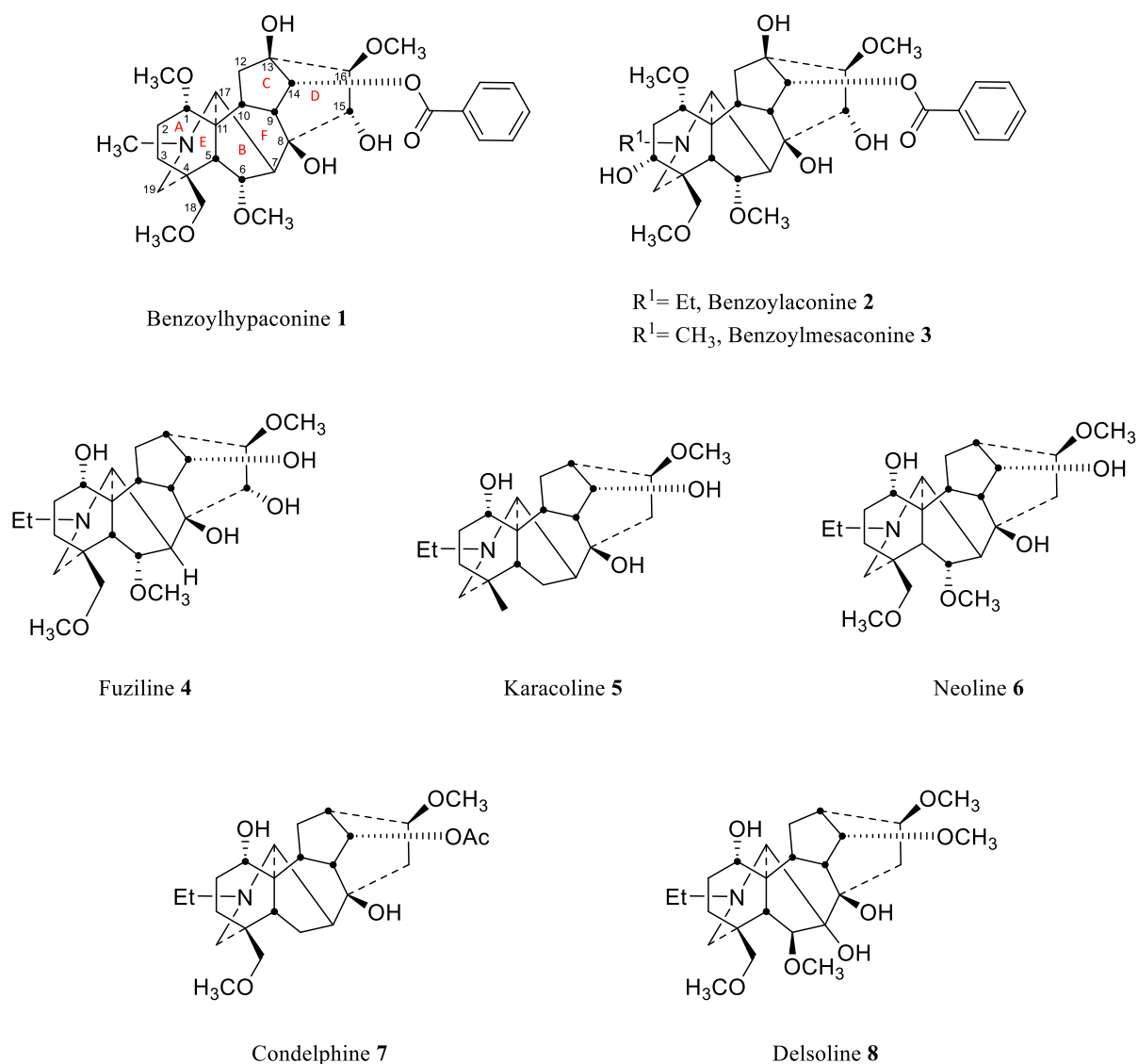


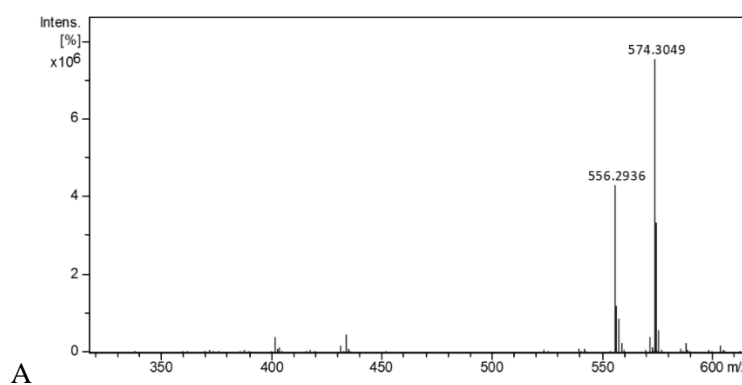
**Figure 2.** Norditerpenoid alkaloids **1-8**.

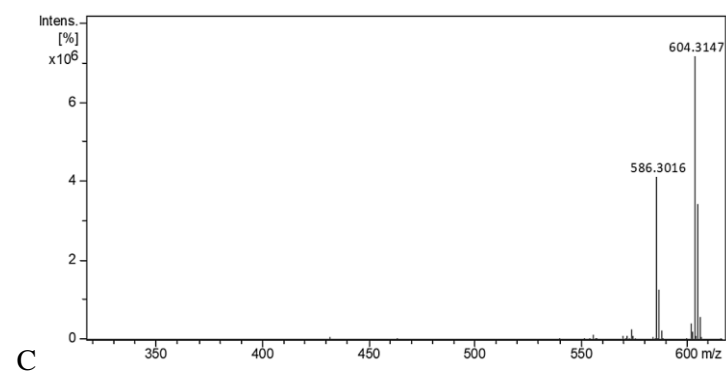
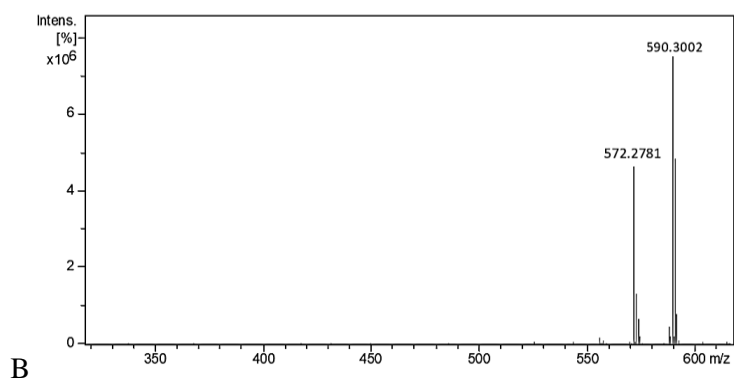


**Table 1. The Detected Signal of the Parent Ion and their Fragment Ion with their Intensities (I%)**

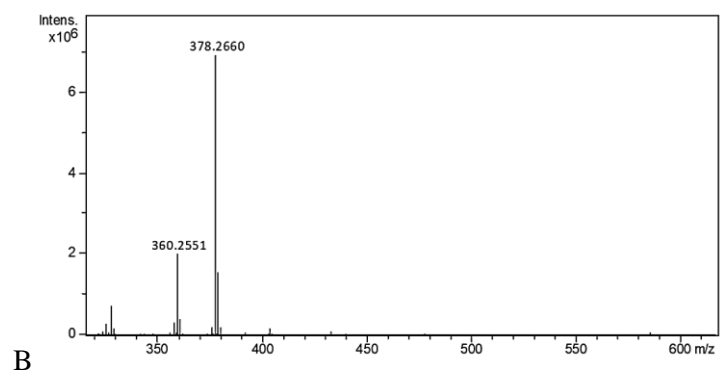
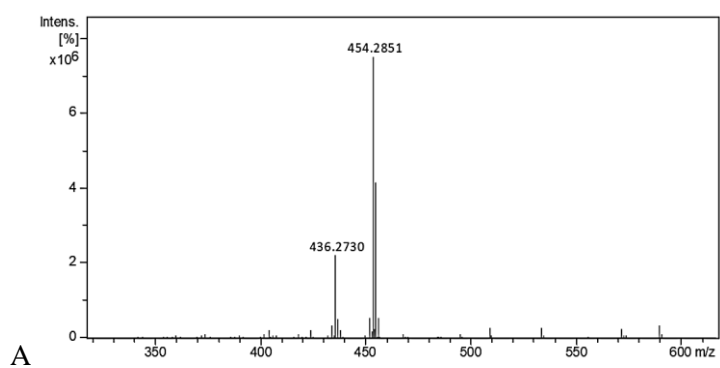
Cmpd	Molecular formula	[M+H] <sup>+</sup>	[M+H] <sup>+</sup>	[M+H-H <sub>2</sub> O] <sup>+</sup>	[M+H-H <sub>2</sub> O] <sup>+</sup>
		<i>m/z</i>	I%	<i>m/z</i>	I%
<b>1</b>	C <sub>31</sub> H <sub>43</sub> NO <sub>9</sub>	574.3049	100	556.2936	57
<b>2</b>	C <sub>31</sub> H <sub>43</sub> NO <sub>10</sub>	590.3002	100	572.2781	62
<b>3</b>	C <sub>32</sub> H <sub>45</sub> NO <sub>10</sub>	604.3147	100	586.3016	58
<b>4</b>	C <sub>24</sub> H <sub>39</sub> NO <sub>7</sub>	454.2851	100	436.2730	30
<b>5</b>	C <sub>22</sub> H <sub>35</sub> NO <sub>4</sub>	378.2660	100	360.2551	29
<b>6</b>	C <sub>24</sub> H <sub>39</sub> NO <sub>6</sub>	438.2926	100	420.2817	27
<b>7</b>	C <sub>25</sub> H <sub>39</sub> NO <sub>6</sub>	450.2941	100	432.2811	31
<b>8</b>	C <sub>25</sub> H <sub>41</sub> NO <sub>7</sub>	468.3015	100	450.2894	33

The APCI spectra of the 1-OMe alkaloids **1-3** were obtained and showed a parent [M+H]<sup>+</sup> ion peak (100%) and a major fragment ion peak [M+H-H<sub>2</sub>O]<sup>+</sup> (Table 1) at position 8 with relative abundance ~60% (Figure 3).





**Figure 3.** APCI mass spectra (A, B, and C) of compounds **1-3** respectively.



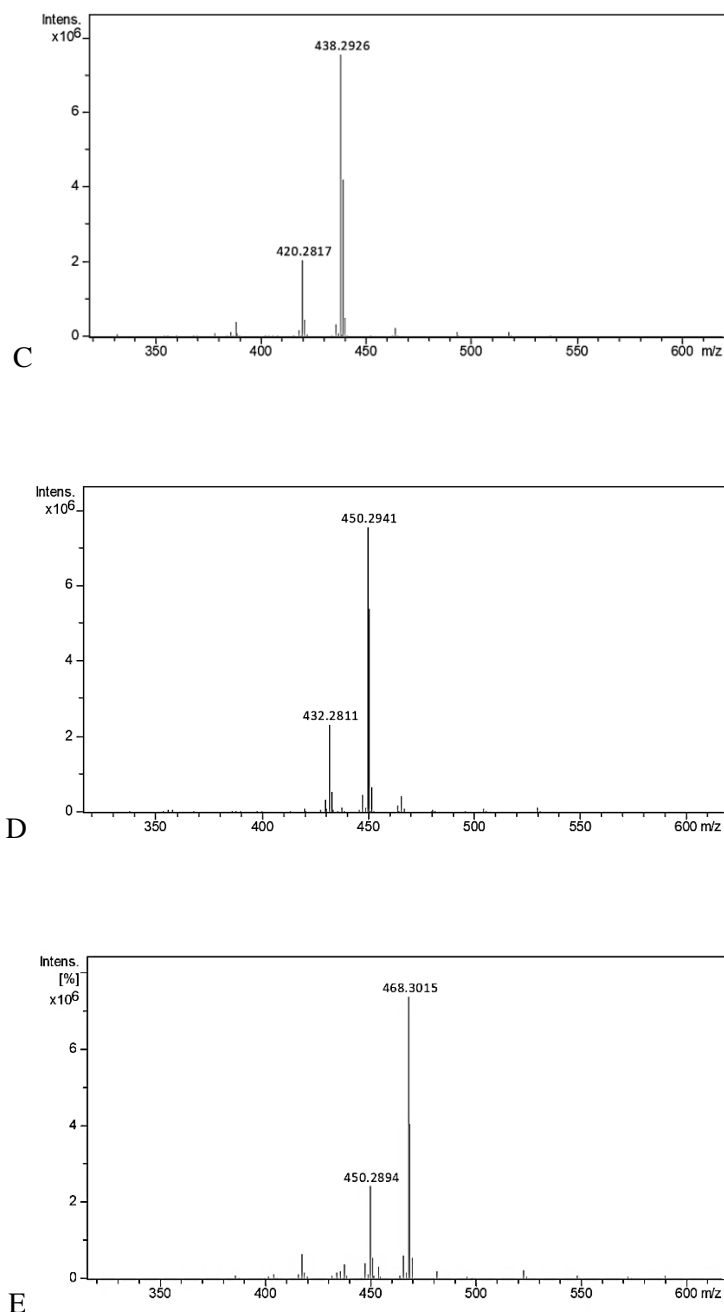


**Figure 4.** APCI mass spectra (A-E) of compounds **4-8** respectively.

The obtained APCI mass spectra of compounds **4-8** were more stable as they showed less fragmentation at position 8 compared to compounds **1-3** (Figure 4). The intensity of the fragment-ion peak observed for compounds **4-8** is around 30% compared to 60% for compounds **1-3** and that indicates the role of conformation in the stabilization of the NDA skeleton.

We have reported that ring A conformations of 1-OMe and 1-OH NDA are different due to the intramolecular H-bond.<sup>15</sup> The tertiary nitrogen is bonded (H-bond) to the 1-OH in

compounds **4-8** and that results in flipping ring A into a boat conformation compared to a chair conformation in compounds **1-3** (Figure 5A). The explanation reported by Wada and co-workers<sup>10</sup> for the stabilization of 1-OH NDA is that the introduced proton, which is the starting point of the fragmentation at position 8 (Figure 5B), is stabilized by an intramolecular hydrogen-bond with the 1-OH where ring A adopts a boat conformation.<sup>15</sup> On the other hand, 1-OMe NDA salts also form intramolecular H-bonds between the methoxy group and the protonated nitrogen and that flips ring A from a chair conformation into a boat<sup>16,17</sup> (Figure 6) and that should result in a stabilization effect similar to 1-OH NDA. Therefore, the reported theory does not explain the observed higher fragmentation of 1-OMe NDA compared to 1-OH NDA.

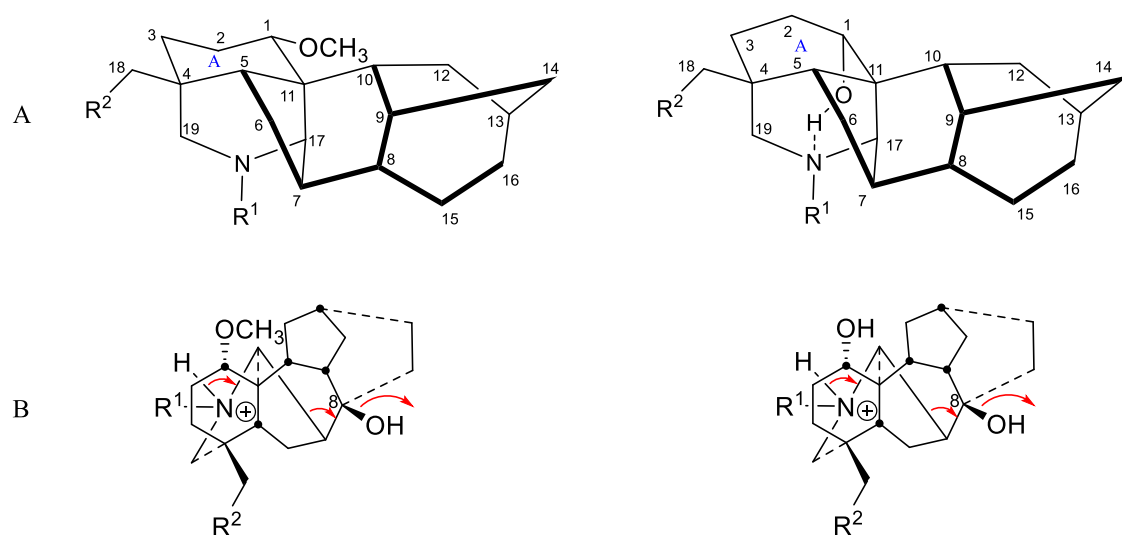


**Figure 5.** A. 1-OH and 1-OMe NDA skeleton, B. fragmentation of 1-OH and 1-OMe NDA at position 8.

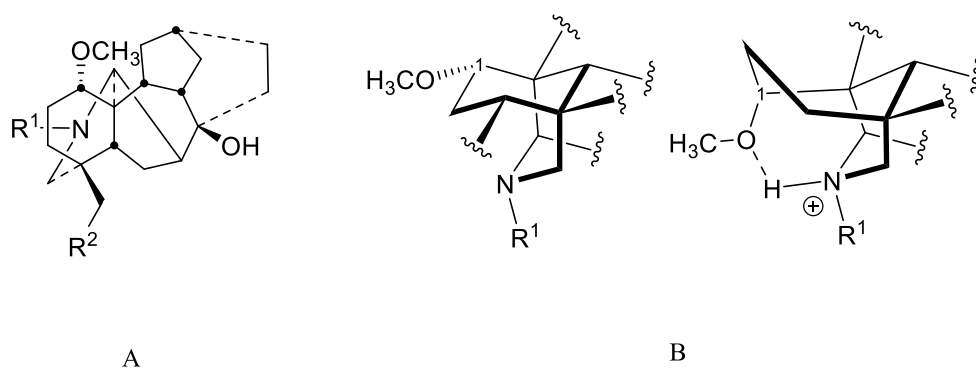


**Figure 6.** A. 1-OMe NDA skeleton, B. Conformation of the AE bicyclic system as a free base (left) and salt (right).

A most reasonable explanation for the difference in the stability of 1-OH NDA and 1-OMe NDA is that the positive charge in 1-OH NDA is delocalized and stabilized over four atoms  $[N-H-O-H]^+$  while the positive charge in 1-OMe NDA is delocalized over three atoms  $[N-H-O]^+$  and therefore 1-OMe NDA has higher tendency to lose the introduced proton on the nitrogen and consequently to lose  $H_2O$  at position 8 (Figure 7).

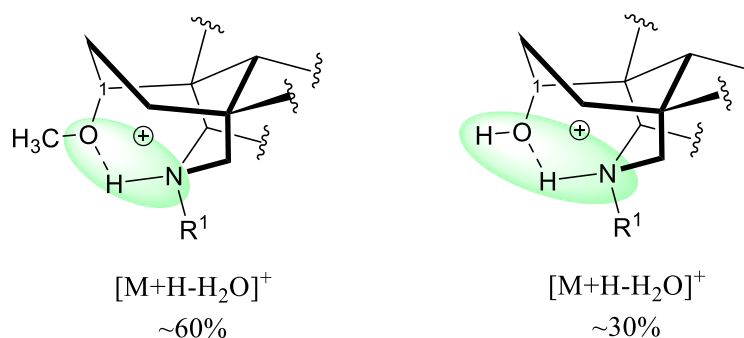


**Figure 7.** Charge delocalisation (green area) in 1-OMe NDA salts (left) and 1-OH NDA salts (right).

## 2. Effect of 1-OH configuration on NDA fragmentation.

The vast majority of NDA are functionalized with an  $\alpha$ -substituent, and it was noted that a  $\beta$ -substituent should lead to less stabilization of the skeleton.<sup>10,11</sup> To investigate the effect of the configuration on the NDA ring A conformation and skeleton MS fragmentation, condelphine **7** was converted into 1-*epi*-condelphine **9** (Figure 8).

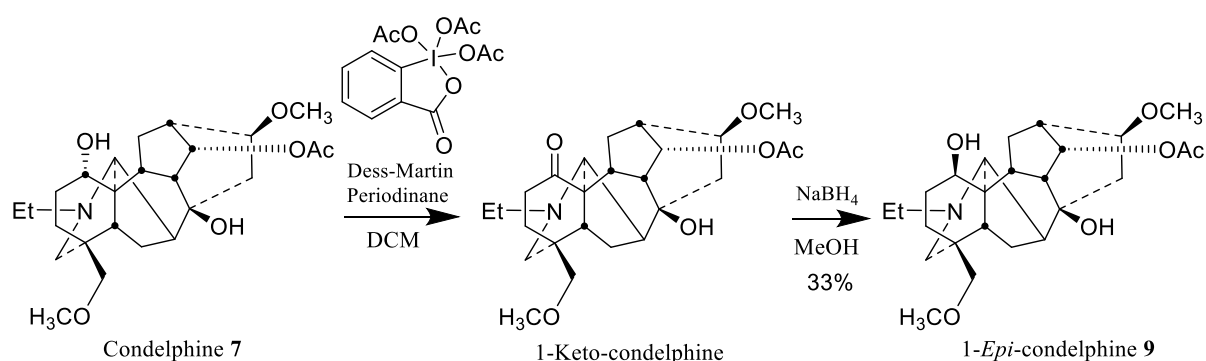


**Figure 8.** Oxidation of condelphine **7** and then reduction to obtain 1-*epi*-condelphine **9**.

The first step of the reaction was oxidation of condelfine **7** ( $R_f = 0.28$  in 10% MeOH/DCM) into 1-keto-condelfine ( $R_f = 0.35$  in 10% MeOH/DCM) using 4 equivalents of Dess-Martin periodinane in anhydrous dichloromethane at 20 °C for 24 h. 1-Keto-condelfine was then reduced with 1 equivalent of  $\text{NaBH}_4$  to obtain 1-*epi*-condelfine **9** (33%). The final mixture was purified using an NX-C18 LC column where 1-*epi*-condelfine **9** eluted after 4.3 min and 1-keto-condelfine at 8.0 min (Figure 9).

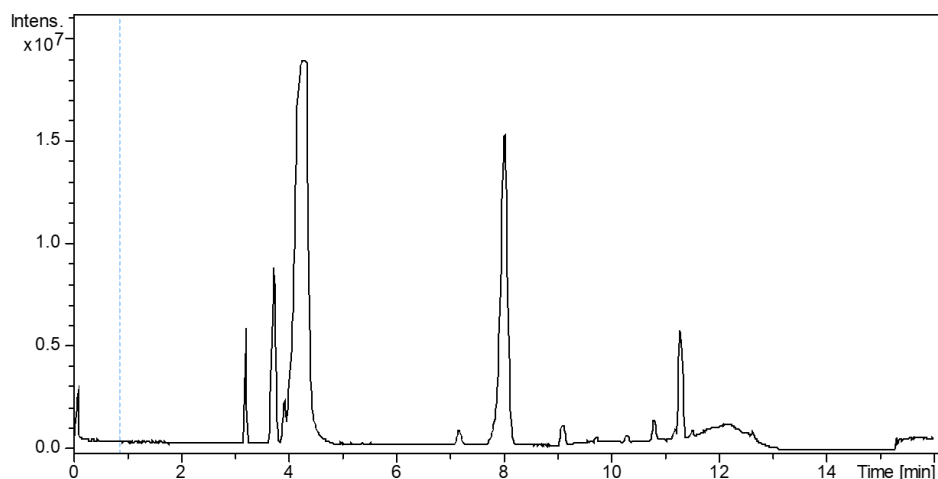


**Figure 9.** LC/MS-ESI ion chromatogram shows 1-*epi*-condelfine signal (4.3 min) and 1-keto-condelfine (8.0 min).

The obtained 1-*epi*-condelfine **9** showed TLC  $R_f = 0.32$  (10% MeOH/DCM) compared to condelfine **7** where the TLC  $R_f = 0.28$  (10% MeOH/DCM). Both compounds were also analysed using an analytical InfinityLab Poroshell 120 EC-C18 (3.0 x 50 mm, 2.7  $\mu\text{m}$ ) column where condelfine **7** elutes at 5.1 min (Figure 10, upper) while 1-*epi*-condelfine **9** elutes at 5.0 min (Figure 10, lower). The reduction of 1-keto-NDA has also been reported using  $\text{NaBH}_4$ <sup>18</sup> where both epimers were isolated and 1- $\beta$ -OH-NDA was the major epimer (3:1 ratio) and that could be due to an effect from nitrogen where the delivery of the hydride complex is easier from the bottom face of the NDA skeleton. The obtained product from 1-keto-condelfine reduction was determined as 1-*epi*-condelfine **9** and the product was not a mixture of epimers.

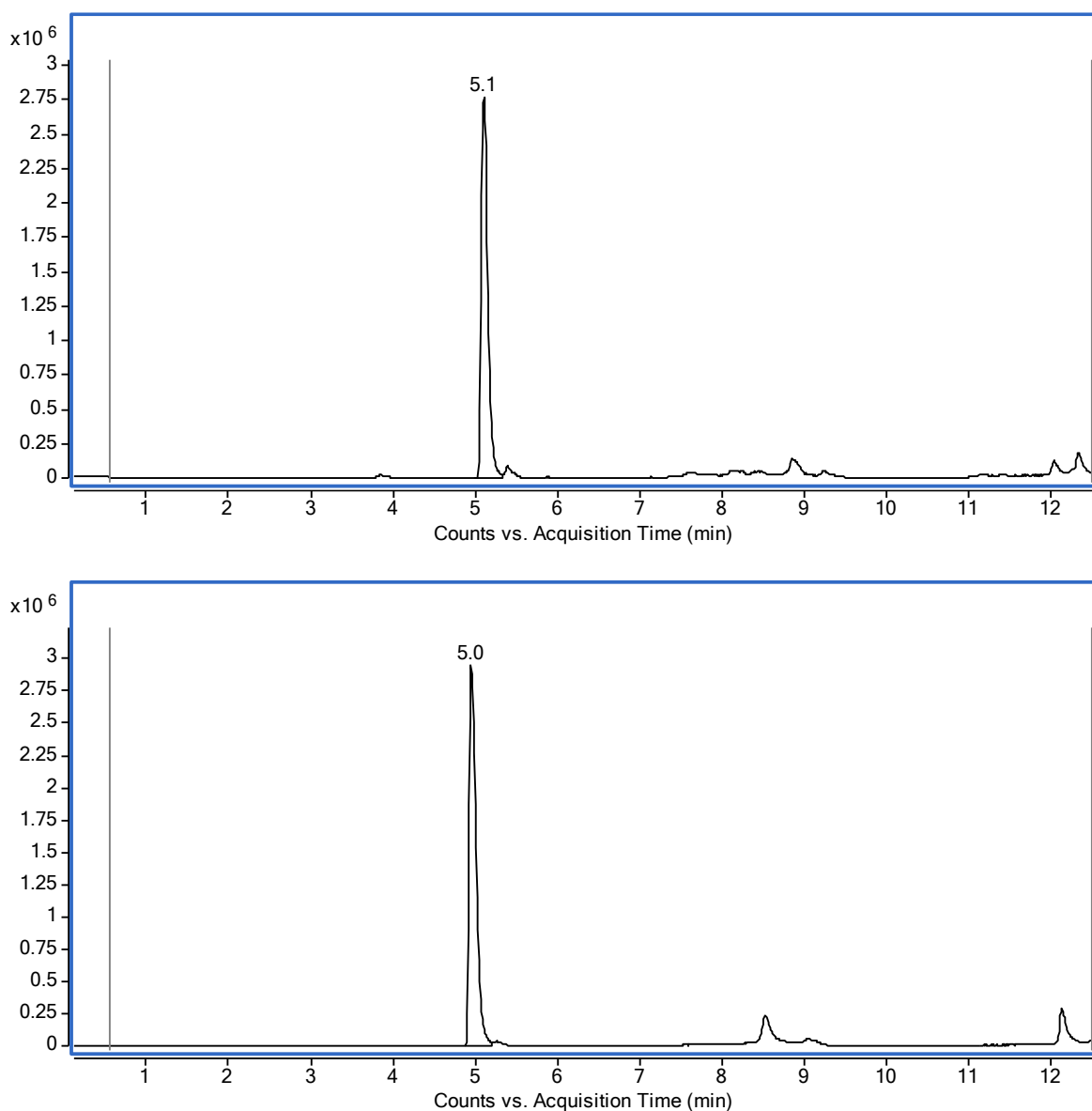


**Figure 10.** LC/MS-ESI ion chromatogram shows condelphine **7** elutes at 5.1 min (upper) and 1-*epi*-condelphine **9** elutes at 5.0 min (lower).

The conformation of ring A of condelphine **7** was studied<sup>15</sup> and it was proved to be a twisted boat conformation due to the intramolecular H-bond with the basic nitrogen atom. Upon oxidation, the hydrogen bonding no longer exists and that being observed in the APCI mass spectrum where the intensity of the fragment peak was 67% compared to 31% for condelphine **7** (Figure 11A). After reduction, 1-*epi*-condelphine **9** shows a 72% fragment ion peak (Figure 11B). This is comparable to 1-keto-condelphine which indicates that the skeleton is no longer stabilized by an intramolecular H-bond.

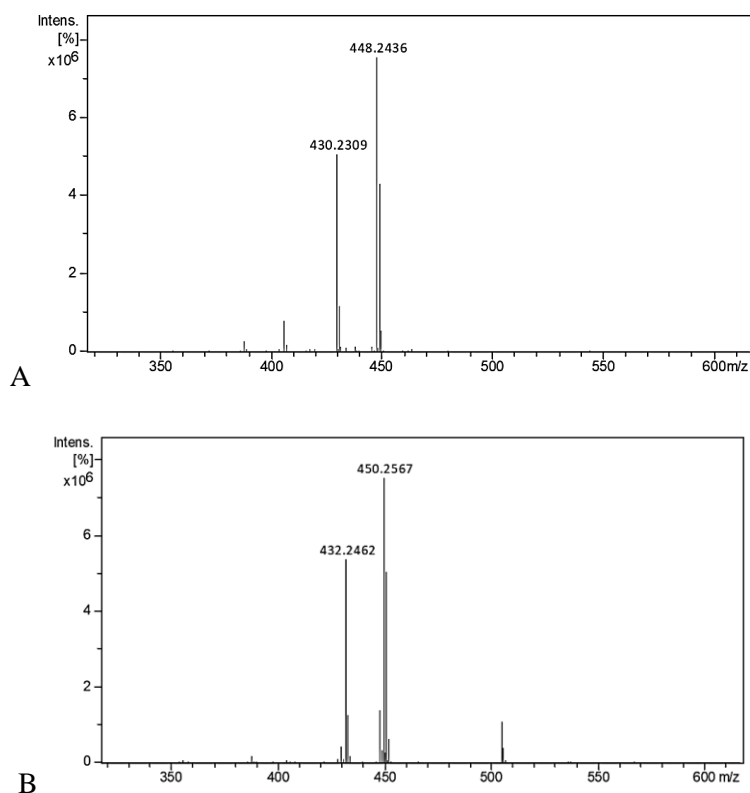


**Figure 11.** APCI mass spectra (A and B) for 1-keto-condelphine and 1-*epi*-condelphine respectively.

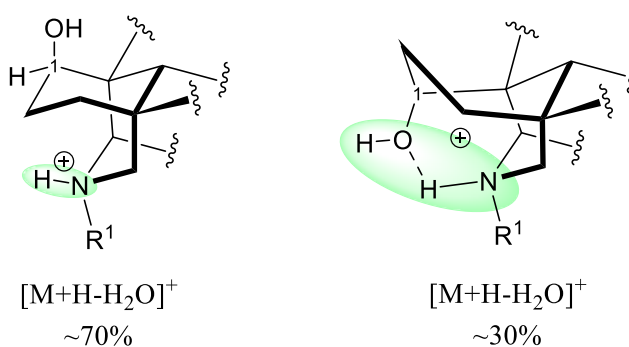


**Figure 12.** Charge delocalisation (green area) in 1- $\beta$ -OH NDA salts (left) and 1- $\alpha$ -OH NDA salts (right).

Figure 12 shows that the skeleton of 1- $\beta$ -OH NDA is not stabilized by intramolecular H-bond as the substituent at position 1 cannot form a H-bond with the nitrogen, and the positive charge is delocalised over 2 atoms compared to delocalisation over 4 atoms in 1- $\alpha$ -OH NDA and that could be the reason for the observed difference in the APCI-MS fragmentation. NMR spectra also support the change of conformation as the chemical shift of the nitrogen in condelphine **7** is



54.2 ppm while 1-*epi*-condelphine **9** has a lower chemical shift (43.8 ppm) for its nitrogen which indicates that the nitrogen in 1-*epi*-condelphine **9** is no longer H-bonded to the 1-OH. The proton at position 1 in condelphine **7** resonates at 3.73 ppm while in 1-*epi*-condelphine **9** it resonates at 4.05 ppm which indicates the change of ring A conformation where it was reported that the proton at position 1 has higher chemical shift in 1- $\beta$ -OH NDA compared to 1- $\alpha$ -OH NDA.<sup>15</sup> Carbon 1 in condelphine **7** resonates at 72.21 ppm<sup>13</sup> while it resonates at 65.00 ppm in 1-*epi*-condelphine **9** which is consistent with the <sup>13</sup>C NMR spectra literature of some NDA and their derivatives where such a decrease in the chemical shift of carbon 1 was observed when a 1- $\alpha$ -OH NDA was converted into the epimeric 1- $\beta$ -OH NDA,<sup>19,20</sup> for example, in the unusual epimerization of the 1- $\alpha$ -OH group in the NDA delphisine. Hydrolysis of delphisine in refluxing water gave 14-*O*-acetyl-1-*epi*-neoline and solvolysis of 8-*O*-acetylneoline in methanol gave 8-*O*-methyl-1-*epi*-neoline. Likewise, solvolysis of delphisine in refluxing methanol gave 8-deacetyl-8-*O*-methyl-1-*epi*-delphisine. For such an epimerization to occur, both an  $\alpha$ -1-OH and an 8-OAc functional groups are necessary.<sup>20</sup>

## CONCLUSIONS

The stability of the NDA skeleton was studied using APCI-MS where it was observed that the alpha ( $\alpha$ )-substituent at carbon 1 affects the stability of the NDA towards fragmentation. It was found that 1-OH NDA are more stable compared to 1-OMe NDA which showed higher intensity of the fragment-ion peak. That difference in stability could be due to the charge delocalisation where the positive charge delocalises in 1-OH NDA over four atoms compared to three atoms in 1-OMe NDA which decreases the chance of the proton transfer in the fragmentation scheme. In addition, the effect of carbon 1 substituent configuration was studied by the synthesis of 1-*epi*-condelphine **9** where it was found that it is less stable in the mass spectrometer compared to condelphine **7** as the nitrogen is no longer bonded to the  $\beta$ -hydroxyl at position 1. The application of APCI-MS is a promising technique to study the 3D configuration of NDA as it leads to a better understanding of their possible 3D-conformations in biological fluids.

## EXPERIMENTAL

**Materials and General Methods.** Fuziline **4**, condelphine **7**, and delsoline (belsoline) **8** were donated by Carbosynth Ltd. (U.K.). Benzoylhypaconine **1**, benzoulmesaconine **2**, benzoylaconine **3**, and neoline **6** were purchased from Carbosynth Ltd. (U.K.). Karacoline **5** was purchased from Latoxan (France). All other chemicals were purchased from Sigma-Aldrich (U.K.) and used as received. Chloroform-d (99.8% D atom, CDCl<sub>3</sub>) was used for NMR experiments purchased from Cambridge Isotope Laboratories (U.S.A.). All other solvents were of HPLC grade, ≥99.9% purity (Fisher Scientific, U.K. and VWR, U.K.).

**Instrumentation.** Analytical thin layer chromatography (TLC) was performed using aluminium backed sheets of precoated silica gel (Merck Kieselgel 60 F254). Compounds were visualized by staining with iodine vapour, and Dragendorff solution, stock solution prepared by mixing bismuth subnitrate (1.7 g) with water (80 mL) and glacial acetic acid (20 mL). Aqueous potassium iodide solution (50% w/v, 100 mL) was added then and stirred until dissolved. The solution was stored in an amber bottle. The working solution was prepared by mixing the stock solution (100 mL) with glacial acetic acid (200 mL) and made up to volume (1 L) with distilled water and stored in an amber bottle. The purification of 1-*epi*-condelphine from 1-keto-condelphine was done using Gemini 5 μm NX-C18 110 Å, LC Column 250 x 10 mm with MaXis HD quadrupole electrospray time-of-flight (ESI-QTOF) mass spectrometric detection (Bruker Daltonik GmbH, Bremen, Germany). The comparison between condelphine and 1-*epi*-condelphine was done using LC-MS analyses performed using an Agilent QTOF 6545 with Jetstream ESI spray source coupled to an Agilent 1260 Infinity II Quat pump HPLC with 1260 autosampler, column oven compartment, and variable wavelength detector (VWD). The MS was operated in positive-ion mode with the gas temperature at 250 °C, the drying gas at 12 L/min and the nebulizer gas at 45 psi (3.10 bar). The sheath gas temperature and flow were set to 350 °C and 12 L/min, respectively. The MS was calibrated using a reference calibrant introduced from the independent ESI reference sprayer. The VCap, Fragmentor, and Skimmer were set to 3500, 100, and 45 respectively. Chromatographic separation of a 5 μL sample injection was performed on a InfinityLab Poroshell 120 EC-C18 (3.0 x 50 mm, 2.7 μm) column

using H<sub>2</sub>O (Merck, LC-MS grade) with 0.1% formic acid (FA, Fluka) v/v and methanol (MeOH, VWR, HiPerSolv) with 0.1% FA v/v as mobile phases A and B, respectively. The column was operated at a flow rate of 0.3 mL/min at 40 °C starting with 1% mobile phase B for 3 min, thereafter the gradient was initiated and run for 2 min to a final 100% B, held at 100% B for 3 min then returned to 1% B, held for re-equilibration for 3.9 min, in a total run time of 12 min. The VWD was set to collect 254 and 320 nm wavelengths at 2.5 Hz. Data processing was automated in Qual B 07.00 with a Find by formula matching tolerance of 10 ppm. <sup>1</sup>H NMR spectra were recorded with a Bruker Avance III (500 MHz) spectrometer at 25 °C. Chemical shifts are given in parts per million (ppm) referenced to the CDCl<sub>3</sub> solvent or its residual CHCl<sub>3</sub> signal, and reported as chemical shift ( $\delta$ ), multiplicity (br = broad, d = doublet, dd = doublet of doublet, m = multiplet, s = singlet, t = triplet), coupling constant ( $J$  absolute values and rationalized to 1 d.p. in Hz), relative integral, and assignment. <sup>1</sup>H-<sup>15</sup>N HMBC spectra were recorded on a Bruker Avance III (<sup>15</sup>N Larmor precession frequency 50.67 MHz) spectrometer at 25 °C. The spectra were externally calibrated with a MeNO<sub>2</sub> solution (50% in CDCl<sub>3</sub>, v/v), recorded and set at  $\delta_N$  379.8 ppm, and the correction factor was measured as -511.72 on our spectrometer. High Resolution Time-of-Flight (HR TOF) mass spectra were obtained on a Bruker Daltonics “microTOF” mass spectrometer using electrospray ionisation (ESI) (loop injection +ve ion mode).

**APCI-MS conditions.** Accurate mass spectrometry analyses were conducted using a MaXis HD quadrupole electrospray time-of-flight (APCI-QTOF) mass spectrometer (Bruker Daltonik GmbH, Bremen, Germany), using a glass syringe (Hamilton) and syringe pump (KD Scientific, Model 781100) for infusions at a flow rate of 3  $\mu$ L/min. Analyses were performed in APCI positive-ion mode with the capillary voltage set to 4500 V, corona discharge 4000 V, nebulizing gas at 0.4 bar, APCI temperature was set at 280 °C and drying gas temperature at 240 °C. The TOF scan range was from 50–1000 mass-to-charge ratio ( $m/z$ ). The MS instrument was calibrated using an APCI tuning solution (Sigma Aldrich, U.K.). All samples were prepared in isopropanol at 20  $\mu$ g/mL. Data processing was performed using the Compass Data Analysis software version 4.3 (Bruker Daltonik GmbH, Bremen, Germany).

**Synthesis of 1-*epi*-condelphine 9.** Condelphine **7** ( $R_f = 0.28$  in 10% MeOH/DCM) (0.0134 mmol, 6 mg) was dissolved in anhydrous dichloromethane (10 mL) under anhydrous  $N_2$  gas, and Dess-Martin periodinane (4 equiv., 0.0535 mmol, 22.7 mg) was added. The reaction mixture was stirred at 20 °C for 24 h and then concentrated under vacuum and the product, 1-keto-condelphine, was used in the next step without purification. The crude 1-keto-condelphine ( $R_f = 0.35$  in 10% MeOH/DCM) was reduced using sodium borohydride (0.013 mmol, 0.5 mg) in anhydrous methanol (5 mL) at 20 °C for 24 h. The mixture was then concentrated under vacuum and purified using HPLC to obtain the title compound **9** (2 mg, 33%) as a pale yellow oil.  $R_f = 0.32$  (10% MeOH in dichloromethane). HRMS (ESI):  $m/z$  calcd. for  $C_{25}H_{40}NO_6$ : 450.2856, found: 450.2836  $[M+H]^+$ .  $^1H$  NMR (500 MHz,  $CDCl_3$ ):  $\delta$  (ppm) (including) = 1.13 (br t, 3H,  $NCH_2CH_3$ ), 2.06 (s, 3H,  $COCH_3$ ), 2.06-2.13 (m, 1H,  $H_{19ax}$ ), 2.30-2.35 (m, 1H,  $H_{19eq}$ ), 2.43-2.57 (m, 2H,  $NCH_2CH_3$ ), 2.64 (dd,  $J = 7.9, 4.8$ , 1H, H13), 2.76 (br s, 1H, H17), 3.01 (d,  $J = 8.8$ , 1H, H18A), 3.15 (d,  $J = 8.8$ , 1H, H18B), 3.27 (s, 3H, 16- $OCH_3$ ), 3.28-3.31 (m, 1H, H16), 3.32 (s, 3H, 18- $OCH_3$ ), 4.05 (t,  $J = 7.0$ , 1H, H1), 4.87 (t,  $J = 4.9$ , 1H, H14).  $^{13}C$  NMR (125 MHz,  $CDCl_3$ ):  $\delta$  (ppm) (including) = 13.3 ( $NCH_2CH_3$ ), 21.1 ( $COCH_3$ ), 36.4 (C13), 48.1 ( $NCH_2CH_3$ ), 56.0 (16- $OCH_3$ ), 56.5 (C19), 59.5 (18- $OCH_3$ ), 63.5 (C17), 65.0 (C1), 76.9 (C14), 78.9 (C18), 82.0 (C16).

## REFERENCES

- (1) Hayes, R. N.; Gross, M. L. [10] Collision-induced dissociation. *Methods in Enzymology* **1990**, *193* (1968), 237–263. [https://doi.org/10.1016/0076-6879\(90\)93418-K](https://doi.org/10.1016/0076-6879(90)93418-K).
- (2) Fetterolf, D. D.; Yost, R. A. Energy-resolved collision-induced dissociation in tandem mass spectrometry. *Int. J. Mass Spectrom. and Ion Physics* **1982**, *44*(1–2), 37–50. [https://doi.org/10.1016/0020-7381\(82\)80037-5](https://doi.org/10.1016/0020-7381(82)80037-5).
- (3) Laprévotte, O.; Serani, L.; Das, B. C. Stereochemistry of electrosprayed ions. 14-Dehydro- and 16-*epi*-14-dehydrovincamine. *J. Mass Spectrom.* **1997**, *32*(3), 339–340. [https://doi.org/10.1002/\(sici\)1096-9888\(199703\)32:3<339::aid-jms498>3.3.co;2-l](https://doi.org/10.1002/(sici)1096-9888(199703)32:3<339::aid-jms498>3.3.co;2-l).
- (4) Laprévotte, O.; Ducrot, P.; Thal, C.; Serani, L.; Das, B. C. Stereochemistry of electrosprayed

- ions. Indoloquinolizidine derivatives. *J. Mass Spectrom.* **1996**, *31*(10), 1149–1155.  
[https://doi.org/10.1002/\(SICI\)1096-9888\(199610\)31:10<1149::AID-JMS408>3.0.CO;2-I](https://doi.org/10.1002/(SICI)1096-9888(199610)31:10<1149::AID-JMS408>3.0.CO;2-I).
- (5) Wu, Z.-J.; Sun, D.-M.; Fang, D.-M.; Chen, J.-Z.; Cheng, P.; Zhang, G.-L. Analysis of matrine-type alkaloids using ESI-QTOF. *Int. J. Mass Spectrom.* **2013**, *341–342*, 28–33.  
<https://doi.org/10.1016/j.ijms.2013.03.002>.
- (6) Czira, G.; Tamás, J.; Kalaus, G. Effects of stereoisomerism on the electron impact fragmentation of some compounds with an eburnane skeleton. *Org. Mass Spectrom.* **1984**, *19*(11), 555–562. <https://doi.org/10.1002/oms.1210191106>.
- (7) Yunusov, M. S. Diterpenoid alkaloids. *Natural Product Rep.* **1991**, *8*(5), 499–526.
- (8) Wang, F. P.; Chen, Q. H. *The C19-diterpenoid alkaloids. The Alkaloids. Chemistry and Biology*, **2010**, *69* (10). Elsevier. [https://doi.org/10.1016/S1099-4831\(10\)69001-3](https://doi.org/10.1016/S1099-4831(10)69001-3).
- (9) Wada, K.; Mori, T.; Kawahara, N. Application of liquid chromatography-atmospheric pressure chemical ionization mass spectrometry to the differentiation of stereoisomeric diterpenoid alkaloids. *Chem. Pharm. Bull.* **2000**, *48*(7), 1065–1074.  
<https://doi.org/10.1248/cpb.48.1065>.
- (10) Wada, K.; Mori, T.; Kawahara, N. Stereochemistry of norditerpenoid alkaloids by liquid chromatography/atmospheric pressure chemical ionization mass spectrometry. *J. Mass Spectrom.* **2000**, *35*(3), 432–439. [https://doi.org/10.1002/\(SICI\)1096-9888\(200003\)35:3<432::AID-JMS954>3.0.CO;2-6](https://doi.org/10.1002/(SICI)1096-9888(200003)35:3<432::AID-JMS954>3.0.CO;2-6).
- (11) Wada, K.; Mori, T.; Kawahara, N. Application of liquid chromatography-atmospheric pressure chemical ionization mass spectrometry to the differentiation of stereoisomeric C-19-norditerpenoid alkaloids. *Chem. Pharm. Bull.* **2000**, *48*(5), 660–668.
- (12) Tarr, M. A.; Zhu, J.; Cole, R. B. Atmospheric Pressure Ionization Mass Spectrometry. *Encyclopedia of Analytical Chemistry*. Chichester, UK: John Wiley & Sons, Ltd, **2006**, pp. 1–34. <https://doi.org/10.1002/9780470027318.a6003>.
- (13) Commisso, M.; Anesi, A.; Dal Santo, S.; Guzzo, F. Performance comparison of electrospray ionization and atmospheric pressure chemical ionization in untargeted and targeted liquid chromatography/mass spectrometry based metabolomics analysis of grapeberry metabolites. *Rapid Commun. Mass Spectrom.* **2017**, *31*(3), 292–300.

<https://doi.org/10.1002/rcm.7789>.

(14) Clench, M. R.; Tetler, L. W. Chromatography: Liquid Detectors: Mass Spectrometry. *Encyclopedia of Separation Science*. Elsevier, **2000**, pp. 616–622. <https://doi.org/10.1016/B0-12-226770-2/00271-4>.

(15) Zeng, Z.; Qasem, A. M. A.; Kociok-Köhn, G.; Rowan, M. G.; Blagbrough, I. S. The 1 $\alpha$ -hydroxy-A-rings of norditerpenoid alkaloids are twisted-boat conformers. *RSC Advances* **2020**, *10*(32), 18797–18805. <https://doi.org/10.1039/D0RA03811C>.

(16) Zeng, Z.; Qasem, A. M. A.; Woodman, T. J.; Rowan, M. G.; Blagbrough, I. S. Impacts of steric compression, protonation, and intramolecular hydrogen bonding on the <sup>15</sup>N NMR spectroscopy of norditerpenoid alkaloids and their piperidine-ring analogues. *ACS Omega* **2020**, *5*(23), 14116–14122. <https://doi.org/10.1021/acsomega.0c01648>.

(17) Qasem, A. M. A.; Zeng, Z.; Rowan, M. G.; Blagbrough, I. S. Norditerpenoid alkaloids from *Aconitum* and *Delphinium*: Structural relevance in medicine, toxicology, and metabolism. *Natural Product Rep.* **2022**, *39*, 460-473. doi 10.1039/D1NP00029B (Highlight).

(18) Pelletier, S. W.; Djarmati, Z.; Lajsic, S.; De Camp, W. H. Alkaloids of *Delphinium staphisagria*. The structure and stereochemistry of delphisine, neoline, chasmanine, and homochasmanine. *J. Am. Chem. Soc.* **1976**, *98*(9), 2617–2625. <https://doi.org/10.1021/ja00425a035>.

(19) Pelletier, S. W.; Mody, N. V.; Sawhney, R. S. <sup>13</sup>C nuclear magnetic resonance spectra of some C 19-diterpenoid alkaloids and their derivatives. *Can. J. Chem.* **1979**, *57*(13), 1652–1655. <https://doi.org/10.1139/v79-266>.

(20) Pelletier, S. W.; Desai, H. K.; Jiang, Q.; Ross, S. A. An unusual epimerization of the  $\alpha$ -OH-1 group of the norditerpenoid alkaloid delphisine. *Phytochemistry* **1990**, *29*(11), 3649-3652.

## Chapter 8

### Synthesis and antagonist activity of methyllycaconitine analogues on human $\alpha 7$ nicotinic acetylcholine receptors

**AIM:** The aim of this study was to synthesize AE-bicyclic analogues of MLA **1** with different nitrogen and ester side-chains to get a better SAR understanding of their activity at human  $\alpha 7$  nAChRs.

<b>This declaration concerns the article entitled:</b>			
Synthesis and Antagonist Activity of Methyllycaconitine Analogues on Human $\alpha 7$ Nicotinic Acetylcholine Receptors			
<b>Publication status (tick one)</b>			
<b>Draft manuscript</b>	<input type="checkbox"/>	<b>Submitted</b>	<input type="checkbox"/>
<b>In review</b>	<input type="checkbox"/>	<b>Accepted</b>	<input type="checkbox"/>
<b>Published</b>	<input checked="" type="checkbox"/>		
<b>Publication details (reference)</b>	Qasem, A. M. A., Rowan, M. G., Sanders, V. R., Millar, N. S., Blagbrough, I. S., 2022. Synthesis and Antagonist Activity of Methyllycaconitine Analogues on Human $\alpha 7$ Nicotinic Acetylcholine Receptors. <i>ACS Bio Med Chem Au ASAP</i> .		
<b>Copyright status (tick the appropriate statement)</b>			
The material has been published with a CC-BY license		<input checked="" type="checkbox"/>	The publisher has granted permission to replicate the material included here
<b>Candidate's contribution to the paper (provide details, and also indicate as a percentage)</b>		<p><b>Formulation of ideas:</b> The candidate contributed to the formulation of the article ideas (60%)</p> <p><b>Design of methodology:</b> The candidate contributed to design the synthesized analogues (70%)</p> <p><b>Experimental work:</b> The candidate contributed to the synthesis and analysis of the synthesized analogues (60%).</p> <p><b>Presentation of data in journal format:</b> The candidate contributed to the paper writing and figures presentation (60%)</p>	
<b>Statement from Candidate</b>	This paper reports on original research I conducted during the period of my Higher Degree by Research candidature.		
<b>Signed (typed signature)</b>	Ashraf Qasem	<b>Date</b>	21/09/2022

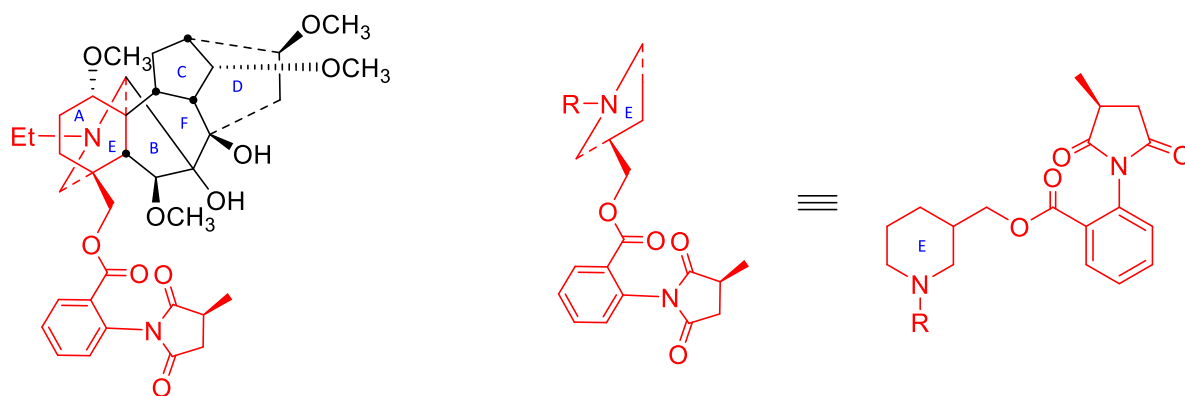
## INTRODUCTION

Nicotinic acetylcholine receptors (nAChRs) are members of a superfamily of ligand-gated ion channels and are receptors for the neurotransmitter acetylcholine (ACh). They are oligomeric proteins in which five transmembrane subunits co-assemble to form a central cation-selective pore. Agonists, such as ACh, bind to a site on the extracellular region of nAChRs and, in doing so, cause a conformational change in the receptor that results in the opening of the transmembrane ion channel and the influx of cations.<sup>1,2</sup> Nicotinic receptors are located at post-synaptic sites (for example on nerve and muscle cells), where they can mediate rapid neuronal or neuromuscular signalling, but they are also located at pre-synaptic sites (for example in the brain), where they can play a more modulatory role. Sixteen nAChR subunits are expressed in humans ( $\alpha 1$ - $\alpha 7$ ,  $\alpha 9$ ,  $\alpha 10$ ,  $\beta 1$ - $\beta 4$ ,  $\gamma$ ,  $\delta$  and  $\epsilon$ ) and these can co-assemble into a diverse array of both homomeric and heteromeric nAChR subtypes with distinct physiological and pharmacological properties.<sup>3</sup> One nAChR subtype that has attracted particular attention is the  $\alpha 7$  nAChR, a homomeric receptor containing five copies of the  $\alpha 7$  subunit. It is expressed in several regions of the brain and has been implicated in a range of neurological disorders.<sup>4</sup>

Signalling through nAChRs can be blocked by the binding of antagonists acting either at the orthosteric agonist binding site (competitive antagonists) or at distinct allosteric sites (non-competitive antagonists).<sup>5</sup> Methyllycaconitine (MLA) **1** is one example of a nAChR competitive antagonist that is highly potent and highly selective for  $\alpha 7$  nAChRs.<sup>6</sup> It forms part of a broader family of norditerpenoid alkaloids (NDA) from *Delphinium* and *Aconitum*, that are highly oxygenated hexacyclic systems and which can exert a variety of pharmacological effects by modulating transmembrane proteins such as nAChRs and voltage gated sodium channels (VGSCs).<sup>7,8</sup> In addition, the potential therapeutic use of MLA **1** has been examined in connection with disorders such as cerebral palsy and Parkinson's disease.<sup>8</sup> MLA **1** and other *Delphinium* alkaloids are also responsible for livestock intoxication<sup>9</sup> due to their action on  $\alpha 1$  nAChRs expressed at neuromuscular junctions.<sup>10</sup> However, it has been reported previously that MLA **1** has higher affinity for  $\alpha 7$  nAChRs compared to other nAChR subtypes.<sup>6,11,12</sup>



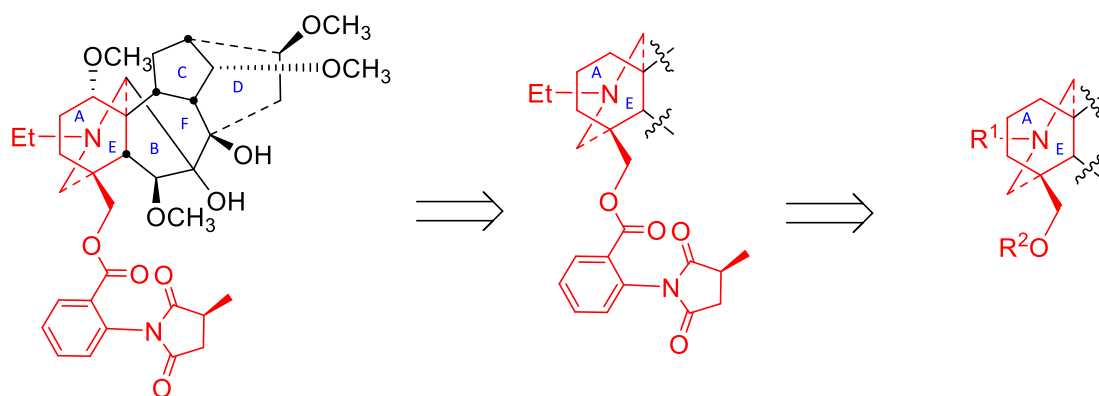
Several structural features of MLA **1** have been studied in our ongoing structure-activity relationship (SAR) studies. For example, it was found that the nitrogen atom plays a key role in the pharmacological action of NDA.<sup>13</sup> Also, the ester side-chain is an important moiety as MLA **1** lost 1000-fold of its activity when converted to neopentyl alcohol lycocotinine.<sup>14-16</sup> Furthermore, the side-chain on the nitrogen atom affects the interaction with the target nAChR. Several piperidine (Ring E) analogues of MLA have been synthesized (Figure 1) with different N-side chains (methyl, ethyl, n-butyl, 2-phenylethyl, 3-phenylpropyl, diethyl ether, and 2-phenylethyl ether) and tested on bovine adrenal  $\alpha 3\beta 4$  nAChRs, where the best analogue had a 3-phenylpropyl N-side-chain.<sup>17</sup> This analogue system was tested on the  $\alpha 7$  nAChR in a competition binding experiment on rat brain preparations using [<sup>125</sup>I] $\alpha$ BGT, where the best analogue (3-phenylpropyl N-side-chain) showed little inhibition with an  $IC_{50} = 177 \mu M$  while other analogues showed no inhibition with  $IC_{50} > 300 \mu M$ .<sup>18</sup>



Methyllycaconitine **1**

**Figure 1.** E-ring analogues system of MLA **1**

The aim of this study was to synthesize AE-bicyclic analogues of MLA **1** with different nitrogen and ester side-chains (Scheme 1) and to examine their ability to modulate the activity of human  $\alpha 7$  nAChRs, with the aim of obtaining a better SAR understanding of these compounds.



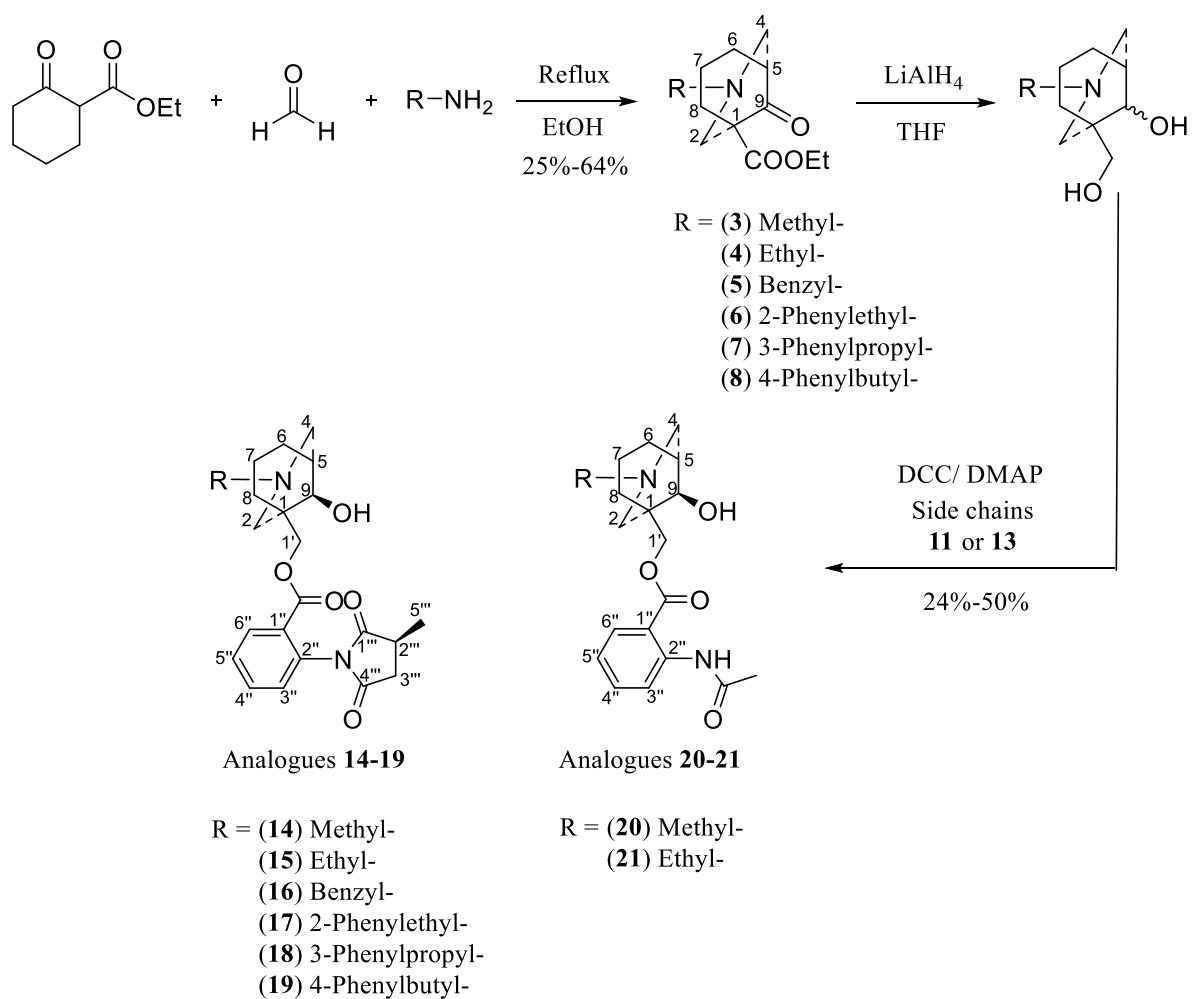
Methyllycaconitine **1**

**Scheme 1.** Relationship of MLA **1** to the target AE-bicyclic system

## RESULTS and DISCUSSION

### 1. Synthesis of the AE-bicyclic core

The synthesis of MLA analogues starts with the core synthesis using the classical double Mannich reaction<sup>18,19</sup> where different amines were used to obtain different N-side chains. The side-chains (methyl, ethyl, benzyl, 2-phenylethyl, 3-phenylpropyl, and 4-phenylbutyl) (Scheme 2) were selected to investigate the importance of the hydrophobic interactions. The reaction was accomplished by heating the reactants under reflux in ethanol for 4 h. As the boiling point of methylamine solution (40 wt % in water) is 48 °C, the synthesis of compound **3** was also achieved at 20 °C for 2 d with no significant drop in yield.



**Scheme 2.** Synthesis of AE-bicyclic analogues **14-21**.

## 2. Reduction of the AE-bicyclic core using LiAlH<sub>4</sub> (LAH)

The reduction of the AE-bicyclic compounds **3-8** was performed using LAH in anhydrous THF under N<sub>2</sub> gas (Scheme 2), and the reaction was monitored by TLC and quenched after 7 h using the Fieser method, where X mL (X = grams of LAH) of water were added slowly followed by X mL of 15% aq. sodium hydroxide solution and then 3X mL of water. The resulting mixture was stirred with magnesium sulfate for 10 min and then filtered over celite and evaporated to dryness. The reduction results in epimeric secondary alcohol at position 9. As an example, cyclohexanone **4** was reduced to get both epimers at position 9. The <sup>1</sup>H NMR methyl triplet signals of the NCH<sub>2</sub>CH<sub>3</sub> showed that the ratio of the isomers is 3:1 (Figure 2). The <sup>1</sup>H NMR spectrum also shows the difference in the intensity of 9-H signals in both epimers (3.60 ppm vs

3.68 ppm) (Figure 2). The full  $^1\text{H}$  and  $^{13}\text{C}$  NMR spectra also showed different intensities of signals for the 3:1 isomeric ratio (SI Figure S1).

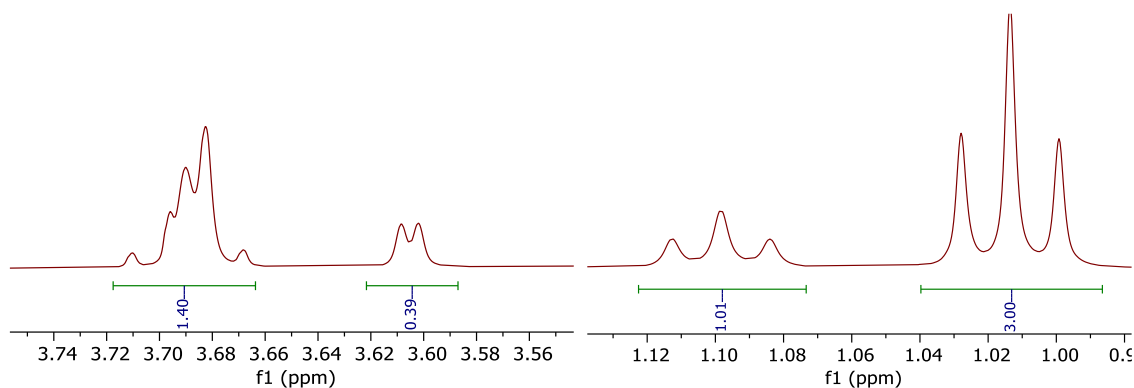


**Figure 2.** The  $^1\text{H}$  NMR (500 MHz) of 9-H proton (left) and the methyl of  $\text{NCH}_2\text{CH}_3$  (right) of the epimeric mixture after reduction of cyclohexanone **4**

The mixture was purified using column chromatography to obtain the major isomer, diol **9**. The  $\beta$ -alcohol was established by NOESY as the proton at position 9 showed a correlation with protons 2ax and 4ax (Figure 3). The methylene protons ( $\text{CH}_2\text{OH}$ ) resonate as two adjacent doublets (3.35 and 3.39 ppm) while they showed as a multiplet in the epimeric mixture (Figure 2). The compounds **3** and **5-8** were reduced and used in the esterification step without purification.

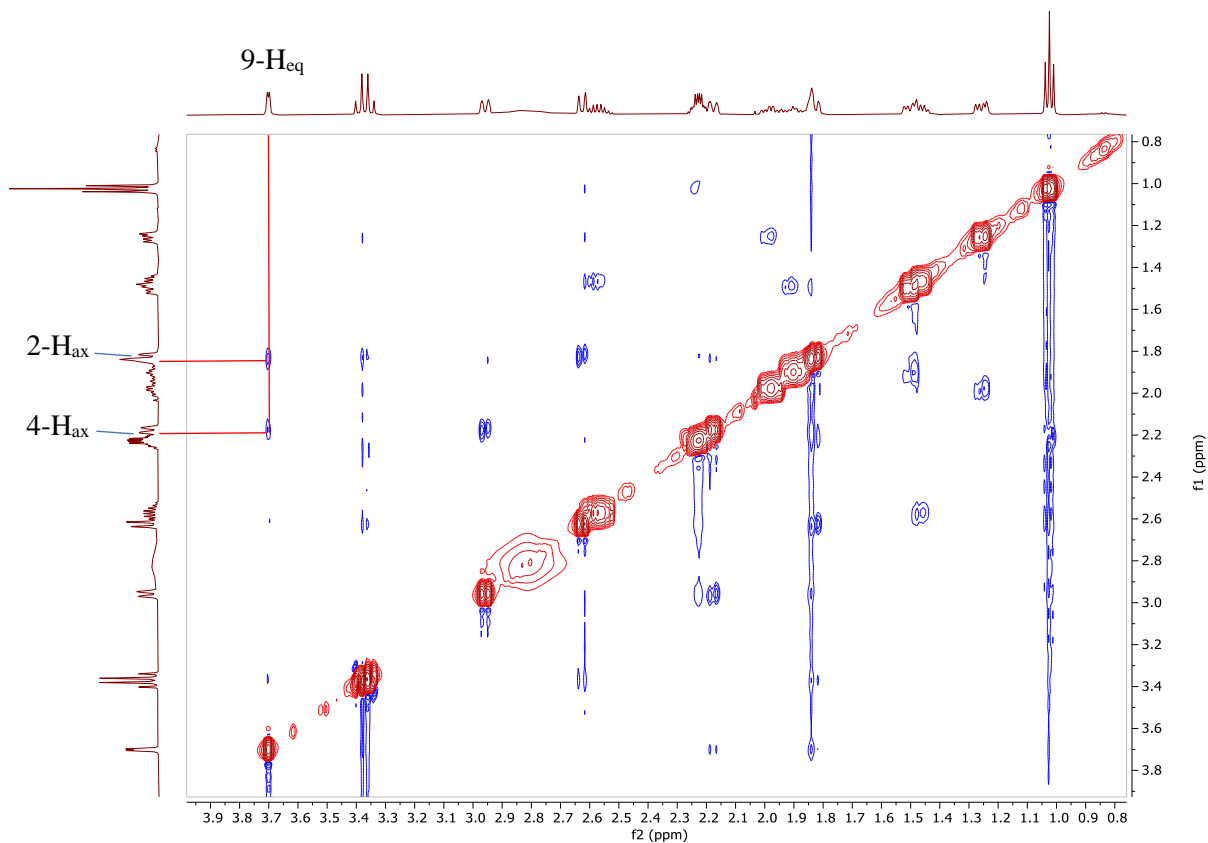
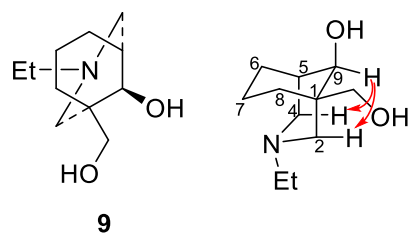


**Figure 3.** NOESY correlation between 9- $H_{eq}$  and 2- $H_{ax}$ , 4- $H_{ax}$  in diol **9**.

### 3. Synthesis of the carboxylic acids side-chains

MLA **1** is a potent nAChR antagonist. Lappaconitine **10** is the most clinically successful NDA where its hydrobromide salt (Allapinin<sup>®</sup>) is used as antiarrhythmic drug.<sup>8</sup> Therefore, their side-chains (Figure 4) were chosen to be attached to the analogues.

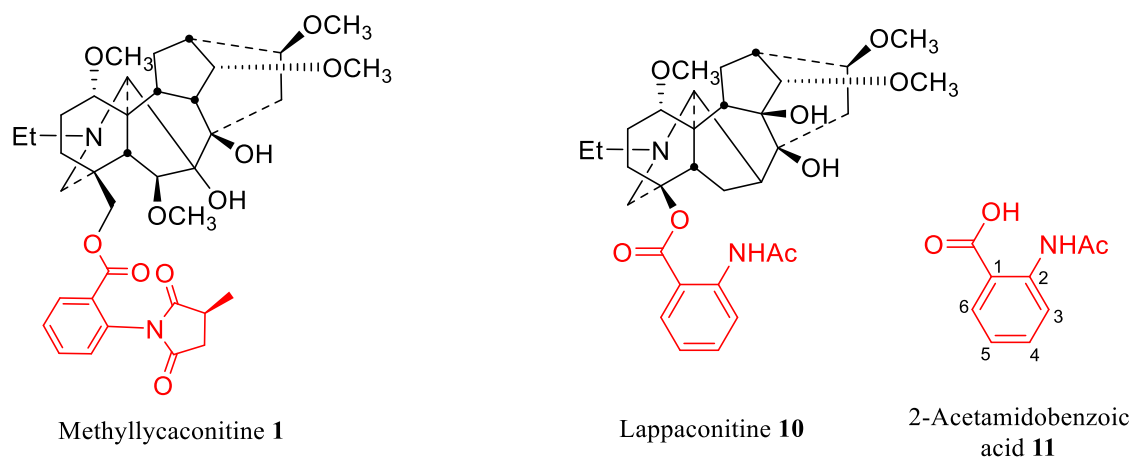


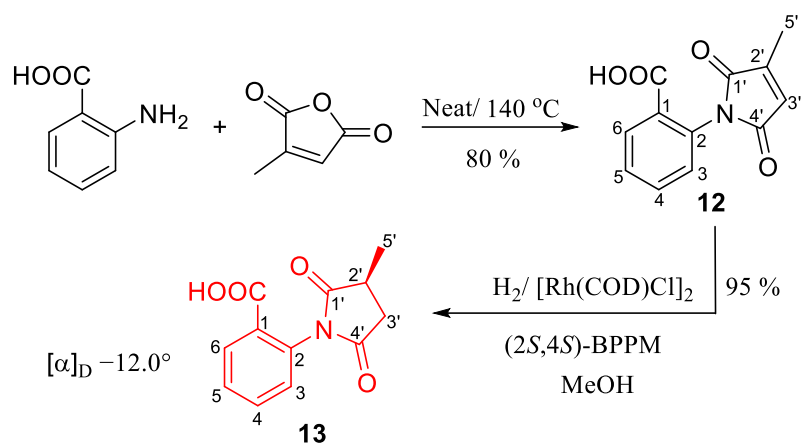
**Figure 4.** Side-chains (red) of methyllycaconitine **1** and lappaconitine **10**

### 3.1. Synthesis of lappaconitine side-chain

The synthesis of 2-acetamidobenzoic acid **11** was accomplished through refluxing anthranilic acid and acetic anhydride in anhydrous tetrahydrofuran under nitrogen gas for 4 h. The reaction was quenched using 1 M aq. HCl and the product was recrystallized from water and ethanol (1:1).

### 3.2. Synthesis of methyllycaconitine side-chain

The first step of MLA **1** side-chain synthesis was performed by neat fusion of anthranilic acid and citraconic anhydride at 140 °C under nitrogen gas for 24 h (Scheme 3).<sup>19-21</sup> Chiral hydrogenation of **12** to get the *S*-enantiomer was tried with (*S*)-ruthenium diacetate (2,2'-bis(diphenylphosphino)-1,1'-binaphthyl) (*S*-Ru(OAc)<sub>2</sub>BINAP) without success. Then it was performed using (2*S*,4*S*)-1-Boc-4-diphenylphosphino-2-(diphenylphosphinomethyl)pyrrolidine (BPPM) coupled with rhodium cyclooctadiene chloride dimer (Rh(COD)Cl)<sub>2</sub>.<sup>22-24</sup> The optical rotation was (-12.0°), consistent with the literature value.<sup>25</sup>



**Scheme 3.** Synthesis of MLA side-chain

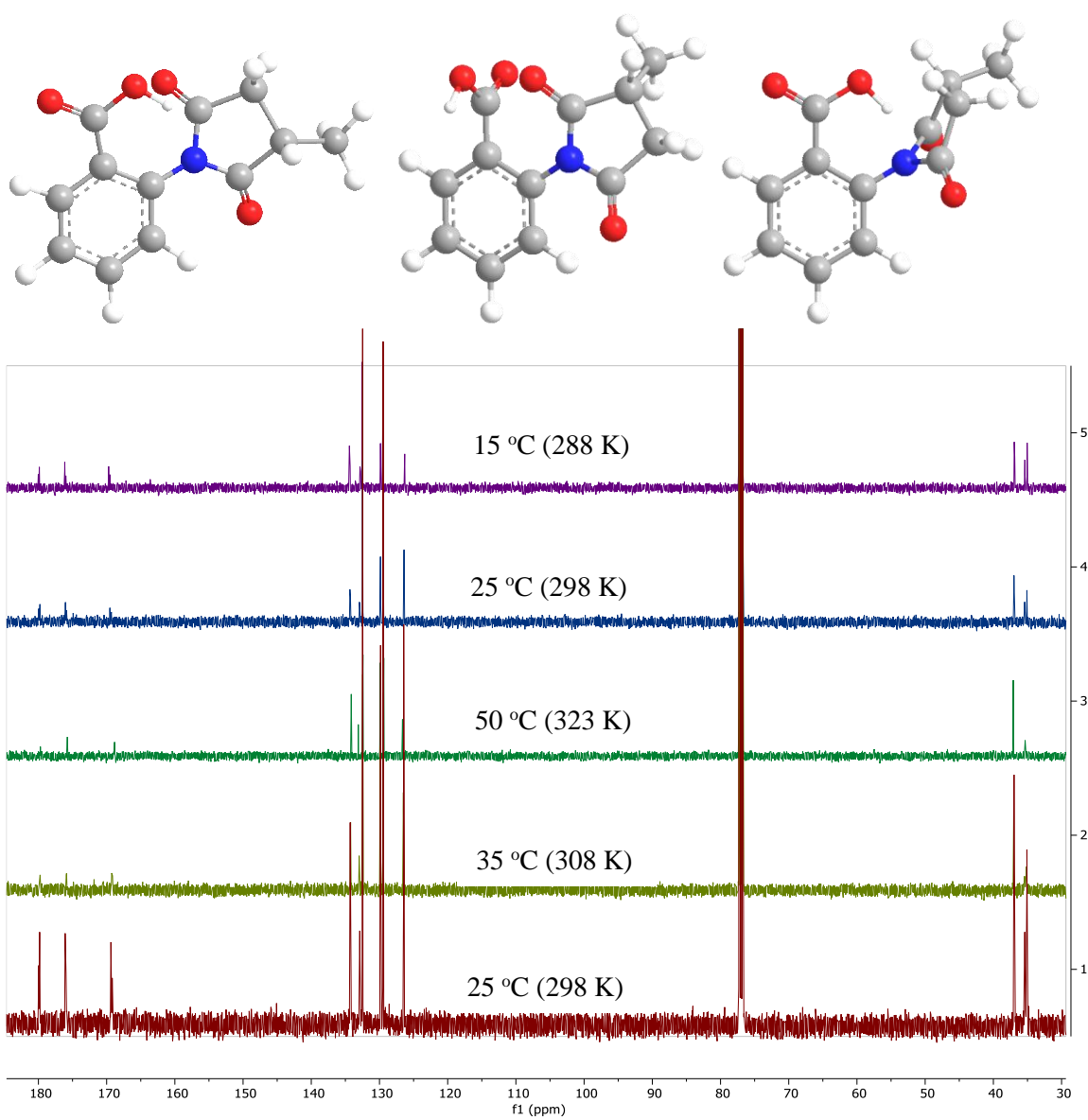


**Figure 5.**  $^{13}\text{C}$  NMR (125 MHz) in  $\text{CDCl}_3$  of **13** at various temperatures.

The  $^{13}\text{C}$  NMR of **13** showed doubling phenomena at 25 °C when measured in  $\text{CDCl}_3$  and that could be due to an intramolecular interaction that hindered the free rotation of the methyl succinimide group. Variable temperature (VT) NMR experiments were performed, and the doubling phenomena disappeared on increasing the temperature to 55 °C where the molecule has more energy to rotate freely, and then re-appeared upon cooling down to 25 °C and 15 °C (Figure 5). To explain the hindrance that results in the NMR doubling, the 3D models in Figure 5 show the clash happens between the carboxylic acid and the methylsuccinimide moiety. NMR of **13** was also measured in  $\text{CD}_3\text{OD}$  to check if the doubling happens due to intramolecular H-bonding or steric clash.  $^{13}\text{C}$  NMR spectra in  $\text{CD}_3\text{OD}$  again showed doubling of the signals (SI Figure S2) consistent with steric hindrance in methylsuccinimido anthranilate **13**.

#### 4. Synthesis of the analogues by esterification

The reduced AE-bicycles were esterified with the naturally occurring NDA side-chains (**11** and **13**) using *N,N'*-dicyclohexyl-carbodiimide (DCC) and 4-dimethylaminopyridine (DMAP) in anhydrous acetonitrile at 40 °C under anhydrous nitrogen gas (Scheme 2). The reaction was monitored and stopped after 24 h and the crude material was purified to homogeneity to yield analogues **14-21**.

The stereochemistry of the hydroxy group at position 9 was determined to be axial by NOESY spectrum as the 9- $\text{H}_{\text{eq}}$  showed correlation with 2- $\text{H}_{\text{ax}}$  and 4- $\text{H}_{\text{ax}}$ . Analogues **14** and **21** were taken as examples and SI Figure S3 shows the NOE correlations in both of them.

The NMR spectra of the analogues were similar, the only major difference observed was for the protons at carbon 1' which showed the roofing effect in analogues **20** and **21** with the 2-acetamido-benzoic acid side-chain where this could be caused by a steric hindrance effect from the side chain. They merge into one multiplet signal in analogues **14-19** with the 2-methylsuccinimidobenzoic acid side-chain. SI Figure S4 shows the  $^1\text{H}$  NMR signal at position 1' in analogues **14-15** and **20-21**.



As we have reported with some naturally occurring NDA,<sup>26</sup> these simple analogues show the effect of steric compression on the axial proton of position 7. The equatorial protons resonate usually at a higher frequency due to the anisotropic effect of the C-C bond.<sup>27</sup> In these bicyclic compounds, the axial proton at position 7 is further downfield due to the interaction with the nitrogen lone pair of electrons. The chemical shift difference that was observed in the bicyclic compounds **3-9** and **14-21** is ~1-1.5 ppm. The axial protons at position 6 and 8 also resonate at a higher chemical shift, which is probably due to 1-3 interactions through space with substituents at positions 1 and 9.<sup>28</sup>

#### 5. Antagonist activity of MLA analogues on human $\alpha 7$ nAChRs

The antagonistic activity of MLA **1** and the analogues **14-21** has been tested on human  $\alpha 7$  nAChRs heterologously expressed in *Xenopus* oocytes. The level of antagonism was measured by the co-application of the analogues [1 nM] with an EC<sub>50</sub> concentration ACh [100  $\mu$ M], after a pre-application of the analogues for 2 min. Responses to ACh in the presence of MLA analogues were normalised to responses to an EC<sub>50</sub> concentration of ACh [100  $\mu$ M] applied in the absence of analogues (Figure 6). MLA **1** inhibited the receptor response to  $3.4 \pm 0.2$  % (n = 4) of normalised responses. In addition, all of the analogues exhibited antagonist effects at human  $\alpha 7$  nAChRs, resulting in significantly reduced agonist responses ( $P < 0.0001$ ; Figure 6). Compounds **16**, **19**, and **17** showed the highest levels of antagonism, agonist responses to  $53.2 \pm 1.9$  % (n = 3),  $56.7 \pm 2.5$  % (n = 3), and  $64.3 \pm 2.2$  % (n = 3) of normalised responses, respectively (Figure 6).

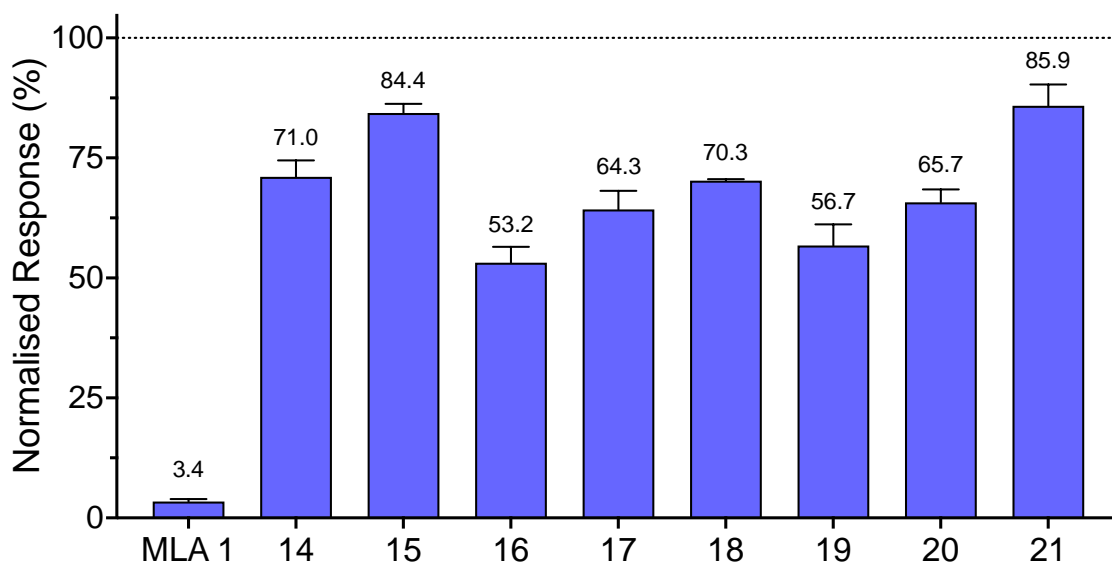


**Figure 6.** Normalized agonist (ACh) response of  $\alpha 7$  nAChRs in the presence of MLA or analogues **14-21**. Data were generated from cloned human  $\alpha 7$  nAChRs expressed in *Xenopus oocytes*. Data are means  $\pm$  SEM of at least three independent experiments.

The antagonist activity of these analogues showed little advantage of the (*S*)-2-methylsuccinimido benzoate ester side chain especially when comparing analogue **14** with **20**. The data of analogues **14-19** highlights the effect of the N-side-chain on the antagonist activity at human  $\alpha 7$  nAChR where the activity is in the following order: benzyl > 4-phenylbutyl > 2-phenylethyl > 3-phenylpropyl > methyl > ethyl (Figure 7). These data indicate that a bulkier N-side-chain (with phenyl moiety) enhances the activity compared to alkane side-chains. The E-ring analogue system developed by Bergmeier, McKay and co-workers<sup>17,18,29,30,31</sup> was tested on bovine adrenal  $\alpha 3\beta 4$  nAChRs and showed that the best analogue, 3-phenylpropyl N-side-chain, inhibits the nicotine-stimulated catecholamine secretion [50  $\mu$ M] by around 86%<sup>17</sup> with an  $IC_{50}$  11.4  $\mu$ M<sup>18</sup> compared to 95% inhibition of the nicotine-stimulated catecholamine secretion [50  $\mu$ M]<sup>17</sup> with an  $IC_{50}$  2.6  $\mu$ M<sup>18</sup> for MLA **1**. In addition, this analogue system was tested on  $\alpha 7$  nAChRs in a competition binding experiment on rat brain preparations using [<sup>125</sup>I] $\alpha$ BGT where the best analogue (3-phenylpropyl N-side-chain) showed only a little inhibition with an  $IC_{50}$  177  $\mu$ M compared to 0.01  $\mu$ M for MLA **1**.<sup>18</sup> The AE-bicyclic analogues showed better activity

compared to the reported one (E) ring system where at the best analogue **16**, benzyl N-side-chain, inhibits the agonist response at human  $\alpha 7$  nAChR to around 53% [1 nM].

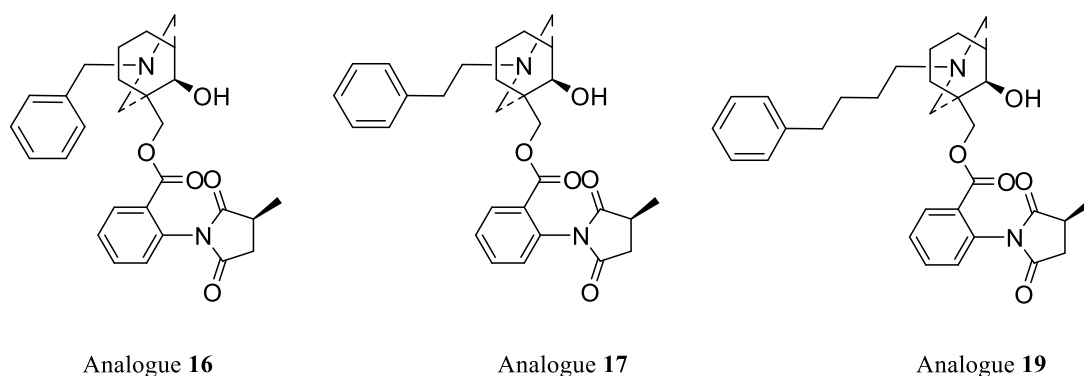


**Figure 7.** The three most active analogues, **16**, **17**, and **19**.

## CONCLUSIONS

Several MLA **1** AE-bicyclic analogues were synthesized with different N-side-chains and ester side-chains. Antagonist effects of synthetic analogues were examined on human  $\alpha 7$  nAChRs and compared to that of MLA **1**. The antagonist activity of these analogues showed little advantage of the (*S*)-2-methylsuccinimido benzoate ester side-chain especially when comparing analogue **14** with **20**. The data from analogues **14-19** highlight the effect of the N-side-chain on the antagonist activity at human  $\alpha 7$  nAChRs, where a bulkier N-side-chain (with a phenyl moiety) enhanced the antagonist activity compared to alkane side-chains. The pharmacological results achieved with these AE-bicyclic analogues, synthesized in three steps, showed better activity compared to the reported one ring system. The best analogue **16**, containing a benzyl N-side-chain, inhibited the agonist response at human  $\alpha 7$  nAChRs to around 53% [1 nM]. However, these are significantly less efficacious than MLA **1** so further optimisation will be required to achieve comparable antagonist activity. In addition, it may be of interest to undertake further studies to examine the selectivity of these novel compounds for  $\alpha 7$  nAChRs by examining their influence on a broader range of nAChR subtypes.

## EXPERIMENTAL

### General Methods

Analytical thin layer chromatography (TLC) was performed using aluminium backed sheets precoated silica gel plates (Merck Kieselgel 60 F254). Compounds were visualized by UV light or by staining with iodine, ninhydrin and *p*-anisaldehyde. Column chromatography was performed over silica gel 200-400 mesh (purchased from Sigma-Aldrich). <sup>1</sup>H NMR spectra were recorded with a Bruker Avance III (500 MHz) spectrometer at 25 °C. Chemical shifts are given in parts per million (ppm) which was referenced to the residual solvent peak, and reported as position ( $\delta$ ), multiplicity (s = singlet, br = broad, d = doublet, dd = doublet of doublets, t = triplet, dt = doublet of triplets, tt = triplet of triplets, q = quartet, qd = quartet of doublets, qt = quartet of triplets, quin = quintet, m = multiplet), relative integral, assignment and coupling constant (*J* in Hz). <sup>13</sup>C NMR spectra were recorded with a Bruker Avance III (125 MHz) spectrometer at 25 °C with complete proton decoupling. Chemical shifts are expressed in parts per million (ppm) referenced to the used solvent, and reported as position ( $\delta$ ). In addition, <sup>1</sup>H-<sup>1</sup>H COSY, <sup>1</sup>H-<sup>13</sup>C HMBC and <sup>1</sup>H-<sup>13</sup>C HSQC correlation spectra were used for the complete assignment of the proton and carbon resonances. <sup>1</sup>H-<sup>1</sup>H-NOESY NMR spectra were recorded in special cases to determine the stereochemistry of diastereoisomers. High Resolution Time-of-Flight (HR TOF) mass spectra (MS) were obtained on a Bruker Daltonics “microTOF” mass spectrometer using electrospray ionisation (ESI) (loop injection +ve and -ve mode). A PerkinElmer 65 spectrum FT-IR spectrometer was used to obtain the IR spectra. Optical rotations were recorded on an Optical Activity LTD high performance Polarimeter using halogen spectral line 589 nm. The final compounds tested for biological activity were all >98% pure, indeed analytical HPLC showed purity of **18** was 98% pure, all the other seven analogues were >99% pure (HPLC traces for compounds **14-21** are provided in the SI). These compounds were also all homogeneous by TLC and NMR.

### Ethyl 3-methyl-9-oxo-3-azabicyclo-[3.3.1]nonane-1-carboxylate (**3**)

A solution of ethyl cyclohexanone-2-carboxylate (4.44 mmol, 0.748 mL, 95%), 2.2 equiv. formaldehyde (9.768 mmol, 0.713 mL, 38% aq v/v) and 1.1 equiv. of methylamine (4.88 mmol,

0.608 mL, 33% in EtOH) in ethanol (25 mL) was stirred at 40 °C for 2 d under N<sub>2</sub>. Then the solution was concentrated under vacuum and purified by column chromatography using 12.5% EtOAc in petroleum ether to yield the title compound **3** (280 mg, 28%) as a yellow oil. R<sub>f</sub> = 0.36 (12.5% EtOAc in petroleum ether). HRMS (ESI): *m/z* calcd. for C<sub>12</sub>H<sub>20</sub>NO<sub>3</sub>: 226.1443, found: 226.1443 [M+H]<sup>+</sup> and *m/z* calcd. for C<sub>12</sub>H<sub>19</sub>NO<sub>3</sub>Na: 248.1263, found: 248.1262 [M+Na]<sup>+</sup>.  $\nu_{\max}$  (NaCl)/cm<sup>-1</sup> 1733 (ester, C=O), 1717 (ketone, C=O). <sup>1</sup>H NMR (500 MHz, CDCl<sub>3</sub>):  $\delta$  (ppm) = 1.26 (t, *J* = 7.1 Hz, 3H, OCH<sub>2</sub>CH<sub>3</sub>), 1.49-1.57 (m, 1H, H7<sub>eq</sub>), 2.00-2.09 (m, 1H, H6<sub>eq</sub>), 2.10-2.17 (m, 1H, H6<sub>ax</sub>), 2.15-2.29 (m, 1H, H8<sub>eq</sub>), 2.25 (s, 3H, NCH<sub>3</sub>), 2.40-2.45 (m, 1H, H5<sub>eq</sub>), 2.50 (dddd, *J* = 14.2, 12.3, 6.3, 2.0 Hz, 1H, H8<sub>ax</sub>), 2.59 (dd, *J* = 11.2, 3.8 Hz, 1H, H4<sub>ax</sub>), 2.76-2.89 (m, 1H, H7<sub>ax</sub>), 2.96 (dd, *J* = 11.3, 1.9 Hz, 1H, H2<sub>ax</sub>), 3.04 (dt, *J* = 11.2, 2.3 Hz, 1H, H4<sub>eq</sub>), 3.11 (dd, *J* = 11.5, 2.2 Hz, 1H, H2<sub>eq</sub>), 4.19 (q, *J* = 7.1 Hz, 2H, OCH<sub>2</sub>CH<sub>3</sub>). <sup>13</sup>C NMR (125 MHz, CDCl<sub>3</sub>):  $\delta$  (ppm) = 13.8 (OCH<sub>2</sub>CH<sub>3</sub>), 20.2 (C7), 34.0 (C6), 36.8 (C8), 44.8 (N CH<sub>3</sub>), 47.1 (C5), 58.5 (C1), 60.9 (OCH<sub>2</sub>CH<sub>3</sub>), 62.3 (C4), 64.0 (C2), 170.9 (ester), 212.3 (C9).

#### Ethyl 3-ethyl-9-oxo-3-azabicyclo-[3.3.1]nonane-1-carboxylate (**4**)

A solution of ethyl cyclohexanone-2-carboxylate (25.07 mmol, 4.09 mL, 98%), 2.2 equiv. formaldehyde (55.154 mmol, 2.19 mL, 38% aq v/v) and 1.1 equiv. of ethylamine (27.577 mmol, 3.99 mL, 70% aq v/v) in ethanol (170 mL) was heated under reflux for 3 h under N<sub>2</sub>. Then the solution was cooled and concentrated under vacuum and purified by column chromatography using 10% EtOAc in petroleum ether to yield the title compound **4** (3.75 g, 63%) as a yellow oil. R<sub>f</sub> = 0.25 (10% EtOAc in petroleum ether). HRMS (ESI): *m/z* calcd. for C<sub>13</sub>H<sub>22</sub>NO<sub>3</sub>: 240.1600, found: 240.1600 [M+H]<sup>+</sup> and *m/z* calcd. for C<sub>13</sub>H<sub>21</sub>NO<sub>3</sub>Na: 262.1419, found: 262.1418 [M+Na]<sup>+</sup>.  $\nu_{\max}$  (NaCl)/cm<sup>-1</sup> 1733 (ester, C=O), 1716 (ketone, C=O). <sup>1</sup>H NMR (500 MHz, CDCl<sub>3</sub>):  $\delta$  (ppm) = 1.10 (t, *J* = 7.2 Hz, 3H, NCH<sub>2</sub>CH<sub>3</sub>), 1.28 (t, *J* = 7.1 Hz, 3H, OCH<sub>2</sub>CH<sub>3</sub>), 1.46- 1.57 (m, 1H, H7<sub>eq</sub>), 2.00-2.18 (m, 2H, H6<sub>ax</sub> and H6<sub>eq</sub>), 2.19-2.28 (m, 1H, H8<sub>eq</sub>), 2.37-2.60 (m, 5H, NCH<sub>2</sub>CH<sub>3</sub>, H5, H8<sub>ax</sub> and H4<sub>ax</sub>), 2.78-2.90 (m, 1H, H7<sub>ax</sub>), 2.94 (d, *J* = 12.0 Hz, 1H, H2<sub>ax</sub>), 3.15 (d, *J* = 11.1 Hz, 1H, H4<sub>eq</sub>), 3.22 (d, *J* = 11.4 Hz, 1H, H2<sub>eq</sub>), 4.21 (q, *J* = 7.1 Hz, 2H, OCH<sub>2</sub>CH<sub>3</sub>). <sup>13</sup>C NMR (125 MHz, CDCl<sub>3</sub>):  $\delta$  (ppm) = 12.7 (NCH<sub>2</sub>CH<sub>3</sub>), 14.1

(OCH<sub>2</sub>CH<sub>3</sub>), 20.5 (C7), 34.1 (C6), 36.8 (C8), 47.2 (C5), 51.1 (NCH<sub>2</sub>CH<sub>3</sub>), 58.8 (C1), 59.9 (C4), 61.0 (OCH<sub>2</sub>CH<sub>3</sub>), 61.6 (C2), 171.1 (ester), 212.6 (C9).

#### Ethyl 3-benzyl-9-oxo-3-azabicyclo-[3.3.1]nonane-1-carboxylate (**5**)

A solution of ethyl cyclohexanone-2-carboxylate (9.95 mmol, 1.62 mL, 98%), 2.2 equiv. formaldehyde (21.89 mmol, 1.6 mL, 38% aq v/v) and 1.1 equiv. of benzylamine (10.9 mmol, 1.2 mL, 99%) in ethanol (70 mL) was heated under reflux for 3 h under N<sub>2</sub>. Then the solution was cooled and concentrated under vacuum and purified by column chromatography using 10% EtOAc in petroleum ether to yield the title compound **5** (750 mg, 25%) as a yellow oil. R<sub>f</sub> = 0.29 (10% EtOAc in petroleum ether). HRMS (ESI): *m/z* calcd. for C<sub>18</sub>H<sub>24</sub>NO<sub>3</sub>: 302.1756, found: 302.1755 [M+H]<sup>+</sup> and *m/z* calcd. for C<sub>18</sub>H<sub>23</sub>NO<sub>3</sub>Na: 324.1576, found: 324.1573 [M+Na]<sup>+</sup>. ν<sub>max</sub> (NaCl)/cm<sup>-1</sup> 1732 (ester, C=O), 1717 (ketone, C=O). <sup>1</sup>H NMR (500 MHz, CDCl<sub>3</sub>): δ (ppm) = 1.27 (t, *J* = 7.1 Hz, 3H, OCH<sub>2</sub>CH<sub>3</sub>), 1.55- 1.65 (m, 1H, H7<sub>eq</sub>), 2.02-2.19 (m, 2H, H6<sub>ax</sub> and H6<sub>eq</sub>), 2.20-2.27 (m, 1H, H8<sub>eq</sub>), 2.44-2.48 (m, 5H), 2.54 (dddd, *J* = 14.1, 12.2, 6.4, 1.9 Hz, 1H, H8<sub>ax</sub>), 2.63 (dd, *J* = 10.9, 2.5 Hz, 1H, H4<sub>ax</sub>), 2.92-3.06 (m, 2H, H2<sub>ax</sub> and H7<sub>ax</sub>), 3.13 (d, *J* = 11.2, 2.4 Hz, 1H, H4<sub>eq</sub>), 3.20 (dd, *J* = 11.5, 2.4 Hz, 1 H, H2<sub>eq</sub>), 3.52 (s, 2H, NCH<sub>2</sub>Ph), 4.19 (qd, *J* = 7.2, 3.0 Hz, 2H, OCH<sub>2</sub>CH<sub>3</sub>), 7.27-7.36 (m, 5H, NCH<sub>2</sub>Ph). <sup>13</sup>C NMR (125 MHz, CDCl<sub>3</sub>): δ (ppm) = 14.1 (OCH<sub>2</sub>CH<sub>3</sub>), 20.7 (C7), 34.1 (C6), 36.7 (C8), 47.2 (C5), 58.9 (C1), 60.3 (C4), 61.1 (OCH<sub>2</sub>CH<sub>3</sub>), 61.8 (C2), 62.1 (NCH<sub>2</sub>Ph), 127.2 (C4 arom), 128.4, 128.7 (C2 arom, C3 arom, C5 arom and C6 arom), 138.3 (C1 arom), 170.9 (ester), 212.4 (C9).

#### Ethyl 3-(2-phenylethyl)-9-oxo-3-azabicyclo-[3.3.1]nonane-1-carboxylate (**6**)

A solution of ethyl cyclohexanone-2-carboxylate (3.17 mmol, 0.517 mL, 98%), 2.2 equiv. formaldehyde (7 mmol, 0.525 mL, 38% aq. v/v) and 1.1 equiv. of 2-phenylethyl amine (3.49 mmol, 0.446 mL, 99%) in ethanol (20 mL) was heated under reflux for 3 h under N<sub>2</sub>. Then the solution was cooled and concentrated under vacuum and purified by column chromatography using 10% EtOAc in petroleum ether to yield the title compound **6** (640 mg, 64%) as a yellow oil. R<sub>f</sub> = 0.30 (10% EtOAc in petroleum ether). HRMS (ESI): *m/z* calcd. for C<sub>19</sub>H<sub>26</sub>NO<sub>3</sub>: 316.1913, found: 316.1912 [M+H]<sup>+</sup> and *m/z* calcd. for C<sub>19</sub>H<sub>25</sub>NO<sub>3</sub>Na: 338.1732, found:

338.1731 [M+Na]<sup>+</sup>.  $\nu_{\max}$  (NaCl)/cm<sup>-1</sup> 1732 (ester, C=O), 1716 (ketone, C=O). <sup>1</sup>H NMR (500 MHz, CDCl<sub>3</sub>):  $\delta$  (ppm) = 1.28 (t,  $J$  = 7.1 Hz, 3H, OCH<sub>2</sub>CH<sub>3</sub>), 1.37-1.45 (m, 1H, H7<sub>eq</sub>), 1.97-2.11 (m, 2H, H6<sub>ax</sub> and H6<sub>eq</sub>), 2.12-2.20 (m, 1H, H8<sub>eq</sub>), 2.42-2.53 (m, H5 and H8<sub>ax</sub>), 2.55-2.68 (m, 4H, H7<sub>ax</sub>, H4<sub>ax</sub> and NCH<sub>2</sub>CH<sub>2</sub>Ph), 2.82 (t,  $J$  = 7.5 Hz, 2H, NCH<sub>2</sub>CH<sub>2</sub>Ph), 3.02 (d,  $J$  = 11.3 Hz, 1H, H2<sub>ax</sub>), 3.18 (d,  $J$  = 11.0 Hz, 1H, H4<sub>eq</sub>), 3.27 (d,  $J$  = 11.4 Hz, 1 H, H2<sub>eq</sub>), 4.21 (q,  $J$  = 7.1 Hz, 2H, OCH<sub>2</sub>CH<sub>3</sub>), 7.18-7.32 (m, 5H, NCH<sub>2</sub>CH<sub>2</sub>Ph). <sup>13</sup>C NMR (125 MHz, CDCl<sub>3</sub>):  $\delta$  (ppm) = 14.1 (OCH<sub>2</sub>CH<sub>3</sub>), 20.2 (C7), 33.8 (NCH<sub>2</sub>CH<sub>2</sub>Ph), 34.1 (C6), 36.8 (C8), 47.2 (C5), 58.5 (NCH<sub>2</sub>CH<sub>2</sub>Ph), 58.8 (C1), 60.2 (C4), 61.1 (OCH<sub>2</sub>CH<sub>3</sub>), 61.8 (C2), 126.0 (C4 arom), 128.3 (C2 arom and C6 arom), 128.6 (C3 arom and C5 arom), 140.1 (C1 arom), 171.1 (ester), 212.5 (C9).

#### Ethyl 3-(3-phenylpropyl)-9-oxo-3-azabicyclo-[3.3.1]nonane-1-carboxylate (**7**)

A solution of ethyl cyclohexanone-2-carboxylate (3 mmol, 0.49 mL, 99%), 2.2 equiv.

formaldehyde (6.6 mmol, 0.48 mL, 38% aq. v/v) and 1.1 equiv. of 3-phenylpropyl amine (3.3 mmol, 0.48 mL, 99%) in ethanol (20 mL) was heated under reflux for 3 h under N<sub>2</sub>. Then the solution was concentrated under vacuum and purified by column chromatography using 10% EtOAc in petroleum ether to yield the title compound **7** (540 mg, 54%) as a yellow oil.  $R_f$  = 0.34 (10% EtOAc in petroleum ether).

HRMS (ESI):  $m/z$  calcd. for C<sub>20</sub>H<sub>28</sub>NO<sub>3</sub>: 330.2069, found: 330.2068 [M+H]<sup>+</sup> and  $m/z$  calcd. for C<sub>20</sub>H<sub>27</sub>NO<sub>3</sub>Na: 352.1889, found: 352.1887

[M+Na]<sup>+</sup>.  $\nu_{\max}$  (NaCl)/cm<sup>-1</sup> 1732 (ester, C=O), 1716 (ketone, C=O). <sup>1</sup>H NMR (500 MHz, CDCl<sub>3</sub>):  $\delta$  (ppm) = 1.28 (t,  $J$  = 7.1 Hz, 3H, OCH<sub>2</sub>CH<sub>3</sub>), 1.52- 1.62 (m, 1H, H7<sub>eq</sub>), 1.83 (quin,  $J$  = 7.2 Hz, 1H, NCH<sub>2</sub>CH<sub>2</sub>CH<sub>2</sub>Ph), 2.05-2.16 (m, 2H, H6<sub>ax</sub> and H6<sub>eq</sub>), 2.21-2.29 (m, 1H, H8<sub>eq</sub>), 2.36 (t,  $J$  = 7.0 Hz, 2H, NCH<sub>2</sub>CH<sub>2</sub>CH<sub>2</sub>Ph), 2.45-2.49 (m, 1H, H5), 2.51-2.61 (m, 2H, H4<sub>ax</sub> and H8<sub>ax</sub>), 2.7 (t,  $J$  = 7.7 Hz, 2H, NCH<sub>2</sub>CH<sub>2</sub>CH<sub>2</sub>Ph), 2.84-2.97 (m, 2H, H2<sub>ax</sub> and H7<sub>ax</sub>), 3.15 (dt,  $J$  = 11.1, 2.4 Hz, 1H, H4<sub>eq</sub>), 3.21 (dd,  $J$  = 11.4, 2.3 Hz, 1 H, H2<sub>eq</sub>), 4.21 (q,  $J$  = 7.1 Hz, 2H, OCH<sub>2</sub>CH<sub>3</sub>), 7.16-7.22, 7.26-7.32 (m, 5H, NCH<sub>2</sub>CH<sub>2</sub>CH<sub>2</sub>Ph). <sup>13</sup>C NMR (125 MHz, CDCl<sub>3</sub>):  $\delta$  (ppm) = 14.1 (OCH<sub>2</sub>CH<sub>3</sub>), 20.6 (C7), 29.1 (N CH<sub>2</sub>CH<sub>2</sub>CH<sub>2</sub>Ph), 33.5 (NCH<sub>2</sub>CH<sub>2</sub>CH<sub>2</sub>Ph) 34.2 (C6), 36.8 (C8), 47.2 (C5), 56.4 (NCH<sub>2</sub>CH<sub>2</sub>CH<sub>2</sub>Ph), 58.8 (C1), 60.4 (C4), 61.1 (OCH<sub>2</sub>CH<sub>3</sub>), 62.0 (C2), 125.8 (C4 arom), 128.37, 128.40 (C2 arom, C6 arom, C3 arom and C5 arom), 142.0 (C1 arom), 171.1 (ester), 212.5 (C9).

Ethyl 3-(4-phenylbutyl)-9-oxo-3-azabicyclo-[3.3.1]nonane-1-carboxylate (**8**)

A solution of ethyl cyclohexanone-2-carboxylate (2.91 mmol, 0.476 mL, 95%), 2.2 equiv. formaldehyde (5.83 mmol, 0.425 mL, 38% aq v/v) and 1.1 equiv. of 4-phenylbutylamine (3.205 mmol, 0.52 mL, 98%) in ethanol (20 mL) was heated under reflux for 3 h under N<sub>2</sub>. Then the solution was cooled and concentrated under vacuum and purified by column chromatography using 10% EtOAc in petroleum ether to yield the title compound **8** (600 mg, 60%) as a yellow oil. R<sub>f</sub> = 0.35 (10% EtOAc in petroleum ether). HRMS (ESI): *m/z* calcd. for C<sub>21</sub>H<sub>30</sub>NO<sub>3</sub>: 344.2226, found: 344.2227 [M+H]<sup>+</sup> and *m/z* calcd. for C<sub>21</sub>H<sub>29</sub>NO<sub>3</sub>Na: 366.2045, found: 366.2044 [M+Na]<sup>+</sup>.  $\nu_{\max}$  (NaCl)/cm<sup>-1</sup> 1733 (ester, C=O), 1717 (ketone, C=O). <sup>1</sup>H NMR (500 MHz, CDCl<sub>3</sub>):  $\delta$  (ppm) = 1.28 (t, *J* = 7.2 Hz, 3H, OCH<sub>2</sub>CH<sub>3</sub>), 1.50- 1.68 (m, 3H, H<sub>7eq</sub> and NCH<sub>2</sub>CH<sub>2</sub>CH<sub>2</sub>CH<sub>2</sub>Ph), 1.66-1.74 (m, 2H, NCH<sub>2</sub>CH<sub>2</sub>CH<sub>2</sub>CH<sub>2</sub>Ph), 2.02-2.16 (m, 2H, H<sub>6ax</sub> and H<sub>6eq</sub>), 2.19-2.25 (m, 1H, H<sub>8eq</sub>), 2.35 (td, *J* = 7.0, 1.4 Hz, 2H, NCH<sub>2</sub>CH<sub>2</sub>CH<sub>2</sub>CH<sub>2</sub>Ph), 2.42-2.46 (m, 1H, H<sub>5</sub>), 2.49-2.57 (m, 2H, H<sub>4ax</sub> and H<sub>8ax</sub>), 2.65 (t, *J* = 7.6 Hz, 2H, NCH<sub>2</sub>CH<sub>2</sub>CH<sub>2</sub>CH<sub>2</sub>Ph), 2.80-2.88 (m, 1H, H<sub>7ax</sub>), 2.91 (dd, *J* = 11.5, 2.0 Hz, 1H, H<sub>2ax</sub>) 3.10 (dt, *J* = 11.2, 2.4 Hz, 1 H, H<sub>4eq</sub>), 3.17 (dd, *J* = 11.4, 2.3 Hz, 1H, H<sub>2eq</sub>), 4.20 (q, *J* = 7.1 Hz, 2H, OCH<sub>2</sub>CH<sub>3</sub>), 7.16-7.21, 7.26-7.31 (m, 5H, NCH<sub>2</sub>CH<sub>2</sub>CH<sub>2</sub>CH<sub>2</sub>Ph). <sup>13</sup>C NMR (125 MHz, CDCl<sub>3</sub>):  $\delta$  (ppm) = 14.1 (OCH<sub>2</sub>CH<sub>3</sub>), 20.5 (C7), 26.7 (NCH<sub>2</sub>CH<sub>2</sub>CH<sub>2</sub>CH<sub>2</sub>Ph), 29.0 (NCH<sub>2</sub>CH<sub>2</sub>CH<sub>2</sub>CH<sub>2</sub>Ph), 34.1 (C6), 35.6 (NCH<sub>2</sub>CH<sub>2</sub>CH<sub>2</sub>CH<sub>2</sub>Ph), 36.8 (C8), 47.2 (C5), 56.8 (NCH<sub>2</sub>CH<sub>2</sub>CH<sub>2</sub>CH<sub>2</sub>Ph), 58.8 (C1), 60.4 (C4), 61.0 (OCH<sub>2</sub>CH<sub>3</sub>), 62.0 (C2), 125.7 (C4 arom), 128.26 (C2 arom and C6 arom), 128.31 (C3 arom and C5 arom), 142.4 (C1 arom), 171.1 (ester), 212.6 (C9).

(9R)-3-Ethyl-1-hydroxymethyl-3-azabicyclo[3.3.1]nonan-9-ol (**9**)

LiAlH<sub>4</sub> (1.756 mmol, 66.6 mg) was added to a solution of cyclohexanone **4** (which was dried under high vacuum for 24 h) (0.878 mmol, 210 mg) in anhydrous THF (5 mL), and the reaction stirred for 7 h at 19 °C under N<sub>2</sub>. Then the mixture quenched with 66  $\mu$ L of water, followed by 66  $\mu$ L of sodium hydroxide solution (15 %w/v), and then 200  $\mu$ L water. The result mixture was stirred with anhydrous magnesium sulfate for 15 min and filtered over celite. The filtrate was concentrated under vacuum and the purified over column chromatography with 5-20% MeOH



in DCM to yield the title compound **9** (60 mg, 34%) as a yellow oil.  $R_f = 0.27$  (20% MeOH in DCM). HRMS (ESI):  $m/z$  calcd. for  $C_{11}H_{22}NO_2$ : 200.1651, found: 200.1648  $[M+H]^+$  and  $m/z$  calcd. for  $C_{11}H_{21}NO_2Na$ : 222.1470, found: 222.1488  $[M+Na]^+$ .  $\nu_{max}$  (NaCl)/ $cm^{-1}$  3413 (OH).  $^1H$  NMR (500 MHz,  $CDCl_3$ ):  $\delta$  (ppm) = 1.03 (t,  $J = 7.2$  Hz, 3H,  $NCH_2CH_3$ ), 1.26 (dd,  $J = 13.0, 5.6$  Hz, 1H,  $H_{8eq}$ ), 1.43-1.54 (m, 2H,  $H_{7eq}$  and  $H_{6eq}$ ), 1.80-2.02 (m, 4H,  $H_{8ax}$ ,  $H_{6ax}$ ,  $H_5$  and  $H_{2ax}$ ), 2.18 (dt,  $J = 11.1, 2.4$  Hz, 1H,  $H_{4ax}$ ), 2.20-2.28 (m, 2H,  $NCH_2CH_3$ ), 2.52-2.61 (m, 1H,  $H_{7ax}$ ), 2.63 (dd,  $J = 11.0, 1.5$  Hz, 1H,  $H_{2eq}$ ), 2.66-2.93 (br, 2H, 9-OH and 1 x-OH), 2.96 (dt,  $J = 11.1, 2.1$  Hz, 1H,  $H_{4eq}$ ), 3.35 (d,  $J = 10.8$ , 1H,  $CHaHbOH$ ), 3.39 (d,  $J = 10.8$ , 1H,  $CHaHbOH$ ), 3.70 (d,  $J = 3.6$  Hz, 1H, 9-H).  $^{13}C$  NMR (125 MHz,  $CDCl_3$ ):  $\delta$  (ppm) = 12.7 ( $NCH_2CH_3$ ), 20.5 (C7), 23.9 (C6), 26.5 (C8), 36.1 (C5), 38.1 (C1), 52.3 ( $NCH_2CH_3$ ), 58.3 (C4), 60.4 (C2), 70.9 (C1), 75.1 (C9).

#### 2-Acetamidobenzoic acid (**11**)

Anthranilic acid (28 mmol, 3.92 g, 98%) was heated under reflux with 5 equiv. acetic anhydride (140 mmol, 13.23 mL) and 1 equiv. anhydrous triethylamine (28 mmol, 3.94 mL, 99%) in THF (20 mL) under nitrogen for 4 h. The reaction mixture was cooled to 19 °C and then in an ice bath, then 20 mL of 1 M aq. HCl was added gradually while the reaction mixture was on ice. The precipitate was filtered and washed with ice-cold water. The product was recrystallized from water and ethanol to yield the title compound **11** (4.2 g, 84%) as pale brown crystals.  $R_f = 0.42$  (10% MeOH in DCM). HRMS (ESI):  $m/z$  calcd. for  $C_9H_8NO_3$ : 178.0504, found: 178.0505  $[M-H]^-$  and  $m/z$  calcd. for  $C_{10}H_{10}NO_5$ : 224.0559, found: 224.0606  $[M+HCOO]^-$ .  $^1H$  NMR (500 MHz,  $CD_3OD$ ):  $\delta$  (ppm) = 2.18 (s, 3H,  $COCH_3$ ), 7.11 (td,  $J = 7.7, 1.2$  Hz, 1H,  $H_5$  arom), 7.52 (ddd,  $J = 8.7, 7.7, 1.7$  Hz, 1H,  $H_4$  arom), 8.05 (dd,  $J = 7.7, 1.7$  Hz, 1H,  $H_6$  arom), 8.52 (d,  $J = 8.4$  Hz, 1H,  $H_3$  arom).  $^{13}C$  NMR (125 MHz,  $CD_3OD$ ):  $\delta$  (ppm) = 25.1 ( $COCH_3$ ), 117.4 (C1 arom), 121.4 (C3 arom), 123.9 (C5 arom), 132.5 (C6 arom), 135.1 (C4 arom), 142.3 (C2 arom), 171.24 (COOH), 171.39 ( $NHCOCH_3$ ).

2-(3-Methyl-2,5-dioxo-2,5-dihydro-1H-pyrrol-1-yl)benzoic acid (**12**)

Neat anthranilic acid (21.6 mmol, 3.02 g, 98%) was stirred with 1 equiv. citraconic anhydride (21.6 mmol, 1.98 mL, 98%) at 140 °C for 24 h under nitrogen then cooled to 19 °C. After that, the crude mixture was dissolved in EtOAc (30 mL). The organic layer was washed sequentially with 1M HCl (2 x 20 mL), water (1 x 20 mL) and brine (1 x 20 mL). The organic layer was dried (MgSO<sub>4</sub>) and filtered, the filtrate was concentrated under vacuum and purified over column chromatography with 10% MeOH in DCM to yield the title compound **12** (4.0 g, 80 %) as a brownish yellow powder.  $R_f = 0.32$  (10% MeOH in DCM). HRMS (ESI):  $m/z$  calcd. for C<sub>12</sub>H<sub>8</sub>NO<sub>4</sub>: 230.0453, found: 230.0458 [M-H]<sup>-</sup> and  $m/z$  calcd. for C<sub>13</sub>H<sub>10</sub>NO<sub>6</sub>: 276.0508, found: 276.0528 [M+HCOO]<sup>-</sup>. <sup>1</sup>H NMR (500 MHz, CDCl<sub>3</sub>):  $\delta$  (ppm) = 2.18 (d,  $J = 1.7$  Hz, 3H, 5' CH<sub>3</sub>), 6.51 (d,  $J = 1.9$  Hz, 1H, H3'), 7.32 (dd,  $J = 7.9, 1.2$  Hz, 1H, H3 arom), 7.52 (td,  $J = 7.7, 1.2$  Hz, 1H, H5 arom), 7.69 (td,  $J = 7.7, 1.6$  Hz, 1H, H4 arom), 8.16 (dd,  $J = 7.9, 1.5$  Hz, 1H, H6 arom). <sup>13</sup>C NMR (125 MHz, CDCl<sub>3</sub>):  $\delta$  (ppm) = 11.3 (5', CH<sub>3</sub>), 127.20 (C1 arom), 128.05 (C3'), 129.15 (C5 arom), 130.54 (C3 arom), 132.16 (C2 arom), 132.44 (C6 arom), 134.25 (C4 arom), 146.4 (C2'), 169.84 (COOH), 170.20 (C4'), 170.87 (C1').

(S)-2-(3-Methyl-2,5-dioxopyrrolidin-1-yl)benzoic acid (**13**)

(2*S*,4*S*)-1-Boc-4-diphenylphosphino-2-(diphenylphosphinomethyl)pyrrolidine (BPPM) (0.649 mmol (5 mol %), 359 mg) and rhodium cyclooctadiene chloride dimer (Rh(COD)Cl)<sub>2</sub> (0.649 mmol (5 mol %), 326 mg, 98%) stirred together in anhydrous toluene (10 mL) under nitrogen gas for 30 min. Then the flask was vacuumed, and hydrogen was introduced. Compound 12 (0.01298 mol, 3 gm) was dissolved in anhydrous methanol (10 mL) and added to the mixture. The reaction was monitored by TLC and stopped after 24 h. The mixture was concentrated under vacuum and purified over column chromatography with 10% MeOH in DCM to yield the title compound **13** (2.9 g, 95 %) as a brownish yellow powder.  $R_f = 0.31$  (10% MeOH in DCM).  $[\alpha]_D -12.0^\circ$  ( $c$  1.0, CHCl<sub>3</sub>). HRMS (ESI):  $m/z$  calcd. for C<sub>12</sub>H<sub>10</sub>NO<sub>4</sub>: 232.0610, found: 232.0613 [M-H]<sup>-</sup>. <sup>1</sup>H NMR (500 MHz, CDCl<sub>3</sub>):  $\delta$  (ppm) = 1.44 (d,  $J = 6.8$  Hz, 3H, 5' CH<sub>3</sub>), 2.53 (d,  $J = 17.9$  Hz, 1H, H3'A), 3.01-3.16 (m, 2H, H2' and H3' B), 7.27 (d,  $J = 7.7$  Hz, 1H, H3 arom), 7.54 (t,  $J = 7.7$  Hz, 1H, H5 arom), 7.70 (t,  $J = 7.7$  Hz, 1H, H4 arom), 8.19 (d,  $J = 7.7$  Hz, 1H, H6

arom).  $^{13}\text{C}$  NMR (125 MHz,  $\text{CDCl}_3$ ):  $\delta$  (ppm) = 16.5 (5'), 35.13 and 35.5 (3'), 37.0 (2'), 125.5 (C1 arom), 129.5 (C5 arom), 129.9 (C3 arom), 132.5 (C6 arom), 132.9 (C2 arom), 134.4 (C4 arom), 146.4 (C2'), 169.2 and 169.4 (COOH), 176.0 and 176.1 (C4'), 179.9 and 180.0 (C1').

((*9R*)-9-Hydroxy-3-methyl-3-azabicyclo[3.3.1]nonan-1-yl)methyl 2-((*S*)-3-methyl-2,5-dioxopyrrolidin-1-yl)benzoate (**14**)

Compound **3** (0.89 mmol, 200 mg) was reduced using LAH (1.78 mmol, 84.2 mg) as described for compound **9**. The crude product was used for the esterification step without purification.

Compound **13** (0.189 mmol, 44 mg) was stirred with DCC (0.189 mmol, 39.4 mg, 99%) and DMAP (0.0189 mmol, 2.3 mg, 99%) in anhydrous acetonitrile under nitrogen gas at 40 °C for 20 min, and then the crude amino alcohol (35 mg) was added. The reaction monitored by TLC and stopped after 24 h. The mixture was concentrated under vacuum and purified over column chromatography with 5% MeOH in DCM to yield the title compound **14** (18 mg, 24 %) as a yellow oil.  $R_f$  = 0.4 (5% MeOH in DCM). HRMS (ESI):  $m/z$  calcd. for  $\text{C}_{22}\text{H}_{29}\text{N}_2\text{O}_5$ : 401.2077, found: 401.2073  $[\text{M}+\text{H}]^+$ .  $^1\text{H}$  NMR (500 MHz,  $\text{CD}_3\text{OD}$ ):  $\delta$  (ppm) = 1.41 (d,  $J$  = 6.7 Hz, 3H, 5'''), 1.44-1.56 (m, 3H, H6eq, H7eq, H8eq), 1.72-1.81 (m, 1H, H8ax), 1.86 (br s, 1H, H5), 1.99-2.07 (m, 1H, H6ax), 2.14-2.21 (m, 4H, N-CH<sub>3</sub>, H2ax), 2.34 (d,  $J$  = 11.4, 1H, H4ax), 2.45-2.63 (m, 2H, H7ax, H3'''A), 2.85-2.91 (m, 1H, H2eq), 2.96 (d,  $J$  = 11.4 Hz, 1H, H4eq), 3.04-3.15 (m, 2H, H2''' and H3'''B), 3.59-3.66 (m, 1H, H9), 3.96-4.11 (m, 2H, H1' A and B), 7.35 (d,  $J$  = 7.4 Hz, 1H, H3''), 7.61 (d,  $J$  = 7.4 Hz, 1H, H5''), 7.73 (d,  $J$  = 7.4 Hz, 1H, H4''), 8.12 (d,  $J$  = 7.4 Hz, 1H, H6'').  $^{13}\text{C}$  NMR (125 MHz,  $\text{CDCl}_3$ ):  $\delta$  (ppm) = 16.2 (5'''), 21.5 (C7), 25.0 (C6), 28.0 (C8), 36.18 (C2'''), 37.33 (C5), 38.00 (C3'''), 39.51 (C1), 46.4 (NCH<sub>3</sub>), 62.30 (C4), 64.44 (C2), 71.78 (C9), 71.80 (C1'), 128.99 (C1''), 130.42 (C5''), 131.10 (C3''), 132.07 (C6''), 133.72 (C2''), 134.50 (C4''), 165.6 (ester), 173.1 (C4'''), 181.8 (C1''').

((*9R*)-3-Ethyl-9-hydroxy-3-azabicyclo[3.3.1]nonan-1-yl)methyl 2-((*S*)-3-methyl-2,5-dioxopyrrolidin-1-yl)benzoate (**15**)

Compound **13** (0.778 mmol, 181 mg) was stirred with DCC (0.778 mmol, 162 mg, 99%) and DMAP (0.0778 mmol, 9.6 mg, 99%) in anhydrous acetonitrile under nitrogen gas at 40 °C for

20 min, and then compound **9** (155 mg) was added. The reaction was monitored by TLC and stopped after 24 h. The mixture was concentrated under vacuum and purified over column chromatography with 5% MeOH in DCM to yield the title compound **15** (130 mg, 40 %) as a yellow oil.  $R_f = 0.44$  (5% MeOH in DCM). HRMS (ESI):  $m/z$  calcd. for  $C_{23}H_{31}N_2O_5$ : 415.2233, found: 415.2233  $[M+H]^+$ .  $^1H$  NMR (500 MHz,  $CD_3OD$ ):  $\delta$  (ppm) = 1.19 (m, 3H,  $NCH_2CH_3$ ), 1.41 (d,  $J = 7.0$  Hz, 3H,  $5''$ ), 1.44-1.55 (m, 3H,  $H_{6eq}$ ,  $H_{7eq}$ ,  $H_{8eq}$ ), 1.66-1.74 (m, 1H,  $H_{8ax}$ ), 1.80-1.87 (m, 1H,  $H_5$ ), 1.97-2.05 (m, 1H,  $H_{6ax}$ ), 2.07-2.12 (m, 1H,  $H_{2ax}$ ), 2.14-2.29 (m, 3H,  $H_{4ax}$  and  $NCH_2CH_3$ ), 2.46-2.57 (m, 1H,  $H_{3'''A}$ ), 2.58-2.69 (m, 1H,  $H_{7ax}$ ), 2.89-2.96 (m, 1H,  $H_{2eq}$ ), 3.00-3.06 (m, 1H,  $H_{4eq}$ ), 3.05-3.14 (m, 2H,  $H_{2'''}$  and  $H_{3'''B}$ ), 3.76 (br s, 1H,  $H_9$ ), 4.00-4.16 (m, 2H,  $H_{1'}$  A and B), 7.36 (d,  $J = 7.8$  Hz, 1H,  $H_{3''}$ ), 7.61 (d,  $J = 7.8$  Hz, 1H,  $H_{5''}$ ), 7.74 (d,  $J = 7.8$  Hz, 1H,  $H_{4''}$ ), 8.13 (d,  $J = 7.8$  Hz, 1H,  $H_{6''}$ ).  $^{13}C$  NMR (125 MHz,  $CDCl_3$ ):  $\delta$  (ppm) = 11.3 ( $NCH_2CH_3$ ), 15.8 ( $5''$ ), 21.3 (C7), 24.8 (C6), 27.9 (C8), 35.7 (C2'''), 37.18 (C5), 37.67 (C3'''), 39.5 (C1), 53.1 ( $NCH_2CH_3$ ), 59.4 (C4), 61.7 (C2), 70.7 (C1'), 72.0 (C9), 128.79 (C1''), 130.50 (C5''), 131.21 (C3''), 132.10 (C6''), 133.82 (C2''), 134.62 (C4''), 165.4 (ester), 175.5 (C4'''), 182.1 (C1''').

((*9R*)-3-Benzyl-9-hydroxy-3-azabicyclo[3.3.1]nonan-1-yl)methyl 2-((*S*)-3-methyl-2,5-dioxopyrrolidin-1-yl)benzoate (**16**)

Compound **5** (1.66 mmol, 500 mg) was reduced using LAH (4.15 mmol, 157.5 mg) as described for compound **9**. The crude product was used for the esterification step without purification.

Compound **13** (0.593 mmol, 138 mg) was stirred with DCC (0.593 mmol, 123.6 mg, 99%) and DMAP (0.0593 mmol, 7.3 mg, 99%) in anhydrous acetonitrile under nitrogen gas at 40 °C for 20 min, and then the crude amino alcohol (155 mg) was added. The reaction monitored by TLC and stopped after 24 h. The mixture was concentrated under vacuum and purified over column chromatography with 5% MeOH in DCM to yield the title compound **16** (140 mg, 50 %) as a yellow oil.  $R_f = 0.48$  (5% MeOH in DCM). HRMS (ESI):  $m/z$  calcd. for  $C_{28}H_{33}N_2O_5$ : 477.2390, found: 477.2385  $[M+H]^+$ .  $^1H$  NMR (500 MHz,  $CD_3OD$ ):  $\delta$  (ppm) = 1.37-1.43 (m, 3H,  $5''$ ), 1.42-1.53 (m, 3H,  $H_{6eq}$ ,  $H_{7eq}$ ,  $H_{8eq}$ ), 1.67-1.81 (m, 1H,  $H_{8ax}$ ), 1.82-1.86 (m, 1H,  $H_5$ ), 1.95-2.06 (m, 1H,  $H_{6ax}$ ), 2.08-2.15 (m, 1H,  $H_{2ax}$ ), 2.21-2.30 (m, 1H,  $H_{4ax}$ ), 2.43-2.63 (m, 1H,  $H_{3'''A}$ ), 2.72-

2.83 (m, 1H, H7<sub>ax</sub>), 2.83-2.91 (m, 1H, H2<sub>eq</sub>), 2.90-2.96 (m, 1H, H4<sub>eq</sub>), 3.01-3.14 (m, 2H, H2''' and H3'''B), 3.34-3.41 (m, 2H, NCH<sub>2</sub>Ph), 3.60-3.68 (m, 1H, H9), 3.95-4.13 (m, 2H, H1' A and B), 7.18-7.30 (m, 5H, NCH<sub>2</sub>Ph), 7.31-7.35 (m, 1H, H3''), 7.56 (td, *J* = 7.7, 1.3 Hz, 1H, H5''), 7.72 (td, *J* = 7.7, 1.5 Hz, 1H, H4''), 7.99 (dd, *J* = 7.7, 1.6 Hz, 1H, H6''). <sup>13</sup>C NMR (125 MHz, CDCl<sub>3</sub>): δ (ppm) = 16.4 (5'''), 22.1 (C7), 25.1 (C6), 28.2 (C8), 36.31 (C2'''), 37.73 (C5), 38.16 (C3'''), 39.54 (C1), 60.1 (C4), 62.40 (C2), 64.38 (NCH<sub>2</sub>Ph), 71.20 (C1'), 72.63 (C9), 127.92 (C4 Ph), 128.87 (C1''), 129.26, 129.75 (C2 Ph, C3 Ph, C5 Ph, C6 Ph), 130.48 (C5''), 131.12 (C3''), 132.00 (C6''), 133.97 (C2''), 134.48 (C4''), 140.5 (C1 Ph), 165.7 (ester), 174.9 (C4'''), 181.6 (C1''').

((9*R*)-9-Hydroxy-3-(2-phenethyl)-3-azabicyclo[3.3.1]nonan-1-yl)methyl 2-((*S*)-3-methyl-2,5-dioxopyrrolidin-1-yl)benzoate (**17**)

Compound **6** (0.634 mmol, 200 mg) was reduced using LAH (1.585 mmol, 60.2 mg) as described for compound **9**. The crude product was used for the esterification step without purification. Compound **13** (0.2 mmol, 46.6 mg) was stirred with DCC (0.2 mmol, 41.6 mg, 99%) and DMAP (0.02 mmol, 2.5 mg, 99%) in anhydrous acetonitrile under nitrogen gas at 40 °C for 20 min, and then the crude amino alcohol (55 mg) was added. The reaction monitored by TLC and stopped after 24 h. The mixture was concentrated under vacuum and purified over column chromatography with 5% MeOH in DCM to yield the title compound **17** (25 mg, 26 %) as a yellow oil. *R*<sub>f</sub> = 0.54 (5% MeOH in DCM). HRMS (ESI): *m/z* calcd. for C<sub>29</sub>H<sub>35</sub>N<sub>2</sub>O<sub>5</sub>: 491.2546, found: 491.2549 [M+H]<sup>+</sup>. <sup>1</sup>H NMR (500 MHz, CD<sub>3</sub>OD): δ (ppm) = 1.37-1.52 (m, 6H, H5''', H6<sub>eq</sub>, H7<sub>eq</sub>, H8<sub>eq</sub>), 1.67-1.80 (m, 1H, H8<sub>ax</sub>), 1.91 (br s, 1H, H5), 1.97-2.08 (m, 1H, H6<sub>ax</sub>), 2.09-2.18 (m, 1H, H7<sub>ax</sub>), 2.34-2.42 (m, 1H, H2<sub>ax</sub>), 2.45-2.60 (m, 2H, H4<sub>ax</sub> and H3'''A), 2.63-2.73 (m, 2H, NCH<sub>2</sub>CH<sub>2</sub>Ph), 2.80-2.89 (m, 2H, NCH<sub>2</sub>CH<sub>2</sub>Ph), 3.02-3.16 (m, 2H, H2''' and H3'''B), 3.18-3.28 (m, 2H, H2<sub>eq</sub> and H4<sub>eq</sub>), 3.63-3.72 (m, 1H, H9), 4.00-4.12 (m, 2H, H1' A and B), 7.12-7.30 (m, 5H, NCH<sub>2</sub>CH<sub>2</sub>Ph), 7.35 (d, *J* = 7.5 Hz, 1H, H3''), 7.61 (td, *J* = 7.5, 1.3 Hz, 1H, H5''), 7.74 (td, *J* = 7.5, 1.5 Hz, 1H, H4''), 8.13 (dd, *J* = 7.5, 1.6 Hz, 1H, H6''). <sup>13</sup>C NMR (125 MHz, CDCl<sub>3</sub>): δ (ppm) = 16.1 (5'''), 20.6 (C7), 24.3 (C6), 27.2 (C8), 33.45 (NCH<sub>2</sub>CH<sub>2</sub>Ph), 35.76 (C2'''), 36.62 (C5), 37.48 (C3'''), 39.58 (C1), 59.46 (C4), 60.81 (NCH<sub>2</sub>CH<sub>2</sub>Ph), 61.30

(C2), 70.00 (C1'), 70.85 (C9), 127.07 (C4 Ph), 128.96 (C1''), 129.29, 129.73 (C2 Ph, C3 Ph, C5 Ph, C6 Ph), 130.50 (C5''), 131.04 (C3''), 132.15 (C6''), 133.26 (C2''), 134.47 (C4''), 139.67 (C1 Ph), 164.5 (ester), 177.9 (C4'''), 180.8 (C1''').

((*9R*)-9-Hydroxy-3-(3-phenylpropyl)-3-azabicyclo[3.3.1]nonan-1-yl)methyl 2-((*S*)-3-methyl-2,5-dioxopyrrolidin-1-yl)benzoate (**18**)

Compound **7** (0.91 mmol, 300 mg) was reduced using LAH (2.28 mmol, 86.3 mg) as described for compound **9**. The crude product was used for the esterification step without purification.

Compound **13** (0.17 mmol, 40.3 mg) was stirred with DCC (0.17 mmol, 36 mg, 99%) and DMAP (0.017 mmol, 2.1 mg, 99%) in anhydrous acetonitrile under nitrogen gas at 40 °C for 20 min, and then the crude amino alcohol (50 mg) was added. The reaction monitored by TLC and stopped after 24 h. The mixture was concentrated under vacuum and purified over column chromatography with 5% MeOH in DCM to yield the title compound **18** (26 mg, 30 %) as a yellow oil.  $R_f = 0.57$  (5% MeOH in DCM). HRMS (ESI):  $m/z$  calcd. for  $C_{30}H_{37}N_2O_5$ : 505.2703, found: 505.2701  $[M+H]^+$ .  $^1H$  NMR (500 MHz,  $CD_3OD$ ):  $\delta$  (ppm) = 1.41 (d,  $J = 7.5$  Hz,  $H5'''$ ), 1.49-1.74 (m, 3H,  $H6_{eq}$ ,  $H7_{eq}$ ,  $H8_{eq}$ ), 1.66-1.88 (m, 1H,  $H8_{ax}$ ), 1.89-1.96 (m, 1H,  $H5$ ), 1.96-2.02 (m, 2H,  $NCH_2CH_2CH_2Ph$ ), 2.04-2.12 (m, 1H,  $H6_{ax}$ ), 2.13-2.26 (m, 1H,  $H7_{ax}$ ), 2.29-2.39 (m, 1H,  $H2_{ax}$ ), 2.42-2.55 (m, 2H,  $H4_{ax}$  and  $H3'''A$ ), 2.57-2.63 (m, 2H,  $NCH_2CH_2CH_2Ph$ ), 2.64-2.74 (m, 2H,  $NCH_2CH_2CH_2Ph$ ), 3.01-3.06 (m, 1H,  $H2_{eq}$ ), 3.05-3.16 (m, 3H,  $H4_{eq}$ ,  $H2'''$  and  $H3'''B$ ), 3.63-3.68 (m, 1H,  $H9$ ), 4.04-4.16 (m, 2H,  $H1' A$  and  $B$ ), 7.12-7.30 (m, 5H,  $NCH_2CH_2CH_2Ph$ ), 7.34 (dd,  $J = 7.7, 1.3$  Hz, 1H,  $H3''$ ), 7.58 (td,  $J = 7.7, 1.3$  Hz, 1H,  $H5''$ ), 7.72 (td,  $J = 7.7, 1.6$  Hz, 1H,  $H4''$ ), 8.10 (dd,  $J = 7.7, 1.6$  Hz, 1H,  $H6''$ ).  $^{13}C$  NMR (125 MHz,  $CDCl_3$ ):  $\delta$  (ppm) = 16.5 ( $5'''$ ), 21.0 (C7), 24.3 (C6), 27.6 (C8), 32.0 ( $NCH_2CH_2CH_2Ph$ ), 34.0 ( $NCH_2CH_2CH_2Ph$ ), 36.64 (C2'''), 36.72 (C5), 38.10 (C3'''), 39.61 (C1), 59.88 (C4), 60.53 ( $NCH_2CH_2CH_2Ph$ ), 61.42 (C2), 70.57 (C1'), 71.67 (C9), 126.98 (C4 Ph), 128.87 (C1''), 129.33, 129.56 (C2 Ph, C3 Ph, C5 Ph, C6 Ph), 130.43 (C5''), 131.06 (C3''), 132.36 (C6''), 133.57 (C2''), 134.43 (C4''), 143.0 (C1 Ph), 166.4 (ester), 177.4 (C4'''), 182.0 (C1''').

((*9R*)-9-Hydroxy-3-(4-phenylbutyl)-3-azabicyclo[3.3.1]nonan-1-yl)methyl 2-((*S*)-3-methyl-2,5-dioxopyrrolidin-1-yl)benzoate (**19**)

Compound **8** (0.58 mmol, 200 mg) was reduced using LAH (1.54 mmol, 55 mg) as described for compound **9**. The crude product was used for the esterification step without purification.

Compound **13** (0.158 mmol, 36.8 mg) was stirred with DCC (0.158 mmol, 32.9 mg, 99%) and DMAP (0.0158 mmol, 1.9 mg, 99%) in anhydrous acetonitrile under nitrogen gas at 40 °C for 20 min, and then the crude amino alcohol (48 mg) was added. The reaction monitored by TLC and stopped after 24 h. The mixture was concentrated under vacuum and purified over column chromatography with 5% MeOH in DCM to yield the title compound **19** (20 mg, 25 %) as a yellow oil.  $R_f = 0.61$  (5% MeOH in DCM). HRMS (ESI):  $m/z$  calcd. for  $C_{31}H_{39}N_2O_5$ : 519.2859, found: 519.2851  $[M+H]^+$ .  $^1H$  NMR (500 MHz,  $CD_3OD$ ):  $\delta$  (ppm) = 1.41 (d,  $J = 7.1$  Hz,  $H5'''$ ), 1.46-1.74 (m, 3H,  $H6_{eq}$ ,  $H7_{eq}$ ,  $H8_{eq}$ ), 1.79-1.97 (m, 4H,  $H5$ ,  $H8_{ax}$  and  $NCH_2CH_2CH_2CH_2Ph$ ), 1.98-2.10 (m, 3H,  $H6_{ax}$  and  $NCH_2CH_2CH_2CH_2Ph$ ), 2.17-2.29 (m, 1H,  $H7_{ax}$ ), 2.33-2.42 (m, 1H,  $H2_{ax}$ ), 2.43-2.52 (m, 2H,  $H4_{ax}$  and  $H3'''A$ ), 2.54-2.61 (m, 2H,  $NCH_2CH_2CH_2CH_2Ph$ ), 2.62-2.77 (m, 2H,  $NCH_2CH_2CH_2CH_2Ph$ ), 2.99-3.05 (m, 1H,  $H2_{eq}$ ), 3.06-3.16 (m, 3H,  $H4_{eq}$ ,  $H2'''$  and  $H3'''B$ ), 3.62-3.66 (m, 1H,  $H9$ ), 4.01-4.18 (m, 2H,  $H1' A$  and  $B$ ), 7.10-7.30 (m, 5H,  $NCH_2CH_2CH_2Ph$ ), 7.34 (dd,  $J = 7.9, 1.3$  Hz, 1H,  $H3''$ ), 7.58 (td,  $J = 7.9, 1.3$  Hz, 1H,  $H5''$ ), 7.72 (td,  $J = 7.9, 1.6$  Hz, 1H,  $H4''$ ), 8.10 (dd,  $J = 7.9, 1.6$  Hz, 1H,  $H6''$ ).  $^{13}C$  NMR (125 MHz,  $CDCl_3$ ):  $\delta$  (ppm) = 16.5 ( $5'''$ ), 21.1 (C7), 24.4 (C6), 28.8 (C8), 32.0 ( $NCH_2CH_2CH_2CH_2Ph$ ), 34.71 ( $NCH_2CH_2CH_2CH_2Ph$ ), 36.33 ( $C2'''$ ), 36.59 ( $NCH_2CH_2CH_2CH_2Ph$ ), 37.19 (C5), 38.05 ( $C3'''$ ), 39.54 (C1), 60.00 (C4), 60.48 ( $NCH_2CH_2CH_2CH_2Ph$ ), 61.26 (C2), 70.35 ( $C1'$ ), 71.70 (C9), 127.07 (C4 Ph), 128.50 ( $C1''$ ), 129.35, 129.50 (C2 Ph, C3 Ph, C5 Ph, C6 Ph), 130.45 ( $C5''$ ), 131.05 ( $C3''$ ), 132.35 ( $C6''$ ), 133.35 ( $C2''$ ), 134.47 ( $C4''$ ), 143.0 (C1 Ph), 166.5 (ester), 177.4 ( $C4'''$ ), 181.9 ( $C1'''$ ).

((*9R*)-9-Hydroxy-3-methyl-3-azabicyclo[3.3.1]nonan-1-yl)methyl 2-acetamidobenzoate (**20**)

Compound **3** (0.89 mmol, 200 mg) was reduced using LAH (1.78 mmol, 84.2 mg) as described for compound **9**. The crude product was used for the esterification step without purification.

Compound **11** (0.189 mmol, 33.8 mg) was stirred with DCC (0.189 mmol, 39.4 mg, 99%) and

DMAP (0.0189 mmol, 2.3 mg, 99%) in anhydrous acetonitrile under nitrogen gas at 40 °C for 20 min, and then the crude amino alcohol (35 mg) was added. The reaction monitored by TLC and stopped after 24 h. The mixture was concentrated under vacuum and purified over column chromatography with 5% MeOH in DCM to yield the title compound **20** (29 mg, 45 %) as a yellow oil.  $R_f = 0.6$  (5% MeOH in DCM). HRMS (ESI):  $m/z$  calcd. for  $C_{19}H_{27}N_2O_4$ : 347.1971, found: 347.1969  $[M+H]^+$ .  $^1H$  NMR (500 MHz,  $CD_3OD$ ):  $\delta$  (ppm) = 1.43-1.59 (m, 3H,  $H_{6eq}$ ,  $H_{7eq}$ ,  $H_{8eq}$ ), 1.78-1.83 (m, 1H,  $H_{8ax}$ ), 1.86 (br s, 1H, H5), 1.99-2.08 (m, 1H,  $H_{6ax}$ ), 2.18 (s, 3H, N- $CH_3$ ), 2.19-2.22 (m, 4H,  $NHCOCH_3$ ,  $H_{2ax}$ ), 2.32 (d,  $J = 11.4$  Hz, 1H,  $H_{4ax}$ ), 2.53-2.61 (m, 1H,  $H_{7ax}$ ), 2.92 (d,  $J = 11.3$  Hz, 1H,  $H_{2eq}$ ), 2.95 (d,  $J = 11.4$  Hz, 1H,  $H_{4eq}$ ), 3.67 (d,  $J = 3.8$  Hz, 1H, H9), 4.08 (d,  $J = 11.0$  Hz, 1H,  $H_{1'A}$ ), 4.14 (d,  $J = 11.0$  Hz, 1H,  $H_{1'B}$ ), 7.19 (td,  $J = 7.7, 1.3$  Hz, 1H,  $H_{5''}$ ), 7.58 (ddd,  $J = 8.6, 7.7, 1.3$  Hz, 1H,  $H_{4''}$ ), 8.05 (dd,  $J = 7.7, 1.3$  Hz, 1H,  $H_{6''}$ ), 8.46 (d,  $J = 8.6$  Hz, 1H,  $H_{3''}$ ).  $^{13}C$  NMR (125 MHz,  $CDCl_3$ ):  $\delta$  (ppm) = 21.3 (C7), 24.48 ( $NHCOCH_3$ ), 24.77 (C6), 28.0 (C8), 37.35 (C5), 39.44 (C1), 46.1 ( $NCH_3$ ), 61.9 (C4), 64.2 (C2), 71.09 (C1'), 72.00 (C9), 116.6 (C1''), 121.5 (C3''), 124.1 (C5''), 131.3 (C6''), 134.8 (C4''), 140.4 (C2''), 167.5 (ester), 169.9 (amide).

((*9R*)-3-Ethyl-9-hydroxy-3-azabicyclo[3.3.1]nonan-1-yl)methyl 2-acetamidobenzoate (**21**)

Compound **11** (0.8 mmol, 143.9 mg) was stirred with DCC (0.8 mmol, 167 mg, 99%) and DMAP (0.08 mmol, 9.9 mg, 99%) in anhydrous acetonitrile under nitrogen gas at 40 °C for 20 min, and then compound **9** (160 mg) was added. The reaction monitored by TLC and stopped after 24 h. The mixture was concentrated under vacuum and purified over column chromatography with 5% MeOH in DCM to yield the title compound **21** (130 mg, 45 %) as a yellow oil.  $R_f = 0.64$  (5% MeOH in DCM). HRMS (ESI):  $m/z$  calcd. for  $C_{20}H_{29}N_2O_4$ : 361.2127, found: 361.2122  $[M+H]^+$ .  $^1H$  NMR (500 MHz,  $CD_3OD$ ):  $\delta$  (ppm) = 1.20 (t,  $J = 7.2$  Hz, 3H,  $NCH_2CH_3$ ), 1.52-1.66 (m, 3H,  $H_{6eq}$ ,  $H_{7eq}$ ,  $H_{8eq}$ ), 1.81-1.92 (m, 1H,  $H_{8ax}$ ), 1.99-2.16 (m, 2H, H5 and  $H_{6ax}$ ), 2.20 (s, 3H,  $NHCOCH_3$ ), 2.24-2.34 (m, 1H,  $H_{7ax}$ ), 2.58-2.80 (m, 4H,  $H_{2ax}$ ,  $H_{4ax}$  and  $NCH_2CH_3$ ), 3.27-3.36 (m, 2H,  $H_{2eq}$  and  $H_{4eq}$ ), 3.82 (d,  $J = 3.5$  Hz, 1H, H9), 4.09 (d,  $J = 11.2$  Hz, 1H,  $H_{1'A}$ ), 4.21 (d,  $J = 11.2$  Hz, 1H,  $H_{1'B}$ ), 7.20 (t,  $J = 7.7$  Hz, 1H,  $H_{5''}$ ), 7.58 (ddd,  $J = 8.7, 7.7, 1.7$  Hz, 1H,  $H_{4''}$ ), 8.07 (dd,  $J = 7.7, 1.3$  Hz, 1H,  $H_{6''}$ ), 8.42 (d,  $J = 8.7$  Hz, 1H,  $H_{3''}$ ).



$^{13}\text{C}$  NMR (125 MHz,  $\text{CDCl}_3$ ):  $\delta$  (ppm) = 11.2 ( $\text{NCH}_2\text{CH}_3$ ), 20.5 (C7), 23.76 (C6), 24.53 ( $\text{NHCOCH}_3$ ), 26.9 (C8), 36.4 (C5), 39.4 (C1), 54.3 ( $\text{NCH}_2\text{CH}_3$ ), 58.90 (C4), 60.63 (C2), 69.88 (C9), 70.16 (C1'), 118.2 (C1''), 121.8 (C3''), 123.9 (C5''), 131.6 (C6''), 135.0 (C4''), 141.5 (C2''), 169.0 (ester), 171.5 (amide).

## Electrophysiological Methods

Oocyte expression studies employed the human  $\alpha 7$  nAChR subunit in plasmid pSP64GL.<sup>32</sup> Oocytes were isolated from adult female *Xenopus laevis* and defolliculated by treatment with collagenase by Victoria R. Sanders and Prof Neil S. Millar,<sup>33-35</sup> University College London, Gower Street, London WC1E 6BT, U.K. funded by a BBSRC Industrial CASE PhD studentship associated with the London Interdisciplinary Doctoral Program (LIDo) and in collaboration with Syngenta [Grant BB/ M009513/1] awarded to Victoria R. Sanders.

## REFERENCES

- (1) Galzi, J. L.; Revah, F.; Bessis, A.; Changeux, J.-P. Functional architecture of the nicotinic acetylcholine receptor: from electric organ to brain. *Annu. Rev. Pharmacol. Toxicol.* **31**, **1991**, 37–72.
- (2) Changeux, J.-P. The nicotinic acetylcholine receptor: A typical ‘Allosteric Machine’. *Philos. Trans. R. Soc. B Biol. Sci.* **2018**, *373*, 20170174.
- (3) Millar, N. S.; Gotti, C. Diversity of vertebrate nicotinic acetylcholine receptors. *Neuropharmacol.* **2009**, *56* (1), 237-246.
- (4) Borroni, V.; Barrantes, F. J. Homomeric and heteromeric  $\alpha 7$  nicotinic acetylcholine receptors in health and some Central Nervous System diseases. *Membranes* **2021**, *11* (9), 664, <https://www.mdpi.com/2077-0375/11/9/664>
- (5) Chatzidaki, A.; Millar, N. S. Allosteric modulation of nicotinic acetylcholine receptors. *Biochem. Pharmacol.* **2015**, *97*, 408-417.

- (6) Wonnacott, S.; Albuquerque, E. X.; Bertrand, D. MLA discriminates between nicotinic receptor subclasses. *Methods Neurosciences* **1993**, 263–275.
- (7) Shen, Y.; Liang, W. J.; Shi, Y. N.; Kennelly, E. J.; Zhao, D. K. Structural diversity, bioactivities, and biosynthesis of natural diterpenoid alkaloids. *Nat. Prod. Rep.* **2020**, 37 (6), 763–796. <https://doi.org/10.1039/d0np00002g>.
- (8) Qasem, A. M. A.; Zeng, Z.; Rowan, M. G.; Blagbrough, I. S. Norditerpenoid alkaloids from *Aconitum* and *Delphinium*: Structural relevance in medicine, toxicology, and metabolism. *Nat. Prod. Rep.* **2022**, 39, 460-473 <https://doi.org/10.1039/d1np00029b>
- (9) Panter, K. E., Manners, G. D., Stegelmeier, B. L., Lee, S., Gardner, D. R., Ralphs, M. H., Pfister, J. A.; James, L. F. Larkspur poisoning: Toxicology and alkaloid structure-activity relationships. *Biochem. Systematics and Ecology* **2002**, 30 (2), 113–128. [https://doi.org/10.1016/S0305-1978\(01\)00123-5](https://doi.org/10.1016/S0305-1978(01)00123-5).
- (10) Dobelis, P.; Madl, J. E.; Pfister, J. A.; Manners, G. D.; Walrond, J. P. Effects of Delphinium alkaloids on neuromuscular transmission. *J. Pharm. Exp. Therap.* **1999**, 291 (2), 538–546.
- (11) Jennings, K. R.; Brown, D. G.; Wright, D. P. Methyllycaconitine, a naturally occurring insecticide with a high affinity for the insect cholinergic receptor. *Experientia* **1986**, 42 (6), 611–613. <https://doi.org/10.1007/BF01955557>.
- (12) Trigg, W. J.; Hardick, D. J.; Grangier, G.; Wonnacott, S.; Lewis, T.; Rowan, M. G.; Potter, B. V. L.; Blagbrough, I. S. Selective probes for nicotinic acetylcholine receptors from substituted AE-bicyclic analogs of methyllycaconitine, *ACS Symposium Series*, (Eds. D. R. Baker, J. G. Fenyves, G. S. Basarab, and D. A. Hunt), **1998**, 686, 194-205.
- (13) Manners, G. D.; Panter, K. E.; Pelletier, S. W. Structure-activity relationships of norditerpenoid alkaloids occurring in toxic larkspur (delphinium) species. *J. Nat. Prod.* **1995**, 58 (6), 863–869. <https://doi.org/10.1021/np50120a007>.
- (14) Hardick, D. J.; Blagbrough, I. S.; Cooper, G.; Potter, B. V. L.; Critchley, T.; Wonnacott, S. Nudicauline and elatine as potent norditerpenoid ligands at rat neuronal  $\alpha$ -bungarotoxin binding sites: Importance of the 2-(methylsuccinimido)benzoyl moiety for neuronal nicotinic

acetylcholine receptor binding. *J. Med. Chem.* **1996**, *39* (24), 4860–4866.

<https://doi.org/10.1021/jm9604991>.

(15) Blagbrough, I. S.; Coates, P. A.; Hardick, D. J.; Lewis, T.; Rowan, M. G.; Wonnacott, S.; Potter, B. V. L. Acylation of lycoctonine: semi-synthesis of inuline, delsemine analogues and methyllycaconitine. *Tetrahedron Lett.* **1994**, *35*, 8705-8708.

(16) Hardick, D. J.; Cooper, G.; Scott-Ward, T.; Blagbrough, I. S.; Potter, B. V. L.; Wonnacott, S. Conversion of the sodium channel activator aconitine into a potent  $\alpha 7$ -selective nicotinic ligand. *FEBS Lett.* **1995**, *365*, 79-82.

(17) Bergmeier, S. C.; Lapinsky, D. J.; Free, R. B.; McKay, D. B. Ring E analogs of methyllycaconitine (MLA) as novel nicotinic antagonists. *Bioorg. Med. Chem. Lett.* **1999**, *9* (15), 2263–2266. [https://doi.org/10.1016/S0960-894X\(99\)00378-9](https://doi.org/10.1016/S0960-894X(99)00378-9).

(18) Bryant, D. L.; Free, R. B.; Thomasy, S. M.; Lapinsky, D. J.; Ismail, K. A.; McKay, S. B.; Bergmeier, S. C.; McKay, D. B. Structure-activity studies with ring E analogues of methyllycaconitine on bovine adrenal  $\alpha 3\beta 4^*$  nicotinic receptors. *Neuroscience Res.* **2002**, *42* (1), 57–63. [https://doi.org/10.1016/S0168-0102\(01\)00304-2](https://doi.org/10.1016/S0168-0102(01)00304-2).

(19) Coates, P. A.; Blagbrough, I. S.; Rowan, M. G.; Potter, B. V. L.; Pearson, D. P. J.; Lewis, T. Rapid and efficient entry to substituted 2-succinimidobenzoate-3-azabicyclo[3.3.1]nonanes: AE-bicyclic analogues of methyllycaconitine. *Tetrahedron Lett.* **1994**, *35*, 8709-8712.

(20) Grangier, G.; Trigg, W. J.; Lewis, T.; Rowan, M. G.; Potter, B. V. L.; Blagbrough, I. S. Synthesis of C5-substituted AE-bicyclic analogues of lycoctonine, inuline and methyllycaconitine. *Tetrahedron Lett.* **1998**, *39*, 889-892.

(21) Barker, D.; Brimble, M. A.; McLeod, M. D. Synthesis of simple analogues of methyllycaconitine — an efficient method for the preparation of the N-substituted anthranilate pharmacophore. *Tetrahedron* **2004**, *60* (28), 5953–5963.

<https://doi.org/10.1016/j.tet.2004.05.024>.

(22) Coates, P. A.; Blagbrough, I. S.; Hardick, D. J.; Rowan, M. G.; Wonnacott, S.; Potter, B. V. L. Rapid and efficient isolation of the nicotinic receptor antagonist methyllycaconitine from Delphinium: assignment of the methylsuccinimide absolute stereochemistry as *S*. *Tetrahedron Lett.* **1994**, *35*, 8701-8704.

- (23) Hardick, D. J.; Blagbrough, I. S.; Potter, B. V. L. Isotopic enrichment by asymmetric deuteration. An investigation of the synthesis of deuteriated (S)-(-)-methylsuccinic acids from itaconic acid. *J. Amer. Chem. Soc.* **1996**, *118* (25), 5897–5903.  
<https://doi.org/10.1021/ja950597w>.
- (24) Barker, D.; Brimble, M. A.; McLeod, M. D. A convenient synthesis of 2-(3-methyl-2,5-dioxopyrrolidin-1-yl)benzoic acid. *Synthesis* **2003**, (5), 656–658.
- (25) Ismail, K. A.; Bergmeier, S. C. Structure–activity studies with ring E analogues of methyllycaconitine. Synthesis and evaluation of enantiopure isomers of selective antagonist at the  $\alpha_3$  nicotinic receptor. *Eur. J. Med. Chem.* **2002**, *37*, 469–474.
- (26) Zeng, Z.; Qasem, A. M. A.; Kociok-Köhn, G.; Rowan, M. G.; Blagbrough, I. S. The 1 $\alpha$ -hydroxy-A-rings of norditerpenoid alkaloids are twisted-boat conformers. *RSC Advances*, **2020**, *10* (32), 18797–18805. <https://doi.org/10.1039/D0RA03811C>.
- (27) Harwood, L. M.; Claridge, T. D. W. 1997. *Introduction to Organic Spectroscopy*. Oxford University Press, p. 39.
- (28) Fleming, I.; Williams, D. H. *Spectroscopic Methods in Organic Chemistry*. 7th ed. Basel: Springer, **2019**, p. 231, <https://doi.org/10.1007/978-3-030-18252-6>.
- (29) Bergmeier, S. C.; Ismail, K. A.; Arason, K. M.; McKay, S.; Bryant, D. L.; McKay, D. B. Structure activity studies of ring E analogues of methyllycaconitine. Part 2: Synthesis of antagonists to the  $\alpha_3\beta_4$  nicotinic acetylcholine receptors through modifications to the ester. *Bioorg. Med. Chem. Lett.* **2004**, *14* (14), 3739–3742.
- (30) McKay, D. B.; Chang, C.; González-Cestari, T. F.; McKay, S. B.; El-Hajj, R. A.; Bryant, D. L.; Zhu, M. X.; Swaan, P. W.; Arason, K. M.; Pulipaka, A. B.; Orac, C. M.; Bergmeier, S. C. Analogs of methyllycaconitine as novel noncompetitive inhibitors of nicotinic receptors: Pharmacological characterization, computational modeling, and pharmacophore development. *Mol. Pharmacol.* **2007**, *71* (5), 1288–1297. <https://doi.org/10.1124/mol.106.033233>.
- (31) Huang, J.; Orac, C. M.; McKay, S.; McKay, D. B.; Bergmeier, S. C. The synthesis of 5-substituted ring E analogs of methyllycaconitine via the Suzuki-Miyaura cross-coupling reaction. *Bioorg. Med. Chem.* **2008**, *16* (7), 3816–3824.

- (32) Broadbent, S.; Groot-Kormelink, P. J.; Krashia, P. A.; Harkness, P. C.; Millar, N. S.; Beato, M.; Sivilotti, L. G. Incorporation of the  $\beta 3$  subunit has a dominant-negative effect on the function of recombinant central-type neuronal nicotinic receptors. *Mol. Pharmacol.* **2006**, *70*, 1350-1356.
- (33) Young, G. T.; Zwart, R.; Walker, A. S.; Sher, E.; Millar, N. S. Potentiation of  $\alpha 7$  nicotinic acetylcholine receptors via an allosteric transmembrane site. *Proc. Natl. Acad. Sci. USA* **2008**, *105*, 14686-14691.
- (34) Young G. T.; Broad, L. M.; Zwart, R.; Astles, P. C.; Bodkin, M.; Sher, E.; Millar, N. S. Species selectivity of a nicotinic acetylcholine receptor agonist is conferred by two adjacent extracellular  $\beta 4$  amino acids that are implicated in the coupling of binding to channel gating. *Mol. Pharmacol.* **2007**, *71*, 389-397.
- (35) Gill, J. K.; Dhankher, P.; Sheppard, T. D.; Sher, E.; Millar, N. S. A series of  $\alpha 7$  nicotinic acetylcholine receptor allosteric modulators with close chemical similarity but diverse pharmacological properties. *Mol. Pharmacol.* **2012**, *81*, 710-718.

## Chapter 9

### Conclusions

This research project is focussed on the characterization of norditerpenoid alkaloids (NDA) in their natural sources by isolation, some aspects of quantification, and detailed analytical chemistry. Analysis of NDA using NMR spectroscopy of various solutions and MS (vapour phase analysis) led to a better understanding of their possible 3D-conformations in biological fluids. The synthesis of small molecule AE-bicyclic NDA analogues with different ester and N-side-chains gave a better understanding of their structure-activity relationships (SAR).

Plants from *Aconitum* and *Delphinium* are well-known as herbal medicines, but it is dose dependent as they also contain highly toxic NDA, e.g. aconitine, and therefore such herbal medicines are banned in the UK. *Delphinium* extracts were well-known for their pediculicide activity where *Delphinium* seeds, pounded and extracted into wine (ethanol), rid the head and body of lice. Packets of *Delphinium* seeds were even reportedly issued to British soldiers at the battle of Waterloo (still for the treatment of body lice). The application of *Aconitum* plants as analgesics in TCM, especially for the treatment of rheumatism, is known since 200–250 A.D. Thus, there is no doubt that *Aconitum* is useful in the clinical treatment. Aconitine, which is the first isolated NDA and thus it is named after this plant, is one of the main toxicological components of every species of *Aconitum*, and this natural product is known to be one of the most toxic NDA in the world. The bioactivities of *Aconitum* alkaloids vary, for instance, aconitine can induce arrhythmia as it maintains cardiac voltage-sensitive sodium channels (VSSCs) in an open-state, thus it could be lethal (depending upon dose). However, its derivative, 3-*O*-acetylaconitine, is less toxic and is allowed to be clinically used as an analgesic in China. Moreover, C<sub>18</sub>-diterpenoid alkaloid lappaconitine isolated from *Aconitum* plants even displays antiarrhythmic activity by the blockade of VSSCs, and its HBr salt, allapinin is an antiarrhythmic agent in China and Russia.

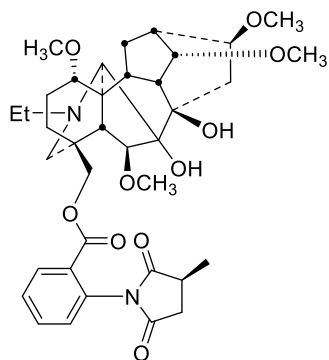
The first theme of this research is the identification of NDA in their natural sources, *Delphinium* and *Aconitum* plants. The phytochemical investigation of *D. elatum* seeds resulted in the isolation of four NDA: methyllycaconitine (MLA) **1**, shawurensine A **2**, shawurensine B **3**, and delpheline **4**. MLA **1** is a potent competitive antagonist at  $\alpha 7$  nAChRs where a rare pharmaceutical preparation, mellictin, was reported in a few countries like Uzbekistan and Kyrgyzstan to be used clinically to treat Parkinson's disease and cerebral palsy. Shawurensine has a similar structure to MLA with a succinimide opened (hydrolysed) side-chain. The SAR importance of the open (by methanolysis) side-chain was reported where it was found that the delavaines ( $LD_{50} = 3.3 \mu\text{g/kg}$ ) are more toxic than MLA **1** ( $LD_{50} = 7.5 \mu\text{g/kg}$ ) when tested in mice. Shawurensine A **2** antifeedant activity was found to be higher than MLA **1** against the larvae of *Spodoptera exigua* (Hübner).

For the use of *Aconitum* plants in TCM, the key for safe application is the dose. Indeed, the poisoning by the clinical use of *Aconitum* plants is widely reported. For the safe clinical administration of *Aconitum* in modern TCM, the total amount of both di- and monoester-type diterpenoid alkaloids is limited in the current Chinese Pharmacopeia. Indeed, due to the various bioactivities of *Aconitum* alkaloids, it is essential to understand the amount of certain key components in detail. Thus, the quantitative analysis on both toxic and pharmacologically active components of *Aconitum* product should be investigated in-depth, for discovering a safe and effective dose of medicinal applications of TCM. Diester norditerpenoid alkaloids (DDA) (mainly aconitine, mesaconitine, and hypaconitine) possess cardiac and analgesic activities, but due to their high toxicity, these herbal preparations are used after processing to convert DDA into monoester diterpenoid alkaloids (MDA) (benzoylaconine, benzoylmesaconine, and benzoylhypaconine) which are less toxic, but still biologically active. The possible safety and effectiveness have been assessed for five *Aconitum* TCM preparations through the quantification of six NDA markers. It was found that the total DDA amount is within the Chinese Pharmacopeia limit and therefore they can be safely used. On the other hand, only Zhi'cao'wu met the Chinese Pharmacopeia limit for the total MDA amount which ensures the preparation efficacy, while the others do not contain enough NDA to show the expected therapeutic activity.

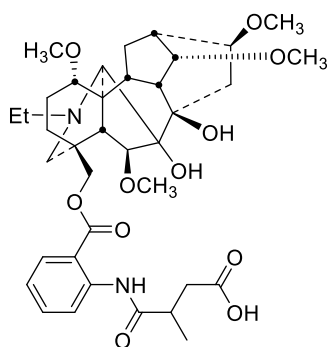
In addition to the safety and effectiveness of TCM, adulteration is a main concern where it is important to identify preparation markers to assess their quality. Therefore, chemical profiling of the selected TCM preparations was accomplished where compounds were identified based on their fragments with comparison to databases. These results highlight the importance of quality control studies on TCM preparations to ensure their effectiveness and safety and therefore it would be more appropriate in modern medicine to formulate medicines of a single component with a desired therapeutic activity, justifying the importance of the work in the following themes of this project where the characterization and analogue synthesis of active NDA will contribute to the drug discovery journey to get potent medicines acting on nAChR and VGSC.

The second theme of this research project is the in-solution characterization of NDA using NMR spectroscopy and mass spectrometry (MS). It was observed using NMR spectroscopy that the A-ring in 1-OH NDA adopts a boat conformation compared to a chair conformer in 1-OMe NDA due to the intramolecular H-bonding between that 1-OH group and the piperidine nitrogen. A rare  $^1\text{H}$  NMR spectroscopic effect of steric compression was observed in 1-OMe NDA in which the lone-pair electrons of the tertiary amine N-atom compress 2-H $\alpha$  through space and therefore they deshield this proton. The A-rings of NDA substituted at C1 with  $\alpha$ -orientated oxygenated functional groups adopt twisted conformers due to the repulsion between atoms attached to C1 (H- or O-atoms in the equatorial position) and 12-He, no matter whether the A-rings are in chair or boat conformations. In addition, a rare  $^{15}\text{N}$  NMR spectroscopic effect of steric compression has been demonstrated in the A/E-rings of several NDA free bases and their synthetic azabicyclic analogues using  $^1\text{H}$ - $^{15}\text{N}$  HMBC NMR spectroscopy. The distribution of the tertiary amine N-atom lone pair of electrons is restricted in the half-cage azabicycles; therefore, the electron density of the N-atom increases and its  $\delta_{\text{N}}$  decreases.  $\delta_{\text{N}}$  of NDA bearing 1 $\alpha$ -OMe significantly increase on protonation. The intramolecular hydrogen bonds between the N-atom and 1 $\alpha$ -OH of 1 $\alpha$ -OH NDA free bases not only stabilize the A-rings, adopting a twisted-boat conformation, but they also increase the  $\delta_{\text{N}}$  of the tertiary amine N-atom. Thus,  $^1\text{H}$ - $^{15}\text{N}$  HMBC spectroscopy has been demonstrated to be an excellent reporter for the analysis of the electron density of substituted piperidine alkaloids. It is particularly useful for certain NDA with complex substitution patterns and half-cage skeleta.

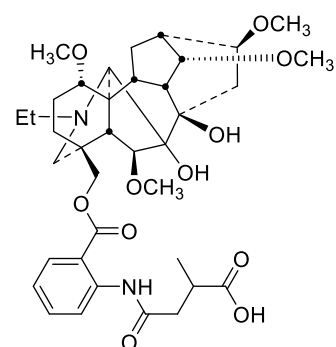




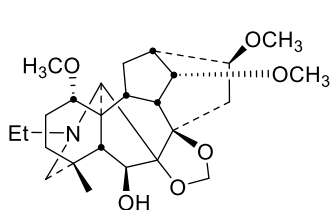
Methyllycaconitine **1**



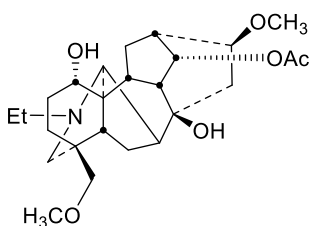
Shawurensine A **2**



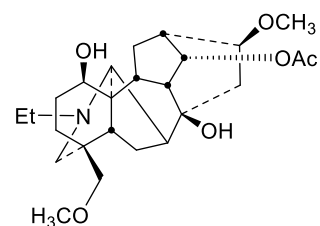
Shawurensine B **3**



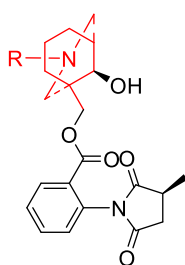
Delpheline **4**



Condelphine **5**

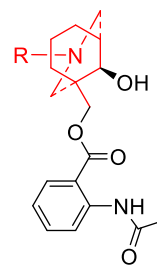


1-*epi*-Condelphine **6**



Analogues **7-12**

- 7** R = Me
- 8** R = Et
- 9** R = benzyl
- 10** R = 2-phenylethyl
- 11** R = 3-phenylpropyl
- 12** R = 4-phenylbutyl



Analogues **13-14**

- 13** R = Me
- 14** R = Et

The stability of NDA skeleton was studied using APCI-MS where it was observed that the alpha ( $\alpha$ )-substituent at carbon 1 affects the stability of NDA towards fragmentation. It was found that 1-OH NDA are more stable compared to 1-OMe NDA which showed higher intensity of the fragment-ion peak. That difference in stability could be due to the charge delocalisation where the positive charge delocalises in 1-OH NDA over four atoms compared to three in 1-OMe NDA which decreases the chance of the proton transfer in the fragmentation. In addition, the effect of carbon 1 substituent configuration was studied by the synthesis of 1-epi-condelphine **6** (by oxidation to the 1-ketocondelphine, followed by borohydride reduction to yield the epimer) where it was found that it is less stable in the mass spectrometer compared to condelphine **5** as the nitrogen is no longer hydrogen bonded to the  $\beta$ -OH at position 1. The application of APCI-MS is a promising technique to study the 3D configuration of NDA as it leads to a better understanding of their possible 3D-conformations in biological fluids.

The third theme of the research project is the synthesis AE-bicyclic analogues of MLA **1** with different nitrogen and ester side-chains to get a better SAR understanding of their activity at human  $\alpha 7$  nAChR. Several MLA **1** AE-bicyclic analogues were designed and synthesized with different N-side-chains and ester side-chains. Any antagonist effects of synthetic analogues were examined (in collaborative studies at UCL) on human  $\alpha 7$ -nAChR and compared to that of MLA. In SAR studies, the antagonist activity of these analogues showed little advantage of the (*S*)-2-methylsuccinimido benzoate ester side-chain especially when comparing analogue **7** with **13**. The data of analogues **7-14** highlight the effect of the N-side-chain on the antagonist activity at human  $\alpha 7$ -nAChR where the activity is in the following order: benzyl > 4-phenylbutyl > 2-phenylethyl > 3-phenylpropyl > methyl > ethyl. These data indicate that bulkier N-side-chain (with a phenyl moiety) enhance the activity compared to alkyl side-chains. The AE-bicyclic analogues showed better activity compared to the reported simple monocyclic system where the best analogue **9**, N-benzyl side-chain, inhibits the agonist response at human  $\alpha 7$ -nAChR to around 53% [1 nM]. However, these bicyclic analogues are significantly less efficacious than MLA **1**, so further molecular optimisation will be required, possibly including more of the rings of hexacyclic MLA, to achieve antagonist activity at concentrations [1 nM] comparable to those of MLA which retains its position as the most potent and selective NDA antagonist at nAChR.

## Appendices

## Appendix 1: Abstracts presented at conferences

<b>Date</b>	<b>Conference and presentation</b>	<b>Place</b>
8-11/9/2019	20 <sup>th</sup> RSC / SCI Medicinal chemistry symposium. Poster	Cambridge, UK
13-15/9/2021	21 <sup>st</sup> RSC / SCI Medicinal chemistry symposium. Poster	Cambridge, UK
17/11/2021	JPAG Pharmaceutical Analysis Research Awards and Careers Fair 2021. Flash Poster	Virtual meeting
30 <sup>th</sup> June-1 <sup>st</sup> July/2022	NMR Discussion Group Postgraduate Meeting. Poster	Manchester, UK
4-6/07/2022	SCT 29 <sup>th</sup> Young Research Fellows Meeting. Flash Poster	Nantes, France
4-8/9/2022	XXVII EFMC International Symposium on Medicinal Chemistry (EFMC-ISMC 2022). 2 Posters	Nice, France
8-9/9/2022	9 <sup>th</sup> EFMC Young Medicinal Chemists' Symposium (EFMC-YMCS 2022). 2 Posters	Nice, France

## Poster Abstract

## Synthesis of AE-Bicycle Analogues of Methyllycaconitine

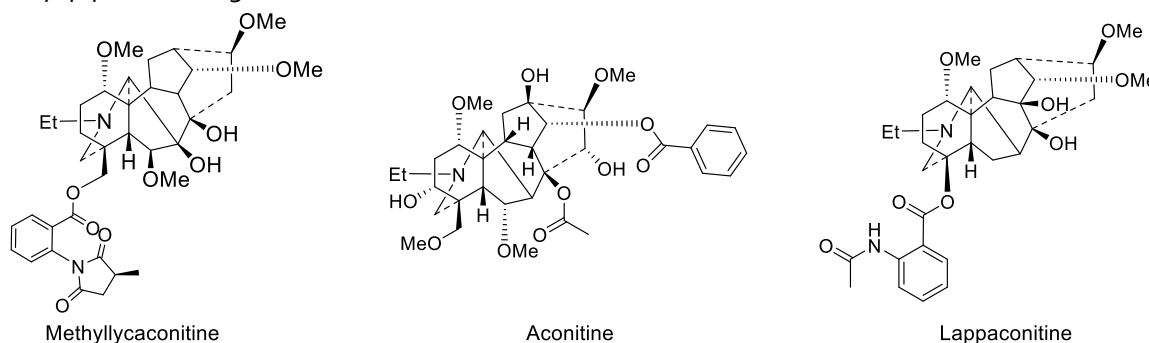
Ashraf Qasem, Michael G. Rowan, and Ian S. Blagbrough

University of Bath

Department of Pharmacy and Pharmacology, University of Bath, Bath BA2 7AY, UK

Email: [aq250@bath.ac.uk](mailto:aq250@bath.ac.uk) [prsisb@bath.ac.uk](mailto:prsisb@bath.ac.uk)

Plants from the genera *Delphinium* and *Aconitum* are used as poisons and as medicines as analgesics and antiarrhythmics in Chinese and Japanese traditional medicine (Benn & Jacyno, 1983; Wang & Chen, 2010). Norditerpenoid alkaloids are the major alkaloid group in the genera *Delphinium* and *Aconitum*. Some of these alkaloids, e.g. methyllycaconitine (MLA) act as competitive inhibitors of nicotinic acetylcholine receptors (nAChRs). However, some, e.g. lappaconitine (allapinine used clinically in Russia), close voltage-gated sodium channels whilst some, e.g. aconitine, keep them in an open conformation. These differences in pharmacological effects encourage studies on the SAR of norditerpenoid alkaloids (Hardick et al., 1996; Bryant et al., 2001; McKay et al., 2007). We are making analogues around the key N-alkyl piperidine ring.



## Acknowledgement

We acknowledge Zarqa University, Zarqa City, Jordan, for funding this PhD studentship.

## References

- Benn, M.H. and Jacyno J.M., 1983. The toxicology and pharmacology of diterpenoid alkaloids. *Alkaloids: Chemical and Biological Perspectives*, 1, pp. 153-210.
- Bryant, D.L., Free, R.B., Thomasy, S.M., Lapinsky, D.J., Ismail, K.A., McKay, S.B., Bergmeier, S.C. and McKay, D.B., 2002. Structure–activity studies with ring E analogues of methyllycaconitine on bovine adrenal  $\alpha_3\beta_4^*$  nicotinic receptors. *Neuroscience Research*, 42, 57-63.
- Hardick, D.J., Blagbrough, I.S., Cooper, G., Potter, B.V.L., Critchley, T. and Wonnacott, S., 1996. Nudicauline and elatine as potent norditerpenoid ligands at rat neuronal  $\alpha$ -bungarotoxin binding sites: importance of the 2-(methylsuccinimido)benzoyl moiety for neuronal nicotinic acetylcholine receptor binding, *J Medicinal Chemistry*, 39, 4860-4866.
- McKay, D.B., Chang, C., González-Cestari, T.F., McKay, S.B., El-Hajj, R.A., Bryant, D.L., Zhu, M.X., Swaan, P.W., Arason, K.M., Pulipaka, A.B. and Orac, C.M., 2007. Analogs of methyllycaconitine as novel noncompetitive inhibitors of nicotinic receptors: Pharmacological characterization, computational modeling, and pharmacophore development. *Molecular Pharmacology*, 71, 1288-1297.
- Wang, F.P. and Chen, Q.H., 2010. The C19-diterpenoid alkaloids. *The Alkaloids: Chemistry and Biology*, 69, pp. 1-577.

## Analogues of methyllycaconitine and lappaconitine

Ashraf M. A. Qasem, Michael G. Rowan, and Ian S. Blagbrough\*

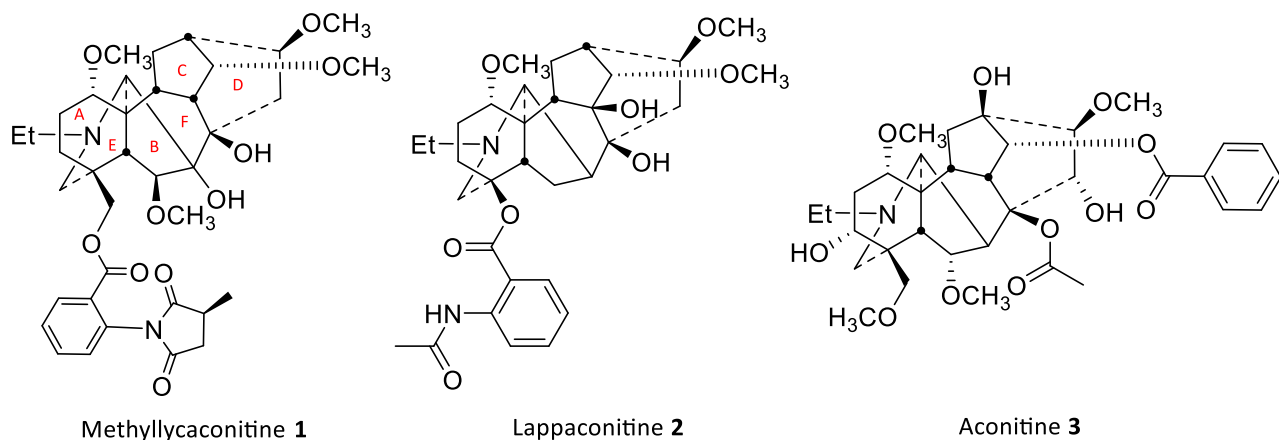
Department of Pharmacy and Pharmacology, University of Bath, Bath BA2 7AY, UK

Email: [prsisb@bath.ac.uk](mailto:prsisb@bath.ac.uk)

I wish to be considered for a Poster Presentation

### Summary

Plants from the genera *Delphinium* and *Aconitum* are used as poisons and as medicines as analgesics and antiarrhythmics in Chinese and Japanese traditional medicine (Benn & Jacyno, 1983). Norditerpenoid alkaloids (NDAs) are the major alkaloid group of these two genera. Methyllycaconitine (MLA) **1**, a highly potent  $\alpha 7$  nicotinic acetylcholine receptor (nAChR) antagonist, and lappaconitine **2**, which is a voltage gated sodium channel (VGSC) blocker and used clinically as antiarrhythmic drug (Allapinin<sup>®</sup>), have been considered drug-like according to several molecular descriptors of the drug-likeness (Turabekova et al., 2008). On the other hand, aconitine **3**, which is an arrhythmogenic alkaloid and keeps VGSCs in their open state (Ameri, 1998), has been considered as a non-drug-like compound (Turabekova et al., 2008). These pharmacological activities encourage SAR studies on NDAs, and we have investigated, through AE-bicyclic analogues, the importance of *N*-alkyl chain length, the ester side-chain, the distance between the amine and the ester side-chain, and how these factors affect the activity at nAChRs and VGSCs.



### Acknowledgement

We acknowledge Zarqa University, Zarqa City, Jordan, for funding this PhD studentship.

### References

- Ameri, A., 1998. The effects of *Aconitum* alkaloids on the central nervous system. *Progress in Neurobiology*, 56, 211-235.
- Benn, M.H. and Jacyno J.M., 1983. The toxicology and pharmacology of diterpenoid alkaloids. in *Alkaloids: Chemical and Biological Perspectives*, 1, 153-210.
- Turabekova, M.A., Rasulev, B.F., Dzhakhangirov, F.N. and Salikhov, S.I., 2008. *Aconitum* and *Delphinium* alkaloids: "Drug-likeness" descriptors related to toxic mode of action. *Environmental Toxicology and Pharmacology*, 25, 310-320.

## Conformational analysis of norditerpenoid alkaloids using NMR and MS

Ashraf M. A. Qasem, Michael G. Rowan, and Ian S. Blagbrough\*

Department of Pharmacy and Pharmacology, University of Bath, Bath BA2 7AY, UK

\*[prsisb@bath.ac.uk](mailto:prsisb@bath.ac.uk)

### Objectives

To analyze the conformations of pharmacologically important norditerpenoid alkaloids (NDA) in solution as this provides details of the bioactive conformations in biological fluids.

### Materials and methods

The analysis of these alkaloids has been undertaken using NMR spectroscopy (Zeng et al., 2020a, 2020b), and mass spectrometry using the LC/MS-APCI method (Wada et al., 2000).

### Results

The NMR results showed a difference between 1-OH and 1-OMe NDA as 1-OH compounds form an intramolecular hydrogen bond with the piperidine ring E N-atom (Fig. 1). Therefore, ring A will adopt a boat conformation compared to the chair ring A in 1-OMe alkaloids (Zeng et al., 2020a). Such intramolecular hydrogen bonding in 1-OH alkaloids leads to a significant increase in the  $\delta_N$  of the N-atom (Zeng et al., 2020b). On the other hand, 1-OH NDA showed better stability (less fragmentation) compared to 1-OMe NDA using LC/MS-APCI (Wada et al., 2000), due to the intramolecular H-bonding.

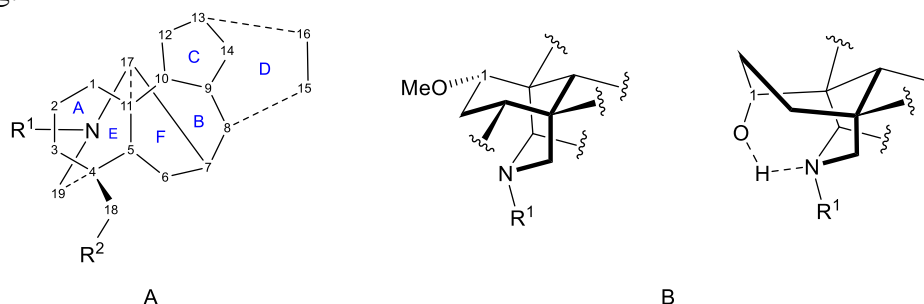


Fig. 1. A. Skeleton and numbering of NDA, B. Conformation of A-ring in 1-OMe NDA (left) and 1-OH NDA (right).

### Conclusions

1-OH NDA adopt a different conformation from 1-OMe and that results in different properties such as their  $pK_a$ . Therefore, it will affect their availability at the binding site and their biological action.

### Acknowledgment

We acknowledge Zarqa University, Zarqa City, Jordan, for funding this PhD studentship.

### References

- Wada, K., Mori, T., Kawahara, N., 2000. Stereochemistry of norditerpenoid alkaloids by liquid chromatography/atmospheric pressure chemical ionization mass spectrometry. *J. Mass Spectrom.* 35, 432–439.
- Zeng, Z., Qasem, A.M.A., Kociok-Köhn, G., Rowan, M.G., Blagbrough, I.S., 2020a. The  $1\alpha$ -hydroxy-A-rings of norditerpenoid alkaloids are twisted-boat conformers. *RSC Adv.* 10, 18797–18805.
- Zeng, Z., Qasem, A.M.A., Woodman, T.J., Rowan, M.G., Blagbrough, I.S., 2020b. Impacts of steric compression, protonation, and intramolecular hydrogen bonding on the  $^{15}\text{N}$  NMR spectroscopy of norditerpenoid alkaloids and their piperidine-ring analogues. *ACS Omega.* 5, 14116–14122.

# NMR analysis of norditerpenoid alkaloids conformation and steric compression

Ashraf M. A. Qasem, Michael G. Rowan, and Ian S. Blagbrough\*

Department of Pharmacy and Pharmacology, University of Bath, Bath BA2 7AY, UK

Email: \*prsisb@bath.ac.uk

Norditerpenoid alkaloids (NDA), from the genera *Aconitum* and *Delphinium*, have a complicated 6 fused and bridged rings. The structural identification of NDA in terms of conformation and configuration is important as their 3D structure is a key factor affecting their biological activities (Qasem et al., 2022). Using NMR, we can analyse the conformation in solution as this provides details of the bioactive conformations in biological fluids.

The NMR results showed a difference between 1 $\alpha$ -OH and 1 $\alpha$ -OMe NDA as 1-OH compounds form an intramolecular hydrogen bond with the piperidine ring E N-atom (Fig. 1). Therefore, ring A will adopt a boat conformation compared to the chair ring A in 1-OMe alkaloids (Zeng et al., 2020a). Such intramolecular hydrogen bonding in 1-OH alkaloids leads to a significant increase in the  $\delta_N$  of the N-atom (Zeng et al., 2020b). In addition, the  $^{15}\text{N}$  chemical shifts of 1 $\alpha$ -OMe norditerpenoid alkaloid free bases significantly increase on alkaloid protonation due to the formation of an intramolecular hydrogen bond between N $^+$ -H and 1 $\alpha$ -OMe. The conformational difference between 1 $\alpha$ -OH and 1 $\alpha$ -OMe results in different steric compression effects in  $^1\text{H}$ -NMR.

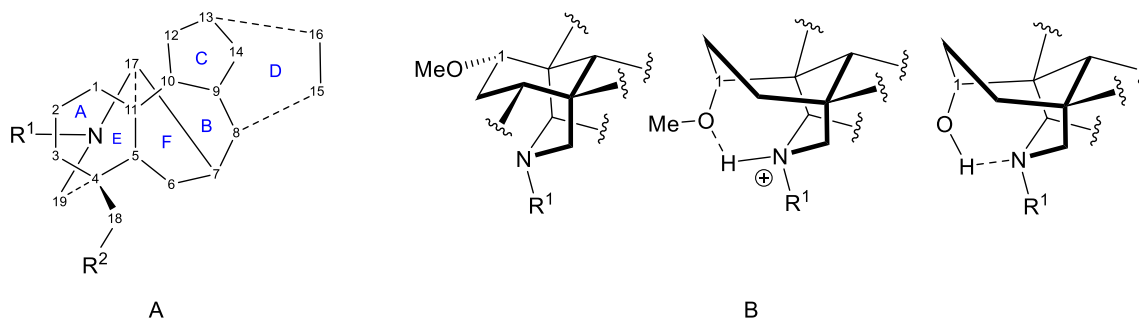


Fig. 1. A. Skeleton and numbering of NDA, B. Conformation of A-ring in 1-OMe free base NDA (left), 1-OMe NDA salt (middle) and 1-OH free base NDA (right).

## Acknowledgment

We acknowledge Zarqa University, Jordan, for funding this PhD studentship.

## References

- Qasem, A. M. A., Zeng, Z., Rowan, M.G., Blagbrough, I.S., 2022. Norditerpenoid alkaloids from *Aconitum* and *Delphinium*: structural relevance in medicine, toxicology, and metabolism, *Nat. Prod. Rep.*, **39**, 460-473.
- Zeng, Z., Qasem, A.M.A., Kociok-Köhn, G., Rowan, M.G., Blagbrough, I.S., 2020a. The 1 $\alpha$ -hydroxy-A-rings of norditerpenoid alkaloids are twisted-boat conformers. *RSC Adv.*, **10**, 18797–18805.
- Zeng, Z., Qasem, A.M.A., Woodman, T.J., Rowan, M.G., Blagbrough, I.S., 2020b. Impacts of steric compression, protonation, and intramolecular hydrogen bonding on the  $^{15}\text{N}$  NMR spectroscopy of norditerpenoid alkaloids and their piperidine-ring analogues. *ACS Omega.*, **5**, 14116–14122.



## NMR and MS analysis of norditerpenoid alkaloids

**Ashraf M. A. Qasem, Michael G. Rowan, and Ian S. Blagbrough\***

Department of Pharmacy and Pharmacology, University of Bath, Bath  
BA2 7AY, UK

Restricted  
to  
organizers

The naturally occurring norditerpenoid alkaloids (NDA) have bridged highly oxygenated hexacyclic skeleta. The analysis of their structures is important to determine their conformation. Solution studies of these alkaloids using NMR spectroscopy leads to a better understanding of their possible 3D-conformations in biological fluids as several of these alkaloids are of pharmacological and even clinical importance (Qasem et al., 2022). We are investigating the effect of C1- $\alpha$  substituents on the conformation of ring A in selected NDA (Zeng et al., 2020 a, b) and studying the through-space interactions and how they affect their MS fragmentation using LC/MS-APCI (Wada et al., 2000).

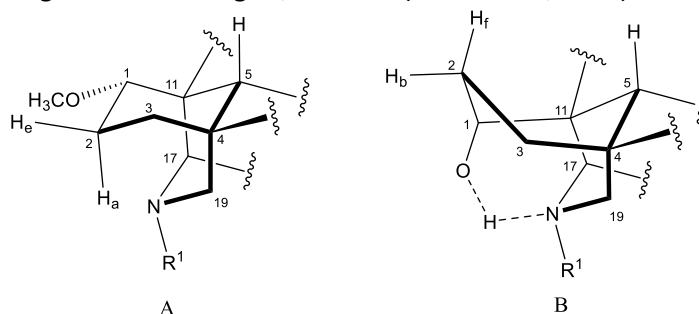


Fig. 1. A. Ring A in a twisted-chair conformation in 1-OMe NDA; B. Ring A in a twisted-boat conformation due to the intramolecular H-bond. a: axial, e: equatorial, f: flagpole, b: bowsprit

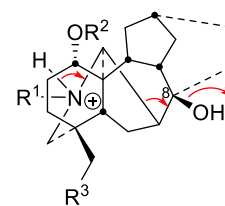
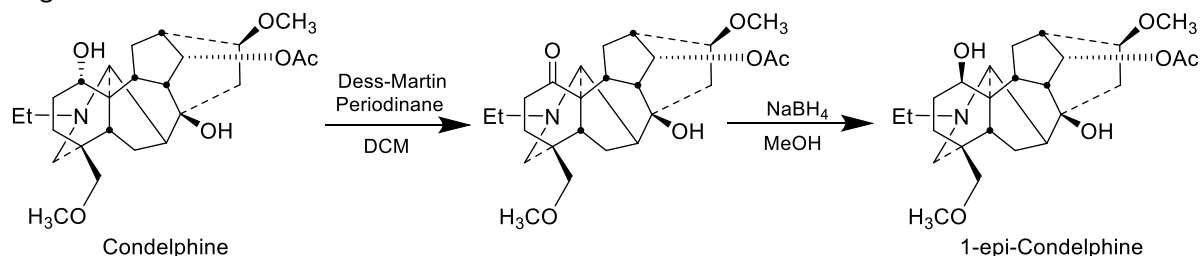


Fig. 2. Fragmentation of NDA skeleton at position 8

In addition, to exclude the effect of structure variability, we have oxidized and then reduced condelphine to get 1-epi-condelphine and to study the effect of 1-OH on NMR and MS fragmentation.



### Acknowledgement

We acknowledge Zarqa University, Jordan, for fully funding this PhD studentship.

### References

- Qasem, A. M. A., Zeng, Z., Rowan, M.G., Blagbrough, I.S., 2022. Norditerpenoid alkaloids from *Aconitum* and *Delphinium*: structural relevance in medicine, toxicology, and metabolism, *Nat. Prod. Rep.*, 39, 460-473.
- Wada, K., Mori, T., Kawahara, N., 2000. Stereochemistry of norditerpenoid alkaloids by liquid chromatography/atmospheric pressure chemical ionization mass spectrometry. *J. Mass Spectrom.* 35, 432-439.
- Zeng, Z., Qasem, A.M.A., Kociok-Köhn, G., Rowan, M.G., Blagbrough, I.S., 2020a. The 1 $\alpha$ -hydroxy-A-rings of norditerpenoid alkaloids are twisted-boat conformers. *RSC Adv.* 10, 18797-18805.
- Zeng, Z., Qasem, A.M.A., Woodman, T.J., Rowan, M.G., Blagbrough, I.S., 2020b. Impacts of steric compression, protonation, and intramolecular hydrogen bonding on the  $^{15}\text{N}$  NMR spectroscopy of norditerpenoid alkaloids and their piperidine-ring analogues. *ACS Omega.* 5, 14116-14122.

\*Correspondence: [prsisb@bath.ac.uk](mailto:prsisb@bath.ac.uk)

# Methyllycaconitine analogues antagonism at human $\alpha 7$ nAChRs

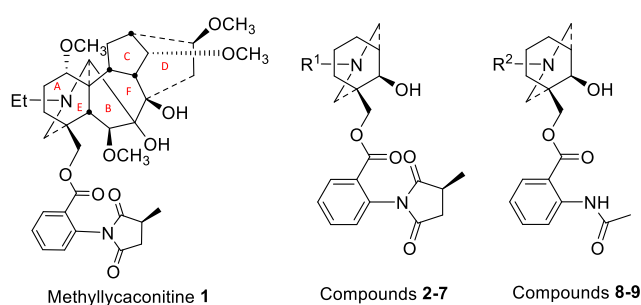
Ashraf M. A. Qasem<sup>1</sup>, Victoria Sanders<sup>2</sup>, Neil Millar<sup>2</sup>, Michael G. Rowan<sup>1</sup>,  
and Ian S. Blagbrough<sup>1\*</sup>

<sup>1</sup> Department of Pharmacy and Pharmacology, University of Bath, Bath BA2 7AY, UK

<sup>2</sup> Department of Neuroscience, Physiology and Pharmacology, University College London, London WC1E 6BT, UK

\*Email: [prsisb@bath.ac.uk](mailto:prsisb@bath.ac.uk)

Norditerpenoid alkaloids (NDAs) are the major alkaloid group of the genera *Delphinium* and *Aconitum*, which are used as poisons and as analgesics and antiarrhythmics in traditional Chinese and Japanese medicine (Shen *et al.*, 2020). Methyllycaconitine (MLA) **1**, a highly potent  $\alpha 7$  nicotinic acetylcholine receptor (nAChR) antagonist, is formulated as Mellictin, reported in clinical use at least in Uzbekistan and Kyrgyzstan for the treatment of Parkinson's disease and cerebral palsy (Qasem *et al.*, 2022). These pharmacological activities encourage SAR studies on NDAs, and we have investigated, through AE-bicyclic analogues, the importance of *N*-alkyl chain length, and the ester side-chain, and how these factors affect the activity at human  $\alpha 7$  nAChRs. The antagonism (normalised response) was measured through the application of these analogues [1 nM] with EC50 ACh. These easily prepared neopentyl esters include promising analogues **8**, **5**, **2**, and **6**.



Cmpd	R <sup>1</sup>	Response %
<b>Methyllycaconitine 1</b>		39
<b>2</b>	Me	77
<b>3</b>	Et	86
<b>4</b>	Benzyl	90
<b>5</b>	Phenylethyl	75
<b>6</b>	Phenylpropyl	80
<b>7</b>	Phenylbutyl	110
	<b>R<sup>2</sup></b>	
<b>8</b>	Me	67
<b>9</b>	Et	100

## Acknowledgements

We acknowledge Zarqa University, Jordan, for funding the studentship of Ashraf M. A. Qasem, and LiDo/BBSRC Doctoral Training Programme for funding the studentship of Victoria Sanders.

## References

Qasem, A. M. A. *et al.* (2022), Norditerpenoid alkaloids from *Aconitum* and *Delphinium* : structural relevance in medicine, toxicology, and metabolism, *Natural Product Reports*, **39**, 460-473. doi: 10.1039/d1np00029b.

Shen, Y. *et al.* (2020), Structural diversity, bioactivities, and biosynthesis of natural diterpenoid alkaloids, *Natural Product Reports*, **37**, 763–796. doi: 10.1039/d0np00002g.

## Norditerpenoid alkaloids analysis using NMR and MS

Ashraf M. A. Qasem, Michael G. Rowan, and Ian S. Blagbrough\*

Department of Pharmacy and Pharmacology, University of Bath, Bath BA2 7AY, UK

\*[prsisb@bath.ac.uk](mailto:prsisb@bath.ac.uk)

The analysis of norditerpenoid alkaloids (NDA) is important to determine their conformation. They have bridged highly oxygenated hexacyclic skeleta. Solution studies of these alkaloids using NMR spectroscopy leads to a better understanding of their possible 3D-conformations in biological fluids as several of these alkaloids are of pharmacological and even clinical importance (Qasem et al., 2022). We are investigating the effect of C1- $\alpha$  substituents on the conformation of ring A in selected NDA (Zeng et al., 2020 a, b) and studying the through-space interactions and how they affect their MS fragmentation using LC/MS-APCI (Wada et al., 2000).

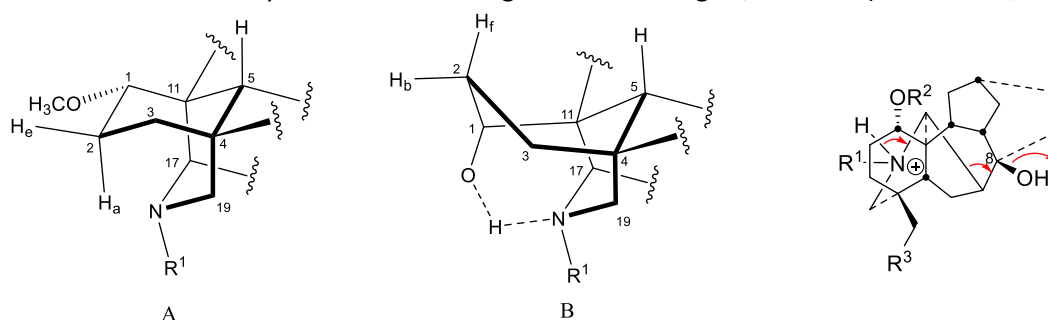
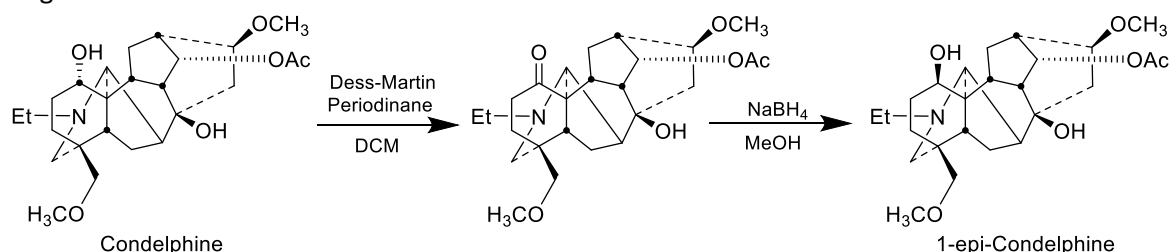


Fig. 1. A. Ring A in a twisted-chair conformation in 1-OMe NDA; B. Ring A in a twisted-boat conformation due to the intramolecular H-bond. a: axial, e: equatorial, f: flagpole, b: bowsprit

Fig. 2. Fragmentation of NDA skeleton at position 8

In addition, to exclude the effect of structure variability, we have oxidized and reduced condelphine to get 1-epi-condelphine and to study the effect of 1-OH on NMR and MS fragmentation.



### Acknowledgement

We acknowledge Zarqa University, Jordan, for fully funding this PhD studentship.

### References

- Qasem, A. M. A., Zeng, Z., Rowan, M.G., Blagbrough, I.S., 2022. Norditerpenoid alkaloids from *Aconitum* and *Delphinium* : structural relevance in medicine, toxicology, and metabolism, *Nat. Prod. Rep.*, 39, 460-473.
- Wada, K., Mori, T., Kawahara, N., 2000. Stereochemistry of norditerpenoid alkaloids by liquid chromatography/atmospheric pressure chemical ionization mass spectrometry. *J. Mass Spectrom.* 35, 432–439.
- Zeng, Z., Qasem, A.M.A., Kociok-Köhn, G., Rowan, M.G., Blagbrough, I.S., 2020a. The 1 $\alpha$ -hydroxy-A-rings of norditerpenoid alkaloids are twisted-boat conformers. *RSC Adv.* 10, 18797–18805.
- Zeng, Z., Qasem, A.M.A., Woodman, T.J., Rowan, M.G., Blagbrough, I.S., 2020b. Impacts of steric compression, protonation, and intramolecular hydrogen bonding on the <sup>15</sup>N NMR spectroscopy of norditerpenoid alkaloids and their piperidine-ring analogues. *ACS Omega.* 5, 14116–14122.

## Appendix 2: Data of single-crystal X-ray determinations of delpheline (s22phar2)

Table 1. Crystal data and structure refinement for s22phar2.

Identification code	s22phar2	
Empirical formula	C <sub>25</sub> H <sub>39</sub> N O <sub>6</sub>	
Formula weight	449.57	
Temperature	150.01(10) K	
Wavelength	1.54184 Å	
Crystal system	Orthorhombic	
Space group	P2 <sub>1</sub> 2 <sub>1</sub> 2 <sub>1</sub>	
Unit cell dimensions	a = 11.98820(9) Å	α = 90°.
	b = 13.21037(11) Å	β = 90°.
	c = 14.32101(13) Å	γ = 90°.
Volume	2268.00(3) Å <sup>3</sup>	
Z	4	
Density (calculated)	1.317 Mg/m <sup>3</sup>	
Absorption coefficient	0.753 mm <sup>-1</sup>	
F(000)	976	
Crystal size	0.308 x 0.189 x 0.172 mm <sup>3</sup>	
Theta range for data collection	4.554 to 72.911°.	
Index ranges	-14 ≤ h ≤ 14, -16 ≤ k ≤ 16, -16 ≤ l ≤ 17	
Reflections collected	49710	
Independent reflections	4522 [R(int) = 0.0268]	
Completeness to theta = 67.684°	100.0 %	
Absorption correction	Semi-empirical from equivalents	
Max. and min. transmission	1.00000 and 0.86657	
Refinement method	Full-matrix least-squares on F <sup>2</sup>	
Data / restraints / parameters	4522 / 0 / 298	
Goodness-of-fit on F <sup>2</sup>	1.102	
Final R indices [I > 2σ(I)]	R1 = 0.0397, wR2 = 0.1109	
R indices (all data)	R1 = 0.0398, wR2 = 0.1110	
Absolute structure parameter	0.01(3)	
Extinction coefficient	n/a	
Largest diff. peak and hole	0.565 and -0.291 e.Å <sup>-3</sup>	

Table 2. Atomic coordinates ( $\times 10^4$ ) and equivalent isotropic displacement parameters ( $\text{\AA}^2 \times 10^3$ ) for s22phar2.  $U(\text{eq})$  is defined as one third of the trace of the orthogonalized  $U^{ij}$  tensor.

	x	y	z	$U(\text{eq})$
N(1)	1133(2)	7230(2)	7776(2)	33(1)
O(1)	4894(2)	5966(1)	7671(1)	28(1)
O(2)	3492(2)	6760(1)	8503(1)	28(1)
O(3)	130(2)	5744(2)	6161(2)	39(1)
O(4)	4498(2)	7660(1)	6488(1)	29(1)
O(5)	3394(2)	2930(1)	7578(1)	33(1)
O(6)	5046(2)	4033(1)	6311(1)	30(1)
C(1)	3822(2)	5685(2)	7282(2)	24(1)
C(2)	4636(2)	6454(2)	8533(2)	30(1)
C(3)	3167(2)	6627(2)	7547(2)	24(1)
C(4)	1908(2)	6495(2)	7364(2)	25(1)
C(5)	959(3)	7073(3)	8776(2)	41(1)
C(6)	-162(3)	7422(3)	9104(2)	48(1)
C(7)	1306(2)	8296(2)	7544(2)	31(1)
C(8)	1687(2)	8500(2)	6532(2)	30(1)
C(9)	2243(3)	9547(2)	6495(2)	37(1)
C(10)	696(2)	8507(2)	5856(2)	34(1)
C(11)	32(2)	7541(2)	5933(2)	34(1)
C(12)	745(2)	6595(2)	5819(2)	29(1)
C(13)	-798(3)	5494(3)	5596(3)	45(1)
C(14)	1916(2)	6608(2)	6292(2)	24(1)
C(15)	2501(2)	7659(2)	6236(2)	25(1)
C(16)	3457(2)	7590(2)	6952(2)	25(1)
C(17)	2653(2)	5771(2)	5819(2)	25(1)
C(18)	2139(2)	4683(2)	5791(2)	32(1)
C(19)	3027(2)	3958(2)	6170(2)	29(1)
C(20)	2902(2)	3853(2)	7236(2)	26(1)
C(21)	2737(3)	2064(2)	7451(3)	52(1)
C(22)	3458(2)	4701(2)	7796(2)	27(1)
C(23)	4097(2)	4502(2)	5908(2)	28(1)
C(24)	6052(2)	4436(2)	5967(2)	37(1)
C(25)	3855(2)	5590(2)	6223(2)	24(1)

Table 3. Bond lengths [Å] for s22phar2.

---

N(1)-C(7)	1.462(3)
N(1)-C(5)	1.463(3)
N(1)-C(4)	1.467(3)
O(1)-C(2)	1.426(3)
O(1)-C(1)	1.450(3)
O(2)-C(2)	1.430(3)
O(2)-C(3)	1.435(3)
O(3)-C(13)	1.415(4)
O(3)-C(12)	1.430(3)
O(4)-C(16)	1.417(3)
O(4)-H(4A)	0.79(4)
O(5)-C(21)	1.400(4)
O(5)-C(20)	1.442(3)
O(6)-C(24)	1.407(3)
O(6)-C(23)	1.417(3)
C(1)-C(3)	1.520(3)
C(1)-C(25)	1.521(3)
C(1)-C(22)	1.556(3)
C(2)-H(2A)	0.9900
C(2)-H(2B)	0.9900
C(3)-C(4)	1.542(3)
C(3)-C(16)	1.569(3)
C(4)-C(14)	1.542(3)
C(4)-H(4)	1.0000
C(5)-C(6)	1.496(4)
C(5)-H(5A)	0.9900
C(5)-H(5B)	0.9900
C(6)-H(6A)	0.9800
C(6)-H(6B)	0.9800
C(6)-H(6C)	0.9800
C(7)-C(8)	1.543(4)
C(7)-H(7A)	0.9900
C(7)-H(7B)	0.9900
C(8)-C(10)	1.533(4)
C(8)-C(9)	1.536(4)
C(8)-C(15)	1.539(3)
C(9)-H(9A)	0.9800
C(9)-H(9B)	0.9800

C(9)-H(9C)	0.9800
C(10)-C(11)	1.508(4)
C(10)-H(10A)	0.9900
C(10)-H(10B)	0.9900
C(11)-C(12)	1.523(4)
C(11)-H(11A)	0.9900
C(11)-H(11B)	0.9900
C(12)-C(14)	1.559(3)
C(12)-H(12)	1.0000
C(13)-H(13A)	0.9800
C(13)-H(13B)	0.9800
C(13)-H(13C)	0.9800
C(14)-C(15)	1.559(3)
C(14)-C(17)	1.569(3)
C(15)-C(16)	1.541(3)
C(15)-H(15)	1.0000
C(16)-H(16)	1.0000
C(17)-C(18)	1.564(3)
C(17)-C(25)	1.571(3)
C(17)-H(17)	1.0000
C(18)-C(19)	1.532(4)
C(18)-H(18A)	0.9900
C(18)-H(18B)	0.9900
C(19)-C(23)	1.517(4)
C(19)-C(20)	1.540(3)
C(19)-H(19)	1.0000
C(20)-C(22)	1.531(3)
C(20)-H(20)	1.0000
C(21)-H(21A)	0.9800
C(21)-H(21B)	0.9800
C(21)-H(21C)	0.9800
C(22)-H(22A)	0.9900
C(22)-H(22B)	0.9900
C(23)-C(25)	1.534(3)
C(23)-H(23)	1.0000
C(24)-H(24A)	0.9800
C(24)-H(24B)	0.9800
C(24)-H(24C)	0.9800
C(25)-H(25)	1.0000

Table 4. Bond angles [°] for s22phar2.

C(7)-N(1)-C(5)	112.3(2)
C(7)-N(1)-C(4)	117.1(2)
C(5)-N(1)-C(4)	113.0(2)
C(2)-O(1)-C(1)	104.88(18)
C(2)-O(2)-C(3)	104.74(18)
C(13)-O(3)-C(12)	113.1(2)
C(16)-O(4)-H(4A)	115(3)
C(21)-O(5)-C(20)	114.6(2)
C(24)-O(6)-C(23)	112.34(19)
O(1)-C(1)-C(3)	98.72(18)
O(1)-C(1)-C(25)	112.44(19)
C(3)-C(1)-C(25)	109.26(19)
O(1)-C(1)-C(22)	106.27(19)
C(3)-C(1)-C(22)	114.9(2)
C(25)-C(1)-C(22)	114.2(2)
O(1)-C(2)-O(2)	108.08(19)
O(1)-C(2)-H(2A)	110.1
O(2)-C(2)-H(2A)	110.1
O(1)-C(2)-H(2B)	110.1
O(2)-C(2)-H(2B)	110.1
H(2A)-C(2)-H(2B)	108.4
O(2)-C(3)-C(1)	101.44(18)
O(2)-C(3)-C(4)	116.3(2)
C(1)-C(3)-C(4)	111.72(19)
O(2)-C(3)-C(16)	111.00(19)
C(1)-C(3)-C(16)	114.4(2)
C(4)-C(3)-C(16)	102.50(18)
N(1)-C(4)-C(3)	118.4(2)
N(1)-C(4)-C(14)	109.9(2)
C(3)-C(4)-C(14)	98.75(19)
N(1)-C(4)-H(4)	109.7
C(3)-C(4)-H(4)	109.7
C(14)-C(4)-H(4)	109.7
N(1)-C(5)-C(6)	113.0(2)
N(1)-C(5)-H(5A)	109.0
C(6)-C(5)-H(5A)	109.0
N(1)-C(5)-H(5B)	109.0
C(6)-C(5)-H(5B)	109.0
H(5A)-C(5)-H(5B)	107.8



C(5)-C(6)-H(6A)	109.5
C(5)-C(6)-H(6B)	109.5
H(6A)-C(6)-H(6B)	109.5
C(5)-C(6)-H(6C)	109.5
H(6A)-C(6)-H(6C)	109.5
H(6B)-C(6)-H(6C)	109.5
N(1)-C(7)-C(8)	115.1(2)
N(1)-C(7)-H(7A)	108.5
C(8)-C(7)-H(7A)	108.5
N(1)-C(7)-H(7B)	108.5
C(8)-C(7)-H(7B)	108.5
H(7A)-C(7)-H(7B)	107.5
C(10)-C(8)-C(9)	108.1(2)
C(10)-C(8)-C(15)	108.8(2)
C(9)-C(8)-C(15)	111.4(2)
C(10)-C(8)-C(7)	111.4(2)
C(9)-C(8)-C(7)	108.5(2)
C(15)-C(8)-C(7)	108.7(2)
C(8)-C(9)-H(9A)	109.5
C(8)-C(9)-H(9B)	109.5
H(9A)-C(9)-H(9B)	109.5
C(8)-C(9)-H(9C)	109.5
H(9A)-C(9)-H(9C)	109.5
H(9B)-C(9)-H(9C)	109.5
C(11)-C(10)-C(8)	111.0(2)
C(11)-C(10)-H(10A)	109.4
C(8)-C(10)-H(10A)	109.4
C(11)-C(10)-H(10B)	109.4
C(8)-C(10)-H(10B)	109.4
H(10A)-C(10)-H(10B)	108.0
C(10)-C(11)-C(12)	113.0(2)
C(10)-C(11)-H(11A)	109.0
C(12)-C(11)-H(11A)	109.0
C(10)-C(11)-H(11B)	109.0
C(12)-C(11)-H(11B)	109.0
H(11A)-C(11)-H(11B)	107.8
O(3)-C(12)-C(11)	108.6(2)
O(3)-C(12)-C(14)	108.88(19)
C(11)-C(12)-C(14)	116.8(2)
O(3)-C(12)-H(12)	107.4

C(11)-C(12)-H(12)	107.4
C(14)-C(12)-H(12)	107.4
O(3)-C(13)-H(13A)	109.5
O(3)-C(13)-H(13B)	109.5
H(13A)-C(13)-H(13B)	109.5
O(3)-C(13)-H(13C)	109.5
H(13A)-C(13)-H(13C)	109.5
H(13B)-C(13)-H(13C)	109.5
C(4)-C(14)-C(12)	115.2(2)
C(4)-C(14)-C(15)	98.05(19)
C(12)-C(14)-C(15)	113.10(19)
C(4)-C(14)-C(17)	111.42(19)
C(12)-C(14)-C(17)	108.2(2)
C(15)-C(14)-C(17)	110.6(2)
C(8)-C(15)-C(16)	109.4(2)
C(8)-C(15)-C(14)	110.1(2)
C(16)-C(15)-C(14)	104.33(18)
C(8)-C(15)-H(15)	110.9
C(16)-C(15)-H(15)	110.9
C(14)-C(15)-H(15)	110.9
O(4)-C(16)-C(15)	109.84(19)
O(4)-C(16)-C(3)	120.2(2)
C(15)-C(16)-C(3)	104.17(19)
O(4)-C(16)-H(16)	107.4
C(15)-C(16)-H(16)	107.4
C(3)-C(16)-H(16)	107.4
C(18)-C(17)-C(14)	115.9(2)
C(18)-C(17)-C(25)	103.35(19)
C(14)-C(17)-C(25)	117.70(19)
C(18)-C(17)-H(17)	106.4
C(14)-C(17)-H(17)	106.4
C(25)-C(17)-H(17)	106.4
C(19)-C(18)-C(17)	107.0(2)
C(19)-C(18)-H(18A)	110.3
C(17)-C(18)-H(18A)	110.3
C(19)-C(18)-H(18B)	110.3
C(17)-C(18)-H(18B)	110.3
H(18A)-C(18)-H(18B)	108.6
C(23)-C(19)-C(18)	101.7(2)
C(23)-C(19)-C(20)	111.7(2)

C(18)-C(19)-C(20)	109.8(2)
C(23)-C(19)-H(19)	111.1
C(18)-C(19)-H(19)	111.1
C(20)-C(19)-H(19)	111.1
O(5)-C(20)-C(22)	105.23(19)
O(5)-C(20)-C(19)	111.9(2)
C(22)-C(20)-C(19)	114.3(2)
O(5)-C(20)-H(20)	108.4
C(22)-C(20)-H(20)	108.4
C(19)-C(20)-H(20)	108.4
O(5)-C(21)-H(21A)	109.5
O(5)-C(21)-H(21B)	109.5
H(21A)-C(21)-H(21B)	109.5
O(5)-C(21)-H(21C)	109.5
H(21A)-C(21)-H(21C)	109.5
H(21B)-C(21)-H(21C)	109.5
C(20)-C(22)-C(1)	119.0(2)
C(20)-C(22)-H(22A)	107.6
C(1)-C(22)-H(22A)	107.6
C(20)-C(22)-H(22B)	107.6
C(1)-C(22)-H(22B)	107.6
H(22A)-C(22)-H(22B)	107.0
O(6)-C(23)-C(19)	111.8(2)
O(6)-C(23)-C(25)	116.2(2)
C(19)-C(23)-C(25)	102.2(2)
O(6)-C(23)-H(23)	108.8
C(19)-C(23)-H(23)	108.8
C(25)-C(23)-H(23)	108.8
O(6)-C(24)-H(24A)	109.5
O(6)-C(24)-H(24B)	109.5
H(24A)-C(24)-H(24B)	109.5
O(6)-C(24)-H(24C)	109.5
H(24A)-C(24)-H(24C)	109.5
H(24B)-C(24)-H(24C)	109.5
C(1)-C(25)-C(23)	112.0(2)
C(1)-C(25)-C(17)	109.32(19)
C(23)-C(25)-C(17)	102.00(19)
C(1)-C(25)-H(25)	111.1
C(23)-C(25)-H(25)	111.1
C(17)-C(25)-H(25)	111.1

Table 5. Anisotropic displacement parameters ( $\text{\AA}^2 \times 10^3$ ) for s22phar2. The anisotropic displacement factor exponent takes the form:  $-2\pi^2 [ h^2 a^{*2} U^{11} + \dots + 2 h k a^* b^* U^{12} ]$

	U <sup>11</sup>	U <sup>22</sup>	U <sup>33</sup>	U <sup>23</sup>	U <sup>13</sup>	U <sup>12</sup>
N(1)	41(1)	37(1)	23(1)	7(1)	5(1)	12(1)
O(1)	29(1)	31(1)	23(1)	-2(1)	-5(1)	1(1)
O(2)	35(1)	31(1)	19(1)	-2(1)	-5(1)	4(1)
O(3)	30(1)	37(1)	50(1)	15(1)	-6(1)	-6(1)
O(4)	30(1)	29(1)	29(1)	4(1)	-2(1)	-5(1)
O(5)	31(1)	24(1)	44(1)	10(1)	-1(1)	0(1)
O(6)	34(1)	28(1)	28(1)	4(1)	4(1)	4(1)
C(1)	27(1)	22(1)	21(1)	1(1)	-3(1)	1(1)
C(2)	35(1)	32(1)	22(1)	-2(1)	-6(1)	0(1)
C(3)	31(1)	25(1)	16(1)	-1(1)	-3(1)	1(1)
C(4)	29(1)	24(1)	22(1)	4(1)	1(1)	2(1)
C(5)	47(2)	51(2)	26(1)	7(1)	6(1)	16(1)
C(6)	46(2)	61(2)	36(1)	7(2)	10(1)	10(2)
C(7)	33(1)	31(1)	29(1)	-1(1)	-3(1)	8(1)
C(8)	34(1)	24(1)	30(1)	3(1)	-4(1)	3(1)
C(9)	45(2)	24(1)	43(2)	4(1)	-4(1)	4(1)
C(10)	36(1)	32(1)	34(1)	9(1)	-6(1)	6(1)
C(11)	30(1)	40(1)	32(1)	9(1)	-6(1)	3(1)
C(12)	31(1)	31(1)	26(1)	6(1)	-4(1)	-2(1)
C(13)	32(2)	40(2)	62(2)	2(1)	-8(1)	-5(1)
C(14)	28(1)	24(1)	22(1)	4(1)	-2(1)	0(1)
C(15)	31(1)	24(1)	22(1)	4(1)	-3(1)	0(1)
C(16)	30(1)	22(1)	23(1)	1(1)	-2(1)	0(1)
C(17)	30(1)	26(1)	19(1)	1(1)	-4(1)	-1(1)
C(18)	37(1)	26(1)	31(1)	0(1)	-12(1)	-2(1)
C(19)	36(1)	24(1)	28(1)	-2(1)	-4(1)	1(1)
C(20)	28(1)	23(1)	29(1)	2(1)	-2(1)	2(1)
C(21)	43(2)	37(2)	76(2)	10(2)	3(2)	-6(1)
C(22)	34(1)	25(1)	23(1)	3(1)	-2(1)	2(1)
C(23)	37(1)	25(1)	21(1)	0(1)	0(1)	2(1)
C(24)	37(1)	35(1)	38(2)	7(1)	2(1)	1(1)
C(25)	27(1)	24(1)	21(1)	1(1)	-1(1)	0(1)

Table 6. Hydrogen coordinates ( $\times 10^4$ ) and isotropic displacement parameters ( $\text{\AA}^2 \times 10^{-3}$ ) for s22phar2.

	x	y	z	U(eq)
H(4A)	5020(40)	7670(30)	6820(30)	46(10)
H(2A)	5123	7052	8621	36
H(2B)	4759	5983	9060	36
H(4)	1674	5793	7536	30
H(5A)	1544	7442	9127	49
H(5B)	1041	6343	8919	49
H(6A)	-208	8160	9051	72
H(6B)	-268	7223	9757	72
H(6C)	-743	7111	8718	72
H(7A)	1872	8578	7975	37
H(7B)	600	8666	7655	37
H(9A)	2394	9729	5844	56
H(9B)	2946	9528	6844	56
H(9C)	1745	10052	6775	56
H(10A)	207	9092	5998	41
H(10B)	972	8585	5208	41
H(11A)	-557	7541	5448	40
H(11B)	-340	7521	6550	40
H(12)	863	6490	5135	35
H(13A)	-600	5581	4937	67
H(13B)	-1424	5940	5750	67
H(13C)	-1012	4789	5709	67
H(15)	2798	7787	5594	30
H(16)	3393	8191	7374	30
H(17)	2755	5984	5154	30
H(18A)	1459	4653	6182	38
H(18B)	1937	4498	5143	38
H(19)	2980	3283	5856	35
H(20)	2088	3846	7390	32
H(21A)	2617	1951	6783	78
H(21B)	2016	2159	7762	78
H(21C)	3118	1476	7721	78
H(22A)	4129	4413	8099	33
H(22B)	2938	4899	8301	33
H(23)	4178	4493	5213	33

H(24A)	6023	4463	5283	55
H(24B)	6675	4006	6162	55
H(24C)	6158	5121	6215	55
H(25)	4403	6075	5947	28

---

Table 7. Torsion angles [°] for s22phar2.

---

C(2)-O(1)-C(1)-C(3)	39.5(2)
C(2)-O(1)-C(1)-C(25)	154.6(2)
C(2)-O(1)-C(1)-C(22)	-79.8(2)
C(1)-O(1)-C(2)-O(2)	-19.1(2)
C(3)-O(2)-C(2)-O(1)	-11.4(2)
C(2)-O(2)-C(3)-C(1)	35.7(2)
C(2)-O(2)-C(3)-C(4)	157.1(2)
C(2)-O(2)-C(3)-C(16)	-86.3(2)
O(1)-C(1)-C(3)-O(2)	-46.2(2)
C(25)-C(1)-C(3)-O(2)	-163.79(19)
C(22)-C(1)-C(3)-O(2)	66.3(2)
O(1)-C(1)-C(3)-C(4)	-170.75(18)
C(25)-C(1)-C(3)-C(4)	71.7(2)
C(22)-C(1)-C(3)-C(4)	-58.2(3)
O(1)-C(1)-C(3)-C(16)	73.3(2)
C(25)-C(1)-C(3)-C(16)	-44.2(3)
C(22)-C(1)-C(3)-C(16)	-174.1(2)
C(7)-N(1)-C(4)-C(3)	57.0(3)
C(5)-N(1)-C(4)-C(3)	-75.9(3)
C(7)-N(1)-C(4)-C(14)	-55.4(3)
C(5)-N(1)-C(4)-C(14)	171.7(2)
O(2)-C(3)-C(4)-N(1)	50.3(3)
C(1)-C(3)-C(4)-N(1)	166.08(19)
C(16)-C(3)-C(4)-N(1)	-71.0(2)
O(2)-C(3)-C(4)-C(14)	168.70(19)
C(1)-C(3)-C(4)-C(14)	-75.5(2)
C(16)-C(3)-C(4)-C(14)	47.4(2)
C(7)-N(1)-C(5)-C(6)	73.1(4)
C(4)-N(1)-C(5)-C(6)	-151.7(3)
C(5)-N(1)-C(7)-C(8)	170.3(2)
C(4)-N(1)-C(7)-C(8)	37.1(3)
N(1)-C(7)-C(8)-C(10)	82.1(3)
N(1)-C(7)-C(8)-C(9)	-159.0(2)
N(1)-C(7)-C(8)-C(15)	-37.7(3)
C(9)-C(8)-C(10)-C(11)	-173.7(2)
C(15)-C(8)-C(10)-C(11)	65.2(3)
C(7)-C(8)-C(10)-C(11)	-54.6(3)
C(8)-C(10)-C(11)-C(12)	-53.4(3)

C(13)-O(3)-C(12)-C(11)	68.9(3)
C(13)-O(3)-C(12)-C(14)	-163.0(2)
C(10)-C(11)-C(12)-O(3)	163.7(2)
C(10)-C(11)-C(12)-C(14)	40.1(3)
N(1)-C(4)-C(14)-C(12)	-51.2(3)
C(3)-C(4)-C(14)-C(12)	-175.8(2)
N(1)-C(4)-C(14)-C(15)	69.1(2)
C(3)-C(4)-C(14)-C(15)	-55.5(2)
N(1)-C(4)-C(14)-C(17)	-174.9(2)
C(3)-C(4)-C(14)-C(17)	60.4(2)
O(3)-C(12)-C(14)-C(4)	-49.4(3)
C(11)-C(12)-C(14)-C(4)	74.0(3)
O(3)-C(12)-C(14)-C(15)	-161.0(2)
C(11)-C(12)-C(14)-C(15)	-37.6(3)
O(3)-C(12)-C(14)-C(17)	76.0(2)
C(11)-C(12)-C(14)-C(17)	-160.5(2)
C(10)-C(8)-C(15)-C(16)	-175.7(2)
C(9)-C(8)-C(15)-C(16)	65.2(3)
C(7)-C(8)-C(15)-C(16)	-54.3(3)
C(10)-C(8)-C(15)-C(14)	-61.7(3)
C(9)-C(8)-C(15)-C(14)	179.3(2)
C(7)-C(8)-C(15)-C(14)	59.8(3)
C(4)-C(14)-C(15)-C(8)	-74.0(2)
C(12)-C(14)-C(15)-C(8)	47.9(3)
C(17)-C(14)-C(15)-C(8)	169.46(19)
C(4)-C(14)-C(15)-C(16)	43.3(2)
C(12)-C(14)-C(15)-C(16)	165.1(2)
C(17)-C(14)-C(15)-C(16)	-73.3(2)
C(8)-C(15)-C(16)-O(4)	-126.5(2)
C(14)-C(15)-C(16)-O(4)	115.7(2)
C(8)-C(15)-C(16)-C(3)	103.5(2)
C(14)-C(15)-C(16)-C(3)	-14.3(2)
O(2)-C(3)-C(16)-O(4)	91.4(3)
C(1)-C(3)-C(16)-O(4)	-22.7(3)
C(4)-C(3)-C(16)-O(4)	-143.8(2)
O(2)-C(3)-C(16)-C(15)	-145.15(19)
C(1)-C(3)-C(16)-C(15)	100.8(2)
C(4)-C(3)-C(16)-C(15)	-20.3(2)
C(4)-C(14)-C(17)-C(18)	74.4(3)
C(12)-C(14)-C(17)-C(18)	-53.2(3)



C(15)-C(14)-C(17)-C(18)	-177.62(19)
C(4)-C(14)-C(17)-C(25)	-48.6(3)
C(12)-C(14)-C(17)-C(25)	-176.17(19)
C(15)-C(14)-C(17)-C(25)	59.4(3)
C(14)-C(17)-C(18)-C(19)	-129.9(2)
C(25)-C(17)-C(18)-C(19)	0.3(3)
C(17)-C(18)-C(19)-C(23)	-28.7(3)
C(17)-C(18)-C(19)-C(20)	89.8(2)
C(21)-O(5)-C(20)-C(22)	155.9(3)
C(21)-O(5)-C(20)-C(19)	-79.4(3)
C(23)-C(19)-C(20)-O(5)	-90.1(2)
C(18)-C(19)-C(20)-O(5)	157.8(2)
C(23)-C(19)-C(20)-C(22)	29.4(3)
C(18)-C(19)-C(20)-C(22)	-82.7(3)
O(5)-C(20)-C(22)-C(1)	137.9(2)
C(19)-C(20)-C(22)-C(1)	14.7(3)
O(1)-C(1)-C(22)-C(20)	-139.7(2)
C(3)-C(1)-C(22)-C(20)	112.3(2)
C(25)-C(1)-C(22)-C(20)	-15.1(3)
C(24)-O(6)-C(23)-C(19)	171.3(2)
C(24)-O(6)-C(23)-C(25)	-72.0(3)
C(18)-C(19)-C(23)-O(6)	171.6(2)
C(20)-C(19)-C(23)-O(6)	54.5(3)
C(18)-C(19)-C(23)-C(25)	46.7(2)
C(20)-C(19)-C(23)-C(25)	-70.4(2)
O(1)-C(1)-C(25)-C(23)	92.8(2)
C(3)-C(1)-C(25)-C(23)	-158.6(2)
C(22)-C(1)-C(25)-C(23)	-28.4(3)
O(1)-C(1)-C(25)-C(17)	-154.86(18)
C(3)-C(1)-C(25)-C(17)	-46.3(3)
C(22)-C(1)-C(25)-C(17)	83.9(2)
O(6)-C(23)-C(25)-C(1)	-51.8(3)
C(19)-C(23)-C(25)-C(1)	70.1(2)
O(6)-C(23)-C(25)-C(17)	-168.6(2)
C(19)-C(23)-C(25)-C(17)	-46.7(2)
C(18)-C(17)-C(25)-C(1)	-90.9(2)
C(14)-C(17)-C(25)-C(1)	38.2(3)
C(18)-C(17)-C(25)-C(23)	27.8(2)
C(14)-C(17)-C(25)-C(23)	157.0(2)

Table 8. Hydrogen bonds for s22phar2 [ $\text{\AA}$  and  $^\circ$ ].

D-H...A	d(D-H)	d(H...A)	d(D...A)	$\angle(\text{DHA})$
O(4)-H(4A)...O(5)#1	0.79(4)	2.11(4)	2.881(3)	165(4)

Symmetry transformations used to generate equivalent atoms:

#1  $-x+1, y+1/2, -z+3/2$